THE UNIVERSITY OF QUEENSLAND

AUSTRALIA

Improved process development for complex silver ores through systematic, advanced mineral characterisation

Jocelyn Andrea Quinteros Riquelme
B. Eng (Mineral Processing) and Metallurgical Engineer

A thesis submitted for the degree of Doctor of Philosophy at

The University of Queensland in December 2014

Sustainable Minerals Institute

Abstract

With the general trend across all commodities towards the treatment of lower grade ores, it is becoming increasingly important to develop robust protocols for comprehensive mineralogical characterisation. The tendency for the complexity of the mineral assemblages in the ore to increase requires the use of more sophisticated tools in order to characterise the ore in the context of the implications of the mineralogy on its process response. Some of the key mineralogical attributes that are used to inform process selection and infer process response include: which minerals host the valuable element (elemental deportment); the type and relative proportions of the minerals present (modal mineralogy); and the grain size, association and liberation characteristics of the valuable minerals.

Silver ores are typically complex in terms of their mineralogical characterisation. There are a wide range of minerals that contain silver in different proportions which can make it difficult to identify them. Additional challenges include the relatively low concentrations of silver (ppm) within an ore, the large number of silver-bearing minerals that can occur in a single deposit and the potential for silver to occur in solid solution in wide range of sulphide minerals. Therefore, understanding the mineralogical attributes of an ore, particularly the deportment of the silver within the ore, is critical in developing an effective flotation processing strategy.

Automated SEM-based systems are a commonly used tool to quantify these attributes for an ore, but the low-grade together with the large number of minerals that are potential hosts for silver means that often, complementary analytical tools must be used in order to properly account for the valuable element.

This thesis aims to develop an appropriate methodology to characterise complex low-grade silver ores for the purpose of developing the most appropriate flotation strategy. As result of this investigation a novel methodology is proposed for the mineralogical characterisation and it consists of three different levels of characterisation using sophisticated analytical techniques. Level 1, the simplest (which included chemical assays, XRD, oxide characterisation of lead and zinc, optical microscopy and MLA), was applied to Toldos ore (oxide ore) and successfully characterised the mineralogy. Level 2, which included laser ablation inductively coupled plasma mass spectroscopy, was needed for Tesorera ore (sulphide ore). Jayula ore (supergene oxide ore) required the added sophistication of Level 3. In addition to the techniques of Level 1 and Level 2, Level 3 included the use of electron micro probe and synchrotron XRD, XRF and XANES methods to estimate the mineralogical attributes of this ore. The insights from the mineralogical characterisation were then

used to inform the metallurgical testing that was undertaken, for example, selective or bulk flotation.

The ore characterisation for Toldos identified the presence of at least eight silver-bearing minerals including coarse grained chlorargyrite and acanthite. Mineralogical analysis of preflotation test samples indicated that acanthite exhibited natural hydrophobicity. These results, together with the mineralogical characterisation, indicated that selective flotation would be an appropriate processing route for this ore. The coarse grained silver minerals required a P80 of 100 μm and a specific dosage of a mix of collectors. The final flow sheet produced a rougher concentrate that contained 4404 ppm of Ag, at a recovery of 83.8%.

In the Tesorera ore, the majority of the silver (>99%) was contained in pyrite, which itself represented approximately 4% of the ore. A bulk flotation strategy using sulphidisation agents and the introduction of mainstream inert grinding (MIG) to generate a P80 of 56 μm, was necessary to recover pyrite minerals to achieve a rougher concentrate of 485 ppm Ag at a recovery of 87.2%.

The mineralogical characterisation of Jayula, during which a previously unreported association was found between silver and barite, accounting for more than 20% of silver in this ore with most of the remainder occurring as fine grained acanthite helped to guide the metallurgical characterisation. The fine grind required a final flow sheet with a P80 of 25 μm and a produced concentrate for which the silver recovery was 80.8% at a grade of 1709 ppm Ag. Again, as with the previous ores, the mineralogical characterisation guided the metallurgical test work.

The outcomes of this research include:

- A systematic method that enables the development of flotation strategies to achieve >80% silver recovery in laboratory rougher separation. Analyses of flotation products were performed on unsized, size-by-size and size-by-liberation bases, opening a broad understanding of the behavior of complex low-grade silver ores.
- The identification of a unique chemical association between silver and barite, which has not been previously reported in the literature and was shown to account for up to 20% of the silver in one of the ores studied.
- A framework for assessing the ‘refractoriness’ of silver ores based on the mineralogical characteristics of the ore and the metallurgical performance.

In summary this work provides a clear demonstration of how powerful a detailed mineralogical study at the onset of a project can be to guide the metallurgical test work for improved recoveries.

Declaration by author

This thesis is composed of my original work, and contains no material previously published or written by another person except where due reference has been made in the text. I have clearly stated the contribution by others to jointly-authored works that I have included in my thesis.

I have clearly stated the contribution of others to my thesis as a whole, including statistical assistance, experimental design, data analysis, significant technical procedures, professional editorial advice, and any other original research work used or reported in my thesis. The content of my thesis is the result of work I have carried out since the commencement of my research higher degree candidature and does not include a substantial part of work that has been submitted to qualify for the award of any other degree or diploma in any university or other tertiary institution. I have clearly stated which parts of my thesis, if any, have been submitted to qualify for another award.

I acknowledge that an electronic copy of my thesis must be lodged with the University Library and, subject to the General Award Rules of The University of Queensland, immediately made available for research and study in accordance with the *Copyright Act 1968*.

I acknowledge that copyright of all material contained in my thesis resides with the copyright holder(s) of that material. Where appropriate I have obtained copyright permission from the copyright holder to reproduce material in this thesis.

Publications during candidature

Peer-reviewed journal paper

Quinteros J., Wightman E., Johnson N.W. and Bradshaw D., 2015. Evaluation of the response of valuable and gangue minerals on a recovery, size and liberation basis for a low grade silver ore. Minerals Engineering Journal, Vol. 74, 150-155.

Peer-reviewed conference papers

J Quinteros-Riquelme, E Wightman, N W Johnson and D Bradshaw., 2014. Applying process mineralogy to complex low-grade silver ores. IMPC 14, Santiago Chile, October 2014.

J Quinteros-Riquelme, N W Johnson, D Bradshaw and E Wightman., 2012. Study of flotation performance in a complex silver ore at laboratory scale. IMPC 12, New Delhi, India, September 2012.

Conference paper

Quinteros-Riquelme J, Wightman E, Johnson NW and Bradshaw D., 2013. Evaluation of the response of valuable and gangue minerals on a recovery, size and liberation basis for a low grade silver ore. Flotation ’13, Cape Town, South Africa, November 2013.

Publications included in this thesis

Quinteros J., Wightman E., Johnson N.W. and Bradshaw D., 2014 – Incorporated in Chapter 5.

Contributor	Statement of contribution
Quinteros J	Conception and design (50%) Analysis and interpretation of data (70%) Wrote the paper (60%)
Wightman E	Conception and design (30%) Analysis and interpretation of data (20%) Wrote and edited paper (20%)
Johnson NW	Conception and design (15%) Analysis and interpretation of data (10%) Wrote and edited paper (15%)
Bradshaw D	Conception and design (5%) Analysis and interpretation of data (0%) Wrote and edited paper (5%)

J Quinteros-Riquelme, E Wightman, N W Johnson and D Bradshaw., 2014 – Incorporated in Chapter 7.

Contributor	Statement of contribution
Quinteros J	Conception and design (60%) Analysis and interpretation of data (80%) Wrote the paper (70%)
Wightman E	Conception and design (40%) Analysis and interpretation of data (20%) Wrote and edited paper (20%)
Johnson NW	Conception and design (0%) Analysis and interpretation of data (0%) Wrote and edited paper (5%)
Bradshaw D	Conception and design (0%) Analysis and interpretation of data (0%) Wrote and edited paper (5%)

J Quinteros-Riquelme, N W Johnson, D Bradshaw and E Wightman., 2012. – Partially incorporated in Chapters 4 and Chapter 7.

Contributor	Statement of contribution
Quinteros J	Conception and design (50%) Analysis and interpretation of data (90%) Wrote the paper (70%)
Wightman E	Conception and design (10%) Analysis and interpretation of data (0%) Wrote and edited paper (5%)
Johnson NW	Conception and design (30%) Analysis and interpretation of data (10%) Wrote and edited paper (20%)
Bradshaw D	Conception and design (10%) Analysis and interpretation of data (0%) Wrote and edited paper (5%)

Quinteros-Riquelme J, Wightman E, Johnson NW and Bradshaw D., 2013. – Partially incorporated in Chapters 3 and Chapter 5.

Contributor	Statement of contribution
Quinteros J	Conception and design (50%) Analysis and interpretation of data (70%) Wrote the paper (60%)
Wightman E	Conception and design (30%) Analysis and interpretation of data (20%) Wrote and edited paper (20%)
Johnson NW	Conception and design (15%) Analysis and interpretation of data (10%) Wrote and edited paper (15%)
Bradshaw D	Conception and design (5%) Analysis and interpretation of data (0%) Wrote and edited paper (5%)

Contributions by others to the thesis

The work in this thesis was discussed with my supervisors, Dr. Elaine Wightman, Prof. Dee Bradshaw and Prof. N.W. Johnson, who also assisted in editing the thesis.

Prof. Tim Napier-Munn provided constant technical revision during the development of this research work.

Prof. William Whiten provided technical support by suggesting the use of Matlab code for identification of elements associated with Ag.

Dr. Elaine Wightman and Ms. Jessica Gray performed the MLA measurements described in Chapter 4, Chapter 5 and chapter 6 in this thesis.

Dr. Rong Fan performed the Synchrotron measurements described in Chapters 3 and 7. John Knights performed the optical microscopy described in Chapters 3, 4, 5 and 6. Dr. David Steele performed the EMPA measurement described in Chapter 3 and 6. ALS-Minerals and hrltesting providing the chemical assays, MODA provided the Laser ablation ion coupled mass spectroscopy analysis used in Chapter 5 and 6 and AMDEL provided the XRD and oxide characterisation described in Chapter 3, 4, 5 and 6.

Statement of parts of the thesis submitted to qualify for the award of another degree

None

Acknowledgements

This thesis would not be possible without the guidance, support, encouragement and generous contribution of my supervisors throughout my studies, and for these reasons I would like to express my appreciation to Dr. Elaine Wightman, Prof. Dee Bradshaw and Prof. Bill Johnson.

Special thanks are for Elaine, my principal supervisor, for all the time that she spent with me in revisions and fruitful technical discussions. Thanks, also to Dee who persuaded me to enroll in the PhD with enthusiasm and conviction. I'll keep both of you in my heart my dear friends.

Bill has guided and was present in any moment that I need his technical support. Also, he showed me that a person must be methodical to have successful in any objective that we have in life.

I am grateful for the guidance received in some of the stages of my PhD from Prof. Bill Whiten and Dr. David Steele.

I would also like to acknowledge the special contribution of Prof. Tim Napier-Munn. He was the one that named the unique chemical association found it in this work, as "jocelynite" (barite_Ag) and contribute with his critical and assertive inputs during the milestones of the PhD. Thanks also to Cathy Evans and Janine Lay for your comments and suggestions during this process.

I would like to acknowledge The University of Queensland and the Julius Kruttschnitt Mineral Research Centre for the support and contributions towards my study. Special thanks to the administrative team: Jill Mann, Heather Barlow and Neva Scott for assisting in the communication of the corrections made by Bill Johnson. Special thanks to Karen Holtham for her great job in the Centre´s library.

Thanks to all the students, past and present; you have made this journey a great time for my life. Thanks to Tim, Simon, Anne, Suping, Vannie, Bianca and Xumeng for the memorable time that we spent together in Brisbane and overseas.

I want to extend my thanks to my beloved parents Manolo and Maite, and my sister Kota for your love, support and absolute confidence in me during my life, and that we kept in touch strongly despite the physical separation of being in the other side of the Pacific Ocean.

And, finally I want to thank God for guiding my life with my Love Gerson and our precious and kind Maite Sophie. Thank you Ochito for bring me to this special journey, for providing me permanent encouragement and support in every decision I take in life.

With Love, Jocelyn.

Keywords

Process mineralogy, silver low-grade complex ores, key mineralogical attributes, flotation recovery, particle size, mineral liberation.

Australian and New Zealand Standard Research Classifications (ANZSRC)

ANZSRC code: 091404, Mineral Processing/Beneficiation , 100%

Fields of Research (FoR) Classification

FoR code: 0914, Resources Engineering and Extractive Metallurgy, 100%

Table of Contents

List of Figures

List of Tables

List of Abbreviations used in the thesis

%	:percentage
µg	:micro gram
µm	:micron
Ag	:silver
AgBr	:broyrite
AgCl	:cerargyrite or chlorargyrite
AgI	:iodyrite
alt	:alyite
As	:arsenic
arg	:argyroodite
Au	:gold
Ba	:barite
BSE	:Back-scattered electron
BSEI	: Back-scattered electron intensity
Char.	:characterisation
CMM	:Centre for Microscopy and Microanalysis
con	:concentrate
Cu	:copper
EDS	:Energy dispersive X-ray spectroscopy
Eh	:Redox potential (mV)
EIV	:Electron interaction volume
EMPA	:Electron micro probe analysis
ENT_i	:Degree of entrainment by particle size class (-)
f	: freibergite
Fe	:iron
g/mol	:grams per mol
g/t	:grams per tonne
ga	:galena
ge	:greenockite
GXMAP	:Ford analysis or grain-based X-ray mapping
Hd	:head
hes	:hessite
jo	:jordanite

L	:Litre
LA-ICP-MS	:Laser ablation inductively coupled plasma mass spectroscopy
ma	:marcasite
MDL	:minimum detection limit
mg/L	:Milligram per litre
m_i	:Mass fractions by size class *i*, relative to size class in feed (-)
M_i	:Mass fractions by size class *i*, relative to total feed (-)
MIBC	:Methyl Isobutyl Carbinol
MIG	: Mainstream inert grinding
min, mins	:minerals
mL	:Millilitres
MLA	:Mineral liberation analyser
MMaST	:Minerals and Materials Science & Technology
Mn	:manganese
Moz	:Million Ounces
MR_i	:Size-by-size mass recovery (-) or (%)
Na_2S	:Sodium sulphide
NaHS	:Sodium Hydrosulphide
NSG	:Non-sulphide gangue
Ox.	:oxide
PAX	:Potassium Amyl Xanthate
Pb	:lead
pg	:pyrargyrite
pH	:Measure of the activity of the hydrogen ion
po	:polybasite
ppm	:part per million
PSD	:Particle size distribution
Py , py	:pyrite
QEMSCAN	:Quantitative evaluation of minerals by scanning electron microscopy
qz	:quartz
QUT	:Queensland University of Technology
Rec	:Recovery of minerals on an unsized basis (-) or (%)
rho	:rhodochrosite
R_{ij}	:Size-by-liberation flotation recovery (-) or (%)
rpm	:Revolutions per minute

RPS	:Rare phase search
R_w	:Water recovery (-) or (%)
S	:sulphur
SD, σ	:Standard deviation
SE	:Secondary electrons
SEM	:Scanning electron microscope
sp	:sphalerite
SPL	:Sparse phase liberation analysis
SPL-dual zoom	:Schouwstra analysis sparse phase liberation analysis
SS	:Solid Solution
Sulp	:sulphide
SXBSE	:Super extended back-scattered electron liberation analysis
SXPS	:Synchrotron X-ray photo spectroscopy
SXRD	:Synchrotron X-ray Diffraction
SXRF	:Synchrotron X-ray Fluorescence
td	:tetrahedrite
ToF – SIMS	:Time of flight secondary ion mass spectroscopy
ToF-LIMS	:Time of flight laser ionization mass spectroscopy
TPH	:Tonnes per hour
UQ	:The University of Queensland
WA	:Western Australia
wt%	:weight percentage
XANES	: X-ray absorption near edge structure
XBSE	:Extended back-scattered electron liberation analysis
XMOD	:X-ray modal analysis
XRD	:X-ray Diffraction
Z	:Average atomic weight of the sample
Zn	:zinc

Chapter I:

Introduction

1.1. Context

One of the current trends in the mining industry is the move towards processing more complex low-grade ores (Mudd, 2010). This presents new challenges and provides an opportunity to perform research that will improve the understanding of how ore mineralogy can affect separation of the minerals via froth flotation. Of particular relevance are the liberation of valuable minerals, the potential activation of gangue minerals and the presence of minerals that generate slimes that may coat the surface of the valuable mineral, rendering it hydrophilic. These characteristics have been widely studied for a range of ores in the context of copper, gold, lead and zinc; however the mineralogical features of deposits containing silver and the associated processing challenges have not been as well studied.

Silver is a noble metal used since ancient times in many fields, namely currency, ornaments and jewellery (Silver Institute, 2013). During the past decade, the demand for this valuable element has increased exponentially as new applications for silver emerged, such as green technologies, medicine and nanotechnologies. High demand for this commodity has increased its price and as a result there is renewed global interest in developing flow sheets to recover silver from low-grade complex oxide and sulphide ores.

Silver has been identified by mineralogists as occurring in hundreds of different silver-bearing minerals that have a wide range of compositions, making silver mineralogy more complex than that of other precious metals, such as gold (Gasparrini, 1993). As a consequence of the complex mineralogy, different metallurgical techniques have been implemented for treating complex silver ores, including amalgamation, leaching, flotation, and roasting processes.

This work is focused on using a combination of mineralogical characterisation and metallurgical test-work to recover silver from three different ore types from a complex low-grade deposit in South America. This work has resulted in the development of a new systematic approach for identifying unknown silver-bearing minerals. Knowledge of the key mineralogical attributes of each ore (including silver deportment, liberation and grain size) are shown to be critical in the

development of the processing strategies used to treat each ore. This thesis only considers flotation as the concentration process.

1.2 Research hypothesis

The research hypothesis is as follows:

"Key mineralogical attributes (elemental deportment, liberation and association minerals) can be determined using a systematic application of mineralogical characterisation tools, from which an effective flotation strategy for low-grade silver ores can be developed"

1.3 Research objectives

The research objectives have been divided into the overall objective and specific objectives; both are described in the following paragraphs.

1.3.1 Overall objective

The overall objective is to develop an appropriate methodology to characterise complex low-grade silver ores for the purpose of developing the most appropriate flotation strategy.

1.3.2 Specific objectives

The following are the specific objectives of this work:

1) To develop a systematic approach to characterise the silver deportment, mineral association and texture in ores, which begins with using traditional microscopic techniques and uses more advanced and sophisticated techniques when needed.
2) To develop a method to identify unknown spectra from MLA analysis, with specific focus on the identification of silver-bearing minerals.
3) Using the information from mineralogical characterisation to develop an appropriate flotation strategy in order to obtain greater than 80% recovery of silver in laboratory rougher flotation tests.
4) Development of a consistent framework that can be used to quantify refractoriness of silver bearing ores.

1.4 Statement of Originality Contribution to Knowledge

This research has made the following contributions to current knowledge:

1) A novel methodology for mineralogical characterization of complex low-grade silver ores, which includes a systematic approach for identifying unknown spectra from MLA-based EDS.
2) Identification of a new association between barite and silver that is not currently described in the published literature.
3) A systematic method that enables the development of flotation strategies to achieve >80% silver recovery in a laboratory rougher process.
4) A framework for assessing the 'refractoriness' of silver based on the mineralogical characteristics of the ore.
5) A comprehensive dataset that includes mineralogical and metallurgical characterization for three complex low-grade silver ore types from a mine site located in Bolivia.

1.5 Scope of the thesis

Mineralogical characterisation provides the attributes of a given ore sample and this key information is then used to select the most appropriate flotation processes to recover the minerals containing the valuable elements present in the ores. There are a range of beneficiation processes that can be used for recovering commodities from silver ores, namely leaching, flotation and amalgamation processes, shown schematically in Figure 1.1. The red dashed box in Figure 1.1 shows which processes are included in this thesis, i.e. the beneficiation process under investigation is flotation. The investigation of other potential beneficiation routes is outside the scope of this work.

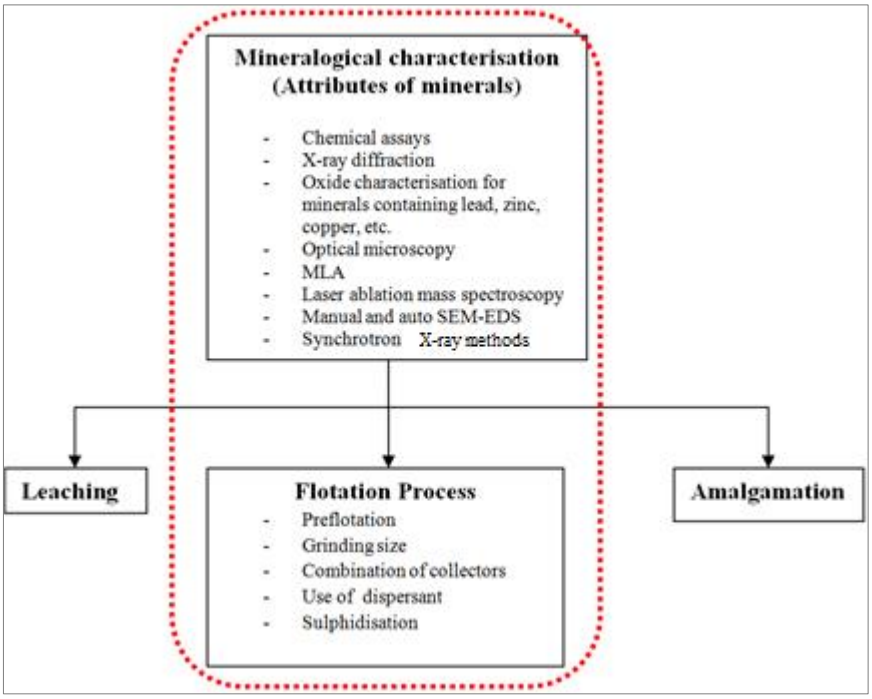

Figure 1.1: Scope of the thesis

A detailed description of the scope of the thesis is provided in Figure 1.2, which shows the inputs, mineralogical characterisation and outputs of the research scope. The inputs are the three case studies that relate to the three different ore types. For each case study, Level 1 mineralogical characterisation was undertaken. If this level of analysis was sufficient to identify the key mineralogical attributes for silver minerals and gangue minerals, then development of a flotation strategy could follow. For cases where the key mineralogical attributes of the ore were unable to be identified, mineralogical characterisation progressed to Level 2 and then Level 3, both incorporating increasingly sophisticated analytical techniques. In terms of the metallurgical characterisation, modal mineralogy will play an important role, not only by providing the deportment of Ag but also to determine the gangue mineralogy. This information will help to develop proper strategies in order to depress the gangue minerals that might dilute the concentrates.

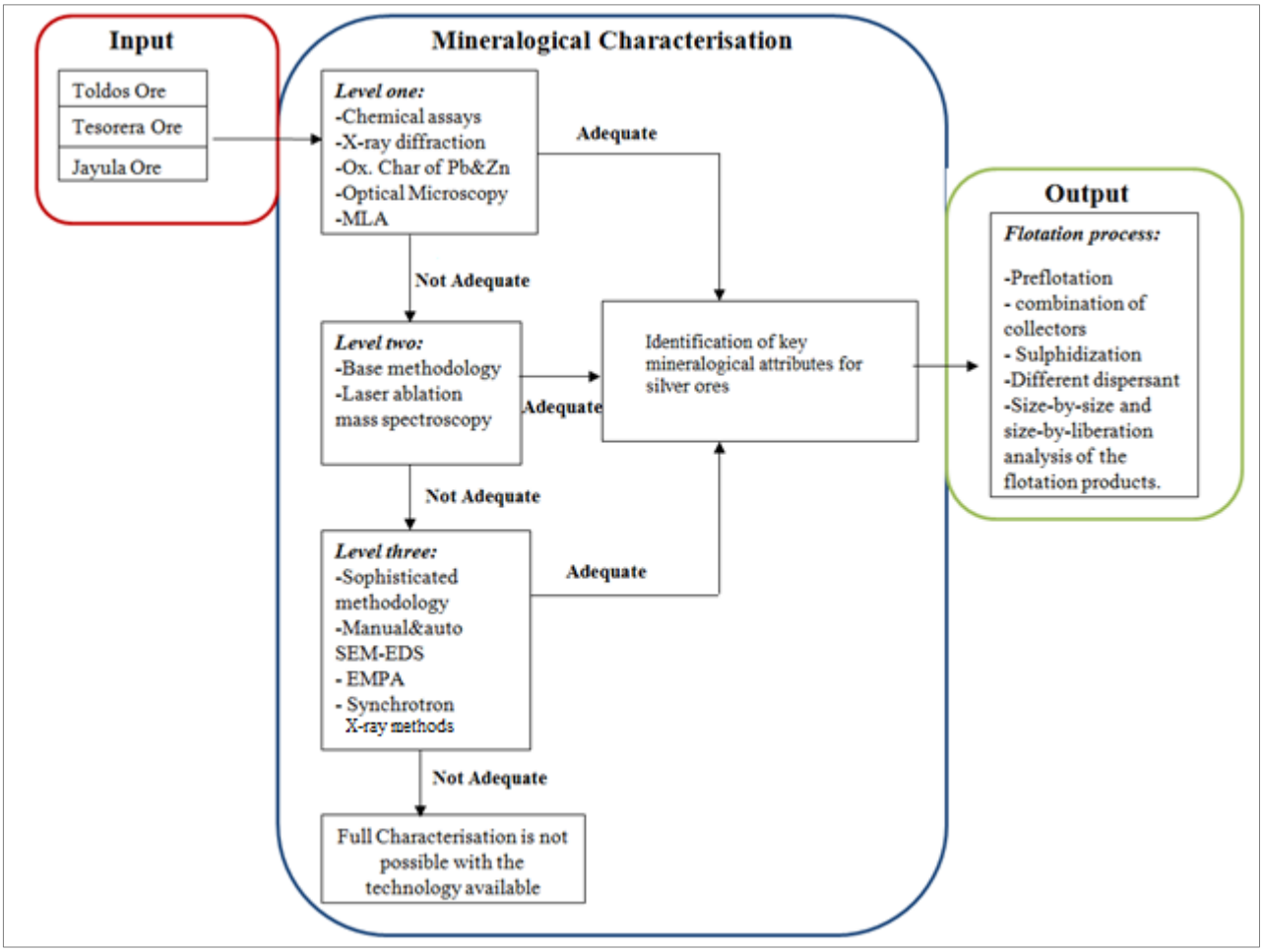

Figure 1.2: Mineral characterisation and beneficiation process to be applied.

1.6 Thesis outline

The following is an outline of the chapters contained in this thesis.

Chapter I presents an overview of this research work and describes the objectives, hypothesis and research path developed for this work.

Chapter II provides a review of the literature relating to the mineralogy of silver, the techniques available for mineralogical characterisation, and a description of the approaches used to characterise gold mineralogy and how these may be applied to characterise silver mineralogy. A description of the strategies used for concentrating silver using flotation is discussed, and finally, two examples describing how process mineralogy is applied in the context of silver are provided.

Chapter III provides details of the experimental methodology used in this research, and provides detailed descriptions of the ores studied. The different levels of the mineralogical characterisation methods used, as well as the flotation characterisation protocols are also described. In addition, the

novel approach for identifying silver minerals that was developed as part of this research is described.

Chapter IV describes the results of the mineralogical characterisation of the oxide low-grade silver ore, where key mineralogical attributes were able to be defined using the Level 1 methodology. This allowed the development of a selective flotation strategy that enabled a concentrate of 4404 ppm Ag with 83.8 % recovery to be achieved in laboratory rougher flotation.

Chapter V describes the results of the mineralogical characterisation of the sulphide ore for which Level 2 characterisation was required in order to define the key mineralogical attributes. A bulk flotation strategy was developed for this ore, which incorporated mainstream inert grinding (MIG) to enhance sulphide liberation and sulphidisation to enhance the recovery of oxidised pyrite. This allowed the production of a concentrate that contained 485 ppm Ag at 87.2% recovery from laboratory rougher flotation.

Chapter VI describes the results of mineralogical characterisation of the oxide supergene ore, for which the key mineralogical attributes could be described following Level 3 characterisation. A selective flotation strategy that incorporated fine grinding of the flotation feed was used to produce a concentrate with 1709 ppm Ag with a recovery of 80.8% from laboratory rougher flotation.

Chapter VII discusses the key findings from this work and the implications in the context of how understanding of the complexity of the ore characteristics will provide insights into the metallurgical response. The concept of refractoriness as it applies to the silver ores studies in this work is also discussed and a framework for describing how refractory a silver ore is likely to be is predictive.

Chapter VIII describes how the objectives and hypothesis outlined in Chapter I were achieved and tested respectively, and identifies potential areas for future work related to complex low-grade silver ores i.e., more complex mineralogical characteristics that results in more complex processing and possible changed the flow sheet design adding more unit process in the treatments.

Chapter II:

Literature Review

This chapter examines the literature relating to the mineralogy and processing of silver ores. It begins with the different silver deposits and silver minerals that can be found worldwide, then reviews the techniques currently used to identify and characterise silver minerals. The literature that describes the metallurgical processing routes for silver minerals is also discussed, with particular emphasis on the different strategies used to float silver minerals. The chapter concludes with literature examples of process mineralogy in the context of silver, leading to the identification of gaps in the literature that will be addressed in this thesis.

2.1 Introduction

Silver has properties that make this valuable element impossible to substitute in most of its applications. Among these properties are its ductility, strength and malleability, its sensitivity to highly reflectant light and its electrical and thermal conductivity. Silver is part of the I-B group in the Periodic Table, its symbol is Ag and its atomic number is 47, with a mass of 107.868 g/mol. Ag has a minimum oxidation number of zero, which allows it to be found in nature in its elemental state (Silver Institute, 2013). Despite silver being a very well-known and widely used element, its mineralogy is quite varied and in most cases complex. Oancea (2007) expressed in one phrase what silver means for mineralogy, declaring that "Silver is an intriguing chemical element with lots of unique characteristics, properties and uses, and presenting with a difficult mineralogy". It is present, at different quantities, in more than 200 minerals; this presents challenges not only in the identification and quantification of silver deportment, but also in the development of metallurgical strategies to treat the ore, particularly if it is of low-grade.

In 2012, Mexico was the top silver producing country in the world with 162.2 million ounces produced, followed by China with 117.0 million ounces and Peru with 111.3 million ounces. Nevertheless, the world's leading primary silver mines are Cannington (BHP Billiton), located in Australia with a production of 32.23 million ounces, followed by Fresnillo (Mexico) and Dukat in Russia (Silver Institute, 2013). Figure 2.1 shows the global silver production between 2005 and

2014. In 2014, it is expected that more than 550 Moz of mined silver will be produced as a by-product from base metal or gold mines (Silver Wheaton, 2013). Figure 2.2 illustrates how silver ore grades (g/t) have been depleting since early 1900 and nowadays the typical grade for silver ores is below 100ppm.

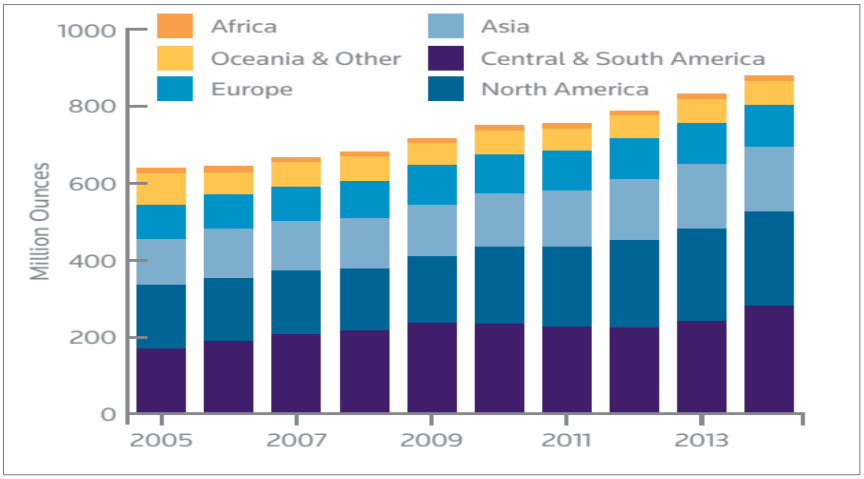

Figure 2.1: Global silver production (from Silver Institute, 2015)

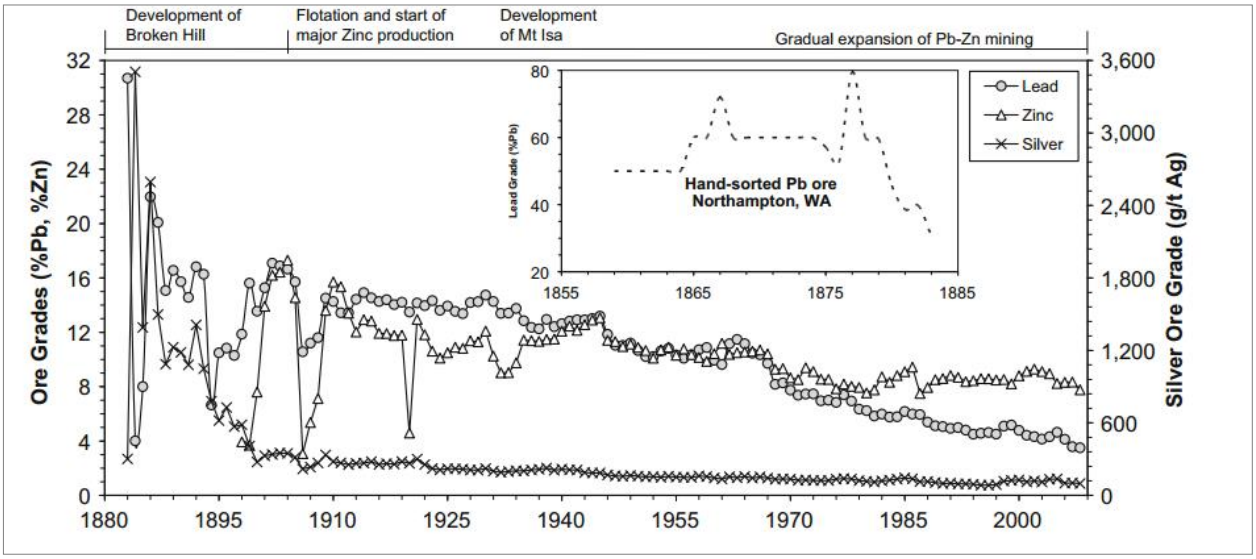

Figure 2.2: Ore grades for silver, lead and zinc (From Mudd, 2010)

The key mineralogical attributes that are critical in the selection of an appropriate processing route include: the relative mineral abundance or modal mineralogy, the deportment of key elements, mineral association and texture, and the consequence of these on the liberation characteristics of key minerals. Different methods for recovering silver have been developed over the last century and these depend on the presence of different silver-bearing minerals in an ore. Examples of potential treatment routes are pressure leaching, cyanide leaching, flotation and roasting.

2.2 Silver mineralogy, types and deposits

2.2.1 Silver mineralogy

The mineralogy of silver has been described as complex by many authors (Gasparrini, 1984A; Chryssoulis and Surges, 1988; Oancea, 2007). This description is based on: i) the wide range of minerals that contain silver in different proportions (*Appendix A* shows a list of silver minerals); ii) relatively low concentrations of silver (ppm) within an ore; iii) the large number of silver-bearing minerals occurring in the same deposit; iv) the instability of some silver minerals; v) the variability within a single deposit; and vi) the presence of silver in solid solution (SS) in a wide range of sulphide minerals, such as galena, sphalerite, and pyrite among others (Mann, 1984; Webster and Mann, 1984). An example of how challenging it can be to quantify silver in low-grade ores is shown in Figure 2.3, which illustrates the variability of silver content in a drill hole sample at increments along the length of the drill core (footage) (Gasparrini, 1993).

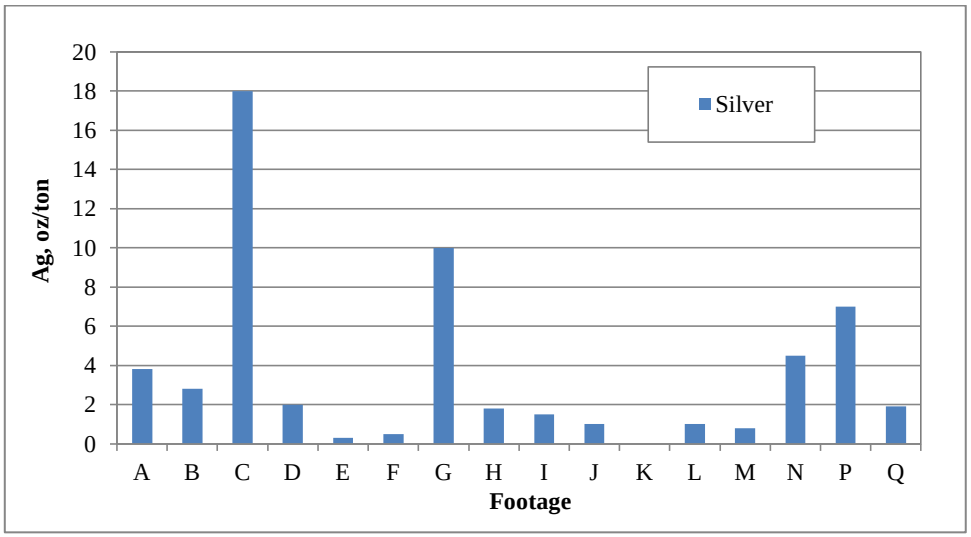

Figure 2.3: Silver content along the same drill hole (after Gasparrini, 1993)

Silver can be found in different geological environments and different ores, where ore is defined as concentrations of minerals that can be exploited for profit. Many silver minerals occur in higher concentrations in hypogene veins, lodes, stockworks and mantos. In addition, it can be present in the supergene zone as secondary silver enrichments, which are near the surface because of the supergene oxidation process (Boyle, 1968). Other occurrences of silver are in copper shales and lead sandstones, in copper-nickel deposits, silver deposits from the tertiary age, and placer deposits (Gasparrini, 1993).

❖ ***Comparison between silver and gold mineralogy***

Silver mineralogy is more complex than gold mineralogy, as stated by Gasparrini (1993), because silver ores typically contain at least five different silver-bearing minerals per deposit while gold deposits usually have only two gold-bearing mineral per deposit. Gold is typically present in stable minerals whereas silver can be present in unstable minerals, i.e. minerals that can modify due to the environmental conditions present in the deposit, making the identification of silver-bearing minerals and the deportment of silver challenging in comparison to gold. Table 2.1 highlights the differences between silver and gold mineralogy. Gasparrini (*op. cit.*) also commented that gold has been more widely studied by researchers than silver; therefore its mineralogy is better understood. Protocols for studying gold mineralogy are discussed in other sections of this chapter. As a comparison, for gold, there are established methods for classifying its process response (such as the definition of refractory gold ores). In contrast, silver process mineralogy is more complex because it is more difficult to quantify, has less well developed methodologies to characterise it and has no established method to classify its process response.

Zhou (2010) also commented on the complexity of silver mineralogy and added that while there are over 60 silver-bearing minerals that contain a considerable amount of silver, only around 20 of them have sufficient economic value to justify recovery through metallurgical processes. *Appendix A* shows the list of more than 200 silver-bearing minerals.

Table 2.1: Differences between gold and silver mineralogy (After Gasparrini, 1993)

Silver	**Gold**
Lower price in stock market	High price in stock market
Higher quantities in ores	Low quantities in ores
Very large number of minerals	Limited number of minerals
Many very common minerals	Native gold / electrum are common minerals
At least 5 or 6 silver-bearing minerals per deposit	Usually two mineral per deposit
Very large-sized grain in minerals	Fine mineral grain size
Unstable minerals	Stable minerals

2.2.2 Different types of silver occurrences

Silver-bearing minerals can be classified into eight groups (Au-Ag alloys, sulphide, selenide, antimonide, telluride, sulphosalts, halide and silver in solid solution), which also can be divided into two different groups: microscopic silver (visible silver) and sub-microscopic silver (invisible silver). Figure 2.4 illustrates some examples of visible and invisible silver.

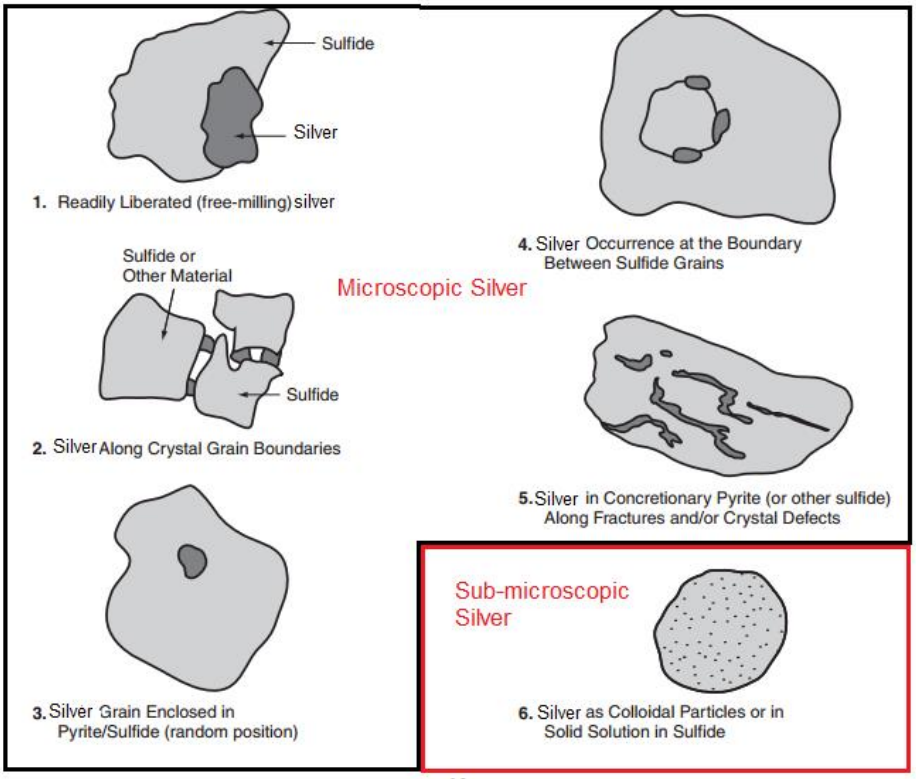

Figure 2.4: Schematic figure of various types of silver as microscopic and sub-microscopic forms (after Marsden and House, 1992)

2.2.2.1. Silver-bearing minerals

Silver can be found in the native form in nature, or it can be associated with a wide range of elements, mainly with gold, copper, lead and zinc and sulphur in different amounts. Silver minerals can be grouped into eight different categories, which are described below:

- **Au-Ag alloys**

This group comprises the Au-Ag alloys, which are kustelite (>50%Ag) and electrum (25-50%Ag), where the amount of silver varies. Native gold (0-15%Ag) and native silver (90%≥Ag) are also part of this group. It is important to note that Ag can form a solid solution series (SS) with Au and Cu because they belong to the same group in the Periodic Table. Examples of the variations of SS that can form in the Ag-Au-Cu system were presented by Allan and Woodcock (2001). Figure 2.5 shows some Au-Ag alloys that are part of this system, with electrum and kustelite being the most notable Au-Ag alloys here. Some Au-Cu alloys are represented as well.

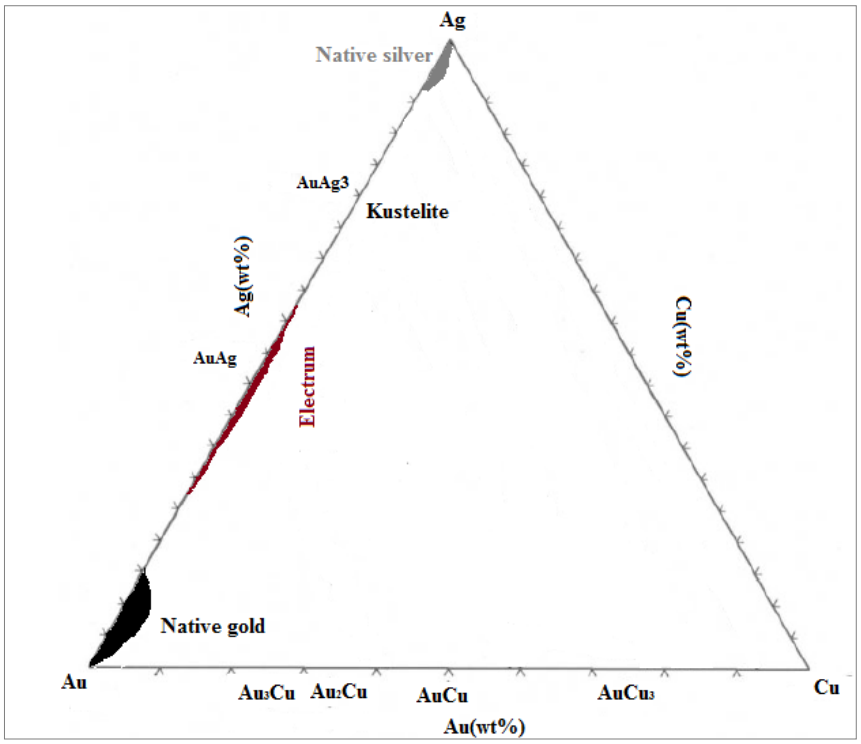

Figure 2.5: Ternary diagram of the gold-silver-copper system (after Allan and Woodcock, 2001).

- **Silver sulphides**

Silver sulphides are mainly represented by acanthite or argentite; both present the same chemical formula of Ag_2S. However, the difference between them arises from the temperature of formation, with acanthite being the stable form of this silver sulphide at normal temperature (Gasparrini, 1984A; Klein, 2002). Dana (1963) also commented that acanthite is the main silver mineral of all silver-bearing minerals.

- **Halides**

The halide group is represented by chlorargyrite or cerargyrite (AgCl), bromargyrite (AgBr) and iodyrite or iodargyrite (AgI). These minerals occur as secondary products in altered or weathered portions of some silver deposits.

- **Silver sulphosalts**

In the group silver sulphosalts, the most common minerals are pyrargyrite (Ag_3SbS_3), freibergite ($(Ag,Cu,Fe)_{12}(Sb,As)_4S_{13}$), tetrahedrite ($(Cu,Fe)_{12}Sb_4S_{13}$), and tennantite ($(Cu,Fe)_{12}As_4S_{13}$). The formulae for the last two minerals does not contain Ag however silver can occur in the lattice. Freibergite, tetrahedrite and tennantite minerals are also called fahlores, because the presence of these minerals can assist in determining the temperature of ore formation (Sack and Brackebusch,

2004). Figure 2.6 illustrates the different spectra (A, B and C) for tetrahedrite, showing the variability of those that can be found in nature, with D representing the pyrargyrite spectrum.

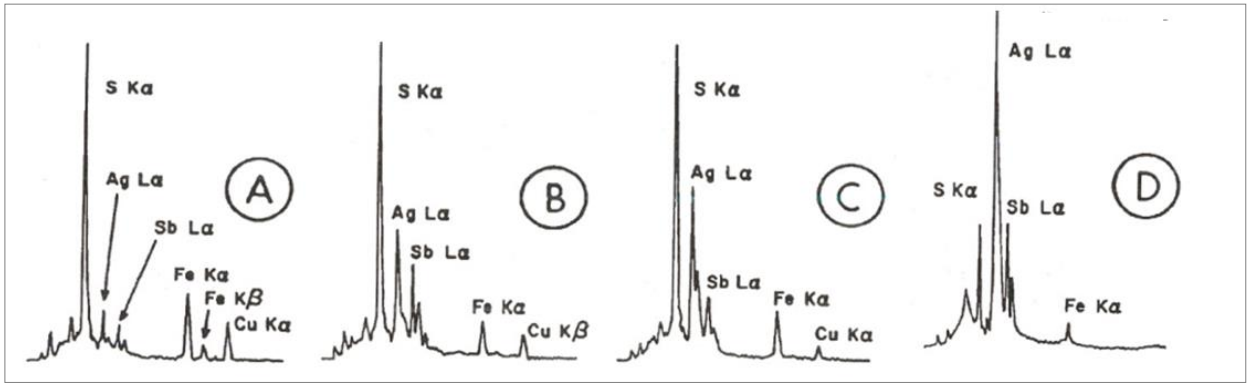

Figure 2.6: A, B, C X-ray spectra for tetrahedrite and D X-ray spectrum for pyrargyrite (from Gasparrini, 1993)

An example of the formation of a series of silver bearing minerals is shown Santo Niño vein (Figure 2.7), which represented a quaternary system of Ag_2S-Sb_2S_3-As_2S_3-Cu_2S. This system represents the series of silver minerals that can occur starting with the precipitation of tetrahedrite with chalcopyrite (represented by Number 1 in Figure 2.7) and then with pyrargyrite and polybasite (Number 2). Subsequently, stephanite (Number 3) is associated with polybasite as a psudomorphic replacement. To finally, minor amounts of acanthite (Number 4) appears as intergrown with pyrargyrite (Gemmell *et al.*, 1989).

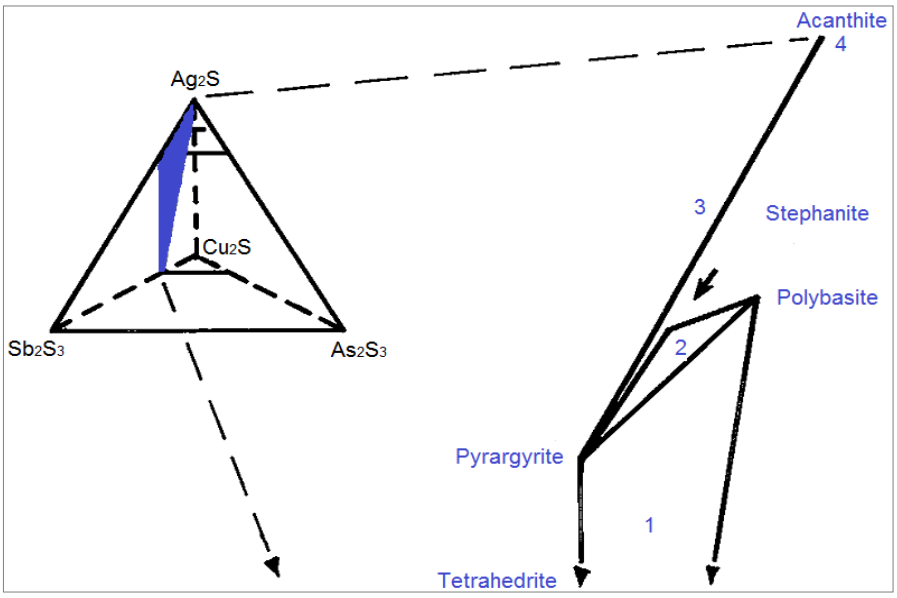

Figure 2.7: Quaternary system Ag_2S-Sb_2S_3-As_2S_3-Cu_2S at Santo Niño vein. The numbers indicate the sequence of minerals corresponding to precipitation from the systems [(Cu,Ag) (Fe,Zn)-Sb-S; Cu-Ag-Sb-S, Ag-Sb-S], [Cu-Ag-Sb-S; Ag-Sb-S], [AgSb-S; Ag-S], and [Ag-S]. (after Gemmell *et al.*, 1989)

- **Silver Tellurides**

The telluride silver group includes hessite (Ag_2Te), empressite (AgTe), stutzite ($Ag_{5-X}Te_3$), petzite (Ag_3AuTe_2) and sylvanite ($(Au,Ag)_2Te_4$). This group is highly associated with Au and sulphides. Hessite is the most common silver telluride found in nature.

- **Selenides**

An example of the silver selenide group is naumannite (Ag_2Se), which can be found associated with quartz and carbonates in hydrothermal veins.

- **Antimonides**

The silver antimonide group is represented by dyscrasite (Ag_3Sb), which can be found mainly in hydrothermal Ag deposits.

- **Silver in solid solution (SS)**

Special attention is required when silver ores contain galena, chalcopyrite, sphalerite, pyrite and other sulphide minerals because silver can be present in those species as SS. The reason that Ag may be present as SS with sulphides comes from the fact that the silver cation can replace iron, manganese, zinc, palladium, nickel and cobalt (Gasparrini, 1984A), making a series of solid solutions with the sulphide minerals mentioned.

SEM images of some silver bearing minerals are shown in Figure 2.8 (SEM images of tellurides) and Figure 2.9 shows (reflected light micrographs showing a number of silver minerals).

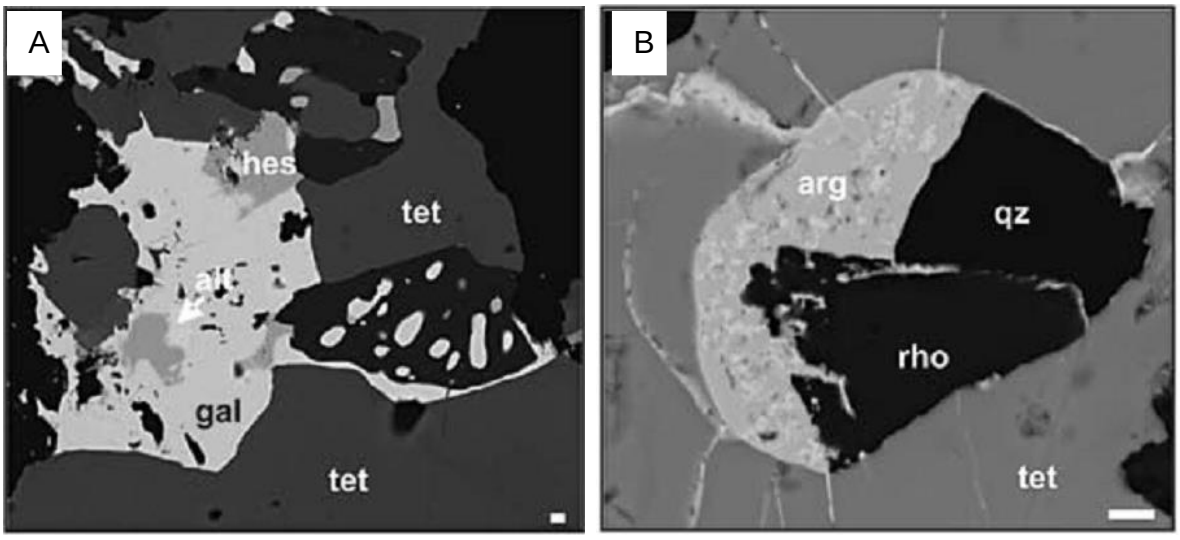

Figure 2.8: A and B are SEM images of telluride occurrences from Rosia Montana. Symbols: hes: hessite, tet: tetrahedrite, alt: altaite, gal: galena, arg: argyrodite, qz: quartz, rho: rhodochrosite (from Tamas *et al.*, 2006)

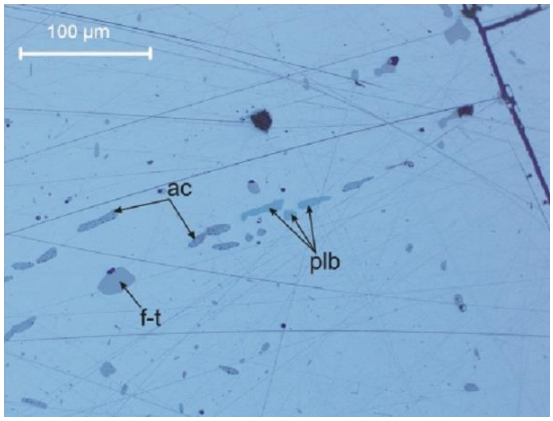

Figure 2.9: A reflected light photomicrograph from Pfunderer Berg. Symbols: ac: acanthite, f-tet: freibergite-tetrahedrite (SS), plb: polybasite (from Krismer *et al.*, 2011).

2.2.2.2. Microscopic and sub-microscopic silver

Silver can be described as microscopic or sub-microscopic depending on whether the minerals are visible under a microscope (Zhou, 2010; Di Prisco *et al.*, 2002; Chryssoulis *et al.*, 1985). A wide range of silver minerals can be classified as microscopic, namely: native silver, electrum, kustelite, acanthite, freibergite and others described in Table 2.2.

Sub-microscopic, or invisible, silver is defined either as very fine inclusion of silver minerals or as silver in solid solution. Silver is commonly found in solid solution with galena, sphalerite, pyrite, bornite, chalcopyrite, covellite, tetrahedrite and tennantite (Zhou, 2010; Di Prisco, *et al.*, 2002).

Table 2.2: Classification of silver by nature and carriers (after Zhou, 2010)

Form	Microscopic Silver	Sub-microscopic Silver
Nature	Visible under microscope, i.e. Scanning electron microscope (SEM)	Invisible under microscope, i.e. Scanning electron microscope (SEM)
Carriers	Native silver, silver-gold alloys, silver sulphides, silver tellurides, silver selenides, silver antimonides, silver sulphosalts and silver halides	Present in galena, sphalerite, pyrite, bornite, chalcopyrite, covellite, tetrahedrite, tennantite, boulangerite, bournonite, arsenopyrite, manganese oxide and kaolinite

2.2.2.3. Stability of silver minerals

Silver minerals can show some degree of vulnerability when being processed, even at normal temperature, pressure and humidity. According to Gasparrini (1993) this is primarily due to the chemistry of silver. As discussed in Section 2.1, silver is part of group 1-B in the Periodic Table and the electronic configuration of the elements in this group plays an important role in the formation of different minerals, and the occurrence of SS with other elements. Gasparrini (*op. cit.*) states: "(t)hey decompose even at normal temperature-pressure conditions: exposure to light, small variations in temperature, atmospheric pressure and humidity are all factors which may alter their chemical

structure", i.e., silver minerals can modify their chemistry due to the environmental conditions. Some silver minerals may show dissolution and redeposition phenomena when they are processed (grinding) or mounted (sample preparation for mineralogical studies) (Gasparrini, 1993 and Chen *et al.* 1988). There are some well-known silver minerals that present difficulties with their stability when they are being processed, for example native silver, electrum and acanthite, making them difficult to work with.

2.2.3 Different silver deposits

Ore deposits may be classified based on the element content of the deposit, the structure of the deposit, ore association, or the interpretation of the processes that control the genesis of the deposit (McQueen, 2005). The genesis of the ore is the most accepted classification by geologists. It includes the elemental composition, mineral distribution, size, shape, and orientation, as well as mineral association. Figure 2.10, from McQueen (2005), illustrates a classification of the genesis of all ore types, namely magmatic, metasomatic, hydrothermal, epigenetic, exhalative-diagenetic, marine sedimentary, residual and supergene, and placer. Note that these deposits are also subclassified as syngenetic (formed with the enclosing rocks) or epigenetic (introduced into pre-existing rocks).

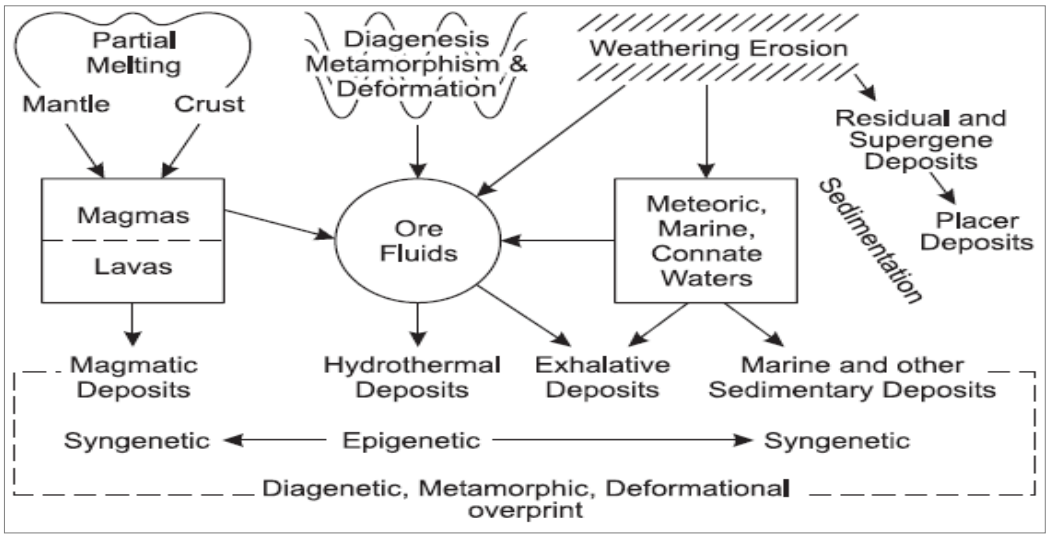

Figure 2.10: Streamlined genetic classification of ore deposits (from McQueen, 2005).

Following this genetic classification, Graybeal and Vikre (2010) described four silver-rich genetic groups, specifically mentioning volcanogenic massive sulphide (VMS), sedimentary exhalative (SEDEX), magmatic-hydrothermal (MH) and lithogene. Table 2.3 describes the geology, metal association and examples of mineral deposits for each one.

Special emphasis applies to the MH deposits on the American continents (especially because the ores used in this thesis are from Minera San Cristobal, which is classified as a magmatic-hydrothermal deposit), which comprise three deposits types: vein, disseminated and carbonate-hosted massive sulphide. Graybeal and Vikre (2010) identified the main alteration mineral assemblages in these types of deposits as:

• High sulphidation: alunite, pyrophyllite, diaspore, kaolinite, silica.
• Low sulphidation: quartz, carbonate, adularia, sericite, epidote.
• Carbonate-hosted massive sulphide: intrusions; replacing permeable carbonate rocks.

Table 2.3: Features of silver-rich genetic groups (after Graybeal and Vikre, 2010)

Genetic group	Geology	Metal associations	Examples of mineral deposit
VMS	• Massive sulphides are syngenetic • Ag (and Au) grades higher where felsic volcanic rocks abundant and boiling occurs; related magmas are primitive • Silver leached from rocks under and adjacent to deposit • Phanerozoic deposits are highest grade on average	Ag-Pb-Zn-Cu-Au	Brunswick 12, Kidd Ck, Greens Ck, Eskay Ck, Hackett River*
SEDEX	• Confined to rift basins, continental margins. Ag leached from rift sequence, transported to basin floor along faults • Form at/near water-rock interface, no igneous or volcanic activity	Ag-Pb-Zn	Broken Hill, Cannington, Mt Isa, Century, Red Dog
MH	In mountain belts above subduction zones, main styles of deposits are vein, disseminated, carbonate-hosted massive sulphide	Ag	Cerro Rico, Guanajuato, Pachuca, Imiter, Ducat, Rochester, Pirquitas, Preciosa*, Fuwan*
		Ag-Au	Comstock, El Peñon, Tonopah, Tayoltita, Coipa, Pascua Lama*, Diablillos*, Palmarejo*, Dolores*
		Ag-Pb-Zn-Cu-Au	Cerro de Pasco, Fresnillo, Peñasquito*, Zacatecas, Huaron, Creede, Casapalca, Leadville, Tintic
		Ag-Pb-Zn	Real de Angeles, Hardshell, Morococha, Sta Eulalia, Pitarrilla*, **San Cristobal*,** Navidad*, Corani*
		Ag- Cu	Equity, Butte veins
Lithogene	Epigenetic; disseminated, veins. Metal leached from rift fill and other rocks by evaporated brines, connate water during compaction, metamorphism.	Ag	Malku Khota *
		Ag-Pb-Zn	Coeur D'Alene, Prognoz, Keno Hill, Ying*
		Ag- Cu	Lubin, Rock Ck – Troy, Cd'A Ag Belt, Dikulushi*
		Ag-Co-Ni-U	Cobalt, Falea*

*New discoveries

Table 2.4 presents a summary of MH group types of silver deposits and the silver minerals present in South America.

Table 2.4: Summary the MH group of silver deposit types and silver minerals present in South America (from Smith, 1988)

Type of deposit	Silver minerals	Comments
Disseminated	Sulphides and sulphosalts	Original hypogene ore at economic silver grade (4.4 kg/t). Can also have local added value from later alteration*. Silver minerals mainly silver sulphides and sulphosalts.
Vein	Sulphides and sulphosalts	Original hypogene ore at economic silver grade (62.2 kg/t). Can also have local added value from later alteration*. Silver minerals mainly silver sulphides and sulphosalts.
Carbonate-hosted massive sulphide	Native silver and chlorargyrite (cerargyrite)	Original carbonate-hosted massive sulphide deposit with silver grade of 7.9 kg/t. Silver minerals present are native silver and chlorargyrite.

*By processes of oxidation, leaching, and/or supergene enrichment

Figure 2.11 illustrates all of the MH deposits worldwide, with all large MH silver deposits (more than 500 Moz) restricted to the eastern side of the Pacific Rim (EPR).

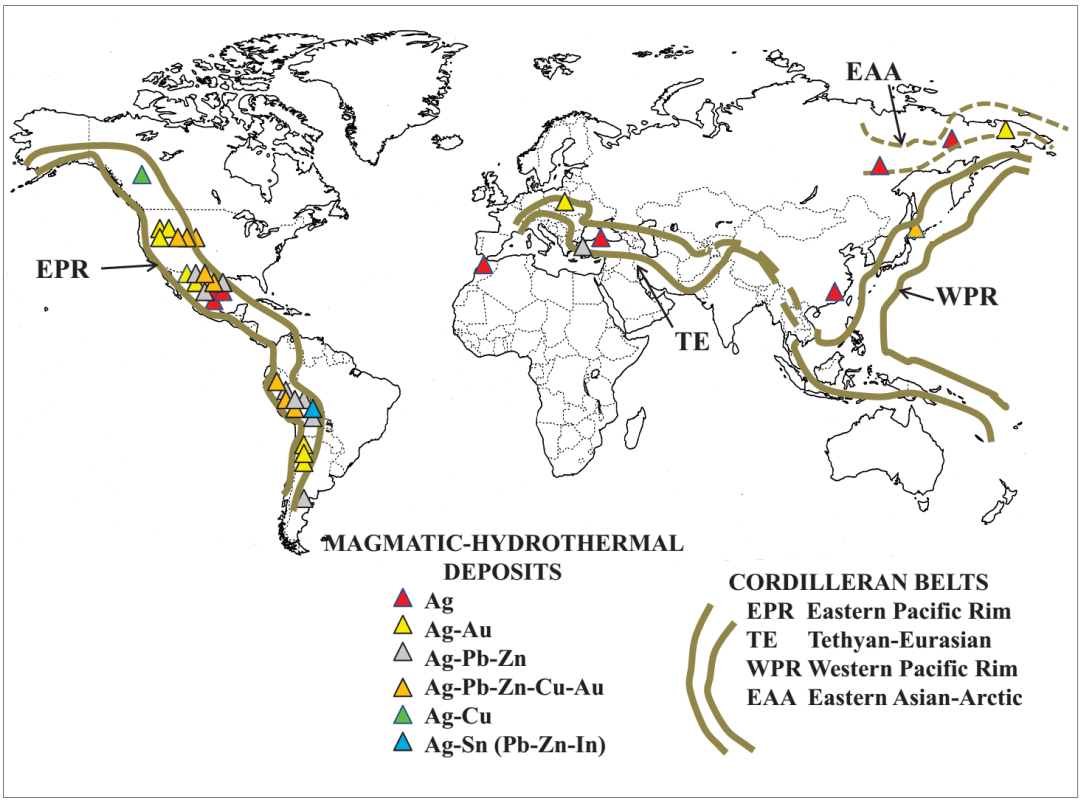

Figure 2.11: Magmatic-hydrothermal deposits worldwide (from Graybeal and Vikre, 2010)

At the Chañarcillo deposit, located in the north of Chile, Warnaars *et al.* (1987) studied three types of silver mineralisation (fissure vein, manto and disseminated), where the main silver production was from the supergene and hypogene zones of the open pit. In the supergene zone native silver, chlorargyrite, silver amalgam, and silver halides were found, while in the hypogene zone stephanite, acanthite, stromeyerite and pearcite-polybasite were observed.

A range of authors have studied the Mexican deposits, which for many years have been the world's leading producers of this commodity. For example, Wandke and Martinez (1928) studied the Guanajuato mining district; the ore there presented disseminations and bands of silver and gold minerals with a quartz-carbonate gangue. The minerals present were sulphides and silver sulpho-antimonides as trace minerals, with some galena, sphalerite and chalcopyrite. Stone and McCarthy (1942) and Cserna (1976) investigated the mineral and element variations in the veins of Fresnillo. The minerals present in these deposits were pyrargyrite, with lesser acanthite, proustite, miargyrite, polybasite, tetrahedrite, galena, sphalerite, and chalcopyrite.

- **Common non-sulphide and sulphide gangue minerals present in silver deposits**

Taggart (1945) and Boyle (1968) described the common non-sulphide and sulphide gangue that can be found in silver deposits. They concluded that quartz, carbonates and barite are the most common. An in-depth study was made by Marley and Hagni (1982), who studied eight Mexican deposits, concluding that quartz was the dominant non-sulphide gangue present in a wide range of ores studied.

2.3 Defining refractory ore

'Refractory' is a term widely used for gold ores, and is strongly related to the amount of gold recovery that can be achieved through the cyanidation process (leaching process). The most commonly used definition states "ores may be termed refractory if they yield inadequate gold extraction by direct cyanidation" (Adams, 2005; Marsden and House, 2006; Dunne *et al.*, 2009; Zhang *et al.*, 2010). However, Collins *et al.* (2013) also commented that "gold that cannot be recovered satisfactorily by conventional gravity concentration or direct cyanide leaching is classified as refractory". Double refractory ores arise basically when gold ore contains sulphides and carbonaceous matter. Table 2.5 shows the classification made by La Brooy *et al.* (1994) for the results obtained through cyanidation using the bottle-roll method.

Table 2.5: Definition of gold refractory ores (La Brooy *et al.*, 1994)

Recovery %	Classification*
< 50 % recovery	Highly refractory
50 – 80 % recovery	Moderately refractory
80 – 90 % recovery	Mildly refractory
90 – 100 % recovery	Non – refractory (free milling)

*Bottle-roll based definition with cyanidation

In terms of silver mineralogy, Leaver and Woolf (1939) commented that silver minerals are also classified as refractory, through the behaviour that they present during cyanidation, while Dorr and Bosqui (1950) attributed this concept to ores that contain manganese minerals. Hause and Hill (1994) used the term, refractory, for small grains of silver minerals present in gangue.

Zhou (2010) claimed the existence, from his own experience, of refractory silver minerals, which he said were pyrargyrite, proustite and stephanite, because the presence of these minerals in an ore causes a decrease in the recovery of silver and other valuable elements present in the ore. He did not mention any particular process for recovery but it is assumed (based on previous work) that he refers to cyanidation.

A systematic approach for defining the refractory nature of gold ores exists (Guay, 1981; Hausen, 1982; Ramadorai, 1991); no such approach exists for silver ores. Therefore, there is an opportunity to adapt the concept of refractoriness to the context of Ag ores.

2.4 Mineralogical characterisation

2.4.1 Techniques used for mineral characterisation

A wide range of micro analytical techniques exists that can be used to examine an ore. During the 1980s, Gasparrini (1984A) noted that optical microscopy and electron microprobe (EMPA) were the techniques used for studying silver carriers in an ore, being that the optical properties were the most important features for the identification of silver deportment at that time. Currently, advanced microscopic techniques provide detailed quantitative information of the minerals present in the ores, directly analyse the structure and composition of the ore, and quantify the key mineralogical attributes (such as modal mineralogy, deportment of the elements, and textures, among other relevant attributes).

Factors that affect the identification of silver minerals are mainly the grain size of the silver minerals (Gasparrini, 1993; Zhou, 2010), textures present in the ore and the detection limits of each microscopic technique used in the mineralogical characterisation (Knights and Patterson, 1988; Basto *et al.,* 1995). In the following paragraphs the techniques used in the present study are described. It is also necessary to comment that there are other micro analytical techniques, which are outside the scope of this work, for example, Sensitive High Resolution Ion microprobe analysis (SHRIMP), Proton induced microprobe (μ-PIXE), among others.

- **Optical microscopy**

Optical microscopy has been used for over 150 years in the field of geology, involving the examination of polished sections to visually identify minerals. It is used to provide information for a sample, including: bulk mineralogy, the identification of grain size, particle compositions and textures (Jones, 1987; Evans, 2010). It requires an expert mineralogist to properly characterise and identify the minerals using the optical properties of the sample, such as reflectivity, colour, hardness, and cleavage, among others. The limit of resolution is from about 5 μm down to 0.5 μm for gold as liberated particles or inclusions, using a magnification of 500x (Zhou *et al.*, 2004).

- **X-Ray Diffraction (XRD)**

X-Ray Diffraction is used to identify minerals, providing information on the minerals present in both qualitative and quantitative terms. Generally, XRD is used to support the identification of gangue minerals present in ores. It uses the unique crystal structure of minerals and is able to unambiguously identify a mineral in a bulk or pure mineral sample (CSIRO, 2011). The limitation of this method is its inability to quantify trace minerals present, because the minimum amounts that can be detected vary between 1 to 5% (Petruk, 2000).

- **Scanning Electron Microscopy (SEM)**

Scanning Electron Microscopy is used in many areas due to the extremely detailed high-resolution images of the surface and near-surface that it can quickly provide (Kohli and Mittal, 2011). When fitted with Energy Dispersive X-ray Spectroscopy (EDS) detectors, SEM's can be used to determine the chemical composition of the materials being studied (Reed, 2005). The back-scattered electron intensity (BSEI) is related to the average atomic weight (mean atomic number) of the material being studied and may be used to differentiate phases if it differs sufficiently. The SEM can be operated manually or automatically.

Figure 2.12 presents a diagram of an electron beam interacting with the sample surface, and the emissions that result from that interaction. These include Auger electrons, X-rays, secondary electrons (SE) and back-scattered electrons (BSE). These emissions provide information about chemical and topographical features and composition of the material being studied. The interaction of the electron beam with the sample surface results in an interaction volume, which is tear-drop in shape and the size of which depends on the e-beam voltage and the atomic weight of the material being studied.

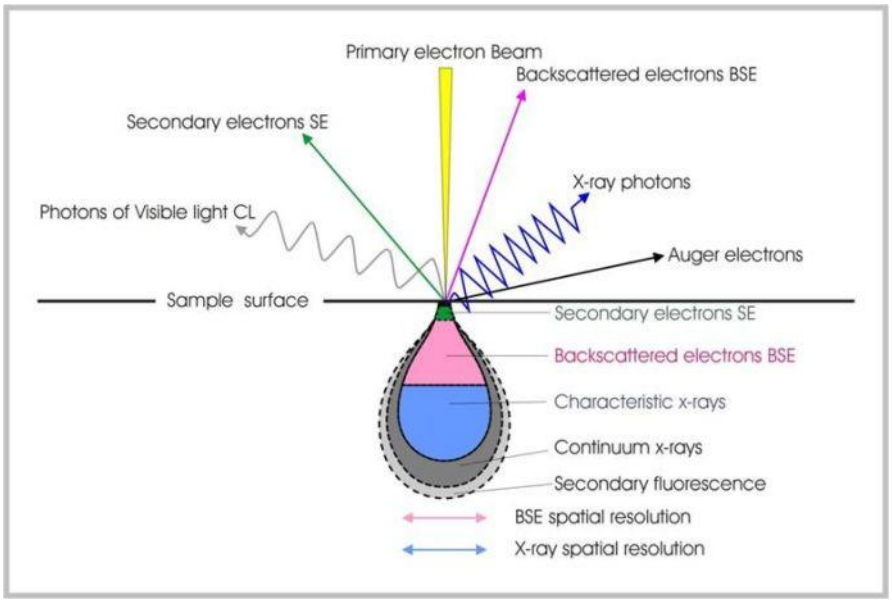

Figure 2.12: Signals emitted through interaction of an electron beam with a solid (After Viljoen and Johnson, 1983)

- **SEM-based automated mineralogical systems**

Automated mineralogical systems are used widely in process mineralogy and mineral characterisation. They can measure key mineralogical attributes in a few hours, such as modal mineralogy, grain size, association and liberation of minerals (Jones and Gravilovic, 1970; Gottlieb *et al.*, 2000; Petruk, 2000; Gu, 2003; Lastra, 2007). *SEM-EDS* are equipped with commercial software that controls the SEM-EDS, making it automatic. There are two well-known software] ucts used worldwide – Quantitative Evaluation of Minerals by Scanning Electron Microscopy (QEMSCAN) and Mineral Liberation Analyser (MLA).

- **Electron microprobe analysis (EMPA)**

Electron microprobe analysis (EMPA) is the most mature of the micro beam analysis techniques, providing quantitative analyses for small areas of polished samples (Reed, 2005). Generally, this method is considered the most useful for the analysis of major and minor elements within a sample, with an accepted minimum detection limit (MDL) for trace elements by wavelength dispersion in the order of 100 ppm (Newbury *et al.*, 1986; Goodall and Scales, 2007; Zhou, 2010). This method is used primarily to quantify the chemical composition of minerals.

- **Laser Ablation Inductively Coupled Plasma Mass Spectrometry (LA-ICP-MS)**

Laser Ablation Inductively Coupled Plasma Mass Spectrometry is used mainly for trace element analysis and for quantification of elements in sulphides (SS), silicates, oxides, carbonates and

phosphates with a detection limit down to around 2 ppm for Au. (Watling *et al.*, 1995; Chryssoulis *et al.*, 2004).

- **Synchrotron- based techniques**

The synchrotron is the most advanced *in-situ* and non-destructive microscopic technique that can be used to identify atomic interaction between minerals and to identify low concentrations of trace elements, being an X-ray source technique. It is often used in combination with X-ray fluorescence (SXRF) for mapping elements in the sample, X-ray photo spectroscopy (SXPS) for analysis of the surface, and X-ray diffraction (SXRD) to identify trace minerals present in samples, along with other techniques, and can significantly improve the analytical sensitivity of those techniques. "Synchrotrons offer a high-brilliance, linearly polarised beam of X-rays, with the possibility of tuning the excitation energy by using a suitable monochromator thus improving significantly the analytical sensitivity … the synchrotron X-ray beam also provides an efficient means of in-situ non-destructive microanalysis, making possible the study of minute samples and the mapping of the analyte" (Basto *et al.*, 1995).

- **Synchrotron XRF (SXRF)** is a highly sensitive technique for chemical analysis, with a range of minimum detection limits from a few parts per million by weight to tens of parts per billion (ppb) for heavy elements dispersed in light matrices. It is used in the assessment of major, minor and trace elements in ores, minerals and rocks, according to Figueiredo *et al.* (1993).
- **Synchrotron XRD (SXRD)** is a method for resolving crystal structures. When SXRD is being used sufficient grains need to be present to show continuous diffraction rings as is shown in Figure 2.13. This indicates that there is a statistically significant number of grains scattering from a 'powder' diffraction pattern (Withers, 2013). Figure 2.13a shows a SXRD which does not represent the pattern of continuous diffraction rings, demonstrating that not enough grains are measured.
- **X-ray absorption near edge spectroscopy (XANES)** is a method that is used to complement the SXRF and SXRD analysis to verify the phases present in the materials evaluated by both techniques mentioned below (Fan and Gerson, 2014).

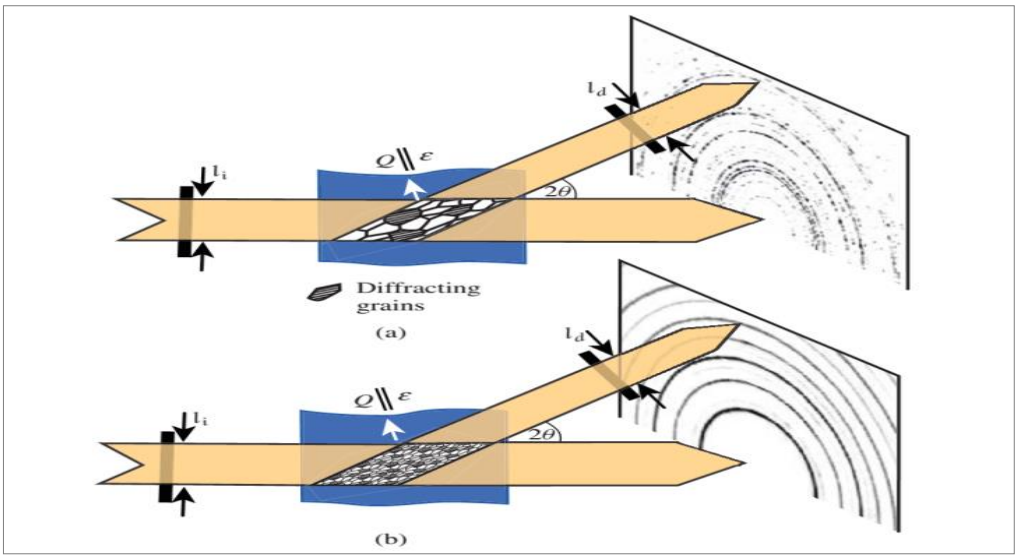

Figure 2.13: Diffraction patterns that can be obtained through SXRD (from Withers, 2013)

The information given by the use of these techniques is shown in Table 2.6.

Table 2.6: Information gained by analytical techniques (from Lamberg, 2011)

Analytical technique	Level of information
Chemical Assays	Elements
MLA/QEMSCAN	Minerals
XRD	Minerals
Mineral conversion	Minerals
EMPA	Elements, minerals
LA-ICP-MS	Elements, minerals
MLA analysis	Elements, minerals, particles
Synchrotron – based methods	Elements, minerals

2.4.2 Key mineralogical attributes

1. **Modal mineralogy:** the relative proportions of minerals present in an ore. Mc Arthur (1996) described the traditional method to measure this as point counting using optical microscopy methods. Currently, the newer methods, such as QEMSCAN, MLA and Quantitative X-Ray Diffraction (QXRD), allow the measurement of modal mineralogy "using a quantitative and unbiased approach" (Bonnici, 2012). QEMSCAN/MLA in some modes uses the point counting approach, in others a different basis is used.
2. **Elemental deportment:** indicates the minerals in which the valuable element is present and what proportion of the total elemental concentration is accounted for by those minerals.
3. **Textures of ores:** According to Bojcevski (2004), texture is closely related to mineral liberation of the ores. There are three different scales that describe texture: macro (ores are at scale of Km-m), meso (ores are at scale of m-cm) and micro (ores are observed at the scale of micrometres – examples of these micro-textural characteristics include mineral grain size and

mineral association). For metallurgists, micro-textures are the most relevant of the textures for consideration of processing properties.

Butcher (2010) and Evans (2010) noted that, in an ore more than one texture may be present with varying deportment of valuable elements. Figure 2.14 illustrates an example of different micro-textures where copper may occur in ores given by Butcher (2010), i.e. copper can be present as chalcopyrite inter-grown with pyrite, discrete native copper, chalcocite rimming pyrite, or others as shown in the figure.

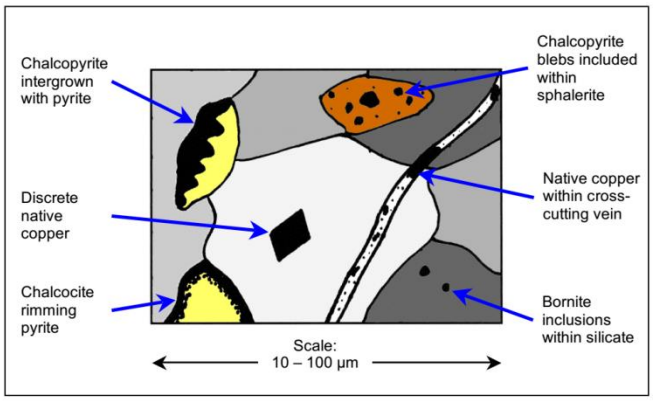

Figure 2.14: Various copper minerals and the textures that may be present in an ore (from Butcher 2010 and modified by Evans, 2010)

Texture also considers grain size and mineral association because together they largely describe the texture of ores.

- ***Grain size:*** As stated by Craig (2001), "(i)t is important to note that size of grains is vital in interpreting growth histories of ores and in predicting the degree of liberation and potential recovery of minerals during processing".

- ***Mineral association:*** describes how the boundary of a mineral is shared with other minerals. These associations have a direct impact on the potential liberation of the target minerals, and therefore on flotation and recovery (Petruk, 2000; Bojcevski, 2004; Goodall and Scales, 2007; Becker *et al.*, 2008).

Butcher (2010) discussed the basic textures that have some influence in flotation – these are equigranular and inequigranular. Also, complex textures have influence on the processing to liberate the valuable minerals, for example: "rims, disseminated inclusions (or exsolutions), or as interstitial phases – as this will control breakage mechanisms during blasting, crushing and grinding (intragranular versus intergranular), and will make it either relatively easy, or difficult (or impossible) to liberate and float effectively" (Butcher, 2010). Figure 2.15 shows the basic and complex textures that affect the processing of the ores.

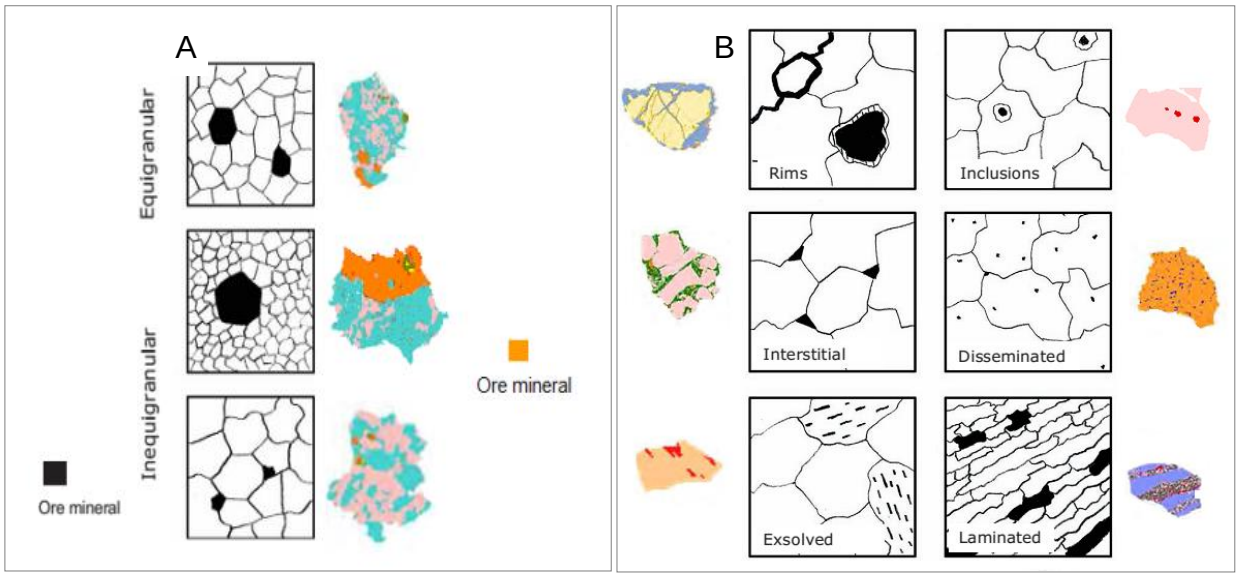

Figure 2.15: A) basic textures; B) complex textures present in an ore that influence processing (after Butcher, 2010).

4. **Degree of liberation:** The degree of particle liberation is a function of the grade and distribution of particles that contain the valuable mineral. Butcher (2010) commented on the modern techniques used to quantify this. He stated that "the degree of mineral liberation can be quantified using a variety of optical and SEM-based image analysis techniques". Figure 2.16 illustrates an ore that starts as unbroken ore and undergoes crushing and grinding to obtain some degree of liberation.

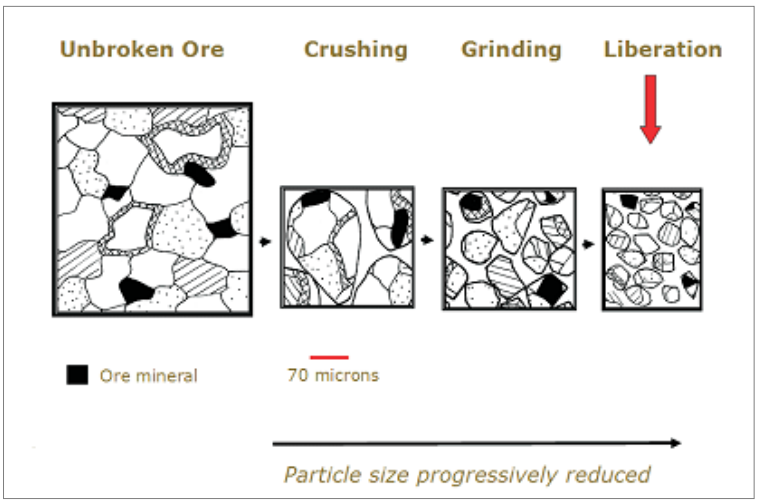

Figure 2.16: From unbroken ore – to obtain liberation of valuable minerals in an ore (from Butcher, 2010.)

Additionally, there is a relationship between the degree of liberation and grain size. The size of grain is crucial on predicting the degree of liberation and therefore the potential recovery of metals during treatment (Craig, 2001). Thus, it is necessary to know the degree of mineral liberation of the feed for complex sulphide ores to design the flow sheet, monitor plant performance and optimise circuits (Johnson and Munro, 2002). They also commented about the ranges of liberation and the

effect on the separation process (Table 2.7) based on their experience with the data and the sulphide flotation process. These numbers will not necessarily be the same for all ores.

Table 2.7: Degree of liberation for minerals of interest (from Johnson and Munro, 2002)

Liberation value for mineral of interest*	Expected or theoretical possible separation process
< 70%	Poor separation results
70% to 80%	Sound of separation results
> 80%	Good separation results

*uncorrected 2D value

The degree of liberation is typically examined by mounting particles into resin and sectioning them to obtain 2D (areal) information (Butcher, 2010). By analysing these particles using optical microscopy or automated SEM, it is possible to classify them into the following groups: liberated particles, binary composites, ternary composites or quaternary composites. This is illustrated in Figure 2.17 where A, B, C and D represent different minerals.

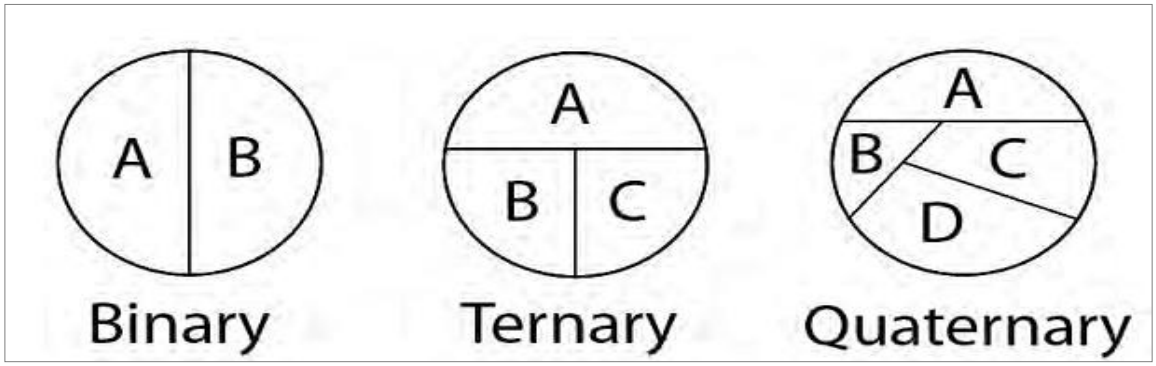

Figure 2.17: Particle compositions for binary, ternary and quaternary composites (from Jones, 1987)

2.4.3 Mineral characterisation for gold

Gold mineralogy has been studied by many researchers including Gasparrini (1993), Chryssoulis *et al.* (2004), Zhou *et al.* (2004), Benzaazoua *et al.* (2007) and Zhou (2013). These researchers have developed well-defined approaches for the mineralogical characterisation of gold. According to Chryssoulis *et al.* (2004), the most common techniques used for gold characterisation are listed in Table 2.8. For bulk mineral analysis, they are EMPA, μ-PIXE and SIMS; and for surface analysis, they are time-of-flight laser ionization mass spectrometry (TOF-LIMS), time-of-flight secondary ion mass spectrometry (TOF-SIMS), vacuum ultra-violet time-of-flight laser ionization mass spectrometry (VUV-TOF-LIMS), vacuum ultra-violet surface analysis by laser ionization (VUV-SALI), and time-of-flight resonant ionization mass spectrometry (TOF-RIMS).

Table 2.8: Techniques most commonly used for gold characterisation (Chryssoulis *et al.*, 2004)

Technique	Type of Analysis
EMPA (EDX/WDX)	Bulk analysis of grains
μ-PIXE	Bulk analysis of grains
SIMS	Bulk analysis of grains
TOF-LIMS*	Surface analysis of grains
TOF-SIMS*	Surface analysis of grains
VUV-TOF-LIMS*	Surface analysis of grains
VUV-SALI*	Surface analysis of grains
TOF-RIMS*	Surface analysis of grains

*TOF-LIMS: Time-of-flight laser ionization mass spectrometry; VUV: Vacuum ultra-violet; SALI: Surface analysis by laser ionization; SIMS: Secondary Ion Mass Spectroscopy; EDX: Energy dispersive X-Ray Analysis; WDX: Wavelength-dispersive X-ray spectroscopy; RIMS: Resonant ionization mass spectrometry (Chryssoulis *et al.*, 2004).

Chryssoulis (*op. cit.*) summarised in Figure 2.18 the detection limits for some techniques used in the characterisation of gold. These techniques can also be used as for silver characterisation.

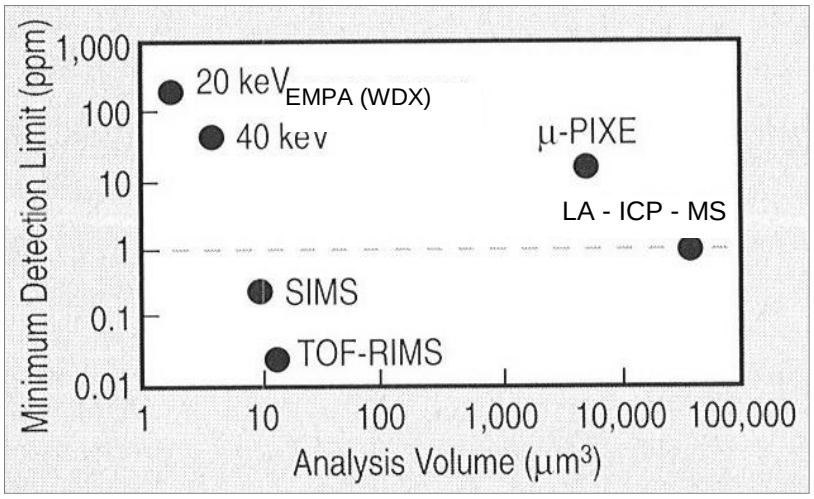

Figure 2.18: Detection limits for some techniques for gold grain measurement and analysis (After Chryssoulis *et al.* 2004).

A well described methodology to follow for gold characterisation is provided by Zhou *et al.* (2004). It starts with sampling, then performing a chemical characterisation, followed by mineralogical characterisation to identify the key mineralogical attributes for gold processing. Figure 2.19 shows the general methodology implemented for gold characterisation.

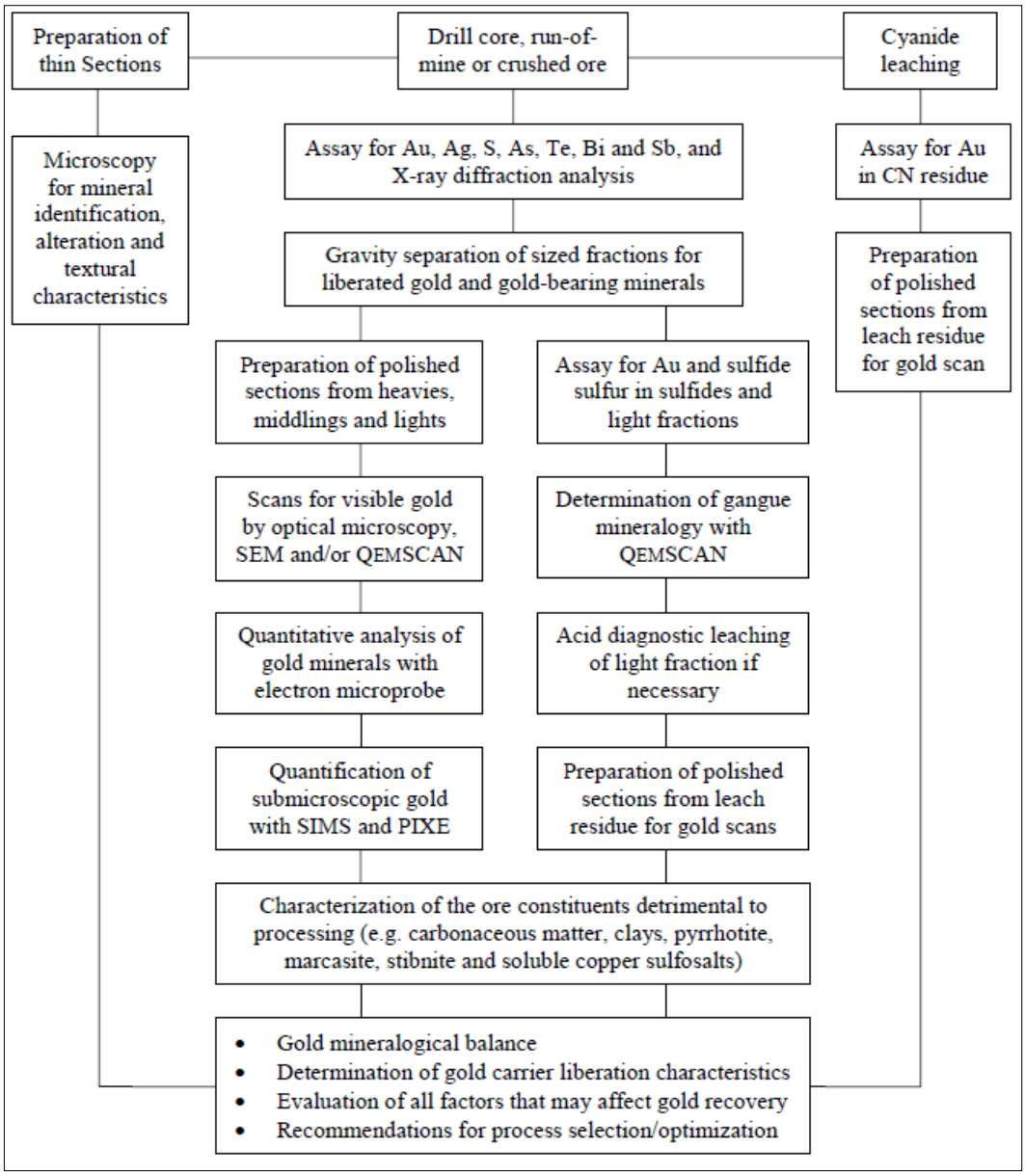

Figure 2.19: Methodology for gold characterisation (from Zhou *et al.*, 2004)

Figure 2.20 illustrates the mineralogical protocol used to find gold association, divided into microscopic and sub-microscopic gold as described by Benzaazoua *et al.* (2007). The following microscopic techniques provide the basis of this methodology: optical microscopy, SEM, EMPA and SIMS.

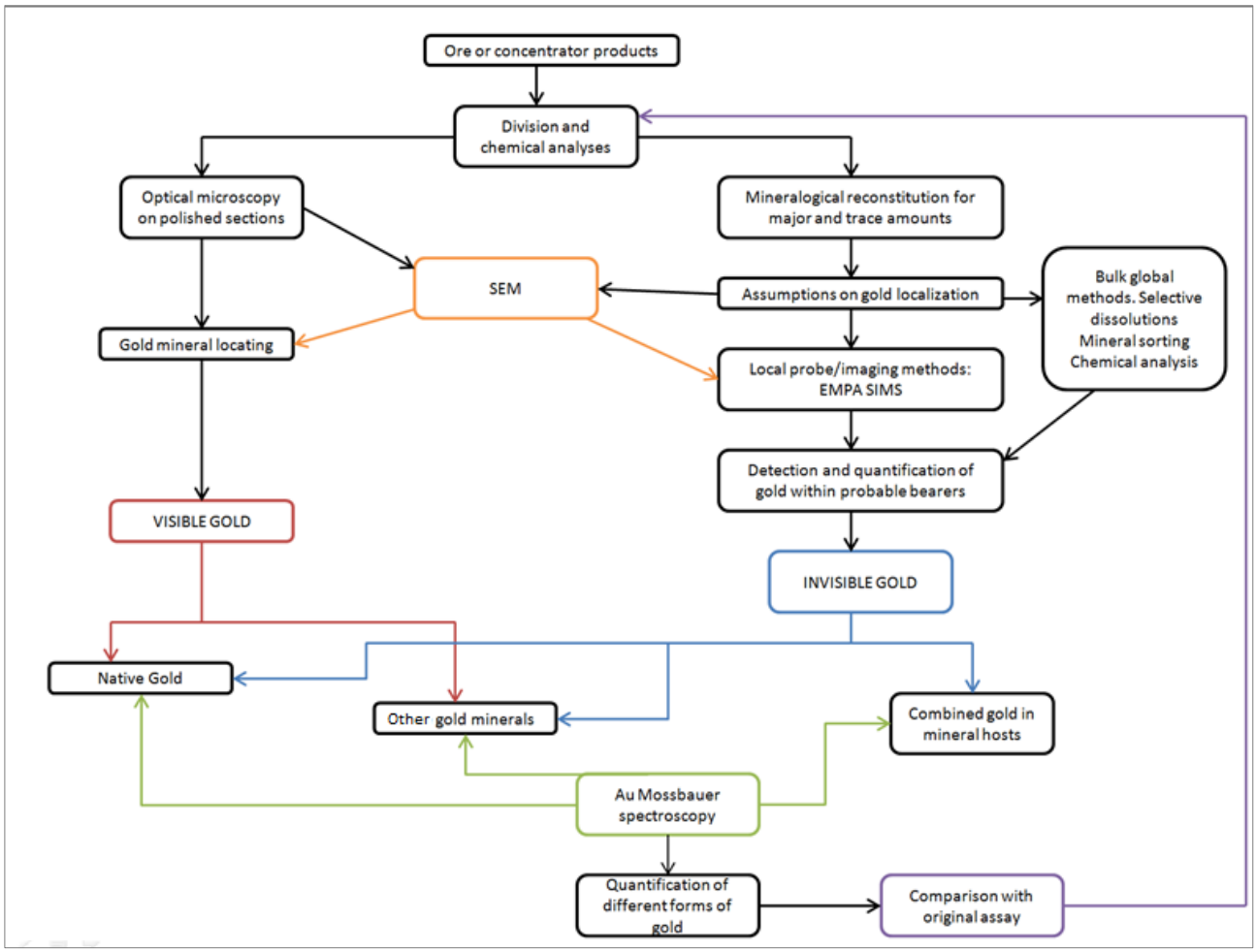

Figure 2.20: Mineralogical characterisation protocols for gold associations (After Benzaazoua *et al.*, 2007)

2.4.4 Mineral characterisation for silver

The mineralogy of silver is more complex than that of gold, as discussed in Section 2.2.1. Although several authors have studied the mineralogy of silver, a systematic approach for the characterisation of silver has not been well defined. This is because silver minerals are complex and time-consuming to identify. Combinations of different techniques need to be applied for each new silver ore, making it impractical to have a strictly defined procedure for silver. A practical framework to systematically characterise silver ores is required.

Many authors have described methods for identifying silver in different contexts; however, a consistent framework for characterisation has not been applied. Petruk (2000) described a number of microscopic techniques that could be used to determine the average level of silver in tetrahedrite, freibergite and tennantite, using microprobe techniques, while for sulphides, such as galena, sphalerite, chalcopyrite and pyrite, the silver content can be determined using PIXE, SIMS and/or LA-ICP-MS. As well, he mentioned that by using point counting and QEMSCAN or MLA, the average weight percentages of the minerals present in the ore could be quantified. Gasparrini's

work provides the most comprehensive description of the implications of silver mineralogy on the mineral processing of silver ores (Gasparrini, 1983; 1984A; 1984B; 1993).

Nevertheless there have been some mineralogical studies performed for different silver mines around the world that apply a mineralogical characterisation method for silver. Some of these are discussed in the following paragraphs.

Cabri *et al*. (1984) performed a trace silver analysis for sulphides from Izok Lake, N.W.T., Canada and from Hilton mine, Mount Isa, Australia, using EMPA and μ-PIXE analysis to determine whether silver was present as dilute solid solutions in the major minerals in these mine sites. Their results concluded that in both mine sites Ag was in solid solution with chalcopyrite.

Gasparrini and Lowell (1985) investigated an ore from the Silvermine District in Missouri, USA, using optical microscopy, SEM and EMPA. Optical microscopy was used at 1250x magnification, while SEM was performed at 12,500x. With these techniques, it was concluded that argentiferous tetrahedrite was present with a range of silver contents, and that one mineral that contained Cu-Fe-Sn-S (mawsonite) was present. EMPA was used to quantify the amount of silver in galena; however, the detection limit of the EMPA (approximately 200 ppm) was insufficient for the measurements and it was concluded that most of the silver was hosted by tetrahedrite.

The ore mineralogy of Real de Angeles was studied by Pearson *et al*. (1988), using optical microscopy and EMPA. The silver was found in solid solution with galena, and other discrete silver minerals were freibergite, stephanite and argentite. Sulphide minerals present were sphalerite and chalcopyrite, and a small amount of pyrite was found in the disseminated ore.

Di Prisco *et al*. (2002) described the Lady Loretta mine as a lead-zinc-silver deposit in the north-west of Queensland, Australia. The mineralogical study was carried out in two phases. The first stage was the determination of silver-bearing minerals using ore microscopy and SEM-EDS microscopy. The second stage was to identify the silver minerals carrying elevated silver. This was determined using EMPA and SIMS. The silver carriers were galena, tetrahedrite, chalcopyrite and pyrite. A similar routine as that used at Lady Loretta was performed by Benzaazoua *et al*. (2002) for Neves-Corvo ore in Portugal. In this case, the routine included an optical microscope (used for mineral and texture identification), SEM (equipped with a microanalysis system), and EMPA (to analyse the chemical compositions of minerals).

These examples demonstrate that the approach used to characterise silver varies widely and there is an opportunity to develop a standard systematic approach to characterise silver in ore deposits.

2.5 Metallurgical process used for silver ores

Silver can be extracted from different sources including: primary silver ores, tailings, from recycling of electronics, or from other origins. Depending of the origin of the silver, there are three possible processes that may be used; these are amalgamation, leaching and flotation. In terms of recovery, silver has largely been obtained as a by-product from gold and base metal sources, such as copper, lead-zinc and cobalt (Carter, 1957; Parashyniak and Phillips, 1978; Shaede *et al.*, 1978; Malhotra and Harris, 1999). In the case of copper ores, silver is separated in the smelter process, followed by refining to produce a silver anode. For lead-zinc ores, the noble metal is recovered as lead bullion, and is then recovered by electrolysis or by other chemical methods.

Gasparrini (1984B) noted that some silver minerals are preferably treated by leaching techniques. For example, native silver, electrum and acanthite are treated by cyanide leaching, while tetrahedrite and pyrargyrite are preferentially treated by flotation. Therefore, when those minerals occur within a same ore, different metallurgical processes may need to be applied to recover silver from that ore. Note that pyrargyrite and other Ag minerals appear in both the leaching and flotation sections of Table 2.9.

There are two important mineralogical attributes that need to be clarified before the appropriate recovery process can be selected. These attributes are: the presence of discrete silver-bearing minerals; and the silver distribution by mineral. This is because different silver-bearing minerals react differently to amalgamation, flotation and leaching agents. Table 2.9 shows various common silver-bearing minerals and the preferred treatment method to recover them.

Table 2.9: Preferred treatments for different silver-bearing minerals (after Woodcock *et al.*, 1976; Marley and Hagni, 1982)

Process	Mineral
Amalgamation	Native Ag
Leaching	Native Ag, chlorargyrite, acanthite, jalpaite, stromeyerite, electrum, miargyrite, stephanite, pyrargyrite, proustite, sternbergite, among others.
Flotation	Native Ag, chlorargyrite, acanthite, polybasite, pyrargyrite, naunannite, aquilarite, guanajuatite, freibergite, sternbergite, Ag in sulphides, among others.

2.6 Froth flotation to recover silver

This research will focus on the froth flotation process, which is used on an industrial scale to selectively separate valuable minerals from non-valuable minerals (Horwood, 1909; Hoover, 1914; Gaudin, 1957; Wills and Napier-Munn, 2006; Fuerstenau, 2007; Fuerstenau *et al.*, 2007; Sandoval-Zambrano, 2013). Since flotation was patented in 1906 by Minerals Separation Ltd, the technology

has evolved to make the processing of low-grade ore economically viable (Wills and Napier-Munn, 2006; Fuerstenau, 2007).

2.6.1 Description of flotation processes

Flotation is a complex process in which valuable minerals are selectively separated from gangue minerals (Lynch *et al.,* 2010). Flotation occurs within a three-phase, solid-liquid-gas system containing finely ground particles, water and chemical reagents, and air. A schematic of the operation of a flotation system is shown below in Figure 2.21. To ensure that the air bubble will preferentially interact with the targeted mineral species, surface - active agents are used to modify the particles' surface rendering them either hydrophilic or hydrophobic. Hydrophobic particles will interact with air-bubbles making them more likely to be recovered in the flotation process. Hydrophilic particles (mostly gangue minerals) will be more likely to drain back into the pulp phase from the froth or remain in the slurry and be transported to the tailings stream.

The bubbles will interact with selected mineralogical particles producing bubble-particle aggregates. Such aggregates will be transported upwards due to density difference. The bubble-particle aggregates will form a froth phase at the top liquid-gas interface and will eventually be reported to the concentrate (Garret, 1979, Nguyen and Schulze, 2004).

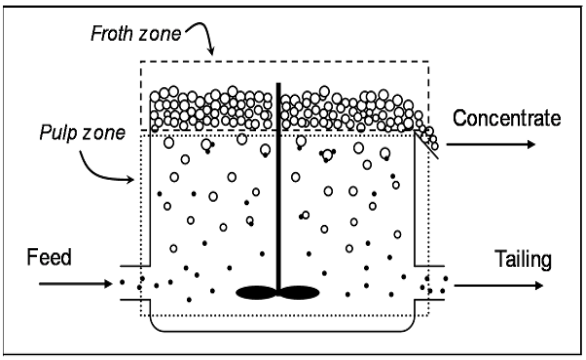

Figure 2.21: Operation of a flotation cell (After Wills, 1988).

Base metals such as copper, lead, zinc and nickel and precious metals such as platinum, gold and palladium often exist either as sulphide minerals or in association with these minerals. For these base metal sulphides, the separation process employed is almost always flotation (Kelly and Spottiswood, 1982). Wills (1998) states that although froth flotation is "the most important and versatile mineral processing technique", the "theory of flotation is complex and not completely understood".

❖ **Particle size in flotation**

Particle size is an important factor governing the attachment with bubbles, especially important are the effect of the coarser and finer particle sizes on the recovery of the valuable minerals. In fact, the probability of collision depends on bubble size, general hydrodynamic conditions in the cell and particle size (Jameson *et al*, 1977). The variation of flotation recovery with particle size follows the general pattern of inverted "u" shape shown in Figure 2.22., where the recovery for fine particles is low, increases with particle size (intermediate region) reaching a maximum and then decreasing for coarser particles. Predictions from laboratory tests can be improved if the mineral recovery from the batch tests is expressed as a function of particle size (Wills and Napier-Munn, 2006).

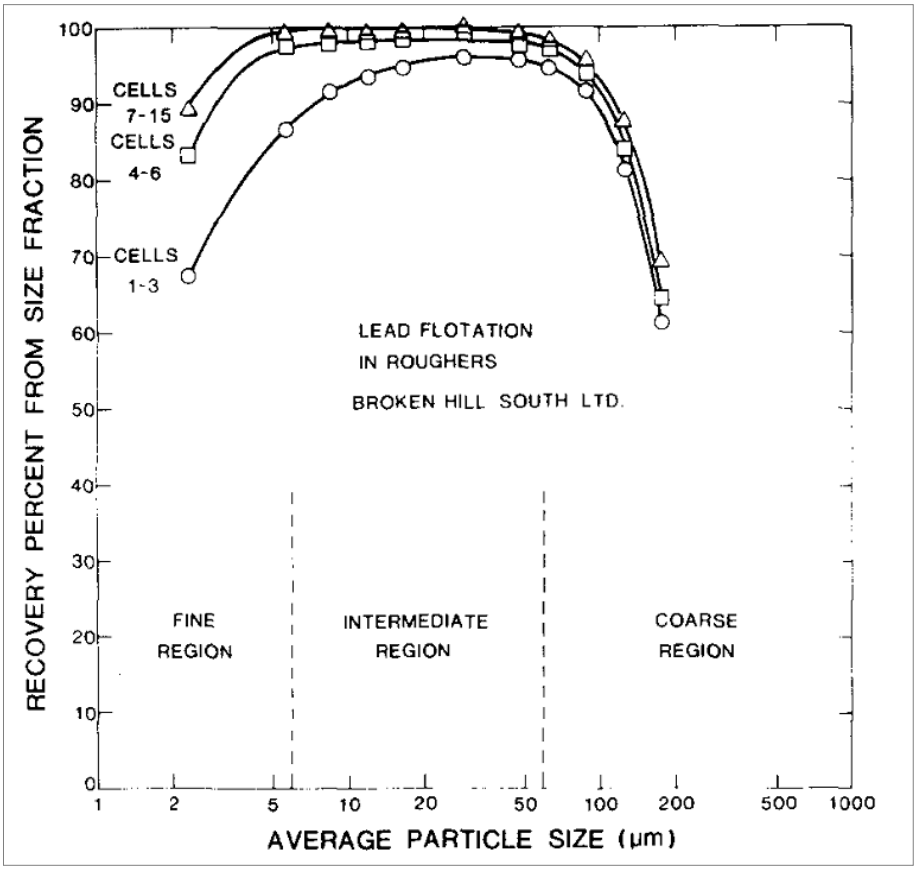

Figure 2.22: Cumulative lead recoveries in the lead rougher circuit at Broken Hill South Ltd. (Trahar, 1981).

Trahar (1981), suggested that composite particles will float less readily than free particles and that a relationship should exist between surface composition and floatability. The determination of an optimum grind size for particles in a given ore depends not only on their grain size, but also on their floatability (Finch *et al.*, 1979). In the case of real complex ores, an initial examination should be made to determine the degree of liberation in terms of particle size so that an estimate of the required fineness of grind can be made (Wills and Napier-Munn, 2006). The potential for liberation

of the minerals contained in the ore and the texture of ore samples can be characterised by using automated image analysis techniques, such as the MLA.

2.6.2 Flotation of silver minerals

Since the early 1930's, a number of researchers have studied the flotation of silver minerals (Hahn, 1927; Hahn, 1929; Gieser, 1931; Leaver and Woolf, 1939). Work by Hahn and Gieser focused on the flotation of oxidised silver ores, while Leaver and Woolf (1939) commented on the factors that affect flotation of silver minerals. Engel and Jackson (1949) studied the flotation of chlorargyrite from an oxide ore. In 1950, Dorr and Bosqui published a book entitled "*Cyanidation and Concentration of Gold and Silver Ores",* in which one of the chapters was dedicated to silver mining. They discussed the treatment of ores that contain silver-bearing minerals and refractory ores (ores containing manganese). Flotation was the main process used to recover silver from Mochito Mill in Honduras, being a high-grade silver ore that contained silver associated with galena and sphalerite. These authors also commented on the reagents used and the conditioning time required for those reagents, which were the same as used for gold. Dorr and Bosqui (*op. cit.)* also commented on the consequences of entrainment, and noted that the possible solution to remediate its effects for gold may also be applied for silver. They stated that "valueless slime, in addition to its detrimental effect in coating gold bearing sulphide, thereby limiting or preventing its flotation, also becomes mixed with flotation concentrate and lowers its value".

Flotation has been applied to a wide range of silver minerals and silver-containing base-metals, using xanthate and dithiophosphate collectors (Leaver and Woolf, 1939; Taggart, 1945; Dorr and Bosqui, 1950; Malhotra and Harris, 1999). Table 2.10 shows data for the flotation of some common silver-bearing minerals treated using flotation and the best recovery achieved for each one.

Currently the strategy adopted for floating silver depends on the amount of metal sulphides present within it. Silver minerals can be recovered either by selective or bulk flotation (Woodcock *et al.*, 2007). Selective flotation is applied to low-grade base metal and sulphide ores; in this type of flotation, silver minerals are floated first while the low-grade minerals are selectively rejected, typically using lime, cyanide or zinc sulphate. Bulk flotation is adopted when the ore has one to five percent of base metals and aims to recover all sulphide minerals into a single concentrate, in order to produce a silver-rich sulphide concentrate.

The use of bulk flotation was reported by Woodcock *et al.* (2007) at the Salar mine in West Siberia. The silver occurrences there were with acanthite, cerargyrite, iodargyrite, native silver and amalgam. Some redeposition of acanthite occurred on goethite as very fine grains less than 2 μm in

diameter. The strategy used was bulk flotation of sulphide minerals; however this was unsuccessful because the dissolution and the redeposition phenomena occurred in the ore.

Table 2.10: Flotation characteristics of the common silver-bearing minerals (after Gasparrini, 1984A and 1993)

Mineral	Flotation Characteristics	Best Recovery
Native Silver	Normal flotation	-
Electrum	Normal flotation	-
Argentite-Acanthite	Normal flotation. Lime has little effect. Recovery is lowered by Fe oxides. Starch helps concentrate grade.	98.5%
Silver halides (Cerargyrite, Bromyrite, Embolite, etc.)	Normal flotation. Lime has little effect. Concentrate grade is lowered by slimes, but improved by starch.	98.8%
Proustite	Lime is deleterious. Grade, but not recovery, is lowered by talcose material. Starch should not be used.	94.5%
Pyrargyrite	Lime is deleterious. Both recovery and grade are lowered by slimes. Starch should not be used. The mineral is very sensitive to changes in flotation conditions. Na sulphide is very harmful in all cases.	97.0%
Stephanite	Lime is deleterious. Grade is lowered by talcose slimes, but starch is effective in correcting the problem.	94.4%
Polybasite	Lime has little effect. Grade is lowered by talcose slimes, but starch is effective in correcting the problem.	98.7%
Tetrahedrite-Tennantite	Lime has little effect. Grade, but not recovery, is lowered by talcose slimes. Starch is effective in correcting the problem. Recovery improves with silver content of the minerals (Boorman *et al.*, 1982).	99.1%
Pb-Zn minerals enclosing fine particles of Ag minerals or containing Ag in solid solution	Lime has little effect. Grade, but not recovery, is lowered by talcose slimes. Starch is effective in correcting the problem.	98% of Pb and Ag in Pb concentrate and 55% of Zinc in Zn concentrate
Copper Ores (Porphyry Copper)	Chalcopyrite, bornite, chalcocite, covellite, native copper, minor oxidised Cu minerals, argentiferous tetrahedrite, Ag sulphide, electrum, pyrite and molybdenite with non-sulphide gangue minerals and alteration products (clay, sericite, hematite and limonite) (0.7% to 1% Cu, 0.05 to 0.1 oz/t Ag).	Cu and Ag recoveries in the region of 90%
Complex Cu-Pb-Zn Ore	Total base metal content of 7%-10%, 1-5oz/t Ag, pyrite is sometimes abundant.	Varies between 85% - 95% Ag with small percent in Zn concentrate if is produced.

According to Gasparrini (1993), “the dissolution and redepositation phenomena which cause the development of coatings over the different mineral particles in the products, through processes similar to those described by Chen and Dutrizac (1988)” give overestimated recovery results when flotation or leaching are chosen to recover silver.

2.6.3 Different strategies for floating silver minerals

There are several strategies that can be assessed for floating silver minerals in an ore that depend on not only the nature of the ore, but also the type of reagents and reagent schemes used.

2.6.3.1 Reagents used in silver flotation

The common reagents used in flotation are pH modifiers, activators, depressants, collectors, frothers and dispersants. In silver flotation, the most accepted reagents are described in the following paragraphs.

- pH modifiers: Used to modify pH during flotation to maximise recovery and selectivity. Lime and soda ash are commonly used in alkaline circuits. In acid circuits, sulphuric acid is widely used. These reagents are found to have small effects on argentite, chlorargyrite, galena and silver sulphides. Proustite and pyrargyrite are depressed by lime (Cytec, 2010).
- Activators: Their function is to increase the effectiveness of the collector. Copper sulphate is the most commonly used reagent to activate pyrite and arsenopyrite which are potential hosts for silver in solid solution.
- Depressants: These reagents are added to reduce gangue recovery and clean the mineral surfaces by removing ions or fine particles, thereby enhancing mineral floatability (recovery and kinetics). A widely used depressant in base metal flotation is cyanide, which depresses all the silver minerals. In some cases the use of cyanide can cause the dissolution of silver to occur. However, new environmental regulations worldwide are minimising the consumption of this depressant (Cytec, 2010).
- Collectors: Mainly used to provide hydrophobicity to the minerals of interest, which contain the valuable elements. The xanthate family of collectors is widely used. There are other collector families that can be used for floating silver, depending on the ore to be treated; these are further described in Chapter 3.
- Frothers: Used to allow stable bubble formation and stabilise the froth, and also to increase flotation kinetics. The most widely used frother is methyl isobutyl carbinol (MIBC).
- Dispersants: Used to reduce the recovery of slimes and to disperse ultra-fine particles in the pulp. The most commonly used are sodium silicate, soda ash and various polyphosphates.

Some examples of industrial applications for reagents selected for silver flotation were first discussed by Dorr and Bosqui (1950). They described the scheme of reagents used in Mochito mine collectors (Aerofloat 25/31, amyl and butyl xanthates, Aerofloat 208 and 404); pH modifiers (sodium carbonate); activators (copper sulphate); depressants (starch); dispersants (sodium silicate)

and sulphidising reagents. Malhotra *et al.* (1987) and Malhotra and Harris (1999) commented that the chemical reagents used in the flotation of Cu-Ag, Co-Ag, or Cu-Ag-Bi in order to obtain concentrates were xanthates and dithiophosphates as collectors, with MIBC, pine oil, or polypropylene glycol as frothers. For pH adjustment, lime was used and it was recommended to work at neutral pH. A study performed by Thompson (2002) investigated the most appropriate scheme of reagents to recover silver from an ore that contained 350 ppm of Ag. In this case, the silver carriers were identified as freibergite, proustite, argentite and pyrargyrite; Ag in solid solution with pyrite, some sphalerite and non-sulphide gangue is also present in the ore. It was possible to use a combination of collectors (thionocarbamate with ethyl xanthate), to produce a concentrate that contained 17500 ppm of Ag at 82% recovery through flotation.

The Cytec Mining Chemicals Handbook (2010) presents a wide range of reagents that can be used for the flotation of silver minerals depending on the type of ore treated. For example, for Cu and/or Pb sulphide concentrates, the recommended collectors to be used for this kind of flotation are AEROFLOAT 242 (from the chemical family of aryl phosphorodithioate), and AEROPHINE 3418A (from the chemical family of dithiophosphinate). For copper sulphide ores with silver present, good recovery is possible using AERO 6931 (from the chemical family of aryl phosphorodithioate) and AERO MX-950 (a modified dithiocarbamate) and AERO MX-6205 (mercaptobenzothiazole). The use of AEROPHINE 3418A was strongly recommended when silver minerals were associated with sulphide minerals in an ore.

Woodcock *et al.* (2007) commented that the separation of tetrahedrite was made with "starvation quantities of collector". This is an indication that large amounts of collectors could be needed to recover silver minerals.

2.6.3.2 Sulphidisation

The recovery of oxidised minerals from old, dumped or supergene ores can be difficult. Therefore, the use of sulphidisation is appropriate to enable these minerals to be recovered by flotation. Sodium sulphide (Na_2S) and sodium hydrosulphide (NaHS) are used as sulphidising agents for oxidised or tarnished sulphide minerals. Any unoxidised sulphide minerals that are present need to be recovered before using the sulphidising agent. Tarnished sulphides can be floated after sulphidisation, but excess sulphide is detrimental. The common amount of sulphidising agent used varies between 500 and 2500 g/t (Onal *et al.*, 2005).

Early work on sulphidisation was performed by Hahn (1927) and Leaver and Woolf (1939), who studied oxidised Zn-Ag ores and silver sulphide minerals in order to examine their behaviour during

sulphidisation. In 1927, Hahn studied the flotation of oxidised lead-silver ores, reviewing the techniques used in the 1920s. At that time, shaking tables and flotation were used for different oxide ores (gold-silver-lead and lead-silver ores). This work was the first attempt at using sulphidisation (sodium sulphide) for silver ores. The procedure was as follows: mixed sulphide and oxidised minerals were treated by a shaking table to concentrate the sulphide minerals, followed by the use of sodium sulphide for the tailings (sulphidisation and flotation stages). Various reagent types were used: dispersants, collectors and sulphidising agents. Hahn (*op. cit.)* also highlighted the problems associated with floating oxidised minerals, which included the presence of colloidal slimes, large amounts of iron and manganese sulphates and soluble salts.

Leaver and Woolf (1939) studied the flotation characteristics of silver sulphides and sulphosalts, i.e. argentite, polybasite, proustite, pyrargyrite and stephanite. Their study demonstrated that all of these silver minerals, including tetrahedrite, float well at a neutral pH with an ethyl xanthate collector and with the use of sulphidisation (sodium sulphide). Other reagents used were sodium hydrate, lime and starch. Slimes containing iron oxide or talc interfered with the grade and recovery of the silver minerals. If free gold was present, Aerofloat 208 could be helpful as a secondary collector (Cytec, 2010). Copper sulphate could help in the activation of zinc, whether it is associated with silver sulphides or sulphosalts.

Extensive work has been performed to determine the best flotation method to recover minerals with different degrees of oxidation (e.g., Pryor, 1953; Fleming, 1953; Boyard, 1954; Rey, 1954; Kleeman, 1968; Lord and Markovic, 1970; Jones and Woodcock, 1979). In 1965, Pryor suggested that oxidised silver ores were aided to float by using a sulphidising treatment followed by the use of a cationic collector or chelating collectors (Pryor 1965; Fa *et al.*, 2005). Rey (1954) pointed out the difficulties of achieving an optimum sulphidisation. However, Jones and Woodcock (1979) later suggested that an optimum amount of sulphidising agent followed by anionic collectors could aid flotation.

A number of researchers have investigated the different flotation strategies using sulphidisation for ores that contain silver on an industrial scale – Amoros *et al.* (1981), Lara (1988), Baum (1988), Allan and Woodcock (2001), and Qing *et al.* (2008) to list some. As an example, Lara's work described the process used at La Encantada, Mexico, where the metallurgical process had been always difficult due to the lack of water and the nature of the ore (which was mainly oxidised lead minerals). The process was described as follows: dry magnetic separation for the coarser-sized fraction of the feed, followed by flotation, which initially floated all sulphide minerals with the rougher sulphide concentrate being the final concentrate, followed by flotation of oxidised minerals

after sulphidisation. The concentrate following sulphidisation was then processed in two cleaning stages to obtain a concentrate that was combined with the final concentrate.

Qing *et al.* (2008) studied a lead-zinc-silver ore with 15% of the galena in an oxidised form, and with silver mineral(s) in a finely disseminated form associated with galena. The developed circuit improved silver recovery and had three stages. The first stage was floating galena in roughing as normal flotation, followed by sulphidisation and rougher recovery of the portion of the galena originally in an oxidized form, the tails from which went to the zinc circuit to produce a marmatite rougher concentrate. For cleaning, the concentrates from the galena rougher and the sulphidised galena rougher were joined and fed to a common regrinding step.

Kim and Stanley (1988) studied natural and synthetic silver minerals that may be present in zinc residues, using flotation as the process selected to treat these materials. The results showed that the majority of silver minerals could be floated with high recoveries at a wide range of pH values using sulphidising agents and also the minerals floated well without sulphidisation. Figure 2.23 shows their results for chlorargyrite, acanthite and native silver, respectively. Native silver recovery is affected by a prolonged period of sulphidisation, with the recovery of the three minerals studied being above 90%.

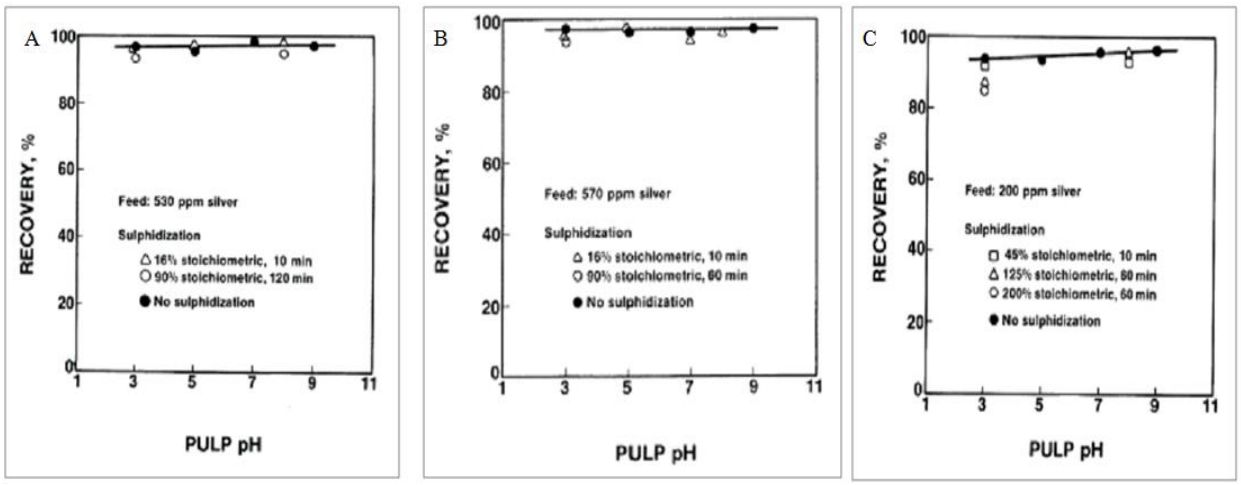

Figure 2.23: A) Recovery of chlorargyrite; B) Recovery of acanthite; and C) Recovery of native silver as a function of pH for all of these (from Kim and Stanley, 1988).

2.6.4 Flotation of refractory silver ores

In the following paragraphs some examples of what have been described as refractory silver ores were treated in the context of flotation or some other processes such as leaching, the sulfur dioxide process, the Caron process and others.

Dorr and Bosqui (1950) investigated the processing of silver minerals contained in refractory ores. The silver occurred in what were described as refractory minerals, such as manganese dioxide, which was difficult to treat. It was possible to process these ores using the sulfur dioxide process after which the silver could be recovered through cyanidation (Crawford, 1934). Another process, which is also used for refractory ores, is called the Caron process, and uses a reducing atmosphere at high temperature; the higher manganese oxides are converted into manganese oxides, which can be treated through a cyanidation process.

An ore from Sonora, Mexico, was studied by Hausen and Hill (1994), who concluded that the silver there was carried by silver-bearing minerals, with a head grade of 265 g/t, which could be recovered by flotation or cyanidation, the yield of Ag reaching 50% to 60%. The recovery of silver was mainly through acanthite (50%) present as coarse particles (70 to 300 μm), while the remaining silver was classified as refractory because it occurred as fine grains of acanthite (2 to 0.2 μm) in quartz gangue, and as freibergite or stylotypite encapsulated in fluorite.

2.6.5 Silver losses in tailings and presences of slimes

Marley and Hagni (1982) noted that silver minerals were lost in tailings as fine inclusions (<5μm) in quartz. They pointed out that silver was encapsulated with quartz, generating a route for the loss of silver.

Leaver and Woolf (1939) investigated the effect of the type of slimes present in flotation, and their effect on silver grade in the concentrate. Table 2.11 illustrates the results of using different types of slime with various silver minerals and using starch as a dispersant. Some solutions for this problem were presented in 1950 by Dorr and Bosqui, in order to remediate the presence of slimes. Those solutions are presented in Table 2.12.

Table 2.11: Summary of the findings by Leaver and Woolf (1939)

Mineral	Type of slime	Effect on Ag recovery	Effect on Ag grade	Effect of starch addition
Chlorargyrite or Cerargyrite	Talc	Nil or minor	Decreased	Recovery maintained Grade increased
	Clay iron oxide	Nil or minor	Decreased	Recovery maintained Grade increased
Acanthite	Clay iron oxide	Slight decrease	Decreased	Starch remedies to large extent
Polybasite Tetrahedrite	Talc	Nil or minor	Decreased	Starch remedies to large extent
Proustite Stephanite	Talc	Nil or minor	Decreased	Starch depressed proustite and stephanite
Pyrargyrite	Talc	Decreased	Decreased	Starch depressed pyrargyrite

Table 2.12: Summary of types of slime present and the remedial action (after Dorr and Bosqui, 1950)

Type of slime	Remedial action
Primary slime from mine	Remove the slime before fine crushing
Carbonaceous slime Talcose slime	Add reagent to make it hydrophilic
Clay slime	Not hydrophobic but attached to valuable minerals Using dispersant helps to deflocculate the pulp
Iron (not hematite) and manganese oxides	Use dispersant and use depressing agent, for example, starch

2.7 Applying mineralogy to increase recovery of valuable metals from ores

Process mineralogy is a science that combines mineralogy and mineral processing, with the capabilities of identifying bulk mineralogy, degree of liberation and the presence of problematic minerals in an ore to develop or improve the processing flow sheet for that ore (Hagni, 1982; Henley, 1983; Hagni, 1986; Baum *et al.*, 2004). There are a number of researchers who have applied process mineralogy to silver (Petruk and Schnarr, 1982; Gasparrini, 1983; 1984A; 1984B; Guerra, 1988; Di Prisco *et al.*, 2002; Chryssoulis *et al.*, 2003; Zhou *et al.*, 2005; Zhang *et al.*, 2006; Holloway *et al.*, 2008; Zhou, 2010). Guerra (1988) studied an ore body that had exhibited good metallurgical performance for silver until some manganese assays were reported as elevated (7.2%). Flotation and cyanidation were tested for the ore with high levels of Mn; however the recoveries of silver were lower, at 29% and 33%, respectively, knowing that the typical recovery of silver is over 80%. Optical microscopy was performed on the tailings to investigate which form of silver present in the ore was lost, but no explanation was found for it. To try to resolve this problem, the author suggested using a metallurgical explanation that silver minerals were present at very fine grains, not detected by optical microscopy, and locked either by gangue minerals or manganese minerals, or even coated by colloidal manganese oxide. Leaching with SO_2 was performed, followed by flotation and then cyanide leaching. The recoveries of silver increased up to 97%. The conclusion of this case study was that the silver minerals were closely associated with manganese oxides, and that the process of leaching with SO_2 followed by flotation and then cyanidation allowed improved recovery of silver.

In 1993, Gasparrini carried out a mineralogical study on silver-copper ore from British Columbia. The search there was focused on the grain size of tetrahedrite, and concluded that the silver content of the fine grains was higher than that of the coarse-sized fraction.

Therefore, before any metallurgical characterisation is attempted, the following key mineralogical factors need to be studied:

- Modal mineralogy
- Silver carriers or silver deportment
- Mineral locking/ liberation
- Grain size
- Mineral association
- Rimming and coating
- Refractory ores
- Silver in solid solution (sub-microscopic silver).

2.8 Key findings

As a consequence of silver having a lower price in the metal market for many years, it has not been a target for recovery in many mine sites around the world. However, with recent increases in its price, those previously uneconomical sources of silver have become more attractive to process. Within this category, it can be seen that old tailings and low-grade ores are now considered new resources of this noble element and offer an important opportunity for opening research, and applying or developing new techniques to recover silver, which necessitates the development of a systematic approach to characterise silver.

Silver mineralogy is more complex than gold mineralogy, due to the variety of silver minerals that may be present in a silver ore. A wide range of grain sizes are also found, and the quantification of silver deportment is difficult to achieve. There are a number of explanations for the difficulties in identifying the deportment of silver: i) silver has different mobility in different environments, which includes the different operational conditions to which the ore is exposed during mineral processing operations; ii) the large number of silver minerals present in an ore, which could affect the accuracy of identifying its mineralogy; iii) the texture of some silver minerals present; and iv) the detection limits of the instruments used to perform the mineralogical characterisation. Therefore, it becomes more important to perform the mineralogical characterisation, in order to develop a clear understanding of which metallurgical processing routes should be tested for both greenfield and brownfield situations.

There is no consistent framework in place to characterise silver mineralogy, as there is for gold. Gold ores can also be characterised using well established methods to determine how refractory the gold is; no such methods exist for silver. In terms of metallurgical processing, there are different strategies that can be applied to recover silver, and these strategies play an important role in developing the flow sheet design for recovering silver. Due to the large number of silver minerals

present within an ore that can react differentially to different metallurgical processes, comprehensive characterisation of the nature of silver minerals within an ore is needed before a suitable processing route can be selected.

The following gaps were identified in the literature review:

i) The development of a standardised approach to determine silver deportment in low-grade silver ores;
ii) A systematic approach to establish appropriate flotation strategies, based on silver deportment, to achieve adequate recovery of silver through rougher flotation stages;
iii) Presentation of a framework that clearly describes what makes silver ores refractory based on the results obtained through this work;
iv) Investigation of the flotation of silver ores on size-by-size and size-by-liberation basis, which is not reported in the literature.

As a result of the identification of these points, the aim of this thesis is to develop an appropriate methodology to characterise complex low-grade silver ores for the purpose of developing the most appropriate flotation strategy.

Chapter III:

Experimental Methodologies

This chapter describes the overall framework used in this research to study three different ore types all from the same deposit. Descriptions of the ores used and of the general test-work procedures are presented, followed by descriptions of the conditions pertaining to the equipment, and the methodologies used for the mineralogical, metallurgical and flotation product characterisation.

3.1. Ores samples

The ores used for this study came from Minera San Cristobal (MSC) in Bolivia, which is classified as a magmatic-hydrothermal Ag-Pb-Zn deposit. It is the 3rd largest silver mine and 5th largest zinc mine in the world (Duran and Block, 2012). More details of MSC can be found in *Appendix B.* These ores were received to be processed in the laboratory of the Julius Kruttschnitt Mineral Research Centre (JKMRC) in Brisbane, Australia. For the metallurgical characterisation, flotation was the process investigated to treat the ores due to the fact that MSC has an existing flotation plant to process the ores; MSC gave the following constraints for the flow sheet process development i.e. Ag recovery over 60%, mass recovery less than 10 % and flotation feed (mill product) size target (P80) of 100 μm.

The three ores are treated as individual case studies in this research: *Toldos ore* (also referred to as *oxide ore*) is an oxide low-grade silver ore (35 kg of ore was received); *Tesorera ore* (also referred to as *sulphide ore*) is a complex sulphide low-grade silver ore (77 kg was received); and *Jayula ore* (also referred to as *supergene oxide ore*) is a complex oxide low-grade silver ore (121 kg was received).

3.2 Approach procedure

The framework used to study the three ores is shown in Figure 3.1, which illustrates the steps used for the sample preparation, and for the detailed mineralogical characterisation of the samples received (ore characterisation), mill product, flotation product as well as the metallurgical characterisation for each of the ores. The approach comprised the following steps:

- ❖ *Sample preparation which included:*
- ✓ Crushing the ore types to 100% passing – 3.35 mm,
- ✓ Sample homogenisation
- ✓ Splitting the sample into charges of 1kg of ore in sealed plastic bags to be stored in the freezer in order to minimise the oxidation effect until further processing.
- ❖ *Detailed mineralogical characterisation of the ore which can be divided into two sections: ore characterisation and mill product characterisation.*
- ❖ *Detailed metallurgical characterisation (including effect of mill product sizing (flotation feed sizing), pre-flotation properties, the effect of collector dosage and the need for sulphidisation) was applied to the ores using a 5-L JKMRC bottom-driven batch flotation cell.*
- ❖ *Each product of the flotation test (concentrates and tailings) was submitted for chemical analysis to evaluate the metallurgical performance (i.e. recovery and grade) of the ore.*
- ❖ *Mineralogical characterisation using MLA was performed on a size-by-size for the flotation products resulting from the conditions which produced the best metallurgical performance from each ore. This was carried out to investigate the influence of the degree of liberation of valuable minerals and how they are locked with other minerals in the ore on the metallurgical performance.*

  ***Note**: that liberation is considered when a particle has only one phase however for practical measurement of liberation a particle is considered liberated when more than 80% of its surface is liberated. Another concept that it is important to mentioning is the degree of liberation that is stated as the fraction of a phase (by mass or volume) present as liberated divided by the mass or volume of the phase present in the population.*

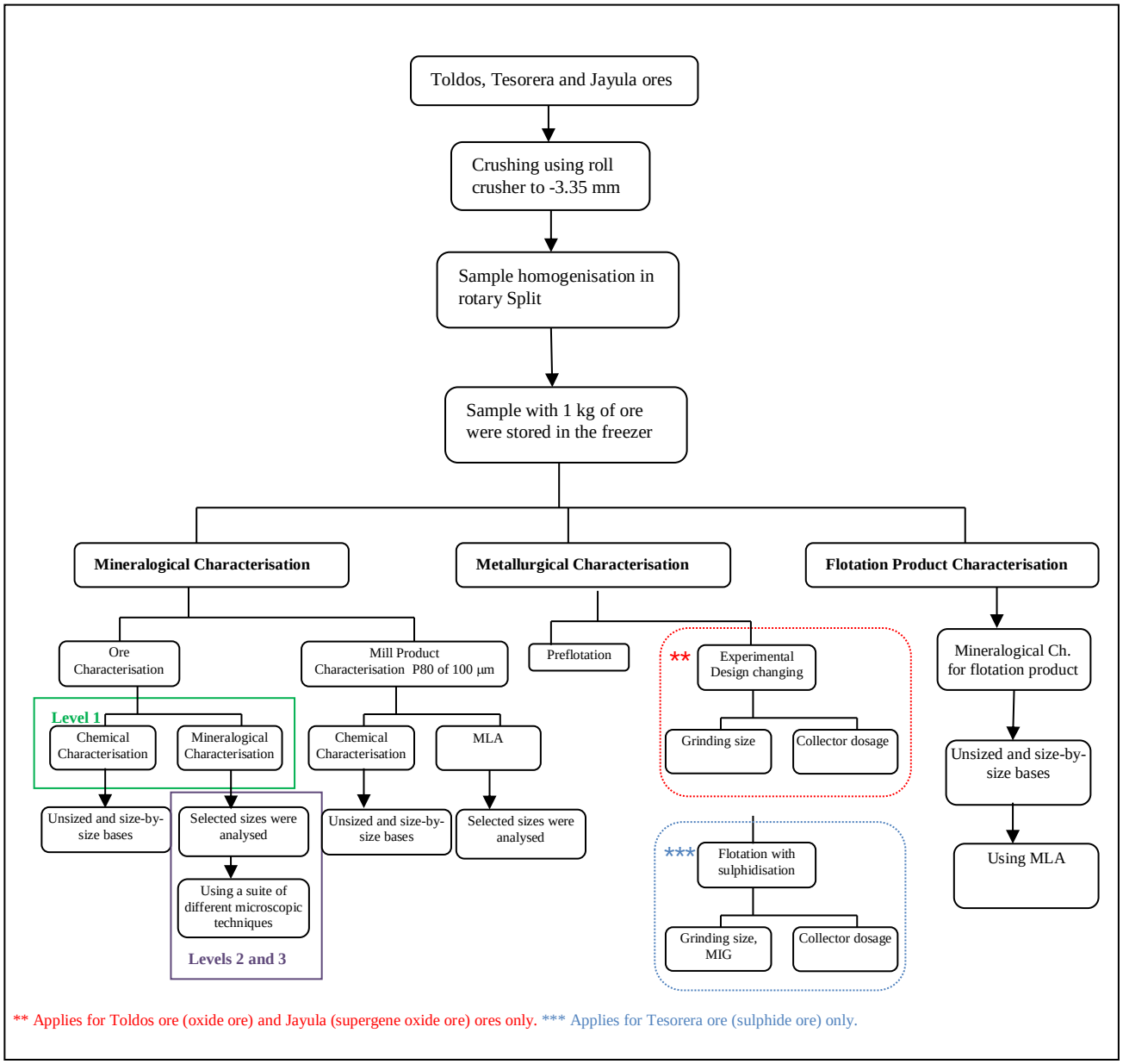

Figure 3.1: Approach procedures for all case studies - Toldos ore (oxide ore), Tesorera ore (sulphide ore) and Jayula ore (supergene oxide ore).

3.3 Sample preparation for the ores

The ores were crushing 100% passing – 3.35 mm by jaw crusher. Stage crushing minimizes the production of fines ahead of grinding. The samples were homogenized and split by rotary splitter and then the sample of each ore was put into charges of 1kg of ore in sealed plastic bags to be stored in the freezer in order to minimise the oxidation effect until further processing.

The sample preparation for ore characterisation is described as follow:

- ✓ Three sub-sample (250 grs each sub-sample) of a 1 kg sample was sieved into 14 size intervals for each ore type, namely +2.36 mm, -2.36/+1.7 mm, -1.7+/1.18 mm, -1.18mm/+850 µm, -

850/+600 μm, -600/+425 μm, -425/+300 μm, -300/+212 μm, -212/+150 μm, -150/+106 μm, -106/+75 μm, -75/+53 μm, -53/+38 μm and -38 μm.

- ✓ A remaining unsized portion (250 grs) of the split sample was kept for further analysis.
- ✓ From these size intervals, selected size fractions were submitted for a range of different analyses as described in the previous section.

3.4 Techniques used in the Mineralogical characterisation for ore, mill product and flotation products

In this section, the experimental conditions of the analytical techniques used for ore, mill product and flotation products characterisation are described, while all the description of the equipment can be found in *appendix C*. Two terms need to be clarified *ore head:* feed samples and *mill product:* the sample prior to entering to flotation.

3.4.1 Chemical assays

The chemical assays were performed on unsized samples (feed head samples, mill product and flotation products) and on size-by-size samples (head, mill product and the flotation products for each ore tested under optimum conditions). Table 3.1 shows the sizes fractions submitted to chemical assays for each ore.

Table 3.1: Samples submitted to chemical assays as unsized and size-by-size bases

Ore	Unsized	Size-by-size
Toldos ore (oxide ore)	Ore head, flotation products	**Ore head:** (+2.36 mm, -2.36/+1.7 mm, -1.7+/1.18 mm, -1.18 mm/+850 μm, -850/+600, -600/+425, -425/+300, -300/+212, -212/+150,-150/+106, -106/+75, -75/+53, -53/+38 and -38 μm). **Mill product and Concentrates and tailings (best performance):** (-150/+106, -106/+53μm, +C2, +C3, +C4, +C5, -C5)
Tesorera (sulphide ore)	Ore head, flotation products	**Ore head:** (+2.36 mm, -2.36/+1.7 mm, -1.7+/1.18 mm, -1.18 mm/+850 μm, -850/+600, -600/+425, -425/+300, -300/+212, -212/+150, -150/+106, -106/+75, -75/+53, -53/+38 and -38 μm). **Mill product and Concentrates and tailings (best performance):** (-150/+106, -106/+53μm, +C2, +C3, +C4, +C5, -C5)
Jayula (supergene oxide ore)	Ore head, flotation products	**Ore head:** (+2.36 mm, -2.36/+1.7 mm, -1.7+/1.18 mm, -1.18 mm/+850 μm, -850/+600, -600/+425, -425/+300, -300/+212, -212/+150, -150/+106, -106/+75, -75/+53, -53/+38 and -38 μm). **Mill product and Concentrates and tailings (best performance):** (-150/+106, -106/+53μm, +C2, +C3, +C4, +C5, -C5)

3.4.2 Oxide characterisation for lead and zinc minerals

The oxide characterisation for lead and zinc minerals were performed in bulk by AMDEL in Melbourne. For lead oxide assays, leaching with ammonium acetate solution was used to selectively

dissolve oxides, and an atomic absorption spectrometer (AAS) analysis was then performed. For zinc oxide assays, a digestion in weak sulphuric acid solution (0.02N) was carried out to extract oxides, followed by an AAS analysis.

3.4.3 X-ray diffraction (XRD)

X-ray diffraction (XRD) analyses were carried out on the bulk samples. These analyses were performed by AMDEL laboratory located in Melbourne.

3.4.4 Optical microscopy

Optical microscopy was performed using the selected size fraction of -425/+300 μm from the ore head. Each ore was mounted in an epoxy polished block section and submitted for optical microscopy by reflected light at hrltesting in Brisbane.

3.4.5 Mineral Liberation Analyser (MLA)

The samples that were analysed by MLA consisted of polished sections of particles of ore head, mill product and flotation product. These polished blocks were made by mixing the particles with a two part epoxy resin to make a block with a diameter of 30 mm. Once the sample block was made, the surface of the block was polished with an automatic polishing machine to provide a high quality flat surface, before being coated by a thin layer of carbon to allow excess electrons to be conducted away from the sample surface. Figure 3.2 shows some blocks used for these analyses.

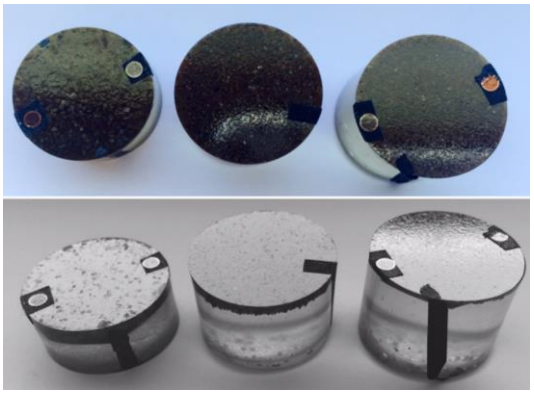

Figure 3.2: Polished block used in this thesis

In this study, four MLA modes were selected for analysis of ore. The ore characterisation was measured with GXMAP so that X-ray mapping of the high BSE phases could be undertaken to capture the complex textures observed in the ores. For the mill product, XBSE was used; and for the flotation products, XBSE was used for the concentrates and a combination of SPL and XMOD was used for the tailings.

a) MLA for Ore characterisation

Two size fractions (-1.18 mm/+850 μm and -425/+300 μm) were chosen to MLA analysis for this type of sample. These size fractions were made in order to preserve the texture in the ore and maximising the number of particles to be measured.

Grain based x-ray mapping (GXMAP) combines the use of X-ray mapping and area X-ray analysis for phase identification. X-ray mapping analysis is used to resolve any overlaps in BSE. For this method, different grains of interest in the analysis can be selected through a BSE trigger (this targets grains within a set BSE threshold), as discussed by Fandrich *et al.* (2007); for these ores a high BSE trigger was selected so that bright phases in the particles underwent X-ray mapping.

The MLA mineral reference library contains the list of minerals identified in each ore (*Appendix D)*; it also contains the corresponding X-ray spectra for each mineral as well as the density and compositional properties of the mineral. Once MLA measurement is complete, the X-ray spectra that are collected during measurement are compared to those in the mineral reference library in the first image processing stage known as classification. The measured X-rays are compared to those in the library using a pattern matching algorithm with user specified matching criteria. If the matching criteria are met the pixels associated with that X-ray spectra are given the mineral name, if no matches are found those pixels are labelled as 'unknown'. The contribution of unknown and low count or no X-ray spectra to the total modal mineralogy is relatively low. For example, in Jayula ore in the -425 /+300 micron size class the amount of unknown is 0.08 wt %, low count and no X-ray are 0.00 wt% for the modal mineralogy. During development of the mineral standard one of the objectives is to minimise the contributions from these types of X-ray spectra to ensure that the minerals present in the sample have been accounted for.

b) MLA for Mill product (Flotation feed) characterisation

The material that was selected for the mineral identification was the mill product for the ore at a P80 of 100 μm for each ore. This was because of the constraints from MSC in developing the project. These samples were analysed using the XBSE mode, and the size fractions analysed were: +106 μm, +53/-106 μm, +C2/-53 μm, +C3/-C2, +C4/-C3, +C5/-C4 and -C5 with the last five fractions created using the cyclosizer.

XBSE uses area X-ray analysis for those ore samples that contained phases with enough contrast in the BSE, collecting the BSE images which were segmented to identify the grain boundaries in each particle (Gu, 2003; Fandrich *et al.*, 2007).

c) MLA for Flotation product characterisation

The material that was selected for the flotation product characterisation corresponds to the best flotation test obtained through the experimental design. The best test of each ore was made by triplicates to have the statistic of it and also the sufficient mass for performing the MLA and chemical analysis. These samples were analysed by: XBSE, SPL_XBSE and XMOD modes. The size fractions analysed were: +106 μm, +53/-106 μm, +C2/-53 μm, +C3/-C2, +C4/-C3, +C5/-C4 and -C5 with the last five fractions created using the cyclosizer.

SPL_XBSE mode searches for target minerals of interest, using a BSE threshold (i.e. using BSE gray-scale range), then using XBSE measurement for each particle that was identified. It is used for samples where the mineral of interest is present at low levels, typically between 0.01 to 1.0 %, being the typical application for PGM, Au, and Ag characterisation, as well as sulphide mineral liberation in tailings, and penalty elements in concentrates.

XMOD was used to characterise the modal mineralogy XMOD uses a similar approach to point counting in optical microscopy. X-ray spectra are collected at each point on a grid intersecting a particle, with spectra typically collected for more than 20,000 data points.

3.4.6 Laser ablation inductively-coupled plasma mass spectroscopy (LA-ICP-MS)

Laser ablation inductively-coupled mass spectroscopy (LA-ICP-MS) was used for a selected size fraction namely the -212/+106 micron size class for Tesorera (sulphide ore) and Jayula (supergene oxide ore) ores; both ores were submitted to MODA (McArthur Ore Deposit Assessments Pty Ltd, located in Burnie, Tasmania) who conducted the analysis. The specific mineral grains analysed for Tesorera ore (sulphide ore) were pyrite (20 grains were measured) with a spot size measurement of 35 μm. In the case of the Jayula ore (supergene oxide ore), three specific minerals were analysed to find silver as solid solution; these were jarosite (5 grains were measured), Pb-phosphates (10 grains were measured) and Pb-arsenates (5 grains were measured). The spot size of the measurement was also 35 μm.

3.4.7 Electron microprobe analysis (EMPA) mapping

EMPA mapping was performed by J. Quinteros and D. Steel using CAMECA SX 50 equipment housed at the JKMRC. The sample analysed was -425/+300 μm. To obtain a map for key elements, the experiment was carried out at 10 kV, with the following elements measured by EMPA: aluminium (Al), arsenic (As), calcium (Ca), iron (Fe), potassium (K), lead (Pb), phosphorus (P),

silicon (Si), silver (Ag) and sulphur (S). These data were combined through a ternary diagram to determine elemental associations as described in *Appendix E*.

3.4.8 Manual SEM-EDS

Manual SEM-EDS was performed on samples prepared in new sample blocks (25 mm diameter). The microscope used was a Philips XL-30 equipped with EDS, held at the Centre for Microscopy and Microanalysis (CMM) at the University of Queensland (UQ) and operated by J. Quinteros. The SEM-EDS was operated at 20 kV. Table 3.2 shows the sample blocks that were measured and the energy used to perform the analyses.

Table 3.2: Conditions used for the manual SEM-EDS on samples of Jayula ore (supergene oxide ore).

Sample block	Size analysed	Energy used, kV
Sample 2	425/+300 μm	20
Sample 3	-1.18mm/+850 μm	20

3.4.9 Auto SEM

The auto SEM used was a Jeol 7001F equipped with EDS and Inca software, located at Queensland University of Technology (QUT) and operated by J.Quinteros. Inca software helped to set the microscope to be an automated SEM-EDS working under fixed conditions for locating bright particles using a threshold of 130.

Two sample blocks of Jayula ore (-1.18mm/+850 μm and 425/+300 μm) were remeasured twice by auto SEM-EDS at 15 kV, with the objective of confirming the chemical composition of silver minerals.

3.4.10 Synchrotron methods

Synchrotron XRF (SXRF) and synchrotron XRD (SXRD) analyses were performed by Minerals and Materials Science and Technology (MMaST) at the University of South Australia and additional analysis was performed using the XANES (X-ray absorption near edge spectroscopy) to complement the SXRF and SXRD analysis to verify the Ag minerals present in the ore. The samples are polished thin sections of two size fractions -1.18 /+850 μm and 38/-75 μm. The samples were built in resin, mounted onto silicon backing plate (0.5 mm tick, Sigma Aldrich) and both samples polished to a thickness of 40 μm for synchrotron microprobe measurements (Fan and Gerson, 2014). *Appendix F* shows details of the results from for synchrotron analysis.

1. SXRF were performed in a section of a substrate of a polished section of 1 cm thick at -1.18 /+850 μm. The substrate has a thickness of 500 μm to map the elements at mapping size (6,100 μm horizontal × 5,400 μm vertical), mapping performed for Ag, As, Cu, Fe, K, Pb, S, Sr and Zn.
2. SXRD measured the grains that contained Ag to then identify possible Ag minerals.
3. The XANES used a bulk analysis of different silver minerals (acanthite, proustite, freibergite and pearcite) as mineral references to check the minerals found through the SXRD and SXRF.

3.5 Experimental methods

3.5.1 Mineralogical characterisation

The objective was to identify the key mineralogical attributes (modal mineralogy, elemental deportment, texture and degree of liberation) necessary for developing an adequate flotation flow sheet for each ore. This characterisation consisted of two stages, one called ore characterisation and the second called mill product characterisation, both characterisations were applied to the three ores under study. Figure 3.3 described the mineralogical characterisation performed under this thesis.

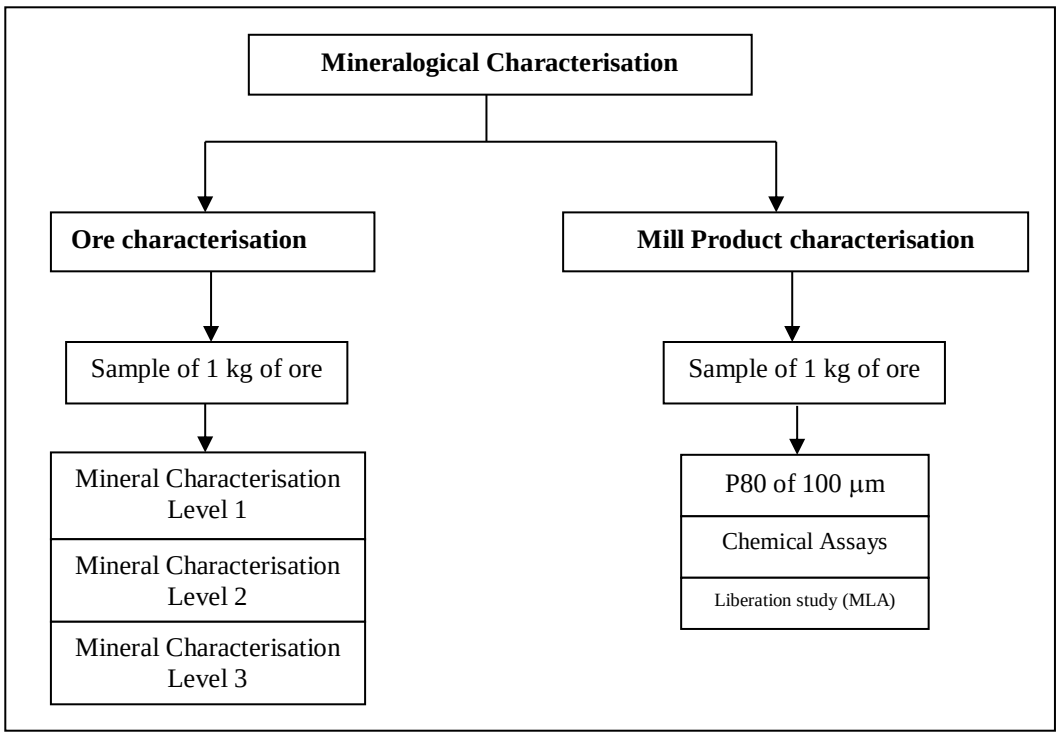

Figure 3.3: Mineralogical characterisation used for the three case studies - Toldos ore (oxide ore), Tesorera ore (sulphide ore) and Jayula ore (supergene oxide ore).

3.5.1.1 Ore characterisation

The ore characterisation was divided into three levels starting with a Level 1. Level 1 was the minimum level of characterisation used to identify key mineralogical attributes and was performed on each ore. When this level of characterisation was insufficient to identify silver deportment, which is one of the key attributes needed for the mineralogical characterisation, additional measurements were required. These measurements were divided into Level 2 and Level 3. A comprehensive description of what comprised each of the levels is provided in the following sections.

1. ***Mineralogical characterisation Level 1***

Level 1 consisted of a combination of complementary techniques that are commonly used in ore characterisation. This level included: chemical assay; X-ray diffraction; optical microscopy; oxide characterisation of lead and zinc; and mineral liberation analysis. This protocol was used for the ore characterisation in this work because each of these analytical techniques complemented the others. A summary of the techniques used is presented in Table 3.3. This level of characterisation was found to be sufficient to describe the mineralogical attributes for the Toldos ore (oxide ore).

2. Mineralogical characterisation Level 2

Mineralogical characterisation Level 2 included all of the analytical techniques described in Level 1 and also incorporated the use of laser ablation inductively couple plasma mass spectroscopy (LA-ICP-MS) to analyse mineral grains that potentially contained Ag in solid solution. This level was applied to both Tesorera (sulphide ore) and Jayula (supergene oxide ore) ores and was found to be sufficient to adequately characterise the mineralogical attributes for the Tesorera ore (sulphide ore).

3. Mineralogical characterisation Level 3

Level 3 was included after Level 1 and 2 and incorporated a highly intensive search for silver-bearing minerals. This resulted in the development of a new protocol for identifying previously unknown spectra for silver minerals which could then be incorporated into the MLA mineral reference library to enable reclassification of measured data and recalculation of the silver deportment. This level was used as the last resort for the ore characterisation, because this technique is time consuming and has higher associated cost due to the equipment needed for it. Only Jayula ore (supergene oxide ore) required the use of this methodology.

Table 3.3 presents the summary of the mineralogical characterisation by levels used for the three ores under study and the sizes that were analysed.

Table 3.3: Summary of the mineralogical characterisation by levels used for the three case studies

Methodology	Techniques	Sizes evaluated
Level 1	✓ Chemical assays	Unsized and size-by-size
	✓ X-ray diffraction	-1.7/+1.18 mm
	✓ Oxide characterisation for lead and zinc	Unsized
	✓ Optical microscopy	-425/+300 μm
	✓ Mineral liberation analyser	-1.18mm/+850 μm and -425/+300 μm
Level 2	✓ Same techniques used in Level 1 and Laser ablation inductively couple plasma mass spectroscopy	-212/+106 μm
Level 3	✓ Same techniques used in Level 2 and novel methodology for identifying the unknown silver minerals	-1.18mm/+850 μm and -425/+300 μm

3.5.1.2 Mill product characterisation

The purpose of the mill product (flotation feed) characterisation was to quantify the level of liberation of the key minerals that were the recovery targets in the flotation process.

- ✓ 1 kg of each ore was ground for 5, 10, 15 and 30 minutes in a laboratory rod mill to develop the grinding calibration curve, with the aim of estimating the time required to achieve a P80 of 100 μm.
- ✓ To validate the calculated grinding time, a sample of each ore was ground for the estimated time and the product sized to confirm that the target had been reached. Table 3.4 shows the grinding time values for each ore at a P80 of 100 μm.

Table 3.4: Grinding times for P80 of 100 μm for each ore under study

Ore	P80	Grinding time (min)
Toldos ore (oxide ore)	100 μm	24.3
Tesorera (sulphide ore)	100 μm	13.5
Jayula (supergene oxide ore)	100 μm	8.3

- ✓ The mill product for each ore was then sieved into seven size fractions (+106 μm, +53 μm, +C1/+C2, +C3, +C4, C5 and –C5, were obtained by wet and dry sieving and cyclosizing). A sub-sample of each size fraction was analyzed by MLA.

3.5.1.3 Characterisation of flotation products

Concentrates and tailings were analysed on a size-by-size basis using chemical assays and liberation data (MLA). This was done to obtain the key metallurgical parameters (recovery, grade, liberation and deportment) and to identify and understand the behaviour of the valuable minerals in each stream obtained by the flotation process. Figure 3.4 illustrates the path used for this characterisation.

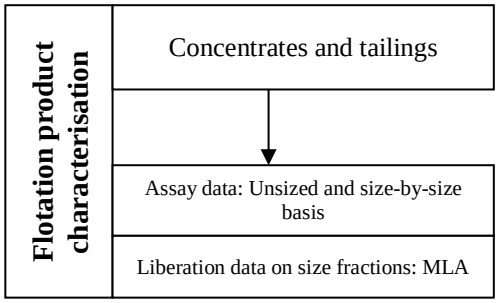

Figure 3.4: Flotation product characterisation used for the three case studies.

The selected size fractions (+106, +53 μm from screening and +C2, +C3, +C4, +C5 and –C5 from the cyclosizer) required that the concentrates be combined in some manner so as to restrict the number of analyses. Table 3.5 shows the size fractions evaluated for each ore and how the concentrates from the ores were combined.

Table 3.5: Size fractions evaluated and the concentrates combined for each ore

Ore	Size fractions evaluated, μm	Concentrate 1	Concentrate 2	Concentrate 3
Toldos ore (oxide ore)	Unsized; +C2;+ C3;+C4/+C5 and –C5	con1+con2	con3+con4	con5
Tesorera (sulphide ore)	Unsized; +53; +C2;+ C3;+ C4; +C5 and –C5	con1	con2+con3+con4	con5+con6+con7
Jayula (supergene oxide ore)	Unsized; +C2; +C3;C4;+C5 and –C5	con1+con2	con3+con4	con5

The liberation data measured using MLA on a size-by-size basis. Overall stream liberation was calculated based on the distribution of the mineral across each size fraction and the liberation within those size fractions. As described in Chapter 2, Table 2.7, in the context of flotation, particles that contain more than 80% of the valuable mineral by weight are considered floatable and for this reason the ‘liberated’ class includes all particles that contain greater than 80% by weight of the mineral of interest.

3.5.1.4 Quantifying silver deportment

As described in the literature review, the identification of silver carriers is complex. The inability to adequately describe silver deportment for two of the ores, i.e. poor reconciliation between the calculated assay from MLA measurement and the chemical assay for silver; was the main driver for

establishing the Level 2 and Level 3 characterisation protocols. The objective of Level 2 characterisation was to identify the presence of silver in solid solution, while the objective of Level 3 characterisation was to identify the remaining hosts for silver that were still not able to be accounted for by Levels 1 and 2 and had been classified as unknown according to the Mineral Reference Library that had been initially developed for each ore.

In this study, MLA was able to identify 12 silver-bearing minerals in these ores which are present on the mineral reference library. The MLA reference library is used to classify spectra collected during measurement, on average 10 X-ray spectra collected from the same point (each point with around 10,000 counts) are used to generate one standard spectrum to be used in the reference library. Figure 3.5 illustrates a standard spectrum of arsenopyrite (A) from one measurement, and B represent the average arsenopyrite spectrum collected and added to the MLA library.

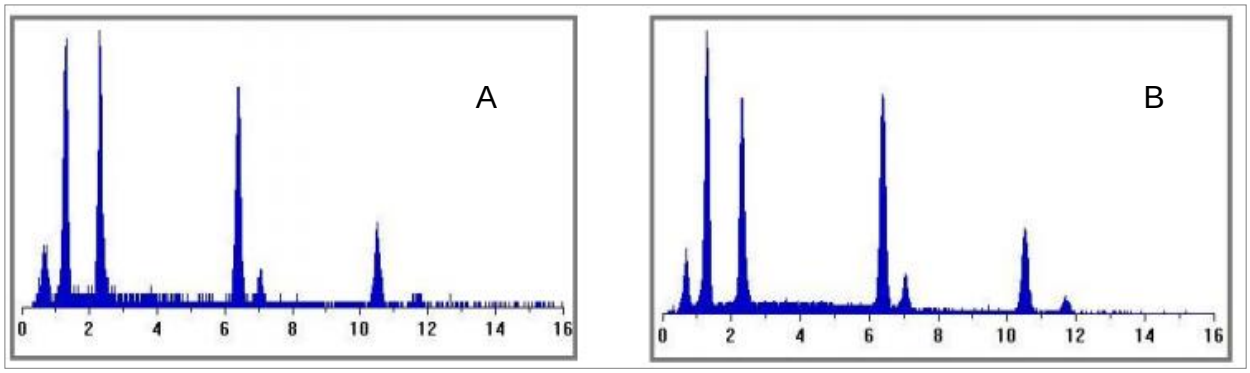

Figure 3.5: A) Arsenopyrite spectrum; B) Average Arsenopyrite spectrum

However, there are some spectra that are misleading or mixed, which are difficult to identify, resulting in those minerals being classified as “unknown”. Unknown minerals are those whose X-ray spectra do not match any in the MLA mineral reference library. This was the case for Jayula ore (supergene oxide ore), in which Ag deportment was not able to be fully reconciled requiring the implementation of Level 3 characterisation.

- ***Novel approach for identification of unknown silver minerals from complex low-grade oxide silver ores.***

This new approach is a combination of manual and auto SEM, EMPA and synchrotron analysis, which were used with the primary objective of identifying silver-bearing minerals that had previously been classified as “unknown”.

The first step in the analysis was to perform elemental mapping using EMPA, to detect any associations between silver and other key elements, such as Pb, S and others. The objective here

was to find any relationship between silver and other elements to assist in the identification of potential minerals hosts for the unaccounted for silver.

The second step in the analysis was to manually search for particles containing grains with high BSE intensity. To clarify the concepts for the purpose of this thesis, the following definitions are worth to mention: grain is always part of a particle or the entire particle and it is composed only for one mineral phase (Figure 3.6). Grains that contain silver are brighter than the grains that contain gangue minerals, which usually have a low BSE value. These bright grains were identified qualitatively using EDS, which was applied in the centre of the grain to search for the spectra that contained silver. Photomicrographs of the surrounding particles were taken for each grain identified that contained Ag, to be available to later identify the grains. The objective was to identify and corroborate spectra that contained Ag.

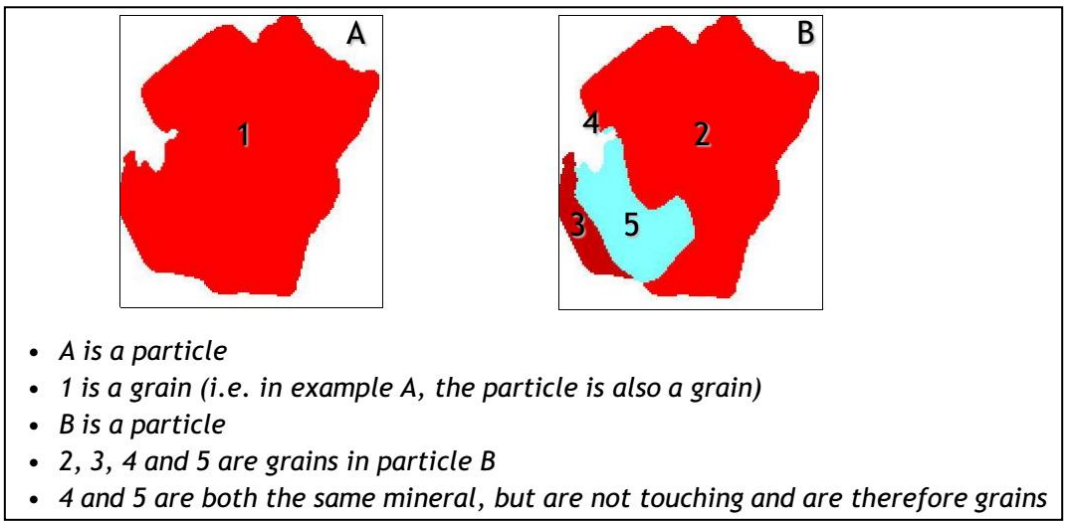

Figure 3.6: Definition of particle and grain.

The third step was to corroborate statistically the presence of new silver minerals or spectra, using an auto SEM-EDS at QUT. In this case, the BSE threshold was set at 120 to identify the bright grains. The results obtained by this apparatus using INCA software helped to identify new spectra, which assisted in improving the silver deportment after being incorporated into the MLA mineral reference library.

Finally, synchrotron analysis using X-ray fluorescence (SXRF) and X-ray diffraction (SXRD) was used to investigate the presence of any other silver minerals that had not been identified through the previous techniques mentioned. Any new spectrum that was identified through this protocol was also incorporated into the MLA mineral reference library.

The new protocol for the identification of unknown silver-bearing minerals is shown in Figure 3.7.

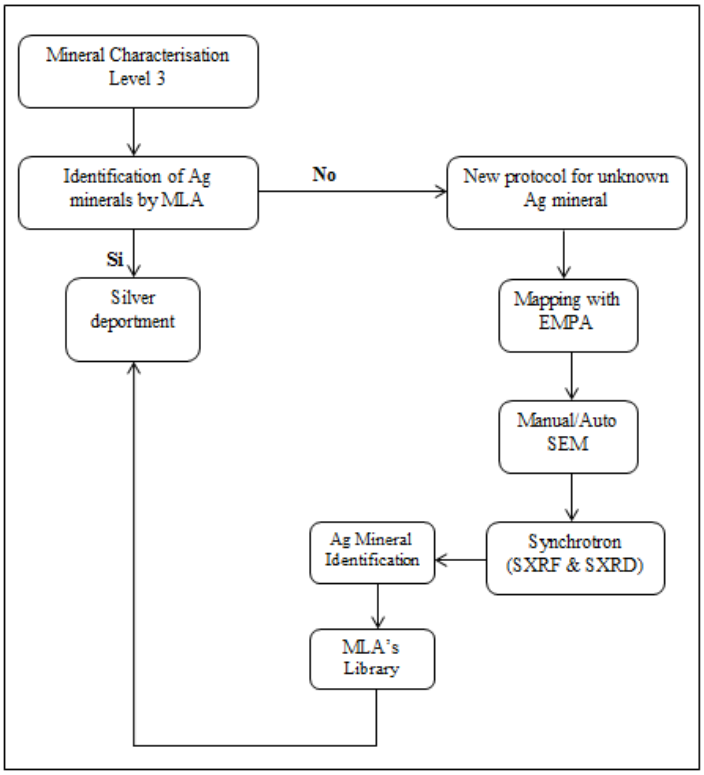

Figure 3.7: New approach to identify the unknown minerals that contain silver

The process is complete when the silver assay reconciliation (MLA assay vs. chemical assay) is adequate, after including solid solution silver in the reconciliation and the addition of any new spectra into the MLA's mineral reference library that were identified as part of Level 3 analysis.

3.5.2 Metallurgical characterisation

For each ore under study, a different flow sheet configuration was used, based on the information obtained from the mineralogical characterisation. In some cases, some of the strategies for floating silver minerals that were discussed in the literature review were adopted; in all cases the flow sheet was optimised to achieve a Ag recovery over 60 %, mass recovery less than 10 % and mill product (flotation feed) size target beginning with a (P80) of 100 μm.

The slurry was transferred from the laboratory batch rod mill (50 % solids) to the 5-litre JKMRC flotation cell (Figure 3.8) with 20 % solids at the natural slurry pH, which was increased (to a pH value depending on the ore type) with the addition of lime during the flotation process. At this point, selective or bulk flotation was undertaken, depending on the silver deportment in the ore. Table 3.6 shows the conditions of the 5-L cell as set for the three case studies.

Figure 3.8: 5-L Flotation cell used for the experiments A: Toldos ore (oxide ore); B: Tesorera ore (sulphide ore) and C: Jayula ore (supergene ore) (Photos taken by J. Quinteros, 2013)

Table 3.6: Conditions for 5-L cell used for the three case studies

Parameter	Unit	Value
Cell volume	L	5
Air flow-rate	L/min	10
Impeller speed	rpm	1000
Percent of solid	wt%	20
Water used in flotation exp.		Brisbane tap water

3.5.2.1 General Batch flotation procedure

The general batch flotation procedure is described in the following lines:

- ✓ The ore was ground at the required P80 using the rod mill at 50 % solids with the required grinding time. After the ore was ground, pH, Eh and temperature of the pulp were measured and recorded.

- ✓ The slurry was then transferred to a 5-L JKMRC bottom-driven batch flotation cell, and fresh water was used to raise the pulp volume of the cell. pH, Eh and temperature of the slurry were measured and recorded. A small injection of air was allowed into the cell to prevent the slurry blocking the air lines of the cell.

- ✓ The pH was adjusted to the required target for flotation using lime. When the pH was adjusted, the impeller was turned on and adjusted to a low speed to prevent solids settling in the bottom of the cell.

- ✓ The required reagents for each ore were introduced into the cell according to the dosage required for each test, with a 1-minute interval between them to allow time for conditioning. The required conditioning time for the sulphidisation stage was 5 minutes. Once the air was changed to nitrogen gas and the sulphidising agent was introduced, the pH, Eh and temperature were recorded at 0, 2, 4 and 5 minutes.

- ✓ The total number of concentrates varied between the ores depending on the strategy used to float the ores. Concentrates were typically collected after 2 minutes of flotation, with the exception of the Toldos ore (oxide ore), for which the first concentrate was collected at 0.3 minutes, the second at 2 minutes, and the following ones at every subsequent 2 minutes of flotation.

- ✓ Each flotation product, and all concentrates and tailings were filtered and dried.

3.5.2.2 Reagents

Different reagents were used for each ore. The function of each type of reagent was briefly described in Chapter 2.

Toldos ore (oxide ore) used activator, pH modifier, a mix of collectors and frother, while Tesorera (sulphide ore) and Jayula (supergene oxide ore) ores used activator, dispersant, pH modifier, sulphidising agent, a mix of collectors and frother. Table 3.7 lists all of the reagents used with these ores. Only some of the reagents provided good flotation responses and these are discussed in the following pages. Note that rigorous optimisation of reagent dosage was not part of the scope of work.

3.5.2.2.1 Collectors

Different collectors were used in this work

- ➢ **Aerophine 3418A**

AEROPHINE 3418A is a sodium-diisobutyl dithiophosphinate (Figure 3.9). It is used at a low dosage, and can provide a significant improvement in the metallurgical parameters for the valuable mineral (recovery and grade). It was developed for copper flotation and activated zinc minerals. However, it was found to be a good collector for complex, polymetallic, and massive sulphide ores. "It is a collector that can also be applied for silver and argentiferous galena" (Cytec, 2010).

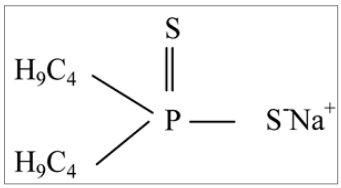

Figure 3.9: Chemical structure of Aerophine 3418A (from Cytec, 2010)

- **Aero 404**

This is used for the flotation of tarnished Pb-Zn minerals, secondary copper minerals and precious metals. It is an excellent collector for pyrite and auriferous pyrite. It is a mercaptobenzothiozole collector.

- **AERO MX-950**

This presents rapid flotation kinetics in coarse middlings, resulting in improved metal recovery. It has demonstrated good recovery of silver. Its formulation corresponds to a modified dithiocarbamate.

- **Potassium amyl xanthate (PAX)**

Potassium amyl xanthate (PAX) is a strong collector (Figure 3.10). Widely used in the flotation of non-ferrous metallic minerals, it is a non-selective collector for sulphide minerals. It is a good collector for the flotation of minerals such as oxidized sulphide, copper and lead ores. It has good results for floating auriferous pyrite.

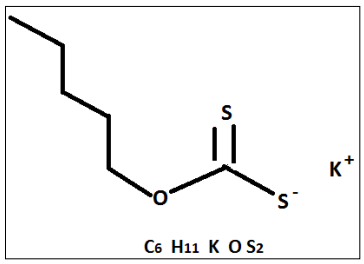

Figure 3.10: Chemical structure of PAX (after Chemical register, 2014)

3.5.2.2.2 Frother

- **Methyl isobutyl carbinol (MIBC)**

Methyl isobutyl carbinol (MIBC) was used as the frother. It comes from the alcohol family. The frother dosage used in all experiments was 75 g/t. Figure 3.11 shows the molecular structure of MIBC.

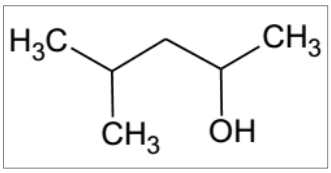

Figure 3.11: Chemical structure of MIBC (after Nicnas, 2014)

Table 3.7: Reagents used in flotation tests

Reagents	Name	Formulation
Activator	Copper sulphate	$CuSO_4$
Dispersant	Sodium silicate	$NaSiO_3$
	D919	Lignosulfonate
	EDTA (ethylenediaminetetra-acetic acid)	
pH modifier	Lime	CaO
	Sulfuric acid	H_2SO_4
Sulphidising agent	Sodium hydrogen sulphide	NaHS
Collector	AERO 404 promoter	Mercaptobenzothiozole formulation
	AEROPHINE 3418A promoter	Dithiophosphinate
	PAX	Potassium amyl xanthate
	AERO MX-950	Modified dithiocarbamate collector (dithiocarbamate and thionocarbamate)
	Aero S-9849 and Aero 6494	Collector (Chelating) alkyl hydroxamates
	Aero 3000C	Collector (Cationic) Amine-based
	Aero 869F	Collector (Anionic) Petroleum sulfonate
	Aero 6697	Alkyl monothiophosphate
	Aero XD-5002 promoter	Modified thionocarbamate
	Sodium oleate	Collector for NSG
	Dodecylsulfonate	Collector for NSG
Frother	MIBC	Methyl isobutyl carbinol

3.5.2.3 Flotation strategies

a) Preflotation

Preflotation tests were performed to determine the presence of floatable minerals in the absence of collector in the ores. The procedures described in this section were used in each case study.

- ✓ 1 kg aliquots of the ore were ground in a laboratory rod mill for the times shown in Table 3.5.
- ✓ The pulp was introduced to the 5L flotation cell and fresh water was introduced (20% of solid was used for flotation).
- ✓ No collectors were used, except frother (MIBC).
- ✓ The concentrates were collected after 2, 4, 6 and 8 minutes of flotation. Only the flotation products of the Toldos ore (oxide ore) case study were analysed through MLA, due to the nature of the silver deportment, which exhibited Ag with natural hydrophobicity.

b) Sulphidisation

- ✓ The pulp was sulphidised with the sulphidising agent (NaHS) after the sulphide concentrates were collected. As air was the gas used for flotation, nitrogen gas was introduced into the cell when NaHS was added in order to change the chemical environment in the pulp to assist in obtaining the required Eh value (-300 mV).

- ✓ After the chemical environment of the pulp had been changed as required, five minutes of conditioning occurred, with the sulphidising agent (NaHS) added at 0, 2, 4 and 5 minutes. The Eh value was set at -300 mV, as measured with a Ag/AgCl electrode.

- ✓ After 5 min of conditioning, the nitrogen was changed to air, and the scheme of reagents was added allowing one minute of conditioning time.

c) Changing grind size

- ✓ Finer P80s were tested for each ore; for Toldos (oxide ore) and Tesorera (sulphide ore) ores a P80 of 50 μm was included, while for Jayula ore (supergene oxide ore), an additional P80 of 25 μm was examined. These extra analyses were made due to the results received from the mineralogical characterisation, indicating that the grain sizes of some of the minerals of interest in each ore were finer and required finer grinding to obtain the necessary degree of liberation.

Figures 3.12, 3.13 and 3.14 show the particle size distribution (PSD) for Toldos (oxide ore), Tesorera (sulphide ore) and Jayula (supergene oxide ore) ores. Note that, for Toldos ore (oxide ore), the PSDs were measured using the Malvern instrument for both P80s, i.e. P80 of 50 and 100 μm. Also, the Malvern instrument was used for Tesorera (sulphide ore) and Jayula (supergene oxide ore) ores to measure P80s of 50 and 25 μm, respectively. The P80 of 100 μm for Tesorera (sulphide ore) and Jayula (supergene oxide ore) ores was measured using dry sieving and the cyclosizer.

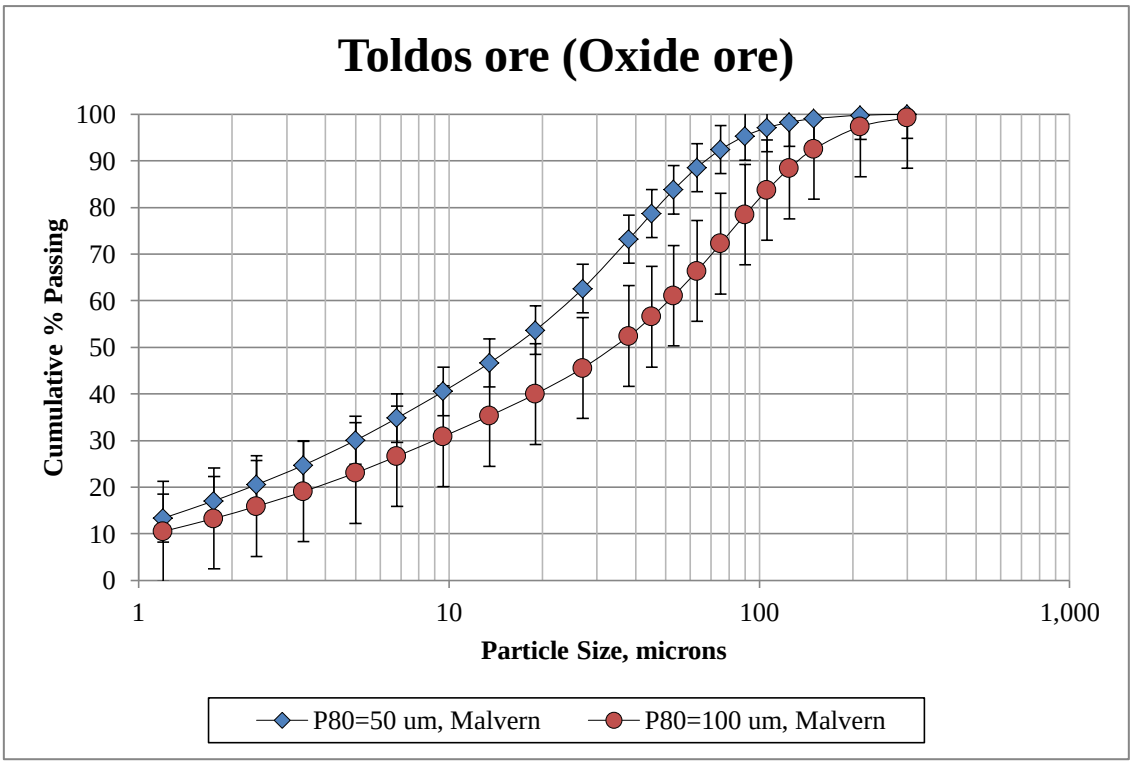

Figure 3.12: Particle size distribution for P80 of 50 and 100 microns for Toldos ore (oxide ore) using Malvern instrument with 95 % confidence.

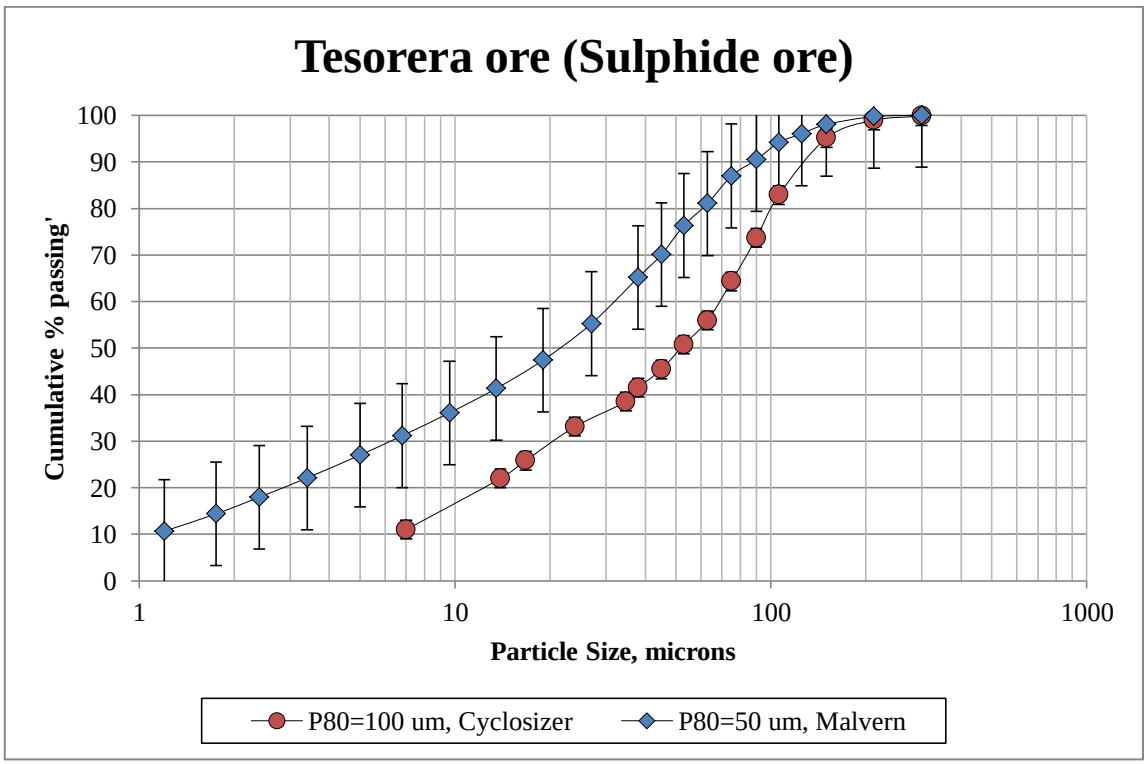

Figure 3.13: Particle size distribution for P80 of 50 and 100 microns for Tesorera ore (sulphide ore) with 95 % confidence.

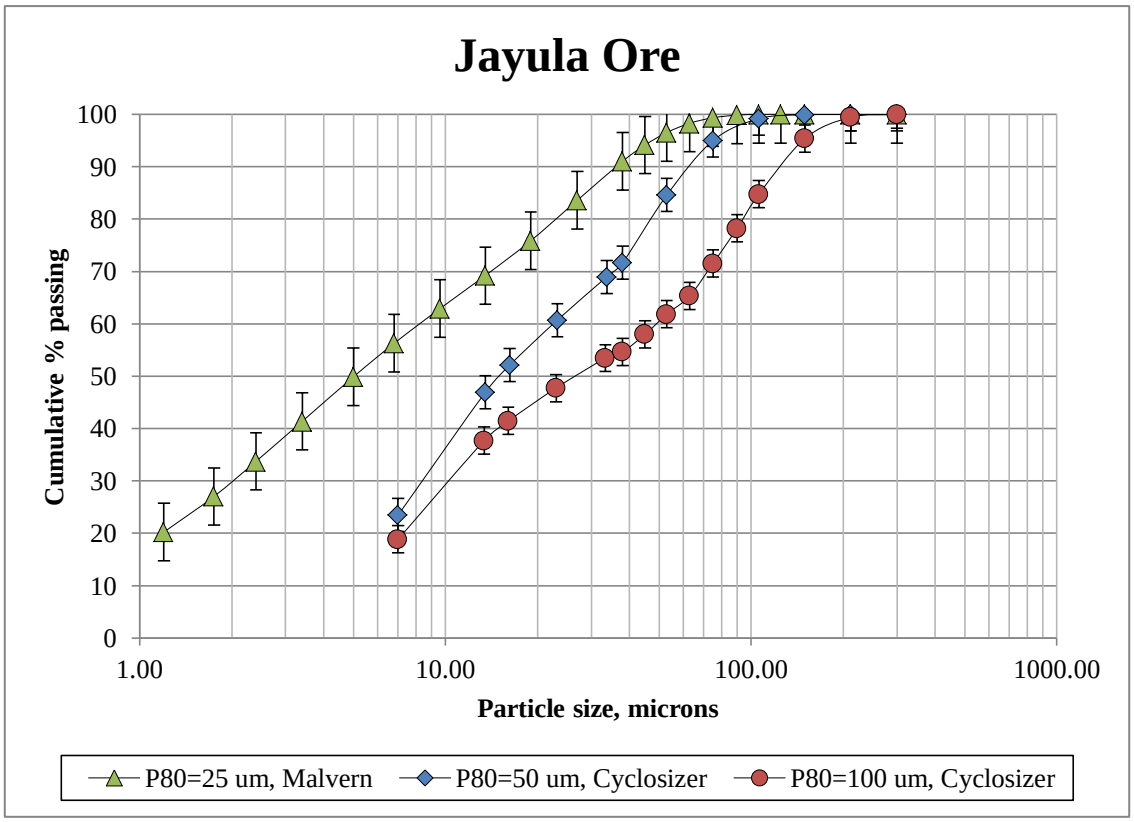

Figure 3.14: Particle size distribution for P80 of 25, 50 and 100 microns for Jayula ore (supergene oxide ore) with 95 % confidence.

➢ **Mainstream inert grinding (MIG) procedure**

Mainstream inert grinding (MIG) is a process applied in some industrial plants at presents (Rule, 2011) and was used in this study for Tesorera ore (sulphide ore). The reasons for choosing this extra grinding step are elaborated in Chapter 5. This new procedure aimed to improve the liberation of the minerals of interest in the coarser particle size fractions, to further increase the recovery in flotation.

MIG was incorporated into the laboratory flotation flow sheet as follows. The ground sample, with a P80 of 100 µm, was wet sieved at 75 µm and the coarse fraction was reground to a P80 value of 50 µm. The reground portion of the feed joined the -75 µm material from wet screening to produce a combined P80 of 56 microns.

3.5.2.4 Experimental design

To improve the flotation results with the Toldos ore (oxide ore) and Jayula (supergene oxide ore) ores, a factorial design (2^2) was proposed and used, aiming to improve understanding of the key flotation parameters that affect the flotation response of each ore. For this study, the 80 percent

passing size of the flotation feed and the collector dosage were tested. The results are described in the Chapters 4 and 6 for Toldos ore (oxide ore) and Jayula ore (supergene oxide ore) respectively.

In the cases of the Tesorera (sulphide ore) and Jayula (supergene oxide ore) ores, the method of changing "one factor at a time" was used to find the best conditions for obtaining optimal recoveries and grades for both ores. For Tesorera ore (sulphide ore) this approach helped to find the best flow sheet configuration which contained the MIG procedure for preparing the feed and using the sulphidising agent and the proper reagents to allow the flotation of this ore.

When the best flow sheet was achieved for each ore replicate tests were performed to obtain an estimate of the experimental error.

3.6 Flotation analysis

3.6.1 Batch flotation test

There are a number of parameters that can be calculated and used to assess the outcomes of a batch flotation test. These calculations are used to understand the flotation response of key minerals and to provide explanations as to their appearance in either the concentrate or tailings streams. These calculations can be performed on an unsized or size-by-size basis, using mass balanced data.

In each case study, the overall elemental, mineral and water recoveries were calculated as well as the rate constants for each test, and the entrainment value based on the following equations.

- The recovery (Rec) is defined as the recovery of the valuable element or mineral in the concentrate out of the total element or mineral present in the feed

$$Rec = \frac{Cc}{Ff} x\ 100 \qquad (3.1)$$

Where, C and F are the solid mass flow in the concentrate and the feed respectively, while c and f are the grades of the valuable minerals present in the concentrate and the feed respectively.

- The water recovery (Rec_w) is calculated as

$$Rec_w = \frac{Wc}{Wf}\ x\ 100 \qquad (3.2)$$

Where W_c and W_f are defined as the water mass flow present in the concentrate and the feed respectively.

- The rate constants (k) for elements and minerals were calculated using Garcia-Zuniga's (1935) equation:

$$\text{Rec} = 1 - \exp^{(-\text{kt})} \qquad (3.3)$$

Where Rec is the overall recovery in a specific flotation time.

- Entrainment is defined as non-selective recovery that affects both valuable and non-valuable minerals since both of these are suspended in the water in the pulp. Entrainment is a major mechanism for the recovery of (liberated) gangue mineral and is, therefore, problematic (Lynch *et al.,* 1981). The degree of entrainment (Savassi *et al.*,1998) needs to be quantified in order to calculate the recovery by true flotation, which is the recovery of particles that are attached to bubbles:

$$ENT = \left(\frac{W_c}{W_T}\right) \qquad (3.4)$$

$$Rec_{ENT} = \left(\frac{1-Rec}{1-R_w}\right) xENTxRec_w \qquad (3.5)$$

$$Rec_{True\ flotation} = Rec - Rec_{ENT} \qquad (3.6)$$

Where ENT is the degree of entrainment, and W_c and W_T are the mass flow rate of tracer in the concentrate and tailings respectively. Rec_{ENT} is the recovery through entrainment, and $Rec_{True\ flotation}$ is the recovery by true flotation.

3.6.2 Size-by-size and Size-by-liberation analysis

Size-by-size and size-by-liberation analyses were performed for each of the flotation products. Calculation of elemental and mineral recovery-by-size was performed using the following equation.

$$Rec_{i,j} = \frac{C_{i,j}}{F_{i.j}} \qquad (3.7)$$

Where

$C_{i,j}$ and $F_{i,j}$ are the flow of particle size "i" and mineral liberation class "j" in the concentrate and feed respectively.

The liberation classes used in this thesis work are based on particle composition and are divided into the following classes: liberated (containing more than 80% of the mineral of interest), binary

composites (containing the mineral of interest and one other mineral) and ternary composites (containing the mineral of interest and at least two other minerals).

3.7 Errors from measurements and calculations

There are many sources of error when flotation experiments are carried out. Examples of these sources of errors are sampling, feed preparation, assaying, by operator, machine and others. It is important to understand the contribution of these errors to uncertainties in the experimental results which will impact on the interpretations made from the data.

3.7.1 Propagation of error analysis of recovery distribution

A propagation of error analysis was performed with respect to overall recovery values. The analysis is acquired from the recovery expression given by Equation 3.1:

$$Rec = \frac{Cc}{Ff} x\ 100$$

The expression for the specific error of the flotation recovery can be estimated using Equation 3.8.

$$Error_{Rec} = \frac{\partial Rec}{\partial C} * SD_C^2 + \frac{\partial Rec}{\partial c} * SD_c^2 + \frac{\partial Rec}{\partial F} * SD_F^2 + \frac{\partial Rec}{\partial f} * SD_f^2 \quad (3.8)$$

The standard deviation (SD) was assumed as 5%, and Rec is recovery.
The partial derivatives can be directly computed as follows:

$$\frac{\partial Rec}{\partial C} = \frac{C}{Ff} \quad (3.9)$$

$$\frac{\partial Rec}{\partial c} = \frac{c}{Ff} \quad (3.10)$$

$$\frac{\partial Rec}{\partial F} = \frac{F}{F^2 f} \quad (3.11)$$

$$\frac{\partial Rec}{\partial f} = \frac{f}{Ff^2} \quad (3.12)$$

3.7.2 Confidence limits

Confidence limits at 95% confidence were used for estimating the confidence in the mineralogical parameters. It was calculated as the following Equation:

$$confidence\ limits = \mu \pm \frac{\sigma}{\sqrt{n}} * 1.96 \quad (3.13)$$

Where:

μ: average
σ: standard deviation
n: number of observations or analysis

3.7.3 Bootstrap resampling methodology

Following the approach of Evans and Napier-Munn (2013) the bootstrap resampling technique was used to double check the confidence limits at 95% for the mineralogical attributes. Evans and Napier-Munn (*op. cit.)* commented that this methodology "provides rapid calculation of the large number of bootstrap samples".

The methodology used the population of the one polished sample block and takes M random subsets of N particles. For the mineralogical attributes M = 500.

The mean (μ) and standard deviation (σ) were calculated across 500 samples. Using Microsoft Excel the methodology was applied to the upper and the lower limits.

3.8 Summary of the methodologies used for each ore

Table 3.8 presents a summary of the methodologies used in each case study, namely Toldos (oxide ore), Tesorera (sulphide ore) and Jayula (supergene oxide ore) ores respectively.

Table 3.8: Methodologies used in each case study

Characterisation	***Toldos ore (oxide ore)***	***Tesorera ore (sulphide ore)***	***Jayula (supergene oxide ore)***
Mineral	Level 1 and mill product (flotation feed) characterisation	Level 2 and mill product (flotation feed) characterisation	Level 3 and mill product (flotation feed) characterisation
Metallurgical	Pre-flotation Flow sheet design Experimental design	Pre-flotation Flow sheet design Experimental design	Pre-flotation Flow sheet design Experimental design
Flotation product	Unsized and size-by-size analysis for concentrates and tailings	Unsized and size-by-size analysis for concentrates and tailings	Unsized and size-by-size analysis for concentrates and tailings

Chapter IV:

Selective flotation for a complex oxide low-grade silver ore: "Toldos Ore"

Chapter 4 describes the results of the mineralogical, metallurgical and flotation product characterisation for Toldos ore (oxide ore). The ore characterisation identified the presence of at least eight silver-bearing minerals including coarse grained chlorargyrite and acanthite. Mineralogical analysis of preflotation test samples indicated that acanthite exhibited natural hydrophobicity. These results together with the mineralogical characterisation indicated that selective flotation would be an appropriate processing route for this ore. An experimental design was used to optimise some of the flotation conditions. The flotation products were studied on an overall and size-by-size basis, with the final flow sheet producing a rougher concentrate that contained 4404 ppm of Ag, at a recovery of 83.8%.

4.1 Mineralogical characterisation

Level 1 characterisation (as described in Chapter 3) was applied to Toldos ore (oxide ore). The results of this characterisation are presented and described in the following sections, giving the key mineralogical attributes that allowed development of an effective flow sheet for recovering silver from this ore.

4.1.1 Level 1

The oxide ore used methodology Level 1 to identify the mineralogical attributes for this ore. The analytical techniques used were chemical assay, XRD, oxide characterisation of lead and zinc, optical microscopy and mineral liberation analyser. In the following sections the output of these techniques is described.

4.1.1.1 Chemical assay

The concentration of silver in the ore was 406 ± 77 ppm, which is the highest silver assay for the three ores under study. Size-by-size analysis of the head (Table 4.1) indicated that the -212/+150 μm size fraction had the highest silver assay (611 ppm) while the finest size fraction evaluated (-38 μm) had the lowest silver assay. The bulk assay for sulphur, lead and zinc showed a low content of these elements, with 0.47%, 0.15% and 0.13% respectively.

Table 4.1: Elemental assays on overall and size-by-size bases of the feed

Size, mm	Ag	Al	As	Cu	Fe	Pb	S	Zn
	ppm	%	Ppm	ppm	%	ppm	%	ppm
Head	406	4.74	640	80	7.74	1520	0.47	1290
+2.36	324	4.9	520	60	7.57	1010	0.37	990
+1.7	326	4.54	680	60	7.61	1310	0.34	1010
+1.18	289	4.58	600	70	8.01	1240	0.37	1090
+0.850	389	4.94	610	80	8.01	1360	0.4	1130
+0.600	533	4.97	710	100	9.1	1580	0.39	1210
+0.425	523	5.39	660	130	8.69	1630	0.45	1230
+0.300	526	5.03	670	120	8.66	1770	0.44	1300
+0.212	522	5.07	710	130	8.84	1930	0.6	1370
+0.150	611	5.2	760	160	8.95	2110	0.46	1480
+0.106	532	5.24	740	140	8.96	2200	0.45	1470
+0.075	508	5.17	780	180	9.13	2280	0.39	1540
+0.053	483	4.58	860	280	9.29	2510	0.44	1620
+0.038	473	5.14	930	650	9.82	2860	0.39	1710
-0.038	265	6.97	870	290	9.81	2660	0.41	2290
Calc Hd	***384***	***5.02***	***659***	***111***	***8.28***	***1535***	***0.39***	***1236***

4.1.1.2 X-ray diffraction (XRD)

X-ray diffraction (XRD) results are shown in Table 4.2, indicating that alkali feldspar is the dominant gangue mineral present in Toldos ore (oxide ore), followed by quartz, with the minor minerals identified as hematite and mica. Mica is likely to be muscovite or illite.

Table 4.2: XRD results for Toldos ore (oxide ore) (provided by AMDEL)

Mineral	Composition	JK2681-3
Quartz	SiO_2	Sub-Dominant (>20%)
Alkali Feldspar	$KAlSi_3O_8$	Dominant (>50%)
Hematite	Fe_2O_3	Minor (5-20%)
Mica	$(X_2Y_{4-6}Z_8O_{20}(OH,F)_4)^*$	Minor (5-20%)

*X is K, Na or Ca, or less commonly, Ba, Rb, or Cs; Y is Al, Mg, or Fe, or less commonly, Mn, Cr, Ti, Li, etc.; Z is Si or Al, however it could include Fe^{3+} or Ti.

4.1.1.3 Oxide characterisation of lead and zinc minerals

The results of this characterisation (Table 4.3) indicated the amount of oxide form that is present for lead (Pb) and zinc (Zn) minerals that can be present in the ores. Toldos ore displayed the highest proportion of lead and zinc oxide for minerals in the three ores under study, with 21.2% and 16.5%, respectively. It is indicated that this ore had an elevated percentage of oxide materials compared to the other ore samples.

Table 4.3: Results for oxide characterisation of lead and zinc minerals present in Toldos ore (oxide ore) (provided by AMDEL)

Element Measurement	Total %
Pb as oxide minerals	21.2
Zn as oxide minerals	16.5

4.1.1.4 Optical Microscopy

The mineralogy from the optical microscopy (Table 4.4) indicated that the matrix present was non-sulphide gangue (NSG), predominately represented by feldspars, quartz and other minerals. Iron oxides (hematite and magnetite) were present as minor minerals in the ore, and mainly associated with the NSG as hydrated and leached occurrences. Knights (2011) described these occurrences as "specular hematite alteration after magnetite". The genesis of the occurrences present in this ore were considered to be from leached, colloformic and partial box work replacement, giving the characteristic colour of the ore as dark brown (Knights, 2011). The observations from optical microscopy were in agreement with the results from XRD analysis.

Table 4.4: Estimated modal volumetric mineral distribution for Toldos ore (oxide ore) (after Knights, 2011)

Volumetric mineral distribution	Mineral present
Dominant (>80 vol %)	Non-sulphide gangue: Feldspar>>quartz>carbonates>clay>mica>barite
Minor (5>x>0.5 vol %)	- Hematite>>magnetite ~ 5% - Lead-iron-arsenates ~1%: beudantite & gabrielsonite - Limonite ~ 0.3%
Sparse* (x<< 0.5 vol%)	Rutile, apatite, arsenopyrite, chlorargyrite, undifferentiated Mn oxides, acanthite, pyrite, native silver & chalcopyrite.

*In petrography sparse mineral distribution is considered as accessory minerals

Sulphide minerals were rare in the ore. Figure 4.1 shows an arsenopyrite grain that was seen as a rhomboid-shaped crystal enveloped by NSG. Two grains of native silver can be seen in the same photomicrograph.

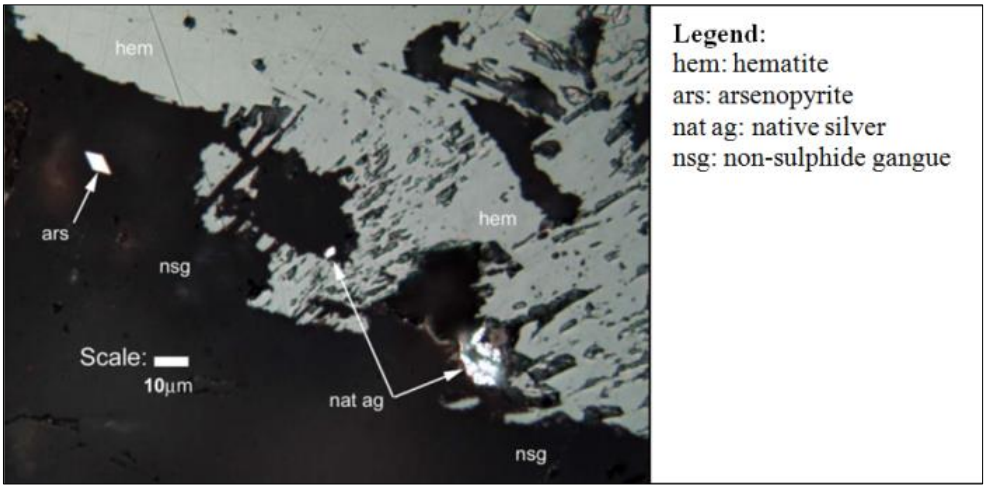

Figure 4.1: Photomicrograph of arsenopyrite, hematite, non-sulphide gangue and native silver (after Knights, 2011).

The silver minerals identified (in order of abundance) were chlorargyrite, followed by possible gabrielsonite (lead-iron bearing arsenate oxy-salt), acanthite and native silver in lesser amounts. Observations from optical microscopy suggested that to upgrade silver from this ore using flotation may be difficult due to the lack of sulphides (Knights, 2011). Figure 4.2 illustrates the occurrence of chlorargyrite (Ag halide). The scale bar indicates that the grain size is relatively coarse for this ore.

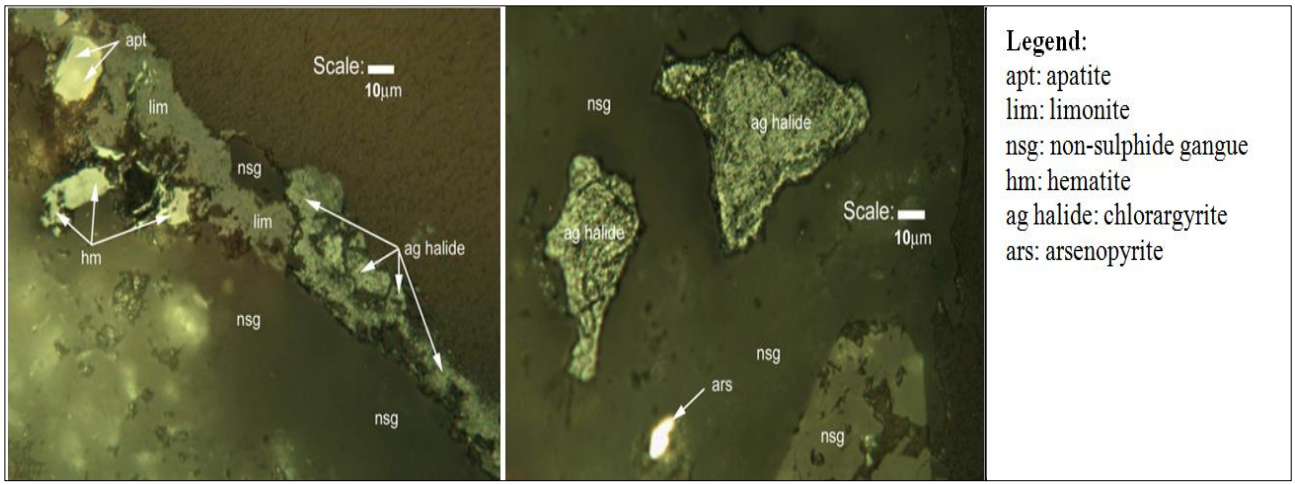

Figure 4.2: Photomicrograph of chlorargyrite, apatite, arsenopyrite, hematite, non-sulphide gangue and limonite (after Knights, 2011).

4.1.1.5 Mineral Liberation Analyser (MLA)

MLA analysed a total of 809,091 grains with 11,134 particles measured (for -425/+300 μm), and 440,275 grains with 4,783 particles (for -1.18mm/+850 μm). Both size fractions were used to estimate the key mineralogical attributes, such as modal mineralogy, elemental deportment, and texture for the ore.

a) Modal Mineralogy

The MLA analysis of Toldos ore (oxide ore) identified the presence of approximately 50 different minerals (see *Appendix D*) with feldspar, quartz, carbonates, clays_micas and iron oxides accounting for the majority of the gangue matrix as shown in Table 4.5. These results were consistent with both optical microscopy and XRD analysis and confirmed the low quantity of sulphide minerals in the ore.

Table 4.5: Modal mineralogy for Toldos ore (oxide ore) with 95% confidence limits included

Mineral	-425/+300 μm		-1.18mm/+850 μm	
	Average, Wt%	St dev	Average, Wt%	St dev
Ag_minerals	0.1±0.06	0.1	0.03±0.02	0.0
Mn(Pb) Oxide	0.6±0.14	0.1	0.1±0.05	0.1
Pb Arsenates	0.2±0.08	0.1	0.1±0.06	0.1
Pb Phosphate	0.3±0.04	0.0	0.2±0.09	0.1
Quartz	15.2±0.50	0.5	13.6±0.56	0.6
Feldspar	54.9±1.64	1.7	62.1±3.13	3.2
Clays_micas	9.0±0.44	0.5	7.5±0.52	0.5
Other Silicates	1.3±0.20	0.2	0.6±0.05	0.1
Fe Oxide	6.7±0.42	0.4	6.7±1.98	2.0
Carbonates	8.1±0.56	0.6	6.3±0.85	0.9
Sulphates	2.9±0.14	0.1	1.9±1.35	1.4
Others	0.5±0.08	0.1	0.9±0.09	0.1
Total	100		100	

b) Elemental deportment

Analysis of the elemental deportment for Toldos ore (oxide ore) focused on Ag carriers due to the presence of large grains of chlorargyrite, native silver and other silver-bearing minerals identified using both optical microscopy and MLA.

Silver deportment was accounted for by the presence of nine different minerals that carry silver, namely chlorargyrite, coronadite, acanthite, gabrielsonite, pyrargyrite, native silver, tetrahedrite, freibergite and arsenopolybasite. Table 4.6 shows the values for -1.18 mm/+850 μm and -425/+300 μm. It is noticed that the silver deportment in acanthite (-425/+300 um fraction) and chlorargyrite (-1.18 mm/+850 um fraction) reported high standard deviations values. This is mainly due to that large particles of both minerals were present in the sample block.

Table 4.6: Elemental deportment for Ag with 95% confidence

Mineral	425/+300 μm		-1.18mm/+850 μm	
	Average, Ag (%)	St Dev	Average, Ag (%)	St Dev
Native Silver	0.4±0.0	0.02	13.3±8.9	9.1
Acanthite	12.3±11.8	12.04	24.9±10.3	10.5
Arsenopolybasite	0.1±0.0	0.03	0.1±0.1	0.1
Pyrargyrite	1.5±0.6	0.62	3.2±1.4	1.4
Tetrahedrite	1.2±0.0	0.00	0.3±0.5	0.5
Freibergite	0.4±0.1	0.14	0.6±0.6	0.7
Chlorargyrite	47.5±30.9	31.52	16.3±24.5	25.0
Coronadite	32.8±26.4	26.91	30.0±9.2	9.3
Gabrielsonite	3.9±2.1	2.19	11.4±9.9	10.1
Total	100		100	

c) Texture:

❖ ***Mineral grain size:***

The mineral grain size distributions of all silver minerals were grouped together to improve the number of observations and the confidence limits were evaluated using the bootstrap resampling technique presented by Evans (2010) and Evans and Naper-Munn (2013). The graph in Figure 4.3 shows that the silver minerals had a mineral grain size with a P80 of approximately 240 μm, this type of particle is expected as the size fraction measured was -425/+300 μm. Pittard, 2010 also argue that when mineralogical analysis is performed in small or trace constituents, that is the case of this thesis i.e., silver; the key constituent is distributed on a small scale in the material to be sampled. Therefore, liberated or not, the coarsest grains of such constituent must be measured and placed into the context of their average

This is consistent with the observations from the optical microscopy. It is reasonably expected that a P80 of 100 μm in grinding would produce a large proportion of liberated Ag minerals. Also, MSC has proposed the constraint that a P80 of 100 μm need to be tested.

From Figure 4.3 and based on the grain size, it can be pointed out that when mineralogical analysis is performed in small or trace constituents, that is the case of this thesis; the key constituent is distributed on a small scale in the material to be sampled. Therefore, "liberated or not, the coarsest grains of such constituent must be measured and placed into the context of their average (Pitard, 2010)". Therefore, in this case P80 of 100 microns is considered to be properly chosen. Indeed this was confirmed with the flotation results and the stepped in the graph helped to choose the P80. If the grains > 100 μm are removed, the P80 of 100 microns was obviously reduced and in that case of course the P80 suggested would be lower than 100 microns.

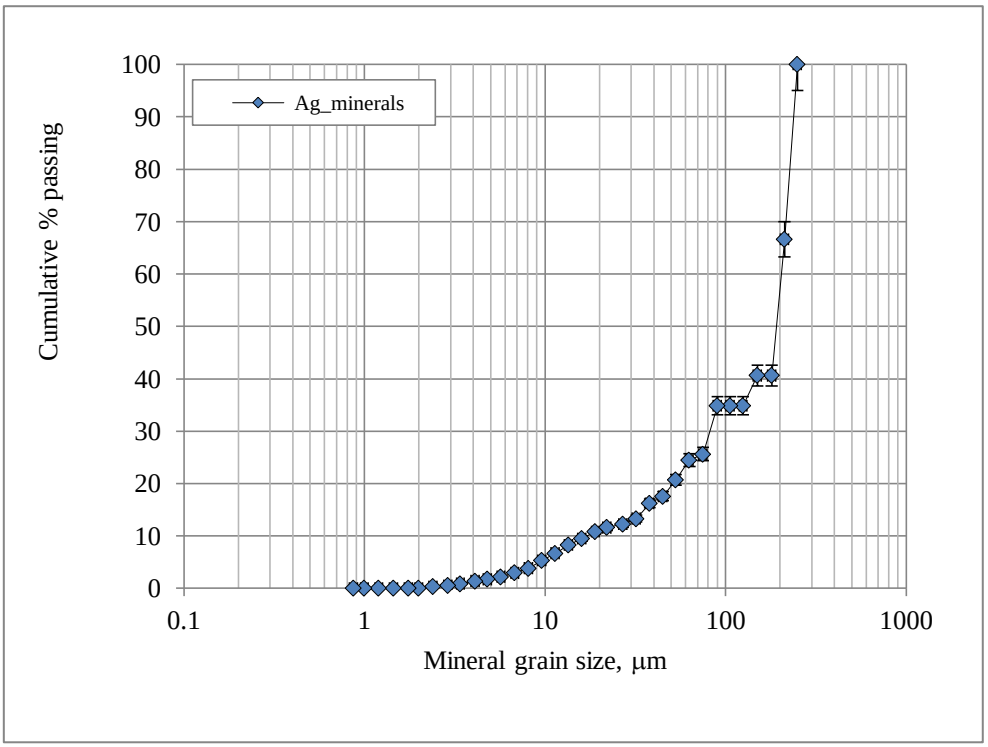

Figure 4.3: Mineral grain size distributions for the combined Ag minerals for Toldos ore (oxide ore).

❖ ***Mineral association:***

The mineral association information was used to find if there were any Ag minerals that tended to associate with any minerals that may be considered problematic in a flotation context e.g. clays. It was also used to establish if any Ag minerals were associated with minerals which were recoverable by flotation, to assist with design of a processing strategy. The results shown in Figure 4.4 indicate that silver-bearing minerals were associated mainly with lead arsenates (32.6% with gabrielsonite), followed by carbonates (siderite and rhodochrosite_siderite) and to a lesser extent, with quartz and hematite. A small amount of silver was found to be associated with lead phosphates, feldspar, sulphates, clays and micas, and other silicates. In addition, 16.2% of the silver-bearing minerals showed free surfaces, i.e, the proportion of the total surface of the Ag minerals that was exposed and ready for flotation or leaching.

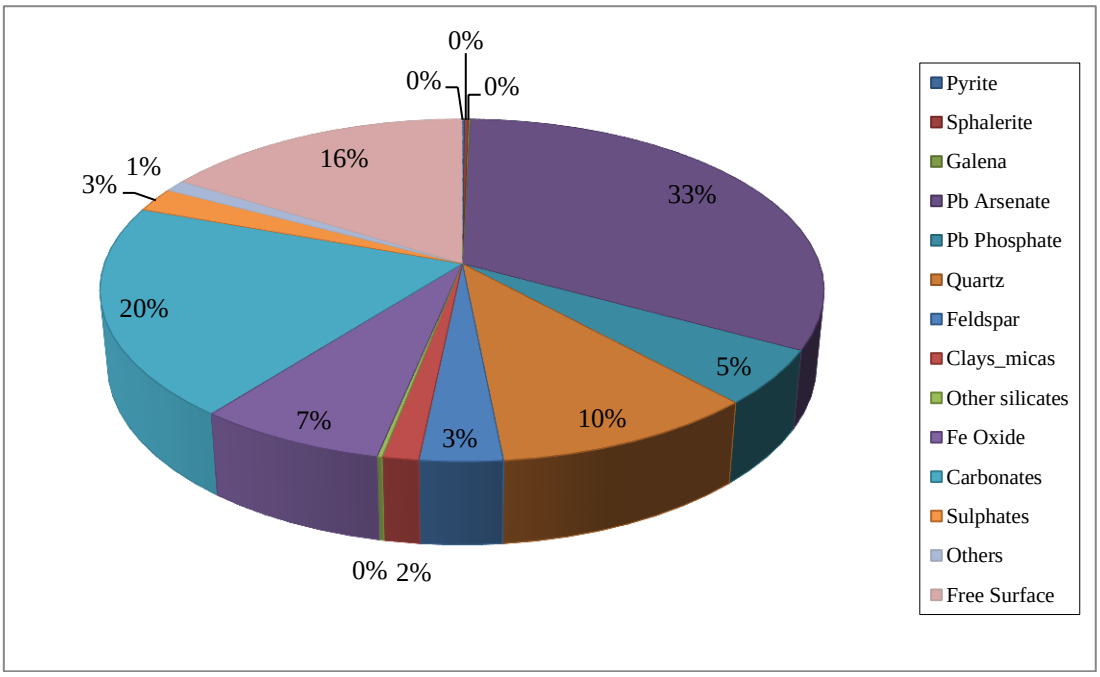

Figure 4.4: Mineral association for silver minerals in Toldos ore (oxide ore) at -425/+300 μm

A range of textures was present in the unbroken ore from Toldos (oxide ore). To illustrate some of these, selected images have been chosen as examples. Figure 4.5 shows examples of the complexity of the mineral textures in different particles in the -425/+ 300 μm size fraction. It can be seen that the Mn(Pb) oxide rims the grains of carbonates and that carbonates are intergrown with Pb phosphates. Figure 4.6 illustrates a complex texture where Ag minerals are intergrown with Pb arsenates and quartz. Also, an example of the compositional variation in this ore is illustrated in Figure 4.7, which shows the BSE image and the elemental mapping for Pb, Mn and Ag; it shows the textural evidence of the growth history of this particle (MnPb) through the bandings. The origin of a band is that, when an ore is forming, different fluids and conditions cause various minerals to precipitate in a sequence. This usually contains variable amounts of minor elements, in this case Ag (Craig, 2001).

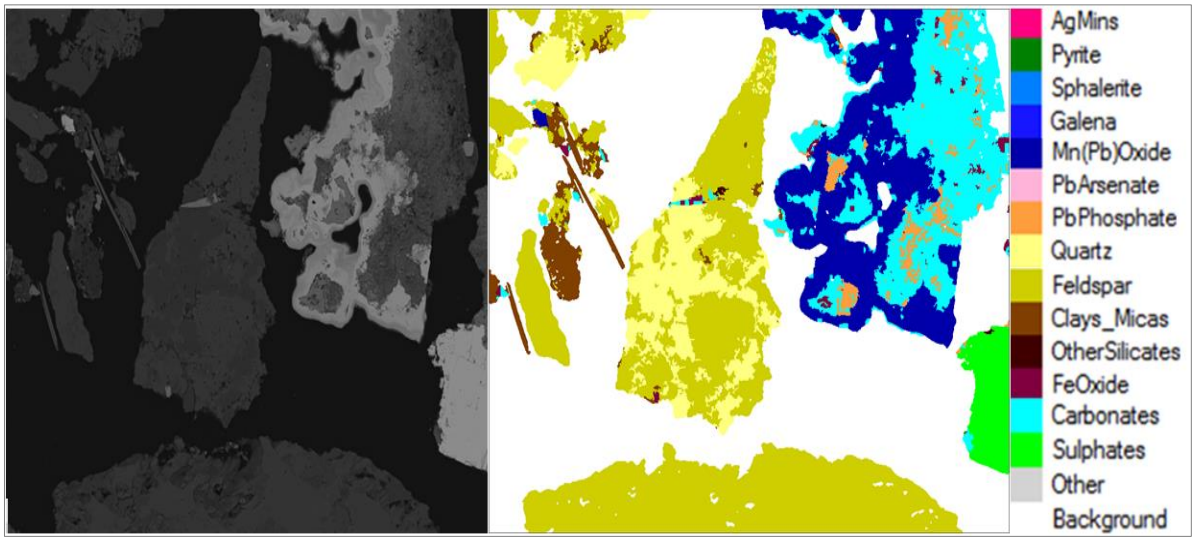

Figure 4.5: BSE and classified images in the -425/ +300 µm size fraction

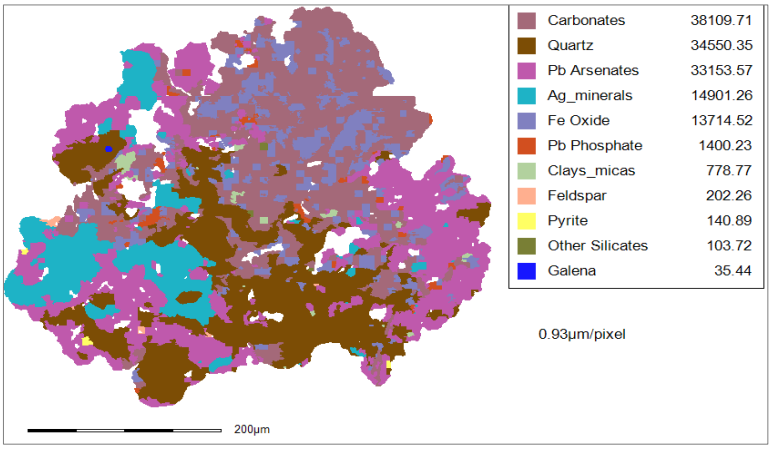

Figure 4.6: MLA image of a particle containing Ag_minerals

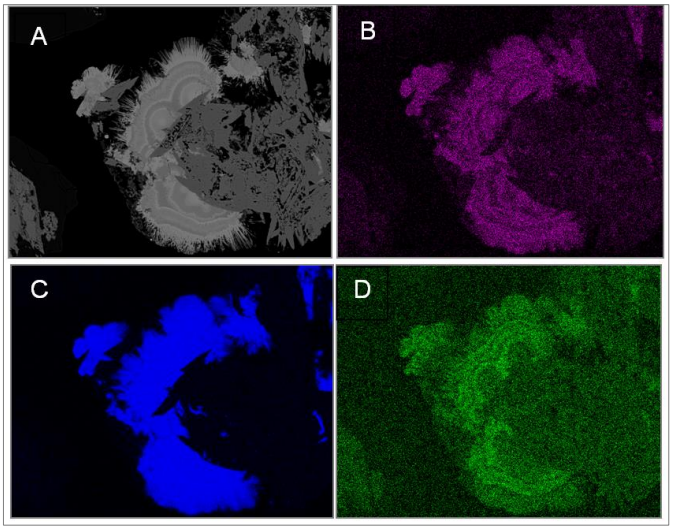

Figure 4.7: Map of Mn(Pb) oxide particle (A) in BSE image, (B), (C) and (D) showing a mapping of lead, manganese and silver elements respectively (from Wightman, 2011).

- ***Assessment from Level 1***

Table 4.7 presents a summary of the outcomes from Level 1 characterisation

Table 4.7: Assessment of Level 1

Techniques	Chemical assay	XRD	Oxide characterisation	Optical microscopy	MLA
Comment	Recalculated head assay for Ag is 384 ppm	Dominant gangue feldspar, followed by quartz	Pb ox: 21.2% Zn ox: 16.5%	Congruent with gangue mineralogy reported by XRD. Ore present as complex textures. Ag deportment: chlorargyrite, Pb arsenates, acanthite, nat. Ag	In agreement with XRD and optical microscopy for gangue mineralogy. Ag min represents 0.1±0.06% of modal mineralogy. Ag deportment: chlorargyrite, coronadite, acanthite, gabrielsonite and other Ag min. Chlorargyrite present as coarse grains thus no fine grinding required for Ag min liberation.

4.1.2 Mill product characterisation for Toldos ore (oxide ore)

The results of a flotation feed characterisation illustrate the status of the ore prior to a flotation test, allowing understanding of the final requirements for grinding in order to develop a flow sheet for processing this complex oxide low-grade silver ore.

For Toldos ore (oxide ore), the levels of liberation by mass of Ag minerals (Ag mins), Pb oxides and NSG were analysed at P80 of 50 microns and the liberation at the P80 of 100 μm was estimated using calculation methods shown in *Appendix G* (Table 4.8). Ag mins and Pb oxides presented a higher degree of liberation at 50 μm when compared with a P80 of 100 μm, while the level of liberation for NSG showed no difference for both P80s. For the Ag mins and the Pb oxides, the change in the level of liberation for the two different feed sizes was modest. This supports that coarse grinding (P80 of 100 μm) will allow reasonable Ag recoveries with the use of flotation as the primary treatment for this ore.

Table 4.8: Level of liberation for Toldos ore (oxide ore) at two P80s

Mineral group	Level of liberation in feed (%)	
	P80	
	100 μm	50 μm
Ag mins	53.7	62.8
Pb oxides mins	55.5	59.1
NSG	99.0	99.0

Key findings of mineralogical characterisation

The results from Level 1 characterisation of the ore resulted in the following key findings:

The valuable element of silver was accounted for by chlorargyrite, coronadite, acanthite, gabrielsonite and other silver minerals (shown in Table 4.6), while the main NSG present were feldspar, quartz and clay_micas.

Silver in the -425/+300 μm fraction of the ore head is mainly associated with Mn(Pb) oxides, followed by Pb arsenates and in lesser extension to Ag_minerals, being these the silver carriers. Complex textures are present in the coarse particulates (-1.18 mm/+850 μm and -425/+300 μm) analysed and include features such as rimming minerals and intergrowth textures.

The mineral grain size for silver minerals (-425/+300 μm size fraction) was coarse in the ore characterisation samples, due to the presence of large grains of chlorargyrite (with a P80 of 240 μm) indicating fine grinding would not be required to achieve sufficient levels of liberation for flotation separation; this was supported by liberation analysis of the flotation feed.

The information gained from the mineralogical characterisation of this ore suggested that selective flotation would be appropriate to recover the silver minerals. The selection of proper reagents (collectors) would selectively render the silver minerals floatable relative to the NSG present, noting that the ore contained minimal base metal sulphides.

4.2 Results of metallurgical characterisation for Toldos ore (oxide ore)

The main objective of the metallurgical characterisation was to investigate how the Toldos ore (oxide ore) would respond to flotation, by using a combination of preflotation (to identify naturally hydrophobic minerals in the ore) and a factorial experimental design (to optimise grind size and reagent addition).

4.2.1 Preliminary preflotation results

Results of the preflotation test are presented in Table 4.9. These results show that more than 40% of the silver can be recovered at grade of 3643 ppm with a mass recovery of 5.7% in the absence of collector indicating the presence of naturally hydrophobic silver minerals. The recovery of other potential elements of interest including copper and zinc were comparatively much lower. This result also indicated the potential for achieving high selectivity for silver through flotation.

Table 4.9: Preflotation results for each concentrate and for the combined concentrate

Streams	Mass		Assays						Recovery (%)					
	grams	%	Ag*	Cu*	Fe (%)	Pb*	S (%)	Zn*	Ag	Cu	Fe	Pb	S	Zn
Feed	1000													
Con 1	11.9	1.2	9505	1225	7.3	4660	0.7	3950	22.1	12.9	1.1	3.6	2.1	3.7
Con 2	5.2	0.5	11195	985	7.3	4520	0.6	3225	11.4	4.6	0.5	1.5	0.8	1.3
Con 3	23.2	2.3	1222	200	7.2	1785	0.4	1705	5.5	4.1	2.2	2.7	2.3	3.1
Con 4	16.8	1.6	485	188	7.4	1654	0.4	1770	1.6	2.8	1.6	1.8	1.5	2.3
Total Con	57.1	5.7	3643	482	7.3	2595	0.5	2331	40.6	24.4	5.4	9.6	6.8	10.5
Tail	944.5	94.3	322	90	7.7	1480	0.4	1205	59.4	75.6	94.6	90.4	93.2	89.5
Recal Feed	1001.6	100.0	511	112	7.7	1544	0.4	1269	100	100	100	100	100	100

*ppm

The concentrates from the preflotation test were analysed by MLA to identify the silver-bearing minerals that exhibited natural hydrophobicity. The results are shown in Figure 4.8, which illustrates that acanthite is the most dominant silver mineral present in the concentrate, followed by native silver, pyrargyrite and chlorargyrite. Acanthite has been reported to exhibit natural hydrophobicity by Hu *et al.* (2009). It was not practical to obtain recovery values for these minerals individually from the preflotation test. MLA analyses on the preflotation tailing would have been required; this was outside the scope of the work.

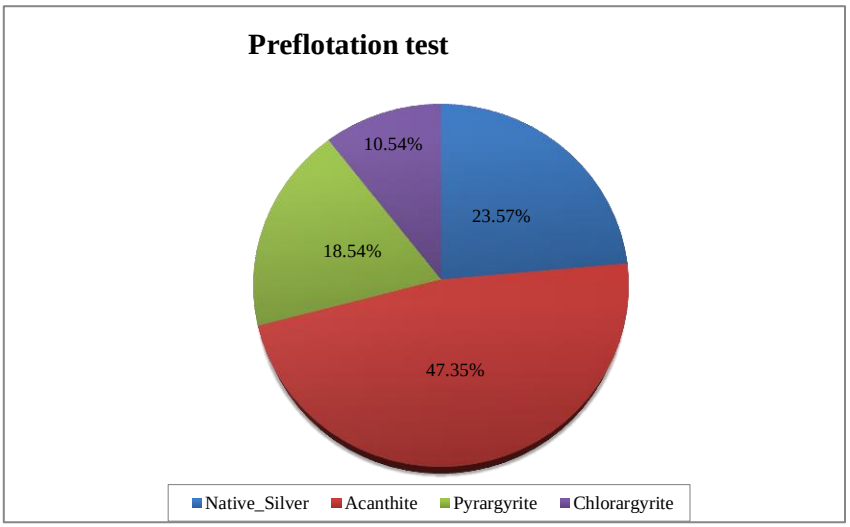

Figure 4.8: Silver-bearing minerals that exhibited natural hydrophobicity in preflotation test.

4.2.2 Experimental design

As the quantity of ore was limited, a decision was made to use a two-factorial experimental design, based on the flotation feed characterisation for this ore. The design included P80 values of 100 microns and 50 microns for the feed sizing, and collector dosages of 250 g/t of 3418A and 375 g/t of 3418A, with the objective being to obtain a reasonable recovery and grade for Ag. The results of the two-factorial design are shown in Table 4.10. These indicate that the best result with respect to grade and recovery was Test B, which used a P80 of 100 μm and a low concentration of collector; the coarse grinding (P80 of 100 μm) was in agreement with the flotation feed characterisation. From the results, the finer flotation feed sizing caused lower grade concentrates due to increased entrainment; higher collector addition also caused lower concentrate grade. The ANOVA test supported the results of the two-factorial design for Test B (*Appendix H)*, where three repeats were performed in order to provide a 95% confidence interval for the results.

Table 4.10: Results of the two-factorial experimental design evaluating P80 and 3148A collector dosage

Test	P80, μm	Collector Dosage, g/t	Ag Rec, %	Ag Grade, ppm	Mass rec, %
A	50	250	76.6	2577	11.8
B	100	250	74.3	4424	6.3
C	100	375	73.6	2771	9.5
D	50	375	75.0	3200	8.9

Figure 4.9 illustrates the grade-recovery curves of silver for the factorial design. From this, it can be seen that Test B had the highest grade and recovery when compared with Tests A, C and D – the improvement in the Ag grade was over 25%, with the most obvious improvements in concentrates 1 and 2.

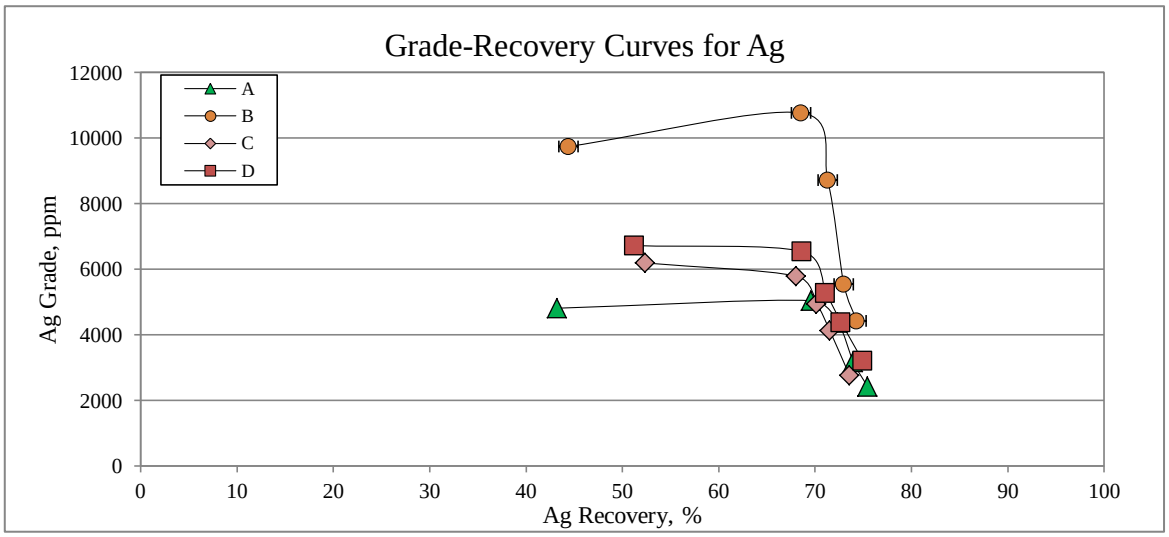

Figure 4.9: Grade-recovery curves for Ag for experimental design, with 95% confidence for Test B.

4.2.3 Flotation flow sheet for Toldos ore (oxide ore)

The literature review showed that selective flotation is often used when an ore contains low concentrations of base metal sulphides, with silver-bearing minerals recovered first in order to selectively reject any gangue sulphide minerals present (Woodcock *et al*., 2007), as well as non-sulphide gangue minerals.

Flow sheet design was performed using the mineralogical attributes provided by the mineralogical characterisation and also considering the metallurgical option of sulphidisation as well as the effects of grinding size and collector dosage (both tested at different levels) to find the best flow sheet configuration for each ore under study.

For the Toldos ore (oxide ore), preflotation was also used to assess its properties and an experimental design focused on obtaining the highest silver recovery possible using froth flotation.

➢ **Final flow sheet for Toldos ore (oxide ore)**

✓ **Grinding time** was selected to provide the flotation feed sizing selected from the experimental design (P80 of 100 microns); a grinding time of 23 minutes was required.

✓ **Selective flotation** was used due to the almost complete absence of sulphide minerals in the ore. Five concentrates were obtained at the following times –30 seconds, 2 minutes, 4 minutes, 6 minutes and 10 minutes. The reagent scheme is shown in Table 4.11. Copper sulphate was retained as a reagent in case some sphalerite existed in the ore; it could only have been present at a low concentration.

Table 4.11: Reagents used on the Toldos ore (oxide ore).

Reagent	Addition (g/t) in Selective Flotation
Sodium Silicate	500
Copper Sulphate	300
Aero 3418A	250
PAX	150
MIBC	115
Lime	36

The most effective flow sheet for this ore is presented in Figure 4.10. Each of the five concentrates was sieved by wet sieving for the +38 microns, and then for the -38 microns, the cyclosizer was used. In total, seven size fractions: -150/+53 μm, -53/+38 μm, +C1/+C2, +C3, +C4, C5 and –C5, were obtained by wet and dry sieving and cyclosizing. To obtain sufficient mass in each size fraction for chemical analysis, three repeats of the final test were performed; this also allowed confidence intervals to be determined.

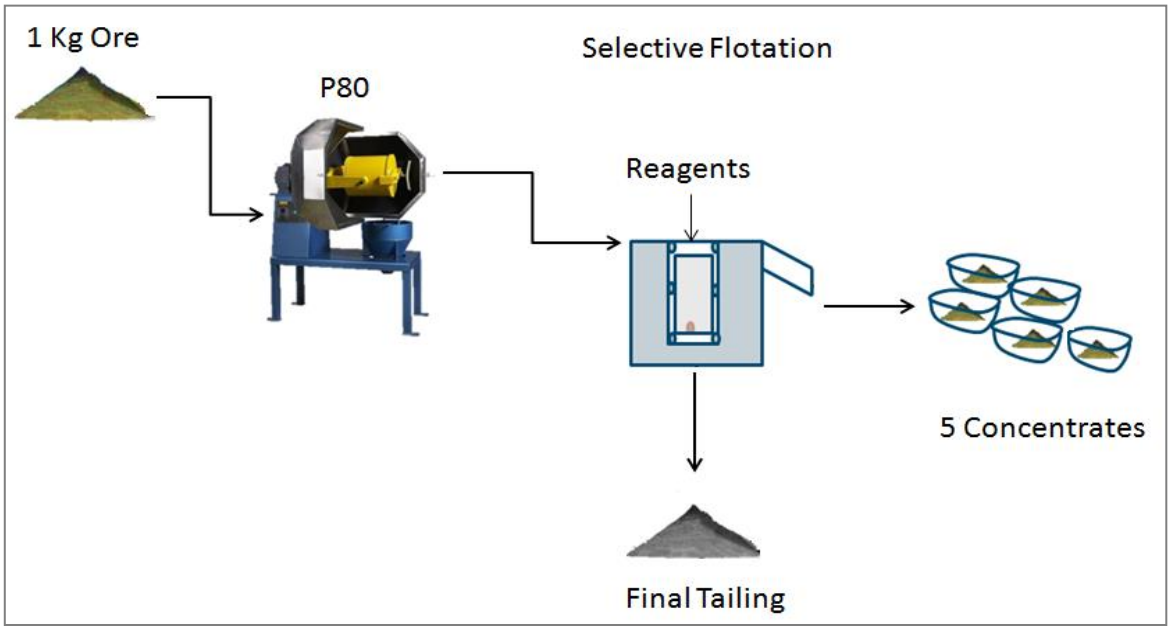

Figure 4.10: Flotation flow sheet for Toldos ore (oxide ore).

The final flow sheet consisted of one stage of rougher flotation. A mix of collectors (dithiophosphinate and xanthate) was used to selectively concentrate the silver. Note that this separation occurred with moderate quantities of the two collectors; no optimisation of the addition of each collector was performed beyond the conditions tested in the experimental design. In the following sections, the results of the batch flotation test and the characterization of the flotation products are presented.

4.2.4 Batch flotation results

Laboratory batch flotation tests were performed according to the final flow sheet with three repeats. Figure 4.11 shows the cumulative grade recovery curve for silver for the final flow sheet. The shape of the grade recovery curve indicates that, at the start for conc 1 and 2, some limited optimisation may be possible. It appears that additional conditioning time/aeration was required. For Concentrates 3, 4 and 5, the cumulative grade decreased as expected with increased recovery, with the final recovery of silver being 83.8% with a grade of 4404 ppm with 8.3% of solid mass recovered.

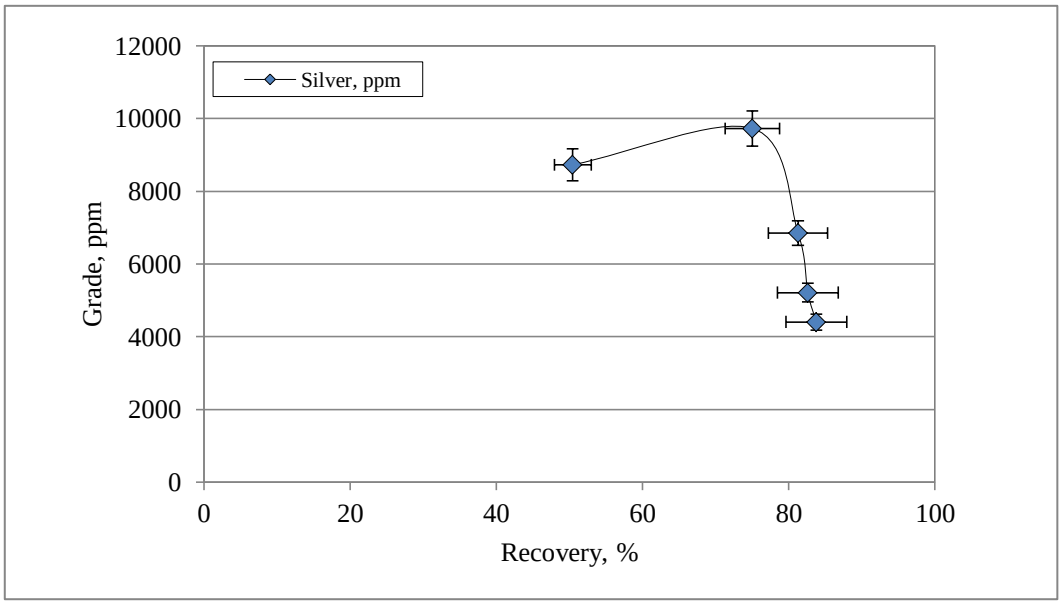

Figure 4.11: Grade-recovery curves for Ag showing 95% confidence limits.

The rates of flotation for various elements in this ore are presented in Figure 4.12, which shows the fraction remaining in the tail (y axis, log scale) with respect to the flotation time (x axis). This figure indicates that silver is exhibiting two-component flotation behaviour with a fast component (concentrates 1 to 3) and a slow component (also recovered in concentrates 1 to 3 but the main component recovered in concentrates 4 and 5). The other elements all exhibited single component (slow) behaviour as would be expected for selective flotation which is targeting silver.

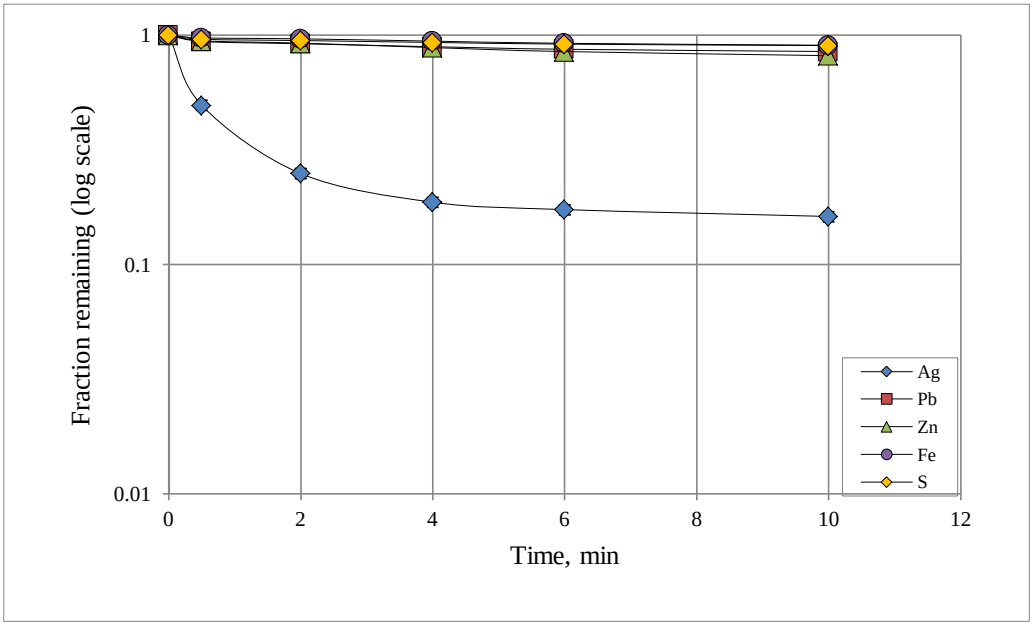

Figure 4.12: Kinetics for elements after mass balancing, with 95% confidence limits.

4.3 Results of characterisation of flotation products

4.3.1 Mineral recovery by size

For analysis of mineral recovery-by-size for Toldos ore (oxide ore), modal mineralogy from the MLA was used, because it provides a good reconciliation between the chemical assays and the MLA’s elemental assays. Note that elemental assay provides the total concentration of elements from various minerals in which they exist. In this ore, Ag assays represented the total concentration from the contributions of nine Ag minerals. However, no element-to-mineral conversion equations existed for this ore. These equations were not developed as part of this thesis, since they are outside the scope of this work; further, it is unlikely that such equations could be developed due to the limited range of elements assays.

The elemental and mineral data were mass balanced using JKSimFloat©. The minerals of interest in the Toldos ore (oxide ore) were the grouped silver minerals native silver, acanthite, arsenopolybasite, polybasite, pyrargyrite, tetrahedrite, freibergite, hessite and chlorargyrite; the rest of the minerals have been grouped as non-sulphide gangue (NSG).

Figure 4.13 shows the mineral recovery-by-size graph for the combined silver minerals and NSG for this ore. The silver minerals give an irregular curve with the recovery-by-size data in comparison to the well-known inverted U shape usually displayed by copper and other minerals in these types of analysis (Figure 4.14). Different zones can be identified in the graph as fine, intermediate and coarse zones. The finest zone (-12 μm) had the highest recovery for silver (91.8%); the intermediate zone (-20/+12μm) illustrated a moderate decrease in the recovery

(80.5%), to then reach 87.0% at -29/+20 μm; and for the coarse zone (-106/+29 μm), recovery decreased to a value of 48.1% of the Ag minerals. The overall recovery for Ag minerals was 68.1% with a grade of 1.12% Ag.

With regard to NSG, its recovery was relatively low in almost all ranges, but the highest recovery occurred in the finest size fraction, with a value of 3.4%.

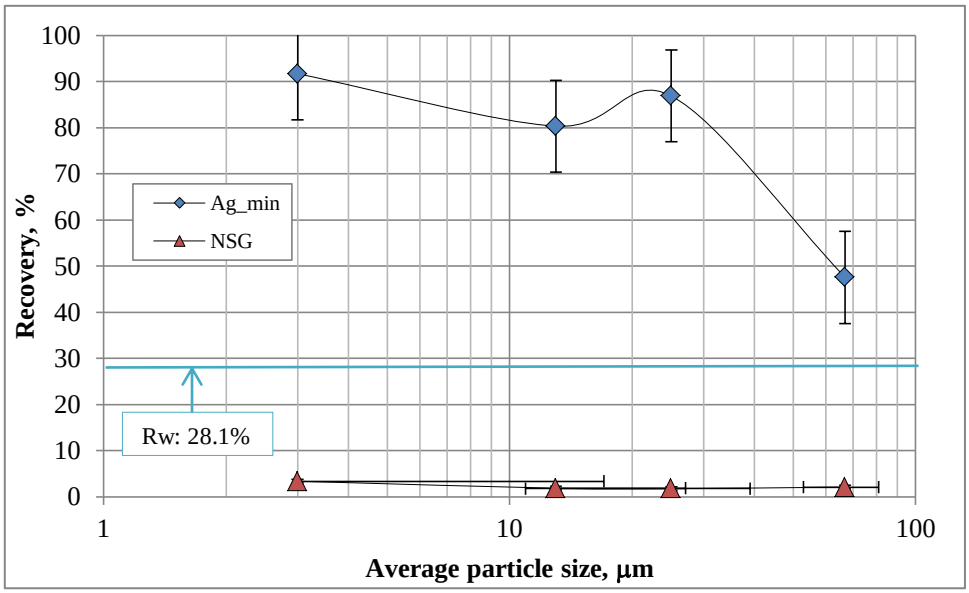

Figure 4.13: Recovery-by-size of the combined Ag minerals, and non-sulphide gangue (NSG).

4.3.2 Recovery-by-size and liberation

The classical liberation analysis by size (using mineral locking data) provides information about whether the phase of interest is liberated or occurs as binary and ternary composites. Figure 4.14 illustrates the recovery-by-size for the silver minerals in this ore based on their locking characteristics. It can be seen that unsized represents the total recovery for all particles identified as liberated, binary and ternary composites, as mentioned in the previous text. The liberated particles of silver minerals show the typical inverted U shape, showing that these minerals have the highest recovery across all size fractions, except the finest size, which has the lowest recovery with 85.5%. The binary composites, i.e. particles that contain two phases, had the highest Ag mineral recoveries in the fine fraction, while this decreased in the intermediate zone, to reach the lowest recovery for binary composites in the coarse region, with a value of 35.5% of the Ag minerals. The ternary composites show an inverted U shape, with the lowest Ag mineral recovery in the finest and coarsest size fraction, and a maximum recovery in the intermediate zone. Finally, the binary composites with NSG diluted the final silver concentrate in the intermediate zone.

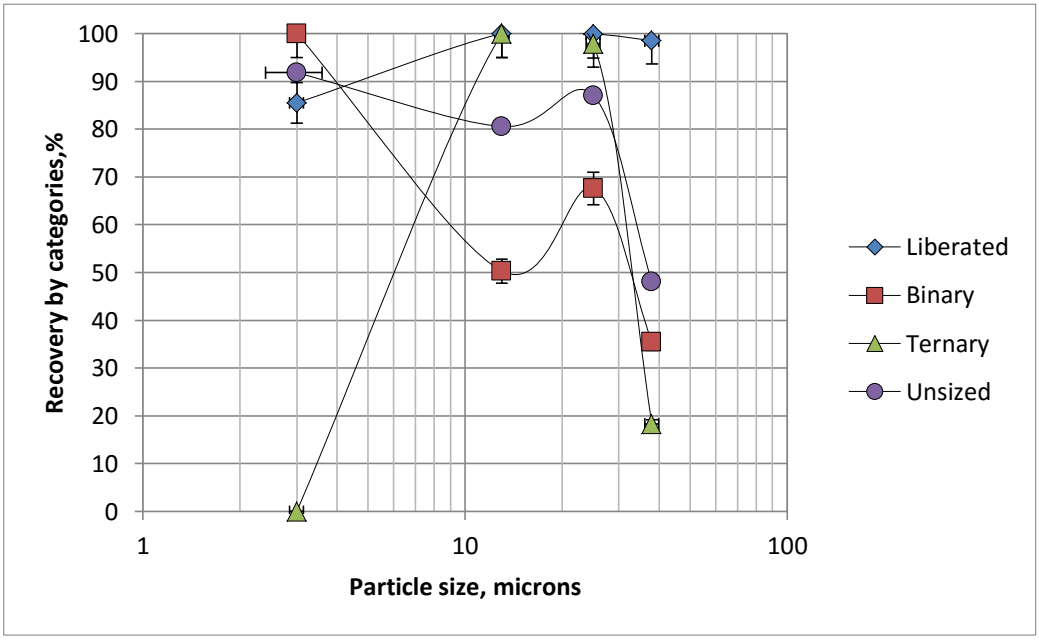

Figure 4.14: Recovery-by-size of Ag minerals for the liberated, binary, ternary and overall unsized categories.

With respect to the loss of silver minerals in the tailings, it can be shown from Figure 4.15 that the losses occur mainly as ternary composites in the coarsest-size fraction (+29 μm) with approximately 48% and in the finest size fraction (+12 μm) as liberated particles. Liberated particles were lost in the finest-size fraction as expected due to the low probability of collision between fine particles and bubbles. For binary composites, the Ag minerals were lost in the coarse-size fraction with approximately 30%, however the total loss of Ag in all size fraction account for 50% approximately.

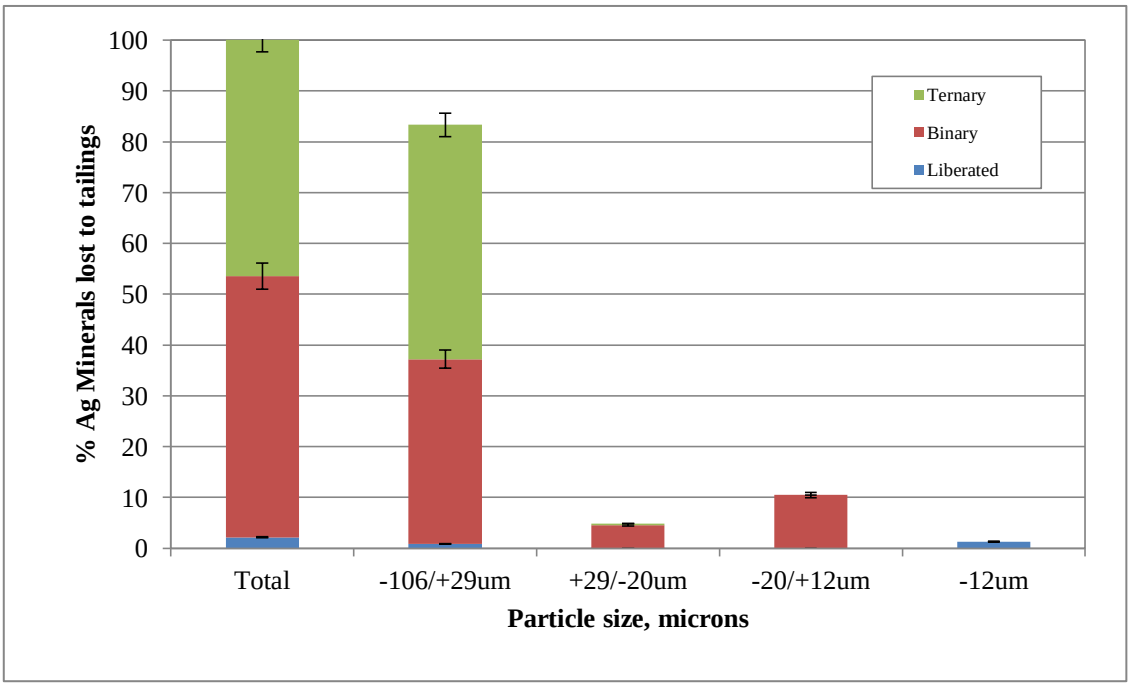

Figure 4.15: Distribution of Ag minerals in rougher tailings with 95% confidence.

4.4 Key findings

Level 1 characterisation of Toldos ore (oxide ore) was undertaken with the aim of developing a flotation flow sheet based on the key mineralogical attributes identified; these included:

1) Gangue mineralogy is represented by NSG, mainly feldspar followed by quartz. The low occurrences of sulphide minerals also indicated that this ore could be classified as an oxide ore. No potentially problematic gangue minerals in the context of flotation were identified.
2) Silver is hosted by chlorargyrite, followed by coronadite and acanthite. The grain sizes of the silver minerals are coarse, indicating that it would not be necessary to grind the flotation feed to a fine size in order to achieve liberation.
3) A significant amount of silver minerals is associated with lead arsenate, followed by carbonate minerals. These minerals do not affect the flotation process.

The use of selective flotation for recovering a rich silver rougher concentrate was successfully undertaken for this complex oxide low-grade silver ore from MSC. The results obtained demonstrate that the use of the flotation process for this type of ore is appropriate, using a combination of collectors and feed particle size distribution (P80 of 100 μm) to obtain a silver concentrate with a grade of 4404 ppm and a recovery of 83.8%. Additionally, a preflotation test showed that acanthite is naturally hydrophobic in this ore.

Chapter V:

Development of a bulk flotation strategy for a complex low-grade sulphide silver ore: "Tesorera ore"

Chapter 5 describes Level 2 characterisation of Tesorera ore (sulphide ore). One of the key distinguishing features of this ore was that the majority of the silver (>99%) was contained in pyrite, which itself represented approximately 4% of the ore. These ore characteristics played a significant role in determining the most appropriate flotation strategy to recover silver from this ore. This chapter describes the series of steps that were undertaken to devise the flotation strategy, and presents the final flow sheet used to achieve a rougher concentrate of 485 ppm Ag at a recovery of 87.2%.

5.1 Mineralogical characterisation

In the following section, the results of the ore and mill product characterisations are discussed, with emphasis on understanding the elemental deportment and liberation of the valuable minerals that needed to be recovered through flotation. As explained in Chapter 3, Level 2 mineralogical characterisation was used for this ore.

5.1.1 Level 2

5.1.1.1 Chemical assays

The silver head assay of this sample was 116±10 ppm. Elemental analysis on a size-by-size basis for silver (shown in Table 5.1) indicated that, in the finest size fraction, the silver assay decreased when compared with the intermediate size fractions, with a value of 78 ppm of silver in the size fraction of -53/+38 microns. For the coarsest size fraction, +2,360 mm, the silver assay (185 ppm) was higher than the intermediate size fractions, +1,700 mm to +425 μm, with an average of 125 ppm. There is a strong correlation between sulphur and silver assays on a size-by-size basis suggesting that sulphide minerals are potential hosts for silver. The chemical assays for selected

other elements are shown in Table 5.1; full details of the elements that were analysed are presented in *Appendix I.*

Table 5.1: Elemental assays on unsized and size-by-size bases for the feed.

	Ag	Al	As	Cu	Fe	Pb	S	Zn
Size, mm	**ppm**	**%**	**ppm**	**ppm**	**%**	**ppm**	**%**	**ppm**
Head	116	4.7	370	30	3.73	1930	3.15	5640
+2.36	185	4.53	600	60	4.68	3050	4.64	14900
+1.7	127	3.93	450	40	4.01	2150	3.60	8060
+1.18	131	4.62	410	50	3.87	2050	3.40	7230
+0.850	113	3.93	380	50	3.66	1760	2.99	5340
+0.600	103	4.81	360	50	3.67	1700	2.82	5300
+0.425	92	4.59	310	50	3.24	1420	2.46	4270
+0.300	87	4.68	290	50	3.14	1390	2.36	3870
+0.212	87	4.94	300	70	3.29	1420	2.43	3800
+0.150	87	3.91	300	90	3.16	1390	2.37	3510
+0.106	93	4.38	330	90	3.61	1570	2.58	3660
+0.075	93	5.69	340	90	3.89	1600	2.67	3580
+0.053	103	4.95	350	160	4.22	1840	2.98	3710
+0.038	110	4.35	400	440	4.39	1960	3.10	3780
-0.038	78	4.12	360	140	3.63	1520	2.21	3670
Calc Hd	***114***	***4.43***	***394***	***72***	***3.77***	***1886***	***3.07***	***6442***

5.1.1.2 X-ray diffraction (XRD)

XRD was used to support the identification of gangue minerals present in the ore. Table 5.2 shows that plagioclase feldspar is the major gangue mineral, followed by the moderate minerals: quartz, alkali feldspar and micas. A minor amount of pyrite (<5%) is also present in this ore.

Table 5.2: XRD results for Tesorera ore (sulphide ore) (provided by AMDEL)

Mineral	Composition	JK2681-2
Quartz	SiO_2	Moderate
Pyrite	FeS_2	Minor
Alkali feldspar	$KAlSi_3O_8$	Moderate
Plagioclase feldspar	$NaAlSi_3O_8$	Major
Mica	$(X_2Y_{4-6}Z_8O_{20}(OH,F)_4)^*$	Moderate

*X is K, Na or Ca or less commonly Ba, Rb, or Cs; Y is Al, Mg, or Fe or less commonly Mn, Cr, Ti, Li, etc; Z is Si or Al, however it could include Fe^{3+} or Ti.

5.1.1.3 Oxide characterisation of lead and zinc minerals

The results shown in Table 5.3 reflect the percentage of Pb and Zn minerals present in an oxide form in the ore. The amounts of oxide minerals are considered as moderate for both elements, representing the insoluble Pb (80.9%) and Zn (91.1%) that may be amenable to the flotation process.

Table 5.3: Results for oxide characterisation of lead and zinc minerals present in Tesorera ore (sulphide ore) (provided by AMDEL)

Element Measurement	% Total
Pb as oxide minerals	19.1
Zn as oxide minerals	8.9

5.1.1.4 Optical Microscopy

The minerals present and their relative abundance from optical microscopy for this ore are presented in Table 5.4. It shows that the main non-sulphide gangue present is feldspar, followed by quartz, clay and micas in declining amounts. As minor minerals present, pyrite, marcasite and sphalerite were identified. The sparse minerals present are rutile, galena, apatite, acanthite and native silver.

Table 5.4: Estimated modal volumetric mineral distribution (Knights, 2011)

Volumetric mineral distribution	Minerals present
Dominant (> 80vol %)	Mainly non-sulphide gangue: feldspar>>quartz>clay>mica
Minor (5 > X > 0.5vol %)	- pyrite + marcasite (~3.5%) (pyrite >> marcasite) - sphalerite (~0.4%)
Sparse (X << 0.5vol %)	rutile, galena, apatite, acanthite and native silver.

Sulphides are present in the ore mainly as pyrite, which shows different textures with colloformic layered / botryoidal concentric fabrics (Figure 5.1). The grain size of pyrite has an average of 3-12 microns, which is disseminated through the non-sulphide gangue and mainly associated with sphalerite. In terms of sphalerite, this is present in low amounts through the non-sulphide gangue (see Figure 5.2).

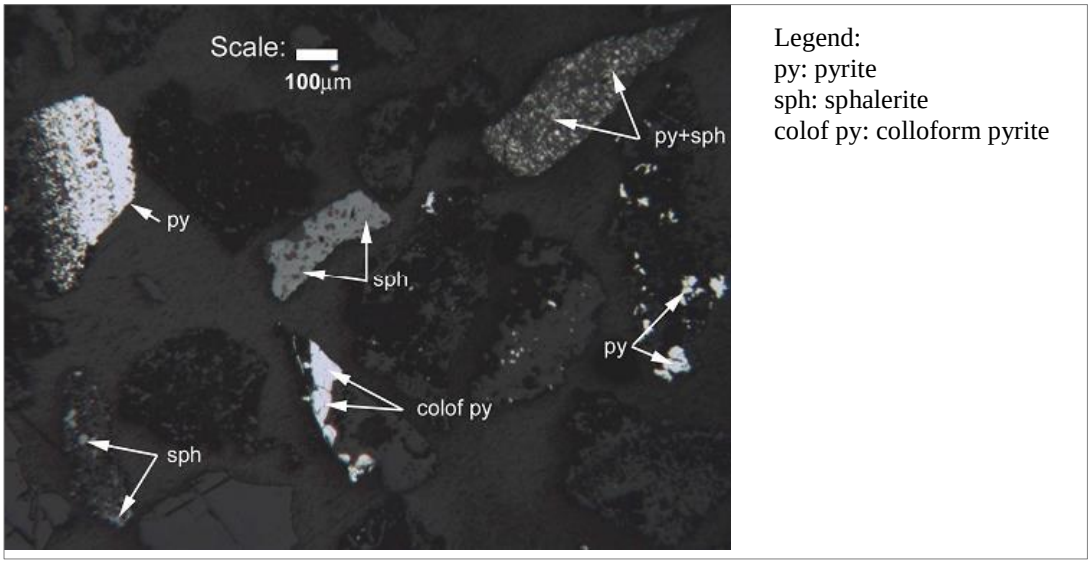

Figure 5.1: Photomicrograph of pyrite, sphalerite and colloform pyrite (after Knights, 2011).

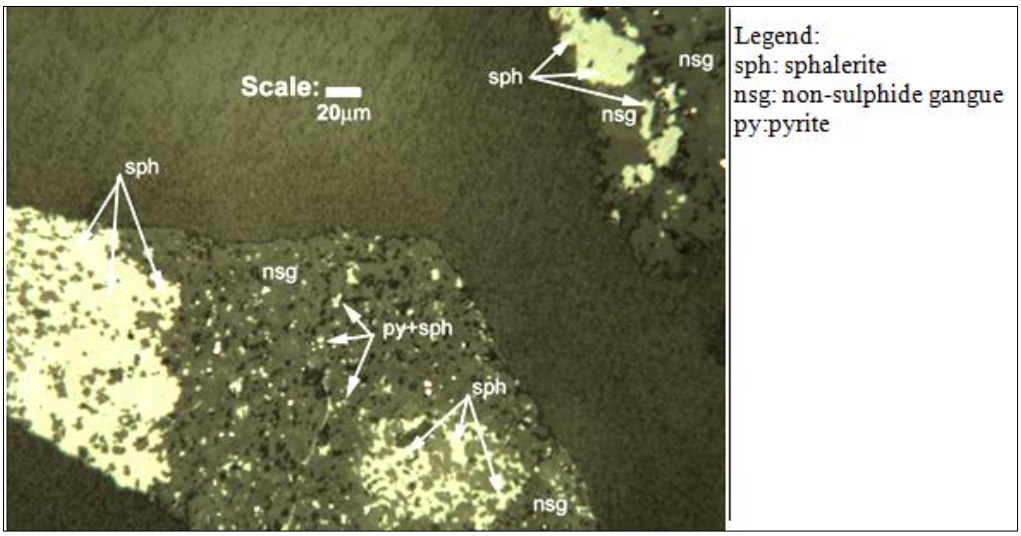

Figure 5.2: Photomicrograph of pyrite, sphalerite and NSG (after Knights, 2011).

The silver minerals identified from optical microscopy were mainly acanthite within layers of colloformic pyrite (Figure 5.3). Native silver, in contrast, was identified as isolated sparse microscopic grains.

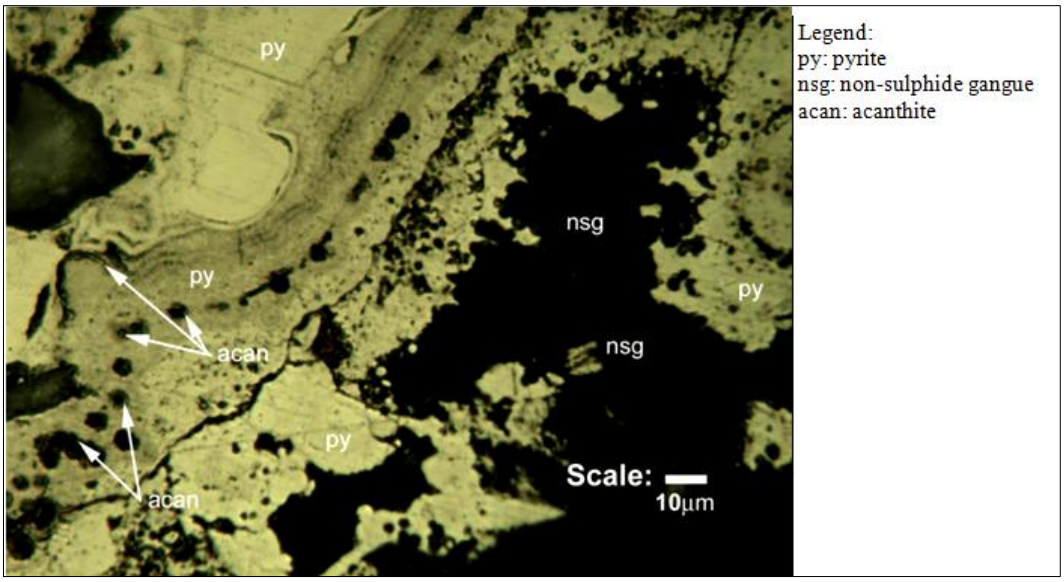

Figure 5.3: Photomicrograph of pyrite, sphalerite and acanthite (after Knights, 2011).

The presence of these two sulphide minerals, pyrite and sphalerite, and silver-bearing minerals suggested the possibility of performing flotation on the ore if it was ground to an appropriate size.

To understand why Level 2 of mineralogical characterisation was used, it is necessary to check the silver assay reconciliation between chemical assays and MLA assays. Figure 5.4 illustrates the graph for Ag reconciliation. From this it can be seen that there is poor reconciliation between the data, demonstrating the need to for a systematic approach that incorporates a range of analytical methods. *Appendix J* show the raw data.

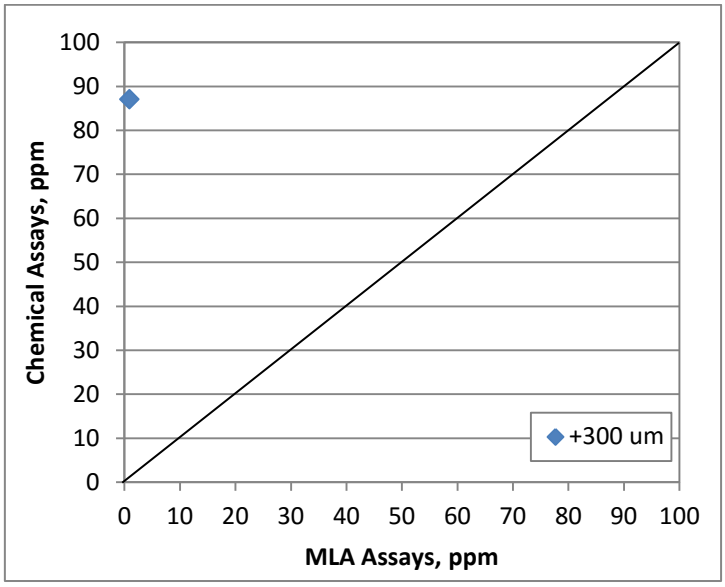

Figure 5.4: Ag assay reconciliation between Chemical and MLA assays

This lead to the addition of laser ablation inductively coupled plasma mass spectroscopy (LA-ICP-MS) to identify silver in solid solution in pyrite and resulted in the creation of Level 2 analysis. The results of this analytical technique are shown in the following section.

5.1.1.5 Laser ablation inductively coupled plasma mass spectroscopy (LA-ICP-MS)

Results from LA-ICP-MS are shown in Table 5.5 only pyrite was evaluated for Tesorera ore. Twenty grains of pyrite were analysed for this ore as a potential carrier of Ag in solid solution. The results were conclusive and indicated that the pyrite carried 2936 $\pm$ 686 ppm of silver. The pyrite also contained a range of other elements including higher amounts of lead and arsenic, and lower amounts of copper and zinc. *Appendix K* shows the results of LA-ICP-MS as supplied by MODA.

Table 5.5: LA-ICP-MS results for Tesorera ore (sulphide ore) with 95% confidence limits

Mineral	Ag, ppm	Fe, ppm	Cu, ppm	Zn, ppm	As, ppm	Pb, ppm
Pyrite	2936$\pm$686	465000$\pm$0	423$\pm$240	293$\pm$345	3253$\pm$1164	37402$\pm$8242

5.1.1.6 Mineral Liberation Analyser (MLA)

The MLA analysed a total of 978,196 grains, with 17,917 particles measured for the size fraction -425/+300 μm, while for the -1.18mm/+850 μm size fraction, 453,952 grains in 7,125 particles were measured. The measurements on both size fractions were used to determine the key mineralogical attributes, such as modal mineralogy, elemental deportment, and texture, which were needed for the ore characterisation.

a) Modal Mineralogy

Preliminary estimation of modal mineralogy for this case study was carried out for two selected size fractions of the mill feed: -425/+300 μm and -1.18mm/+850μm. Table 5.6 shows that the gangue mineralogy was represented predominantly by feldspar and quartz. Lesser amounts of clays_micas and pyrite (3.8%) in +300 μm size fraction were found. Similar results were found for the +850 μm size fraction.

Table 5.6: Modal mineralogy for Tesorera ore (sulphide ore)

Mineral Groups	-425/+300 μm		-1.18mm/+850 μm	
	Average	St. Dev	Average	St. Dev
Ag minerals	0.0±0.0	0.0	0.0±0.0	0.0
Pyrite	3.8±0.44	0.5	5.3±1.13	1.3
Sphalerite	0.5±0.12	0.1	0.5±0.43	0.5
Galena	0.0±0.02	0.0	0.0±0.01	0.0
Quartz	18.6±0.93	1.1	22.0±4.19	4.8
Feldspar	67.6±1.30	1.5	62.2±3.38	3.9
Clays_micas	7.8±0.50	0.6	7.6±2.97	3.4
Other silicates	0.1±0.02	0.0	0.2±0.19	0.2
Iron Oxide	0.1±0.05	0.1	0.2±0.19	0.2
Carbonates	0.6±0.06	0.1	0.6±0.29	0.3
Sulphates	0.4±0.08	0.1	0.3±0.21	0.2
Other	0.5±0.06	0.1	1.2±0.35	0.4
Total	100		100	

b) Elemental deportment

Key elements were selected for elemental deportment analysis, namely: silver, iron, sulphur and zinc. The elemental deportment for silver was quantified by a combination of LA-ICP-MS and MLA results. Table 5.7 presents the lists of Ag carriers for both sizes measured. The results were conclusive and indicated that pyrite was the main silver carrier (97.8% at +300 μm and 99.2% at +850 μm). A small amount of silver was found to be in silver minerals including coronadite, tetrahedrite, pyrargyrite, chlorargyrite and gabrielsonite. Zinc deportment is shown in Table 5.8 which indicates that sphalerite is the main zinc-bearing mineral in both size fractions measured. Pyrite is the main sulphur host in the ore, hosting 89.1% at +300 μm (Table 5.9). Therefore, the decision was made to use sulphur as a proxy for pyrite in comparing the flotation results for this ore.

Table 5.7: Elemental deportment for Ag with 95% confidence limits

Mineral	Ag			
	-425/+300 μm		-1.18mm/+850 μm	
	Average, %	St Dev	Average, %	St Dev
Pyrargyrite	0.2±0.05	0.06	0.1±0.00	0.00
Tetrahedrite	0.5±0.14	0.17	0.2±0.00	0.00
Freibergite	0.0±0.00	0.00	0.0±0.00	0.00
Chlorargyrite	0.1±0.05	0.05	0.0±0.00	0.00
Coronadite	1.5±0.17	0.20	0.4±0.00	0.01
Gabrielsonite	0.0±0.01	0.01	0.0±0.00	0.00
Pyrite	97.8±0.1	0.10	99.2±0.22	0.22
Total	100		100	

Table 5.8: Elemental deportment for Zn with 95% confidence limits

Mineral	Zn			
	-425/+300 μm		-1.18mm/+850 μm	
	Average, %	St Dev	Average, %	St Dev
Sphalerite_Fe	2.5±0.30	0.3	2.6±1.32	1.5
Sphalerite	97.5±0.30	0.3	97.4±1.32	1.5
Total	100	0.0	100	0.0

Table 5.9: Elemental deportment for S with 95% confidence limits

Mineral	S			
	-425/+300 μm		-1.18mm/+850 μm	
	Average, %	St Dev	Average, %	St Dev
Pyrite	89.1±0.01	0.0	91.9±6.59	7.5
Pyrrhotite	1.0±0.00	0.0	0.6±0.10	0.1
Sphalerite_Fe	0.2±0.07	0.1	0.3±0.28	0.3
Sphalerite	6.9±1.82	2.1	6.1±6.06	6.9
Galena	0.1±0.08	0.1	0.1±0.05	0.1
Barite	2.5±0.60	0.7	1.0±0.69	0.8
Beudantite	0.1±0.00	0.0	0.0±0.00	0.0
Total	100		100	

c) Texture:

❖ *Mineral grain size*

The mineral grain size information (Figure 5.5) illustrates that the silver minerals show a finer grain size distribution when compared to the sulphide minerals present in the ore. The silver mineral grains show a P80 of 22 μm, followed by galena (P80 of 100 μm) and then by sphalerite (P80 of 118 μm), while pyrite, which is the main silver carrier in this ore, has a P80 of 115 μm.

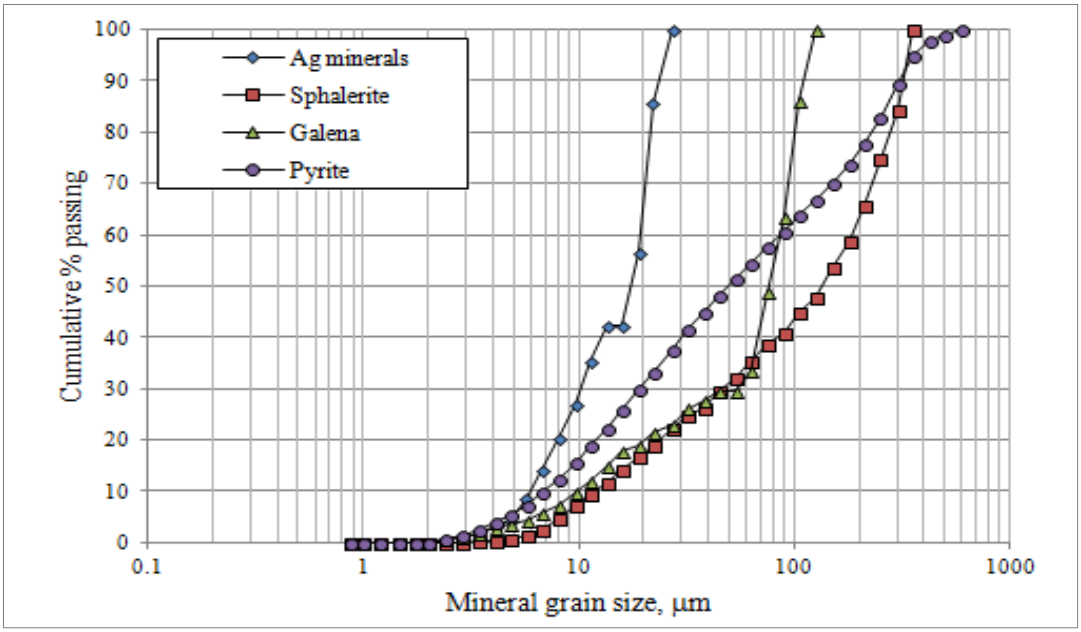

Figure 5.5: Mineral grain size distribution for Tesorera ore (sulphide ore)

❖ *Mineral association*

The mineral associations indicated if there was pyrite that tended to be associated with problematic minerals (clays or any antagonistic minerals for the flotation process). The results in Figure 5.6 show that pyrite is associated mainly with quartz (44.4%), followed by feldspar (orthoclase and plagioclase) and to a lesser extent with clay_micas (8.5%) and others (4.0%). A small amount of pyrite (4.4%) was found associated with free surface (i.e. the surface is available for flotation or leaching).

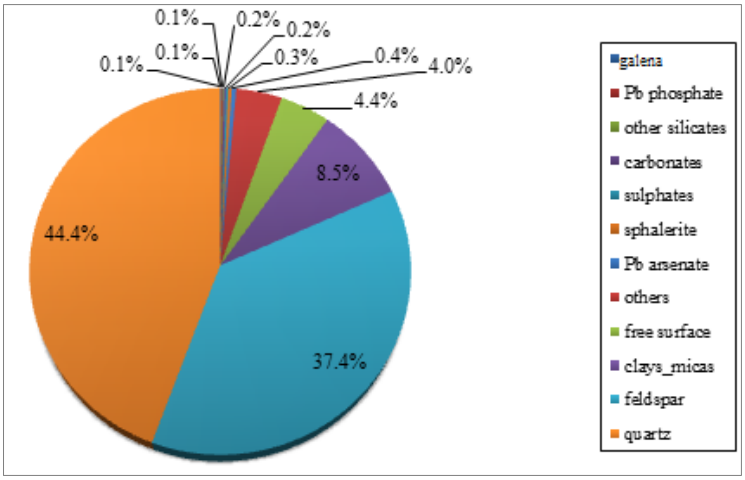

Figure 5.6: Mineral association for pyrite in Tesorera ore (sulphide ore) at -425/+300 µm.

Complex textures are present in this ore (as indicated by the optical microscopy), and these can be seen from Figures 5.7 (A to C), which illustrate the complexity of the mineral textures in different

grains in the -425/+300 μm size fraction. Figure 5.7 A shows a particle of pyrite which has rims and inclusions with quartz. In B, the particles present inclusions of pyrite in feldspar. In C, some grains of pyrite are present in quartz in the centre of the image and some others pyrite grains are hosted by feldspar in the upper left corner of the image C.

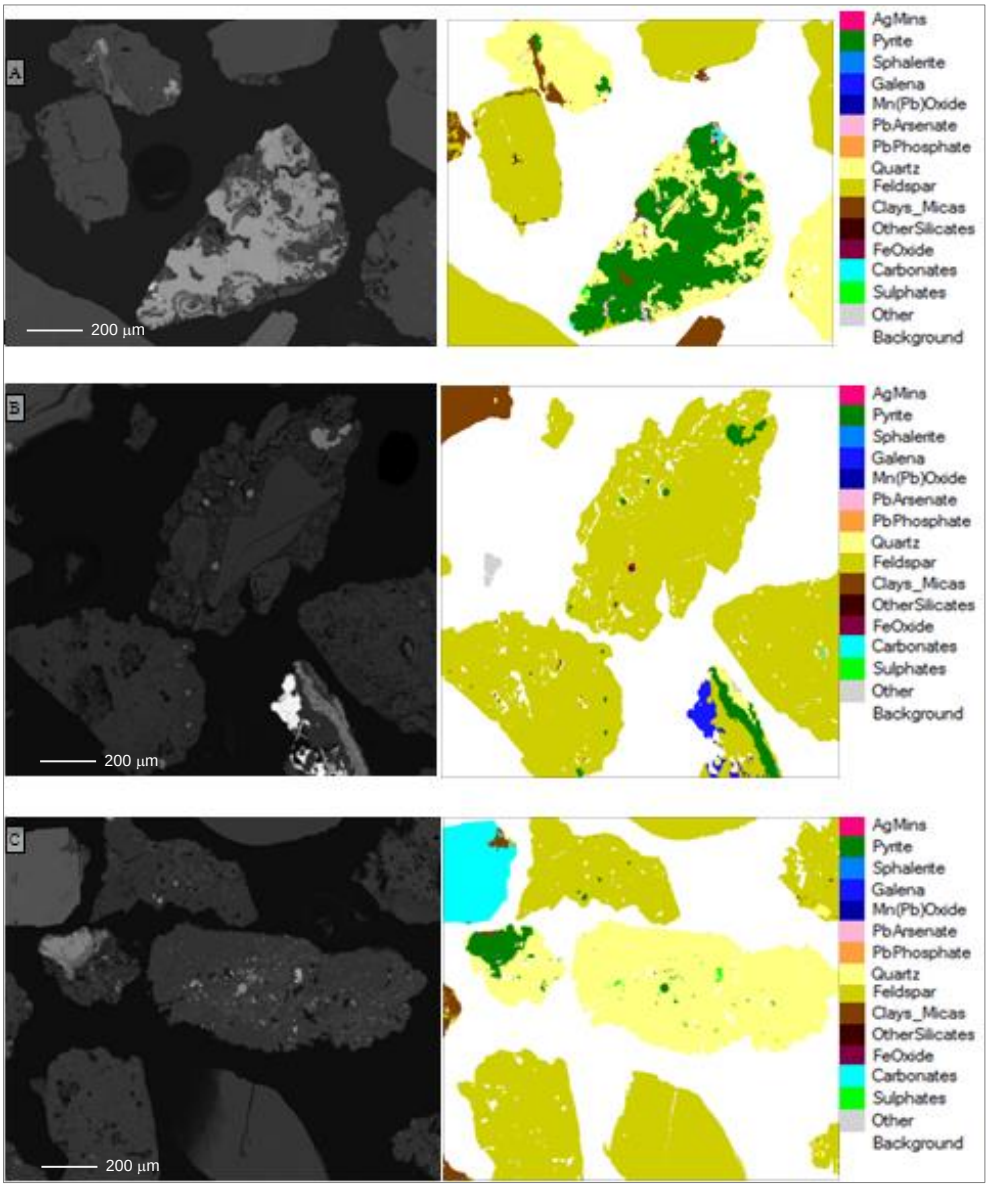

Figure 5.7: A, B, & C left: BSE images; and A, B, & C right: classified MLA particle images from the -425/+300 μm size fraction.

- ***Assessment from Level 2***

Table 5.10 shows a summary of the assessment of Level 2 of the mineralogical characterisation.

Table 5.10: Assessment of Level 2

Techniques	Chemical assay	XRD	Oxide mineral characterisation	Optical microscopy	LA-ICP-MS	MLA
Comment	Recalculated head assay for Ag is 114 ppm	Dominant gangue is feldspar, followed by quartz and mica	Pb ox. mineral: 19.1% Zn ox. mineral: 8.9%	Congruent with gangue mineralogy reported by XRD. Ore present complex textures. Ag deportment: acanthite within layers of colloformic pyrite.	Pyrite grains contain Ag in ss with a value of 2936±686 ppm of Ag in pyrite	In agreement with XRD and optical microscopy for gangue mineralogy. Ag deportment: >97% of Ag as ss in pyrite. Pyrite present a P80 of 115 µm, and Ag min present a P80 of ~ 20µm. Therefore an intermediate P80 is required

5.1.2 Mill product characterisation for Tesorera ore (sulphide ore)

MLA analysis was conducted on the mill product by size to determine the level of liberation of key minerals. The liberation results for pyrite and sphalerite (illustrated in Table 5.11) revealed that the liberation level for pyrite is poor (40.9%) for the production of a pyrite concentrate, which was the mineral targeted for recovery from this ore; the feed contains a relatively large quantity of low quality composites containing pyrite. In the case of sphalerite, it can be seen that only 30% is liberated. Also shown in Table 5.11 is the distribution of sulphide minerals by size; these data indicate that a large proportion of the pyrite is in the coarser size fractions (+53 microns) where pyrite liberation is less than 30 %, providing the motivation to use the mainstream inert grinding (MIG) procedure with this ore.

Table 5.11: Liberation for pyrite and sphalerite in the ore after grinding to 80% passing 100 µm

Size Fraction	Pyrite distribution	Pyrite Liberated (%)	Units of liberated pyrite	Sphalerite distribution	Sphalerite liberated (%)	Units of liberated sphalerite
+106 µm	16.0	31.0	4.96	13.5	6.4	0.86
+53 µm	35.7	28.9	10.32	35.4	6.3	2.23
+35 µm	20.7	45.7	9.46	18.2	26.7	4.86
+24 µm	8.5	50.5	4.29	9.5	54.0	5.13
+17 µm	7.2	61.4	4.42	7.4	60.8	4.50
+14 µm	3.1	62.5	1.94	4.2	77.7	3.26
-14 µm	8.8	62.5	5.50	11.8	77.7	9.17
Total	100.0		40.9	100.0		30.0

The ore contains 51.5 ± 2.4% of feldspar and 26.4±2.5% of quartz with, in this analysis, 6.7±1.7% of pyrite which, as shown earlier, was 40.9% liberated. Table 5.12, illustrates the modal mineralogy of the mill product.

Table 5.12: Modal mineralogy for mill product with 95% confidence limits

Mineral Groups	Average	St. Dev
Ag_min	0.0±0.0	0.0
Pyrite	6.7±1.7	2.1
Sphalerite	0.7±0.2	0.2
Galena	0.0±0.0	0.0
Other	1.2±0.1	0.2
Mn(Pb)Oxide	0.0±0.0	0.0
PbArsenate	0.1±0.1	0.1
PbPhosphate	0.0±0.0	0.0
Quartz	26.4±2.5	3.2
Feldspar	51.5±2.4	3.0
Clays_micas	11.7±2.0	2.5
OtherSilicates	0.1±0.0	0.1
Fe Oxide	0.2±0.1	0.1
Carbonates	0.6±0.1	0.2
Sulphates	0.8±0.2	0.2
Total	100	

Key findings of mineralogical characterisation

According to the information obtained through the mineralogical characterisation, the ore should be processed through flotation, but considering that silver is present mainly as solid solution in pyrite, a pyritic concentrate is needed to recover silver. The degree of liberation at a P80 of 100 microns for the mineral of interest is not adequate for obtaining a good flotation response (based on the information presented in Table 2.7.

5.2 Results of metallurgical characterisation for Tesorera ore (sulphide ore)

The development of a rougher flotation flow sheet for Tesorera ore (sulphide ore) was driven by the mineralogical characterisation that is described in the previous section, which provided the mineralogical attributes needed for developing an appropriate flow sheet to recover silver from this complex sulphide low-grade silver ore. Also, it is important to mention that previous flotation test were performed in this ore, being also a base to understand the behaviour of this ore. The results of these tests are shown in *Appendix L*.

5.2.1 Preliminary Preflotation Results

The preflotation assessment showed that none of the minerals present in the ore exhibited natural floatability. The results for the preflotation test are given in Table 5.13, showing that only 1.7% of

the mass was recovered, with the following recoveries for elements: 1.4% silver, 7.1% copper, 1.6% iron, 2.6% lead, 1.7% sulphur and 8.5% zinc.

Table 5.13: Preflotation results for each concentrate and for the combined concentrate for Tesorera ore (sulphide ore)

Streams	Mass		Assays						Recovery (%)					
	grams	%	Ag, ppm	Cu, ppm	Fe, %	Pb, ppm	S, %	Zn, ppm	Ag	Cu	Fe	Pb	S	Zn
Feed	1000													
Con 1	3.9	0.4	95	210	3.5	3530	3.4	33600	0.3	1.6	0.4	0.7	0.4	2.2
Con 2	4.7	0.5	92	220	3.5	2800	3.1	30300	0.4	2.0	0.5	0.7	0.5	2.4
Con 3	7.9	0.8	93	230	3.6	2620	3.2	29400	0.7	3.5	0.8	1.1	0.8	3.9
Total Con	16.5	1.7	93	222	3.5	2884	3.2	30637	1.4	7.1	1.6	2.6	1.7	8.5
Tailings	964.7	98.3	114	50	3.6	1880	3.2	5660	98.6	92.9	98.4	97.4	98.3	91.5
Recal Feed	981.2	100	114	53	3.6	1897	3.2	6080	100	100	100	100	100	100

5.2.2 Flotation flow sheet for Tesorera ore (sulphide ore)

As noted in the literature review, bulk flotation and sulphidisation are used when there is a low concentration of base metal sulphide minerals in the ore, and when the sulphide surface of the minerals of interest may be tarnished or oxidized. Accordingly, based on the mineralogical characterisation, bulk flotation in combination with sulphidisation stages, was selected as the most appropriate flotation strategy to be used for recovering silver in this ore.

Various flotation strategies were used to finally achieve the best flotation flow sheet for this ore. The preliminary flow sheets and the operational conditions from the different batch tests were presented in Chapter 3. Figure 5.8 presents a summary of the series of various stages used to identify the final flow sheet used. The first step was to perform the preflotation test; various mixtures of collectors and various dosages were tested to find the best flotation conditions for the sulphide minerals; then the incorporation of the sulphide and non-sulphide flotation was achieved, the sulphidisation step was added; and finally, the addition of the MIG step to the flow sheet aimed to obtain a higher recovery and grade as a final product.

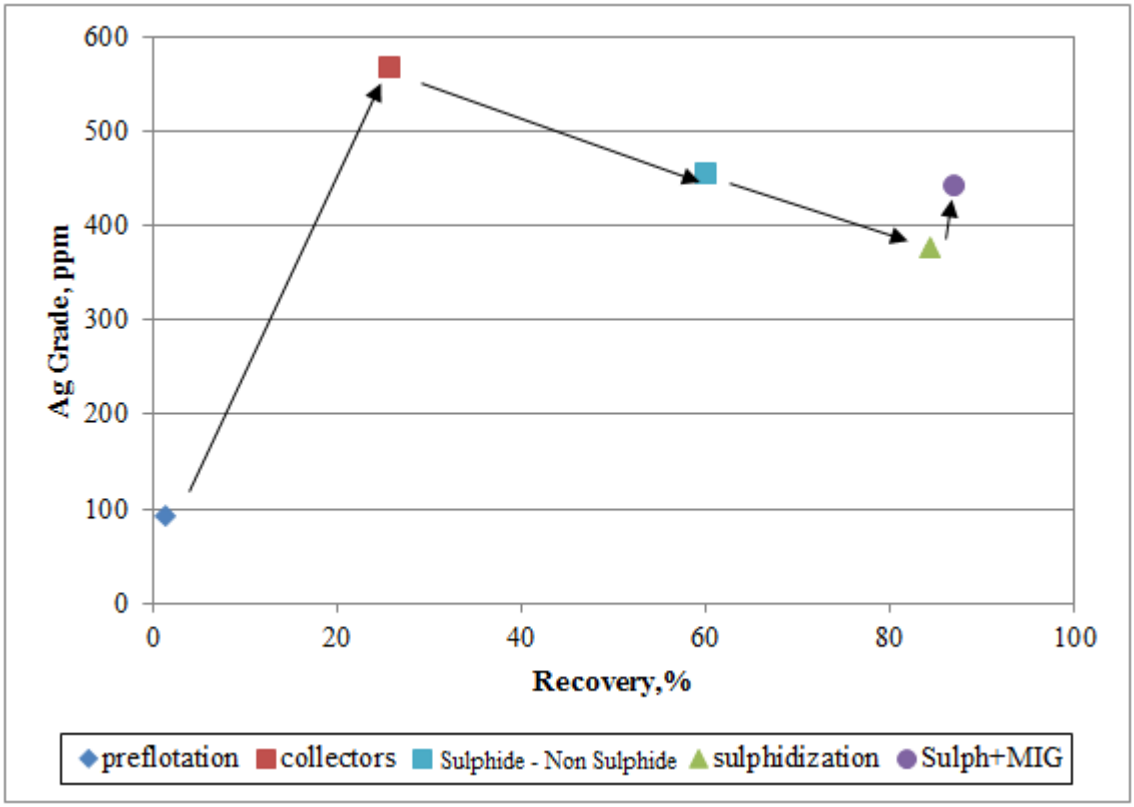

Figure 5.8: Summary of the different flotation strategies used in Tesorera ore (sulphide ore)

The flow sheet consists basically of two flotation rougher stages that are the core of this process; these are the ***sulphide flotation stage*** and the ***non-sulphide flotation stage.*** A complementary approach of MIG was evaluated at the beginning of the flow sheet to improve the liberation of pyrite and sphalerite for upgrading the recovery of these target minerals. Between the two flotation stages, ***sulphidisation*** was incorporated to create a pseudo-sulphide surface on the minerals that did not respond to the sulphide flotation and were to some degree tarnished or oxidized during processing or from the nature of the ore.

➢ **Final flow sheet for Tesorera ore (sulphide ore)**

✓ **Grinding time** was selected for a P80 of 100 microns with a required time of 13.5 minutes. After this period of time, MIG was used to ensure that there was less solid and silver in the coarse size fractions. The P80 after MIG was 56 μm.

✓ **Bulk flotation** was used to recover a concentrate that contained the sulphide minerals, both unoxidized and oxidized. This flotation was divided into two main stages (Figure 5.9), described as follows:

❖ ***Sulphide flotation:*** The sulphide flotation stage was performed using a scheme of reagents (Table 5.14). Four concentrates were collected, with each concentrate being collected every

two minutes (8 minutes in total). The pulp potential during the sulphidisation step was -100 mV SHE at pH = 7.

- ***Non-sulphide flotation:*** The remaining pulp in the cell was sulphidised with sodium hydrogen sulphide (NaHS) with five minutes of conditioning time. The pulp potential was measured using a platinum electrode coupled with an Ag/AgCl/3.0M KCl reference electrode. The pulp potential was set at 150 mV SHE. Three concentrates were collected in this stage, every two minutes of flotation (6 minutes in total).

For this ore, the flow sheet is presented in Figure 5.9. Before each stage, one minute of conditioning time was allowed for each reagent (with the exception of NaHS) introduced into the pulp (see Table 5.14), starvation quantities of collectors were used for this flow sheet. Optimization of the collector dosage is suggested but is outside of the scope of this thesis.

Table 5.14: Reagents used on the Tesorera ore (sulphide ore)

Reagent	Addition (g/t) in sulphide flotation	Addition (g/t) in non-sulphide flotation
Sodium silicate	1000	-
Copper sulphate	450	300
Aero 404	600	400
PAX	400	500
MIBC	120-140	60, 100
NaHS	-	3950-4200
Lime	50-100	-
Sulphuric acid	1.25	-

In total, seven size fractions: -150/+53 μm, -53/+38 μm, +C1/+C2, +C3, +C4, +C5 and –C5, were obtained by wet and dry sieving and cyclosizing. To obtain sufficient mass in each size fraction for analysis three repeats of the final test were performed i.e., four test were done, this also allowed confidence intervals to be determined.

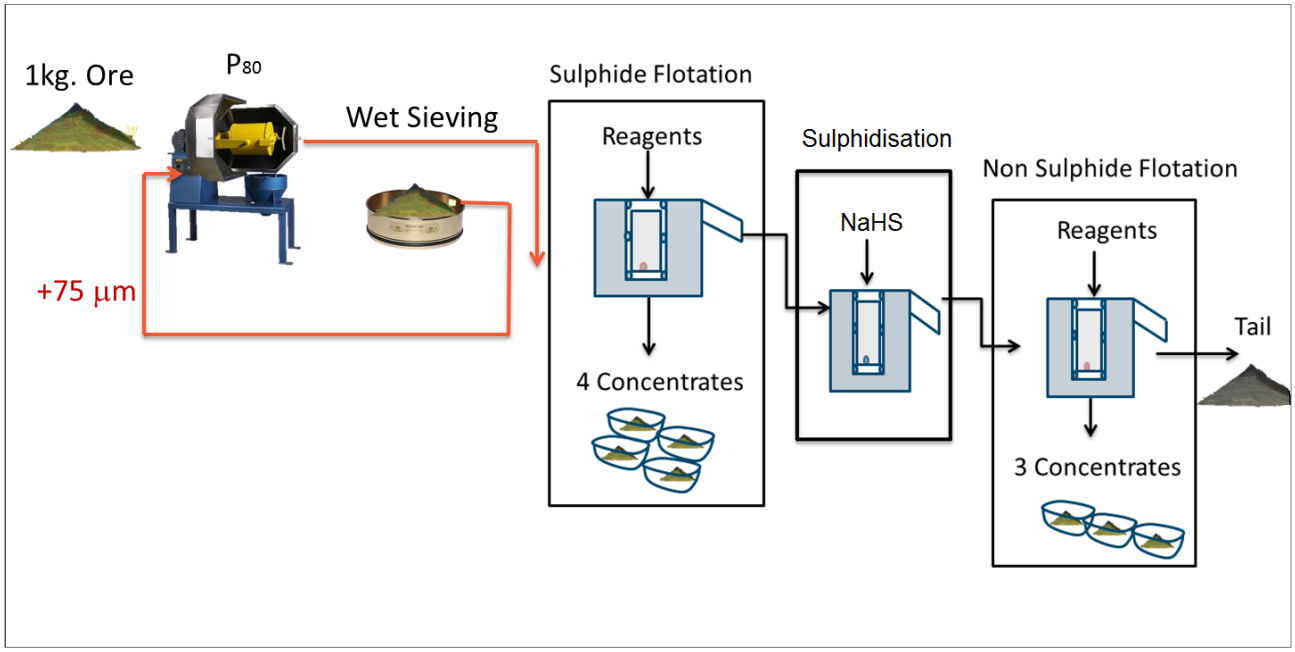

Figure 5.9: Flow sheet for Tesorera ore (sulphide ore).

5.2.3 Flotation of Tesorera ore (sulphide ore)

From the mineralogical analysis, the implications for processing this ore were: firstly, to maximise recovery of the discrete silver minerals and the sulphide minerals (pyrite and sphalerite), which respond to the sulphide mineral flotation conditions; and secondly, to maximise the recovery of minerals considerably modified from their original form by the use of sulphidisation technology. It is noted that the pyrite in this ore is an important silver carrier, and that it exists at a relatively high feed grade (6.7%), requiring substantial additions of reagents such as collector(s) and activator(s) for recovery at this head grade. From the elemental deportment, pyrite is the major mineral containing sulphur; therefore S could be considered the proxy for the pyrite for subsequent analysis of the flotation process. Table 5.15 shows the distribution of various elements and of two minerals for the ore sample ground to a size of 80% passing 100 µm. It can be seen that the sulphur and silver distributions are quite similar to that of pyrite. The sphalerite and zinc distributions were similar as well.

Table 5.15: Distribution of solid, elements and minerals by size for the ore sample at a P_{80} of 100µm.

Size Fraction, µm	Solid, %	Ag, %	Pb, %	Zn, %	S, %	Sphalerite	Pyrite
+106	17.2	17.3	16.8	19.6	17.7	13.5	16.0
+53	32.2	36.8	35.9	35.2	37.0	35.4	35.7
+35	12.1	18.3	19.1	14.4	18.8	18.2	20.7
+24	5.4	7.2	6.7	6.2	7.5	9.5	8.5
+17	7.3	5.6	5.3	5.2	5.9	7.4	7.2
+14	3.8	2.6	2.7	2.9	2.9	4.2	3.1
-14	22.0	12.2	13.5	16.5	10.2	11.8	8.8
Total	100	100	100	100	100	100	100

5.2.4 Batch flotation results

Bulk flotation was performed using a number of different strategies, including sulphidisation, MIG, and the mixture of collectors. The investigation of the relative benefits of these different approaches (see preliminary results and Figure 5.8) in combination with the knowledge gained from the mineralogical characterisation allowed the development of a suitable processing technique to recover silver from this ore.

The cumulative grade and recovery results for the final flow sheet, based on chemical assays, are shown in Table 5.16. The combined rougher concentrate produced a silver grade of 485 ppm at a recovery of 87.2%.

Table 5.16: Cumulative grade and recovery for combined concentrates

Stream	Unsized cumulative grade				Unsized cumulative recovery, %			
	Ag, ppm	Fe, %	S, %	Zn, %	Ag	Fe	S	Zn
Con 1	1021	18.3	24.5	14.6	35.9	20.8	34.1	79.8
Con 2	673	13.8	15.9	6.0	62.6	41.4	58.7	87.2
Con 3	485	11.0	11.9	3.3	87.2	63.8	84.5	92.6
Tailings	23	2.0	0.7	0.08	12.8	36.2	15.5	7.4
Rec. Feed	135	4.2	3.4	0.87	100	100	100	100

The grade recovery curves in Figure 5.10 show the similar trends displayed by silver and sulphur in this system. The close agreement between the S and Ag was a direct result of the silver deportment in this ore, as described in the previous section. The average grade of Ag in pyrite represented the maximum silver grade that could be achieved theoretically (see Table 5.5).

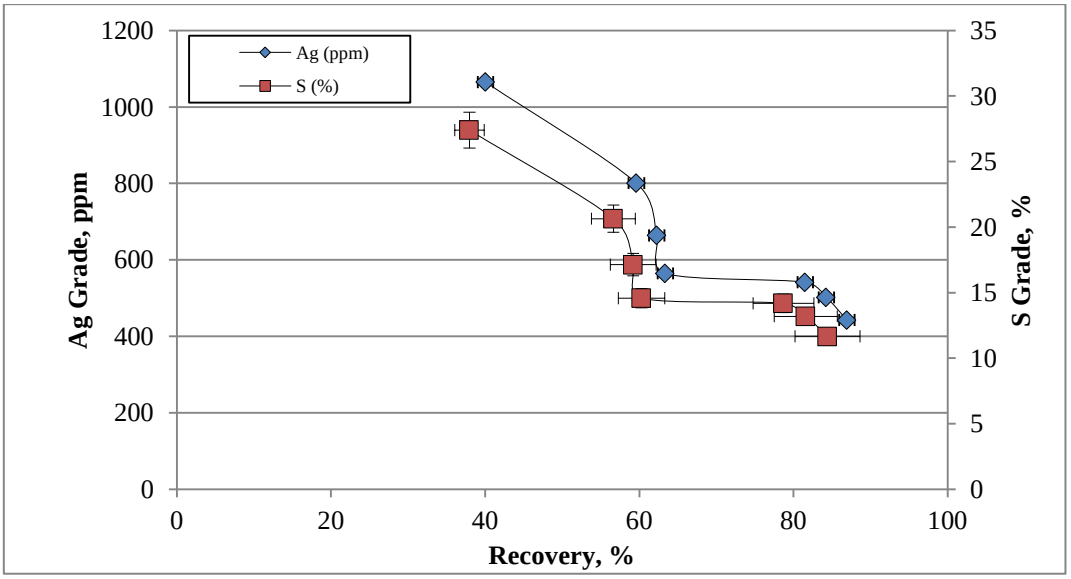

Figure 5.10: Grade recovery curves for flotation test.

Figure 5.11 presents the flotation response (log fraction remaining versus time) for three elements, namely silver, zinc, and sulphur. The relative responses of these elements to the sulphidisation stage are indicated by the change in slope in the curves between 8-10 minutes of flotation; the elements that responded most strongly to this stage were silver, and sulphur (which due to elemental deportment can be treated a proxy for pyrite); while sphalerite (for which Zn can be used as a proxy) exhibited a minor change in flotation response due to sulphidisation. The response of pyrite to sulphidisation indicates that there was some oxidised or surface-altered pyrite present in the ore.

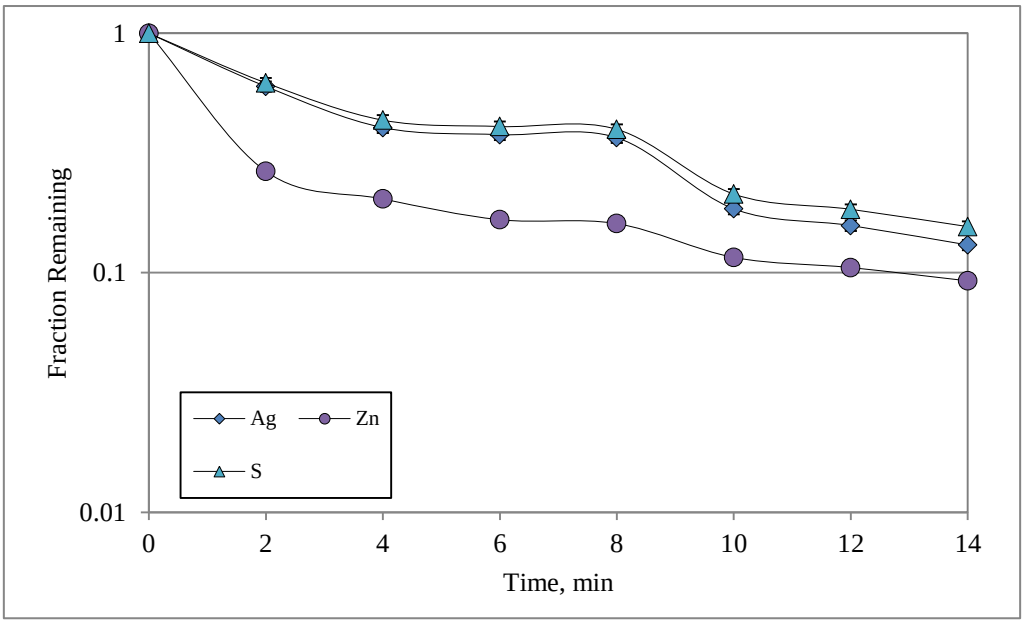

Figure 5.11: Rate curves for selected elements.

5.3 Results of flotation products characterisation

No element-to-mineral conversion equations existed for this ore. These equations are not developed in this research. All streams were measured at the size fractions described in section 5.2.2 and the modal mineralogy from MLA measurements was used to perform the mineral recovery-by-size calculations.

5.3.1 Mineral recovery by size

The results from this mineral mass balance by size are presented in Figure 5.12, the minerals selected were pyrite (the dominant sulphide and primary silver carrier in the ore); sphalerite (because all the zinc was represented by it) and NSG which contained the remaining minerals. The pyrite and sphalerite profiles had a similar trend in recovery for all size fractions. The overall recovery–by-size trends did not follow the typical inverted U shape; both sphalerite and pyrite

showed a high level of recovery for all size fractions analysed (within experimental error). The NSG showed the typical entrainment trend, with an increase in recovery at the fine fractions. Removing recovery by entrainment will give the more typical shape for pyrite and sphalerite recovery in the finer fractions. It would also appear that for this ore, due to the relatively fine mill product size, the usual drop-off in recovery at coarser size fractions is not observed.

Water recovery is also indicated in Figure 5.12, with the overall water recovery for the flotation test being 29.3%. This value correlates with the recovery of NSG in the ore in the finer size fractions.

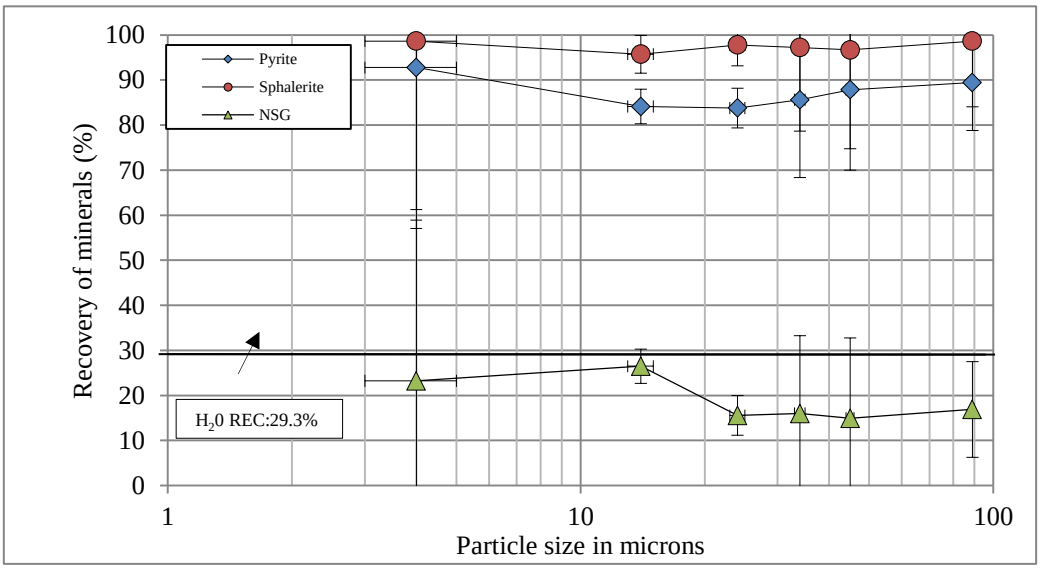

Figure 5.12: Recovery by size of pyrite, sphalerite and non-sulphide gangue (NSG)

5.3.2 Recovery by size and liberation

Incorporating mineral liberation into the recovery-by-size analysis was done using mineral locking data from the MLA measurements. Mineral locking data provide information on the distribution of the mineral of interest in a number of particle classes, including: liberated (particles that contain >95% by weight of the mineral of interest); binary (particles that contain the mineral of interest and one other mineral); and ternary (particles that contain the mineral of interest and more than one other mineral). The flotation tailing and products can then be analyzed to determine the response of these different classes of particles during flotation; the recalculated mill product can be obtained by summing the tailing and the products.

The characteristics of pyrite-containing particles in the mill product are shown in Figure 5.13, which shows that approximately half of the pyrite falls into the liberated class, with much of the remainder present as binaries with NSG.

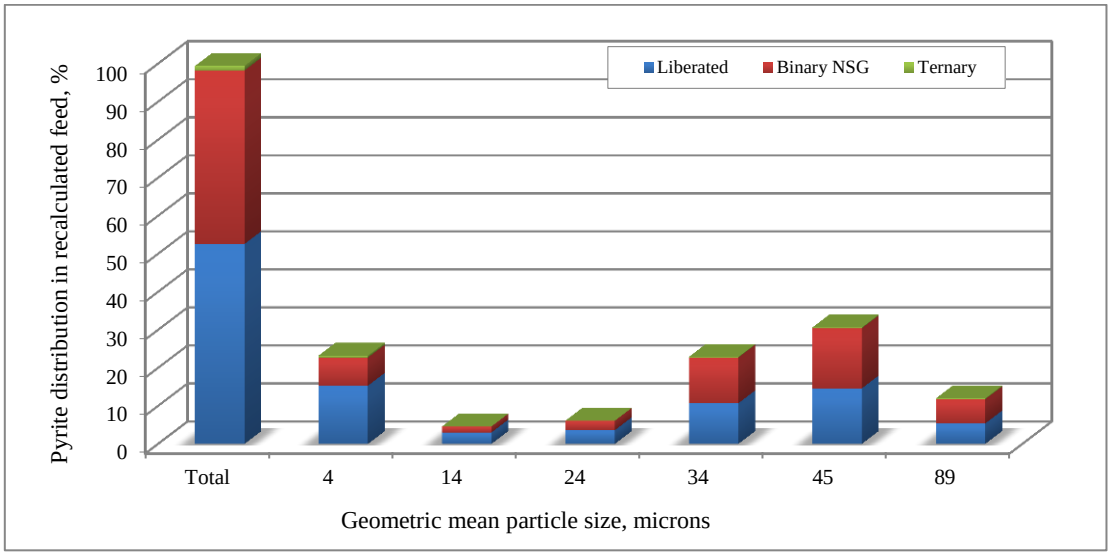

Figure 5.13: Pyrite distribution in recalculated mill product

Figure 5.14 shows the pyrite distribution recovered in the concentrates and shows the contribution of binary, ternary and liberated forms for the six size fractions under study. The pyrite reached 27% with respect to the pyrite in the concentrate at 45 μm, which was the highest value for this mineral in the ore. The percentage of liberated pyrite was higher in the small size fraction of 4 μm, followed by the 45 μm size fraction. In the intermediate zone the percentage of liberated pyrite is higher than for the binary composite; ternaries are seen in small proportions in this region. The mineral locking for pyrite in binaries is a higher proportion in the coarse size fraction (45 μm).

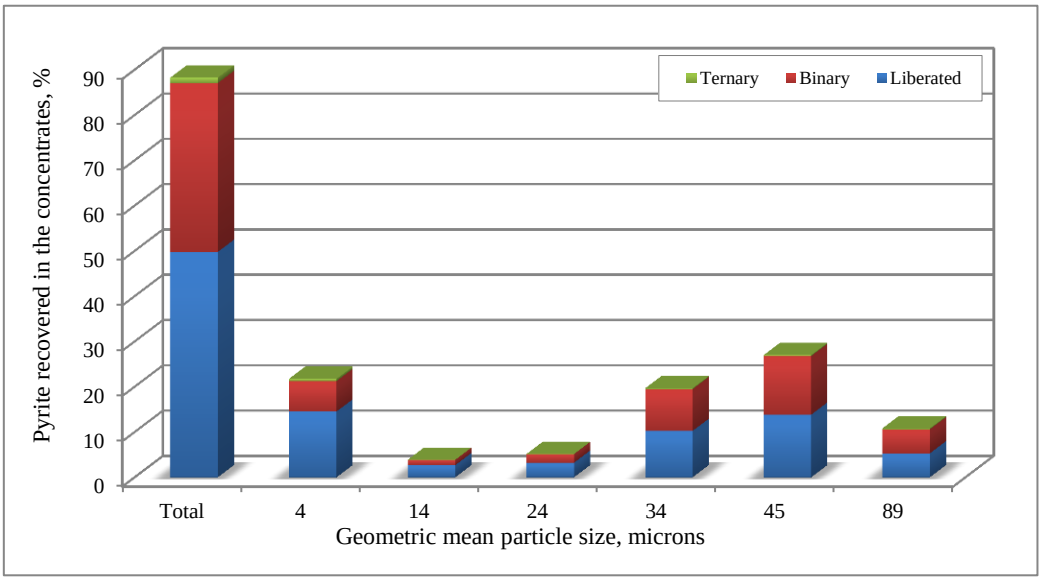

Figure 5.14: Mass balanced recovery of pyrite by size

The analysis of the tailings provides information on where the valuable mineral has been lost. Pyrite losses are predominantly as the result of pyrite being present in binary composites as shown in Figure 5.15. The main pyrite losses occur in the coarser size fractions where pyrite is present mostly

in binary composites with a small proportion of the pyrite present in the composites with NSG i.e. the binaries are low in pyrite content. In the finer fractions, an increased proportion of the lost pyrite is as liberated pyrite (Figure 5.15).

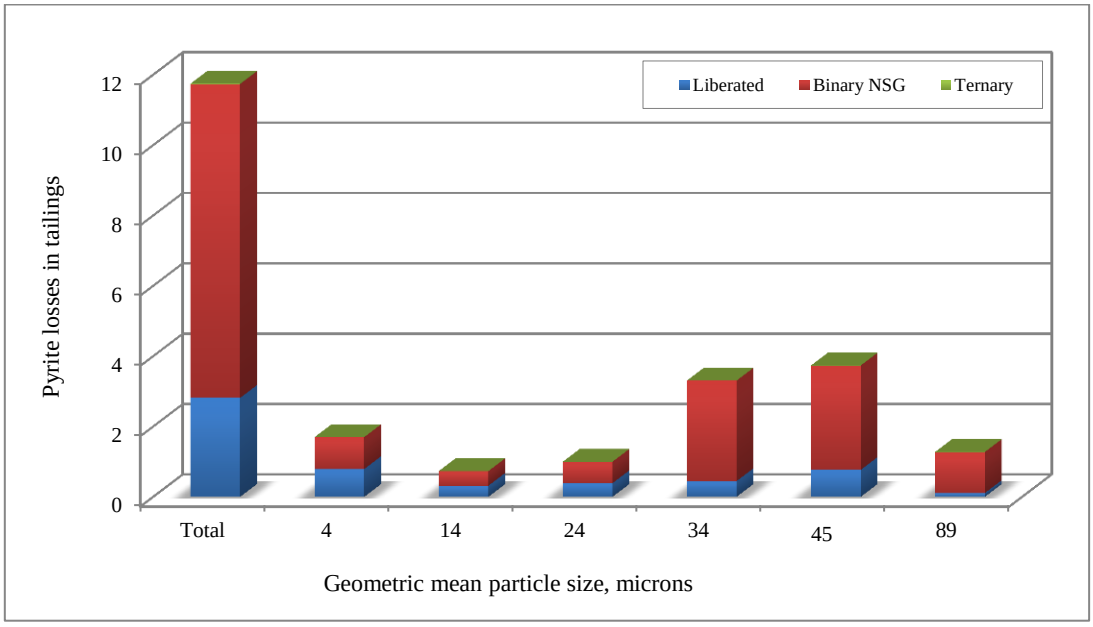

Figure 5.15: Pyrite losses in the tail by size.

5.4 Key findings

A comprehensive mineralogical assessment was undertaken using Level 2 characterisation. The mineralogical characterisation supported the use of a flotation process to recover silver through the production of a pyrite concentrate. The key findings for Tesorera ore (sulphide ore) are summarised below:

1) Gangue mineralogy was represented mainly by feldspar and quartz in this case study. The gangue mineralogy did not pose any significant issues with regard to the selection of flotation as the separation process.
2) Silver occurred mainly as solid solution in pyrite (99% of the silver in the mill product from the mineralogical characterisation). Therefore, the flotation process was developed to target the recovery of pyrite.
3) Pyrite was not well liberated in the mill product and a large proportion of the pyrite was present in the coarser size fractions which show poor liberation of pyrite, which resulted in the incorporation of mainstream inert grinding (MIG)
4) Sulphidisation resulted in an increase of 18.4% in pyrite recovery indicating that a proportion of the pyrite in the feed was tarnished or oxidized.

5) The grain size of the silver minerals was relatively fine. If these minerals had represented a recovery target, the mill product size may have been a consideration in the development of the flow sheet because a much finer feed sizing would have been needed.

This case study shows that pyrite, which in almost all processing of base metal ores is considered as gangue, can be the most important mineral. It can carry the valuable element, which transforms this gangue sulphide mineral into the most important mineral to be recovered. Enhancing the recovery of pyrite was supported by the mineral characterisation for this ore, which was the most important stage for understanding the deportment of silver prior to flotation testing.

A combination of collectors, a dispersant, an activator, a sulphidising agent and the MIG procedure were used to improve the silver grade and recovery. As a result of these conditions, a silver recovery of 87.3% with a grade of 485 ppm was obtained from the ore, through batch rougher flotation tests performed in two main stages, namely sulphide flotation followed by flotation of non-sulphide minerals after sulphidisation.

The liberation study by size indicated that pyrite was mainly recovered in the liberated form, followed by binary composites and, to a lesser extent, as ternary composites. The main losses of this mineral were as binary composites in the 45 μm fraction (-53 μm/+38 μm) and the size fraction below this one.

Chapter VI:

Development of a selective flotation strategy for a supergene silver ore: “Jayula ore”

Chapter 6 describes the Level 3 characterisation used for Jayula ore, during which a previously unreported association was found between silver and barite, which accounted for more than 20% of silver in the ore. The metallurgical implications of floating a supergene ore are discussed in terms of flow sheet design. This discussion is followed by analysis of the product from the optimised process, on a size-by-size and size-by-liberation basis. The final flow sheet with a P80 of 25 μm produced a concentrate for which the silver recovery was 80.8% at a grade of 1709 ppm Ag.

6.1 Overview of complex mineralogy present in Jayula ore

In the following section, the results of the Level 3 ore characterisation are discussed with the emphasis on understanding the silver deportment and the liberation of the silver minerals that were the recovery targets in flotation.

The discussion begins with the most relevant results from chemical assays and a description of the new protocol that was developed to find the silver minerals that were not initially identified from MLA analysis. This was then used to inform the standard MLA analysis from Level 1. This protocol, together with the other tools used in the Level 3 characterisation, provides an overall picture of the mineralogical characteristics for this ore.

6.2 Mineralogical characterisation

6.2.1 Level 3

6.2.1.1 Chemical assay and MLA assay reconciliation

a) Chemical assays

The silver assay for this ore had an approximate value of 112±5 ppm. The assay by size data shown in Table 6.1 indicate that the coarsest size fractions have the highest silver assays (> 115 ppm); below -425/+300 μm microns, the value of silver decreases from 99 ppm to 31 ppm of silver at 38 μm. This ore had the lowest grade in the finest size fraction (-38 μm), 31 ppm, when compared with the other two case studies Toldos ore, at 265 ppm of Ag, and Tesorera ore, at 78 ppm of Ag. The presence of sulphur was also evaluated on a size-by-size basis, showing a similar assay value through almost all size fractions with a sulphur grade of 0.4% S (with the exception of +75 μm and the fine size fractions of +38 and -38 microns that contained 0.5% S). This lower grade of S suggested that this ore was an oxide ore. The chemical assays for other selected elements are shown in Table 6.1; the complete dataset for chemical assay for this ore feed is presented in *Appendix I.*

b) MLA calculated assays

A standard output from MLA analysis is the calculated chemical assay, which is based on the chemical composition of the minerals in the sample and their relative abundance. A standard quality control (QC) step in any MLA analysis is the comparison of these values to the bulk chemical assay. Figure 6.1 shows the comparison between the values of the chemical assay and the MLA chemical assays for silver in the -425/+300 μm and -1.18mm/+850 μm size fractions. It is evident that the MLA silver assay underestimated the bulk chemical assay. The values for the MLA assays were 44 ppm at -425/+300 μm, and 109 ppm at -1.18mm/+850 μm. Possible reasons for the poor reconciliation between the chemical assay and MLA calculated assay include: the low grade of Ag in combination with the relatively small number of particle sections measured in the coarse size fractions (i.e. poor sampling statistics), and the very fine grain size of the observed Ag minerals in combination with the coarse particle size measured (i.e. the pixel size for the measurement was at or below the limits of the Ag mineral grain size for the samples measured, the pixel size at -425/+300 μm being 0.93 μm/pixel). The initial inability to reconcile the silver assays drove the development of the protocols used in Level 3 characterisation but also indicated that this ore would present a challenge in terms of the ability to use flotation to produce an acceptable concentrate. A wide range of analytical tools was investigated to try to discover the nature of the unaccounted-for silver. This

led to the discovery of a previously unreported chemical association between silver and barite that is described in section 6.2.1.5.

Table 6.1: Elemental assays on unsized and size-by-size basis for Jayula ore.

Size, mm	Ag	Al	As	Ba	Cu	Fe	Pb	S	Zn
	ppm	%	ppm	ppm	ppm	%	ppm	%	ppm
Head	112	3.5	530	3320	90	3.2	5880	0.4	710
+2.36	189	4.8	480	3310	70	4.0	4470	0.4	560
+1.7	151	3.9	490	3960	70	3.6	4980	0.4	610
+1.18	160	4.0	500	4800	70	3.7	4980	0.4	600
+0.850	138	4.4	500	3650	80	3.7	4930	0.4	600
+0.600	126	4.3	510	3940	80	3.6	4980	0.4	600
+0.425	115	3.7	510	4260	90	3.3	5120	0.4	630
+0.300	99	4.3	500	4360	80	3.5	5220	0.4	640
+0.212	98	4.1	490	5080	90	3.4	5400	0.4	660
+0.150	89	2.9	520	5660	100	3.1	5540	0.4	690
+0.106	79	4.9	530	6370	90	3.7	5760	0.4	710
+0.075	78	5.0	530	6590	100	3.7	5920	0.5	740
+0.053	69	4.8	540	6180	120	3.8	6300	0.4	800
+0.038	64	5.8	560	5900	200	4.0	6470	0.5	820
-0.038	31	4.9	580	2110	120	3.0	7580	0.5	850
Calc Hd	***104***	***4.4***	***523***	***3891***	***94***	***3.5***	***5780***	***0.4***	***690***

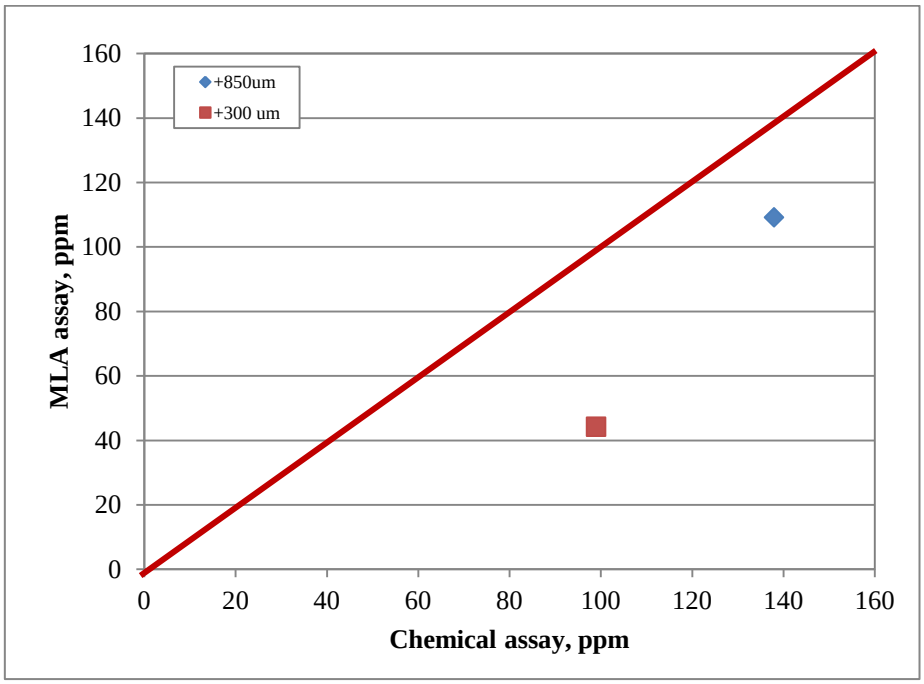

Figure 6.1: Parity chart of chemical and MLA assays for silver at -425/+300 µm and -1.18mm/+850 µm.

After applying Level 2 characterisation to the Jayula ore, the results were still not conclusive with respect to silver deportment. This is due to only 15% of the silver deportment was identified as

known silver minerals, namely, acanthite, pyrargyrite, and chlorargyrite, being more than 80% of the silver deportment not accounted by MLA in the size fraction corresponding to -425/+300 µm. Considering these results, it was decided to pursue in the searching of the silver deportment, resulting in a new protocol for identifying the unknown silver carriers being developed, which is described in section 6.2.1.5.

6.2.1.2 X-ray diffraction (XRD)

As explained in Chapter 3, the size fraction used for the XRD analysis was +1.18 mm, and the objective of this analysis was to support the identification of gangue minerals. Table 6.2 shows the results for the qualitative XRD measurements for Jayula ore. It can be seen that the most abundant mineral in the ore is quartz at more than 50%, with kaolinite as the sub-dominant mineral, with more than 20% present in the ore. In small quantities (minor) is the alkali feldspar group, representing minerals such as orthoclase, anorthoclase, microcline and sanidine. The plagioclase feldspar group is present at the trace mineral level, lower than 5%.

Table 6.2: X-ray diffraction results for Jayula case study (AMDEL).

Mineral	Composition	JK2681-1
Quartz	SiO_2	Dominant (>50%)
Kaolinite/greenalite	$Al_2Si_2O_5(OH)_4$ / $Fe_6Si_4O_{10}(OH)_8$	Sub-dominant (>20%)
Alkali feldspar	$KAlSi_3O_8$	minor (5-20%)
Plagioclase feldspar	$NaAlSi_3O_8$	Trace (<5/%)

6.2.1.3 Oxide characterisation for lead and zinc minerals

The results shown in Table 6.3 reflect the percentage of lead (Pb) and zinc (Zn) minerals that are present in oxide form in the ore. The amount of oxide is considered as moderate for both elements, representing the insoluble Pb (89.6%) and Zn (94.4%) that are amenable to the flotation process.

Table 6.3: Results for oxide characterisation of lead and zinc minerals present in Jayula (AMDEL).

Element measurement	% Total
Pb as oxide minerals	10.4
Zn as oxide minerals	5.6

6.2.1.4 Optical microscopy

One of the main features of this ore is its yellow appearance. This comes from the presence of amorphous iron, resulting in colouration that ranges from diffuse concentrated yellow-brown to rich red-brown, characteristic of the presence of iron oxides like goethite (moderately hydrated) and hematite.

Quartz is the main NSG with a coarse grain size, followed by kaolinite, then feldspar and carbonates. Some silver minerals are observed – those are native silver in a range of 2-20 μm in length by 1-5 μm wide. Acanthite is also observed in the ore. Other minerals that are present and identified in the ore are presented in Table 6.4.

Table 6.4: Estimated modal volumetric mineral distribution (from Knights, 2011)

Volumetric mineral distribution	Mineral present
Dominant (> 80vol%)	Mainly non-sulphide gangue: quartz>>kaolinite>feldspar>carbonates
Minor (5 > X > 0.5vol%)	- Lead iron arsenates (~1%) (beudanite + gabrielsonite) - Limonite – hematite – magnetite (~0.5%)
Sparse (X << 0.5vol%)	Rutile, apatite, pyrite, native silver, acanthite, chalcocite.

Complex textures were identified in the Jayula ore, with the following images showing some examples of them. Figure 6.2 shows a series of disseminated complex lead-iron arsenate oxy-salts, gabrielsonite ($PbFeAsO_4(OH)$). This complex oxy-salt is present as discontinuous rimming features, with a size that varies between 3 and 5 μm. Figure 6.3 illustrates the granular rimming of colloform limonite ($2Fe_2O_{3*}3H_2O$) with undifferentiated lead-iron bearing arsenate. It also shows discoloured, iron-stained non-sulphide gangue.

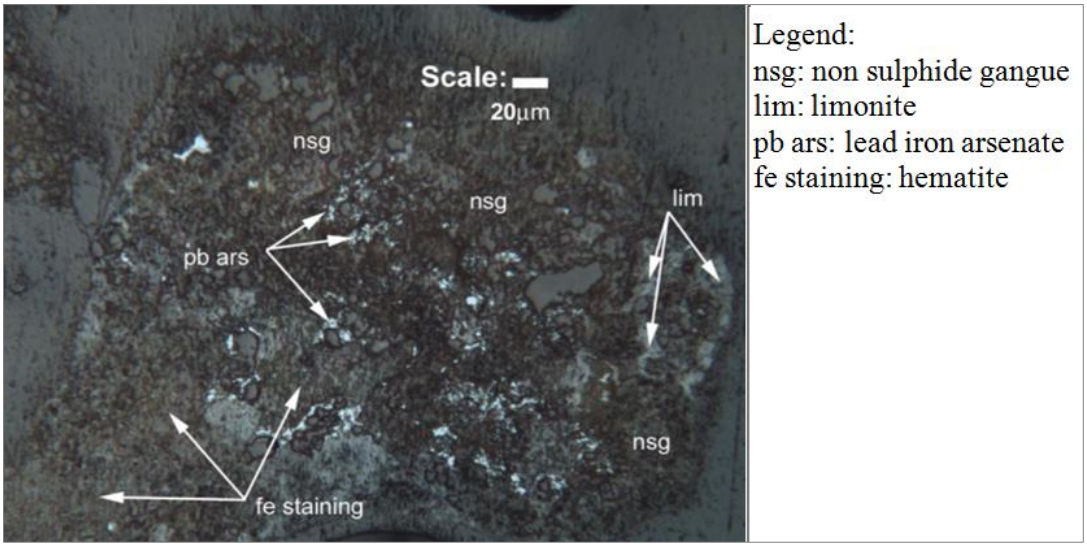

Figure 6.2: Photomicrograph of disseminated complex lead-iron arsenate oxy-salts (from Knights, 2011).

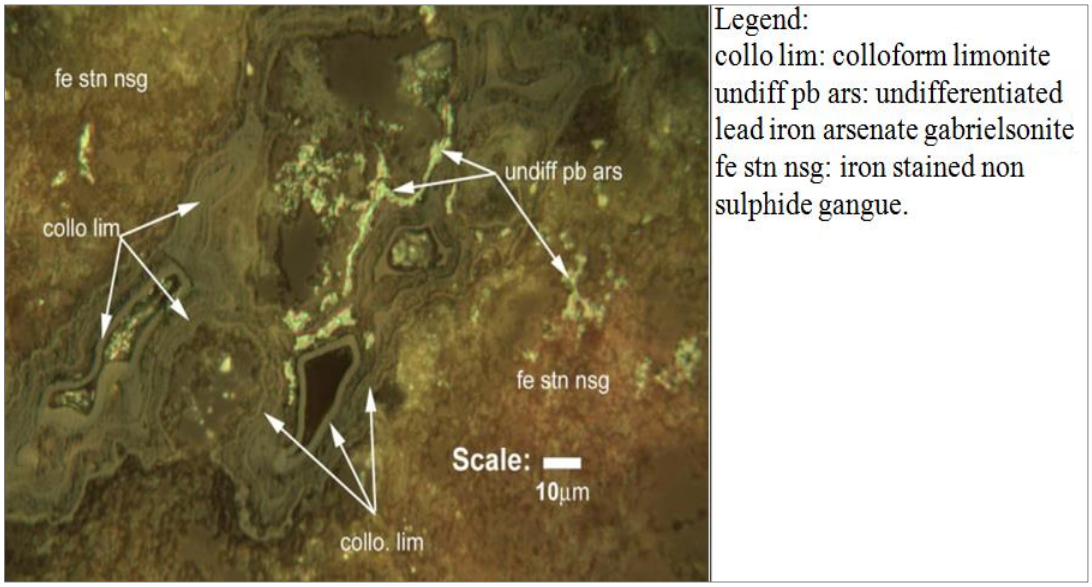

Figure 6.3: Photomicrograph of granular rimming of colloform limonite (from Knights, 2011).

The photomicrograph shown in Figure 6.4 (A) illustrates some native silver enclosed with non-sulphide gangue, while (B) shows pyrite and acanthite enclosed with the non-sulphide gangue.

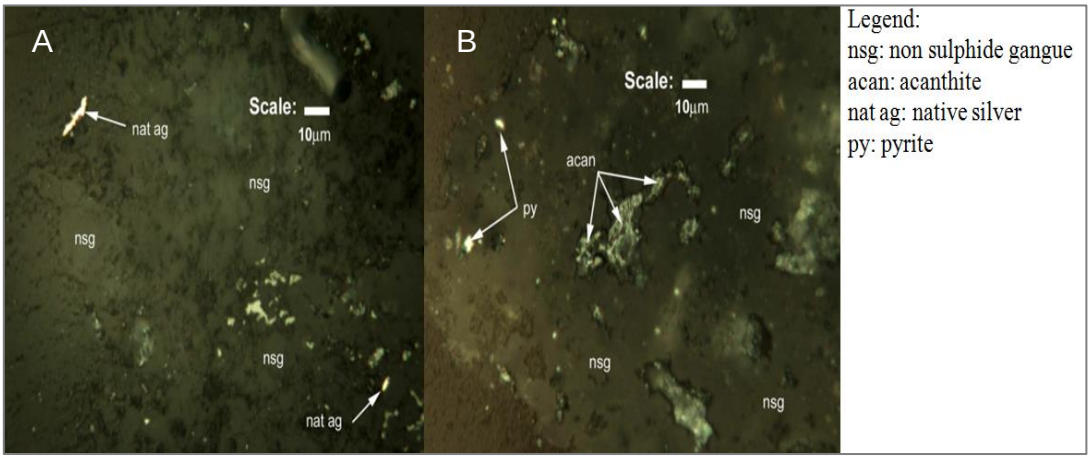

Figure 6.4 A) at left photomicrograph containing native silver and Figure 6.4 B) at right photomicrograph containing acanthite (from Knights, 2011).

Optical microscopy indicated of the presence of grains of native silver. Native silver is amenable to recovery through the flotation process, assuming liberation is possible.

6.2.1.5 Laser ablation inductively coupled plasma mass spectroscopy (LA-ICP-MS)

The results showed that the average amount of silver present in these minerals was relatively low. For Pb phosphates an average 9 ppm of Ag was found; for Pb arsenates 266 ppm of Ag and for Jarosite 173 ppm of silver were contained in the minerals. Attention is on the discrepancy between the quantity of As content in Pb phosphate and Pb arsenate that have only ~0.05% difference, with a

much larger error in the As content of the Pb arsenate, it was expected that a significant difference in As content between a phosphate and an arsenate, given the same cation of Pb, with the arsenate containing much more As than the phosphate, but the values are similar. The uncertainties are related to the measurements in the assays i.e., that during measurement and classification there were probably some misclassification and when the samples were sent for analysis, there may well have been some inconsistency. However, these Pb phosphates and arsenates are easily identified through MLA because the compositions of Pb Phosphates is half of what it is in Pb arsenates, as is shown in *Appendix J*, which shows the elemental composition of each of the minerals used in Jayula Ore. Therefore, there is no problem for MLA differentiated and recognising these spectra. Table 6.5 presents the average results of silver content for the minerals analysed. *Appendix K*, shows the individual results by MODA.

Table 6.5 LA-ICP-MS results (supplied by MODA)

Mineral, average	Ag, ppm	Al, ppm	Si, ppm	Fe, ppm	Cu, ppm	Zn, ppm	As, ppm	Pb, ppm
Pb phosphates	9±5.4	71164±27065	37028±14995	776678±758101	750±371	5644±3184	6580±1367	95941±56913
Pb arsenates	267±442	16183±8948	11549±6958	436351±21735	822±401	3444±2889	7109±5973	119474±62644
Jarosite	173±109	9940±8007	34219±29326	489461±63048	160±114	3084±3123	4753±2018	41403±24046

6.2.1.6 Establishing a new protocol to identify unaccounted silver carriers in complex ores (Level 3)

This section describes the steps undertaken to identify the possible sources of the unidentified (from MLA analysis) silver in the ore. During the course of this analysis a chemical association between silver and barite was found that has not been reported in the literature; this will be referred to as barite_Ag. In order for barite_Ag to be officially recognised as a new mineral, the following are required: the isolation of a certain quantity of the mineral grains; a high quality EMPA; a series of high quality crystallographic analyses (XRD); and identification of the optical properties. This thesis focuses on the identification of silver hosts but the process of gaining recognition for new minerals is outside the scope of this work.

The new protocol begins with elemental mapping using EMPA, followed by manual and auto SEM, and finally Synchrotron XRD and XRF. The description of this approach is given in Chapter 3, Section 3.4.1.2. Figure 6.5 illustrates the approach used for the identification of the silver minerals that remained unidentified following Level 1 and Level 2 characterisation.

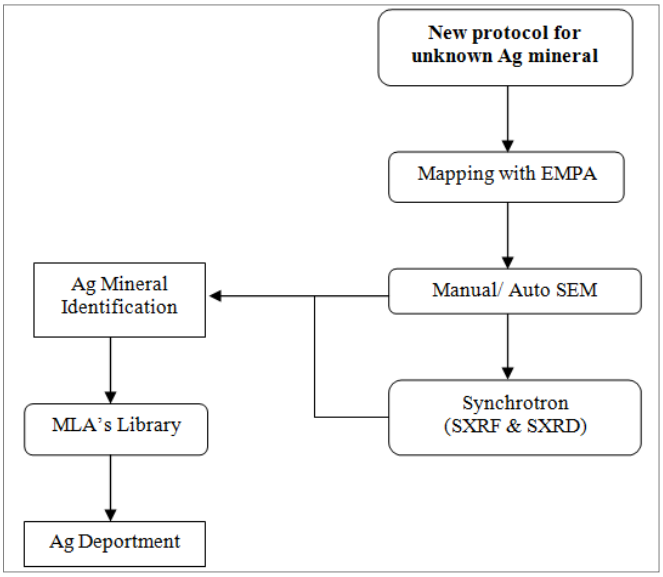

Figure 6.5: Protocol for analysing the unknown minerals that contain silver.

A. Step 1 – Mapping with EMPA

The first technique used to help locate the missing silver after MLA analysis was to map the -425/+300 μm size fraction, to search for the presence of silver in the sample. Other elements were also mapped at that stage of the research. The elements that were mapped and considered important at that stage of the project were silver (Ag), aluminium (Al), arsenic (As), calcium (Ca), iron (Fe), potassium (K), phosphorus (P), lead (Pb), sulphur (S) and silicon (Si). At that stage of the research, barite_Ag had not been identified, and therefore barium was not included in the elements that were mapped by EMPA. Figure (6.6) shows the maps of elements measured by EMPA. The area measured was one square centimetre of the sample block, which gave a square matrix of 1024x1024 pixels. In the figure, the grains containing higher amounts of the elements measured have the highest colour intensity.

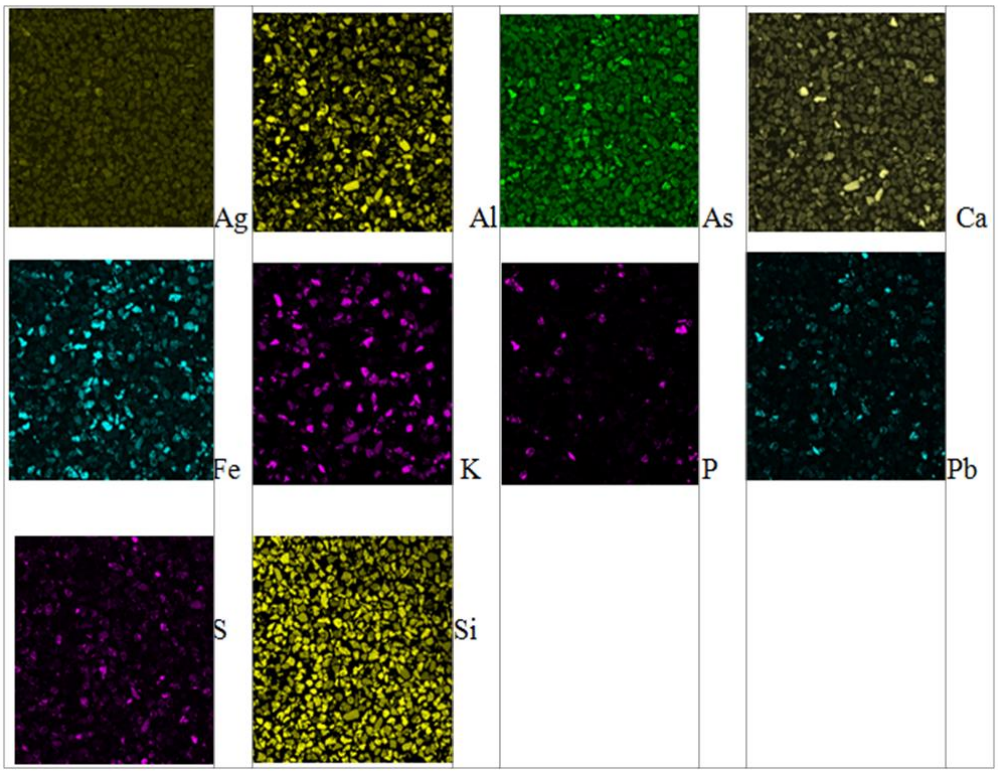

Figure 6.6: X-ray maps for Sample 1 (matrix 1024x1024)

The numeric matrix generated could be correlated mathematically in ternary diagrams, in order to understand the elemental association with silver, and to find any relationship that would help to find the unknown silver carriers in the ore. The analysis of those matrices was performed by selecting the highest values of silver, using a small program developed in Matlab (*Appendix E*), which provides small matrices. Ternary diagrams were plotted, using ioGas software. In Figure 6.7, the most significant ternary diagram that relates Ag-Si-S is presented; the data analysed are shown as a ternary diagram, which associated silver with silicon and sulphur. The points are related to the composition of the highest population of these related grains, and suggest that there was an association between silicon and silver (because mineral grains that contain Ag are very fine and the matrix is mainly quartz).

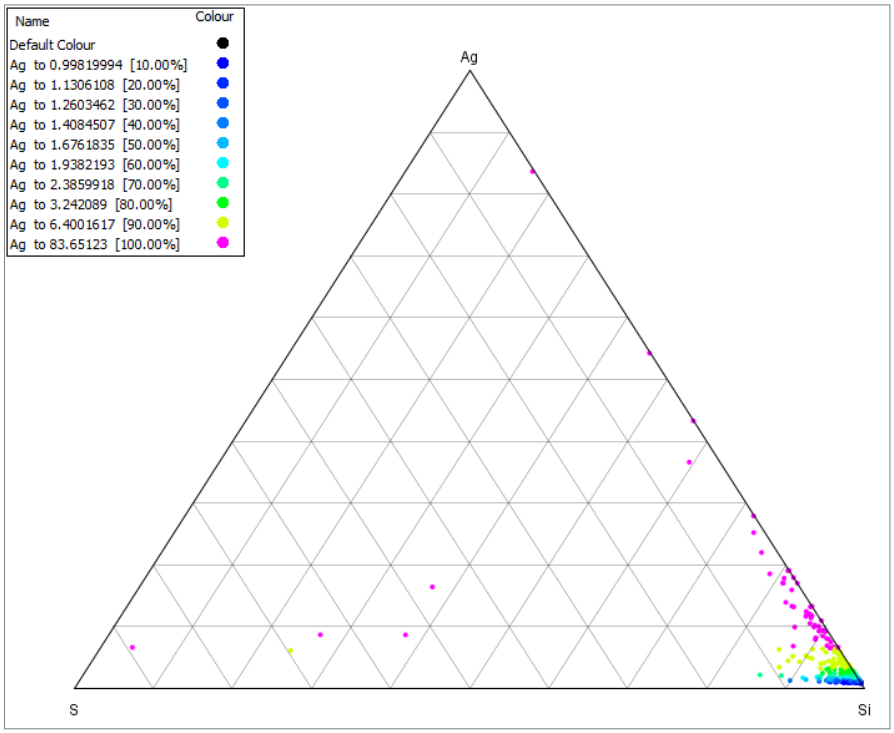

Figure 6.7: Ag-S-Si ternary diagram association

B. Step 2 - Manual SEM

In Chapter 3, the conditions used in re-analysing the size fraction of -425/+300 μm by manual SEM-EDS were described. Table 6.6 shows the fourteen bright grains identified that contained silver and between four and 10 other elements. All of the grains containing Ag also included oxygen (O) and silicon (Si), because they are part of the matrix in which the very fine grains occur and they appear in the X-ray spectra as the result of being sampled by the interaction volume. The grain size evaluated had sizes ranging between 2 and 20 microns.

Table 6.6: Grains identified by manual SEM-EDS that contain silver

Grain no.	Element														
	C	O	F	Mg	Al	Si	P	S	Ti	Fe	As	Ag	Te	Ba	Pb
1		x			x	x	x	x		x		x		x	
2		x			x	x		x	x	x		x			
3		x			x	x	x	x		x		x		x	
4		x				x		x		x		x		x	
5	x	x			x	x				x		x			x
6	x	x		x		x		x		x		x		x	
7		x			x	x		x				x			
8		x			x	x		x		x		x			
9	x	x	x		x	x	x	x		x	x	x			
10	x	x			x	x	x	x		x		x	x		x
11	x	x				x		x				x		x	
12	x	x			x	x	x	x		x	x	x			
13		x				x		x				x			
14	x	x				x		x		x		x		x	

Figure 6.8 illustrates an EDS image with the particle containing Grain 5 as referred in Table 6.6. The other bright grains in the particle were not considered in the Ag analysis due to the EDS measurements showed that they do not contain Ag. The Figure, also shows the spectrum of the energy (kV) on the x-axis and the intensity of x-rays detected on the y-axis. The X-ray spectrum generated by EDS for Grain 5 includes Ag, Pb, Fe, Al and Si apart from O and C, being these last two present in all measurement.

In Table 6.6, there are six different grains containing silver and barium along with other elements. The mineral reference library (used during MLA image processing to identify the spectra collected online for the measurement) did contain a spectrum for barite, but did not include a spectrum containing Ag and Ba. Just to clarify, the barite_Ag association was found using the manual SEM with an example of the spectrum shown in Figure 6.9 where is possible to appreciate a particle with various grains, one of them containing barite_Ag. The matrix of this sample is quartz, which accounts for the presence of Si in the spectrum. It should be noticed that barite_Ag association is a very fine grained, and might be a mixture of quartz/ barite/ silver/ acanthite or others, or probably might be a new series of solid solution between Barite and acanthite in a matrix of quartz.

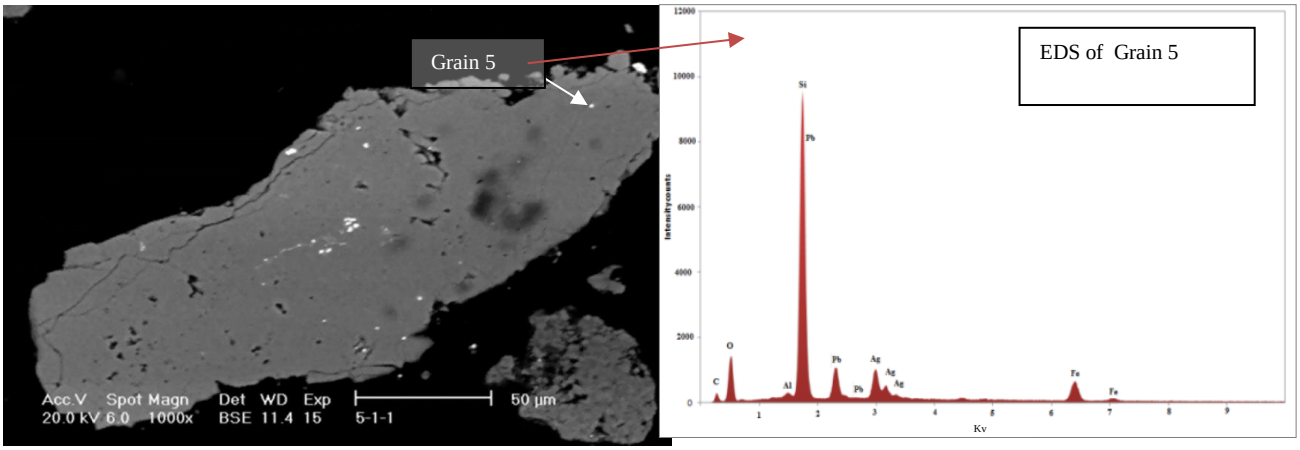

Figure 6.8: Particle with Grain 5 measured referred to table 6.5 containing a silver-bearing spectrum identified by EDS.

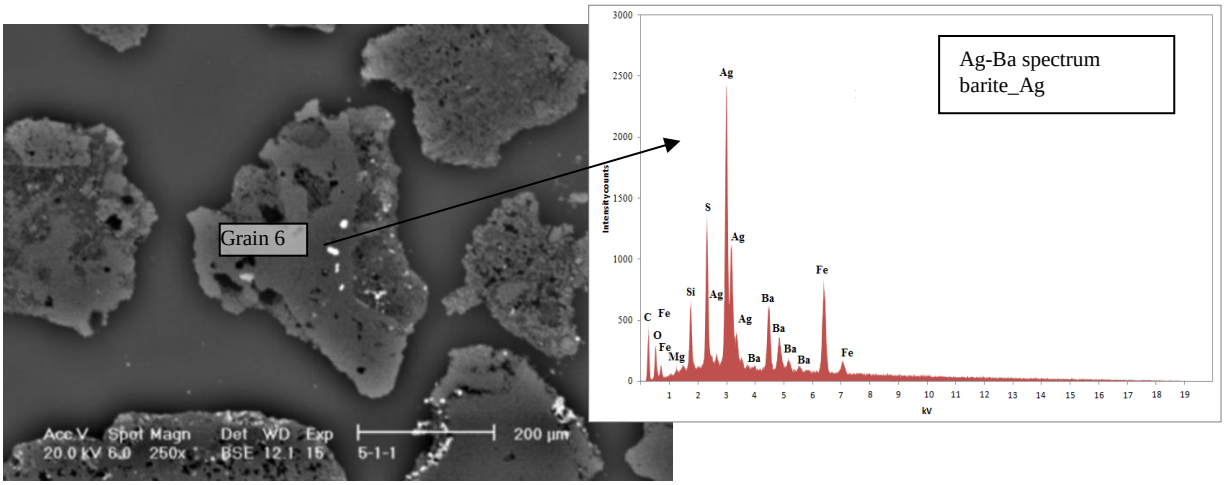

Figure 6.9: Particle with different grains including Grain 6 containing Ag-Ba seen in the ED spectrum.

The results from optical microscopy indicated the presence of native silver in the Jayula ore. Previous MLA results (Wightman, 2011) did not identify native silver in the samples analysed. Sample 3 prepared by J.Quinteros was analysed by manual SEM-EDS, and a grain of native silver was found in the sample, confirming the existence of it in the Jayula ore. This result complemented the results of the optical microscopy analysis, which needed to be confirmed with the MLA results. Figure 6.10 shows a grain of native silver identified in a particle in Sample 3.

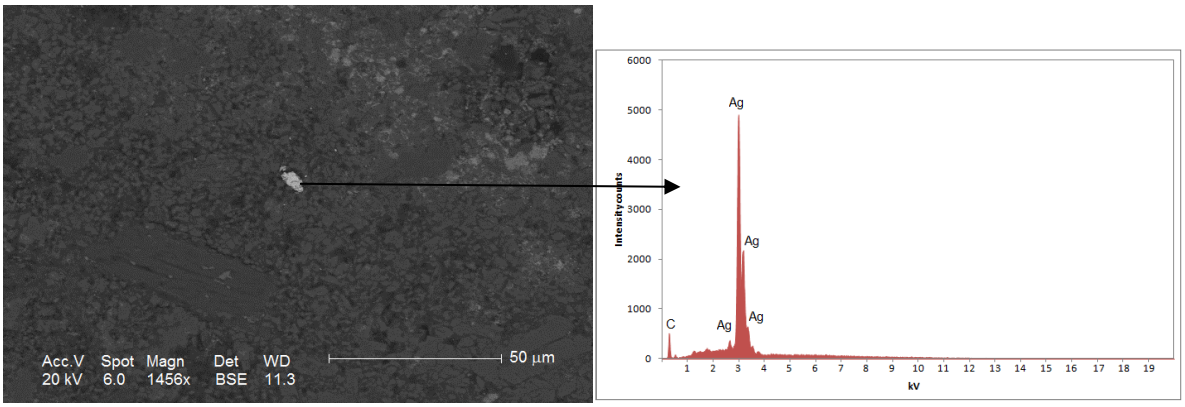

Figure 6.10: Particle with a grain of native silver identified by EDS.

The results from the manual SEM-EDS made it necessary to investigate whether the composition of barite_Ag was consistent for this sample. Therefore, to gather more confidence in the data, auto SEM was used to target the grains of interest.

C. Step 3 - Auto scanning electron microscope (Auto SEM)

Two samples from each of the -425/+300 µm and -1.18mm/+850 µm size fractions were measured twice by a Jeol 7001F SEM, equipped with EDS and using Inca software to set the parameters to quantify the composition of barite_Ag. The objective of this measurement was to identify more rapidly the grains that exhibited the barite-Ag spectra in the sample blocks. The results from the measurement of the samples are presented as a summary in Table 6.7 and the number of grains analysed that had the barite-Ag spectra confirmed the presence of barite_Ag. These measurements are not a repeat samples as two different blocks for each size fraction were measured. Figure 6.11 illustrates the compositional variability of barite_Ag. To account for this, three spectra containing varying amounts of Ag and barite were incorporated into the MLA's reference library and the samples were reclassified to determine the contribution of this new spectrum to the quantification of silver in the ore.

Table 6.7: Summary from the measurement at auto SEM

Sample	Test 1	Test 2	Test 3	Test 4
	-425/+300 µm	-425/+300 µm	-1.18mm/+850 µm	-1.18mm/+850 µm
No of Ag grains	57	83	624	286
No of grains measured	7676	2127	16640	988
Average area of grain, microns	21.01	0.47	10.19	1.07
No. of Ag-Ba spectra	34	35	297	178

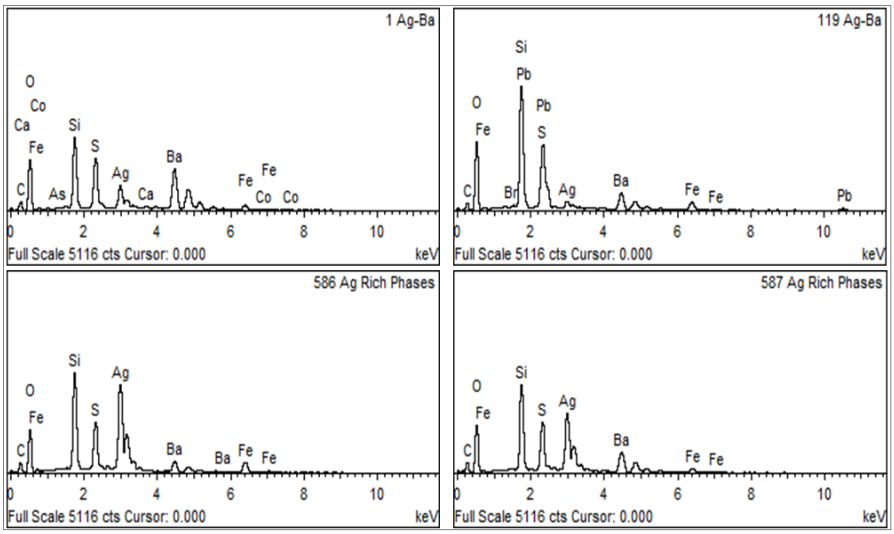

Figure 6.11: New spectra of Ag-Ba with different amounts of silver and barium.

Even with the incorporation of barite_Ag into the MLA mineral reference library the reconciliation between the MLA calculated assay and chemical assay was still not acceptable with more than 45% of the silver unaccounted for at -425/+300 µm and more than 20 % at -1.18mm/+850 µm. For this reason the highest resolution techniques currently available were used in order to try to understand the behaviour of silver in this ore, leading to the use of the synchrotron as part of this thesis work.

D. Step 4 – Synchrotron Methods

The synchrotron incorporates three techniques described in Chapter 3. In this section the results of the combination of SXRF and SXRD with XANES are discussed.

a) Synchrotron XRF (SXRF) mapping to find Ag hotspots

The results of the SXRF mapping of the -1.18mm/+850 µm size fraction (Map size: 6,100 µm horizontal (h) × 5,400 µm vertical (v)) analysing Ag, K, S, Fe, Cu, Zn, As, Pb and Sr are shown in Figure 6.12. The conditions used were described in Section 3.4.1. Frame B in the figure shows a SXRF image that was analysed for Ag, K and S, containing two hotspots of Ag inside the yellow box. These two hotspots were analysed using the XANES spectra. For frames C and D, Fe, Cu and

Zn and As, Pb and Sr were analysed respectively. Once the Ag spots were identified, synchrotron XRD was applied on the spots to identify the possible minerals.

Additionally, for the +38 μm size fraction, two other spots (3 and 4) were identified. Figure 6.13 illustrates the spots, which were analysed for silver-sulphur-iodine (Ag-S-I) and silver-potassium - sulphur (Ag-K-S), respectively. These analyses then were evaluated using XANES to identify some Ag minerals to be incorporated in the MLA's Library.

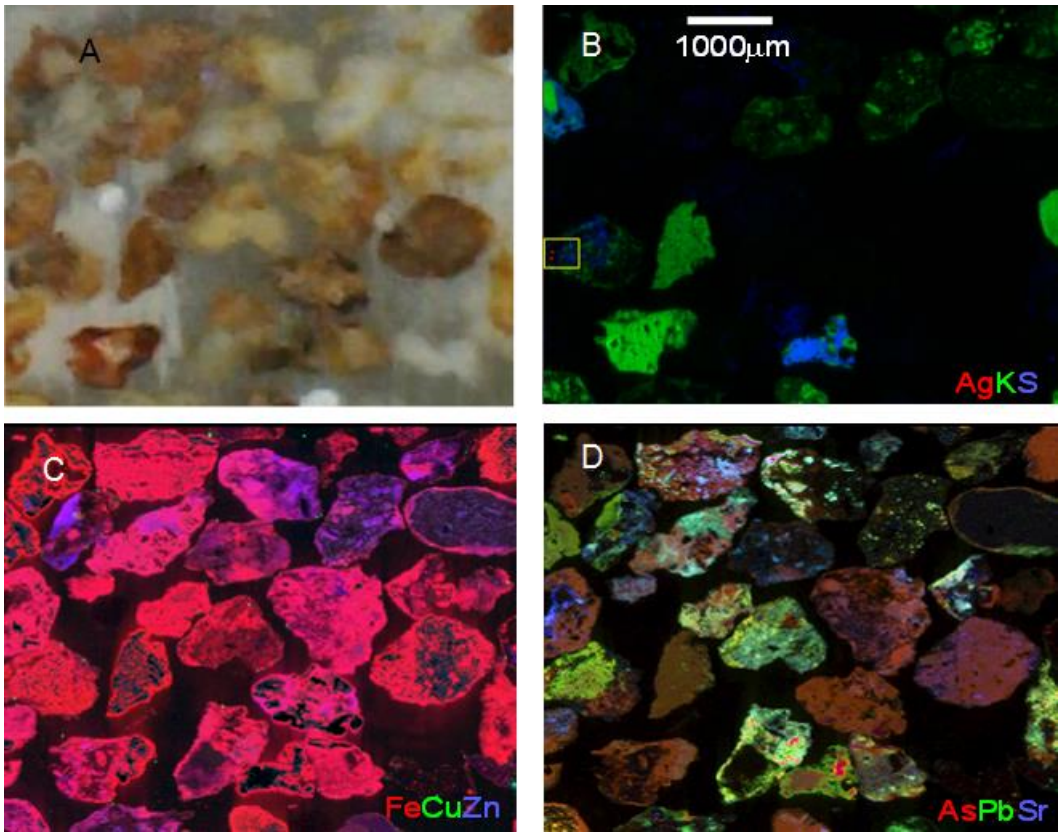

Figure 6.12: Synchrotron XRF mapping of Ag, A) is an optical image of the section measured (from Fan, 2013).

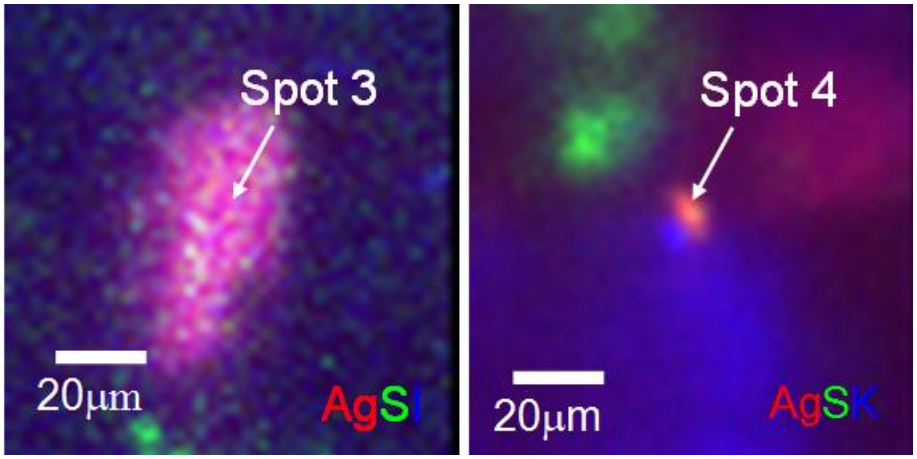

Figure 6.13: SXRF spots containing Ag at +38 μm (from Fan, 2013)

b) Synchrotron XRD for Ag spots

SXRD and XANES were applied on the silver hotspots 1, 3 and 4. Figure 6.14 shows the 2D diffraction rings for the SXRD analysis on spot 1. It illustrates the crystal structure of a continuous diffraction ring that satisfies Bragg’s Law; however, there were a few grains that suggest the presence of quartz but not for specific silver minerals.

The SXRD for spots 3 and 4 (Figures 6.15 and 6.16) showed different single large grains in both hotspots. These represent an insufficient sampling of grains to produce a continuous diffraction ring in the 2D diffraction graph.

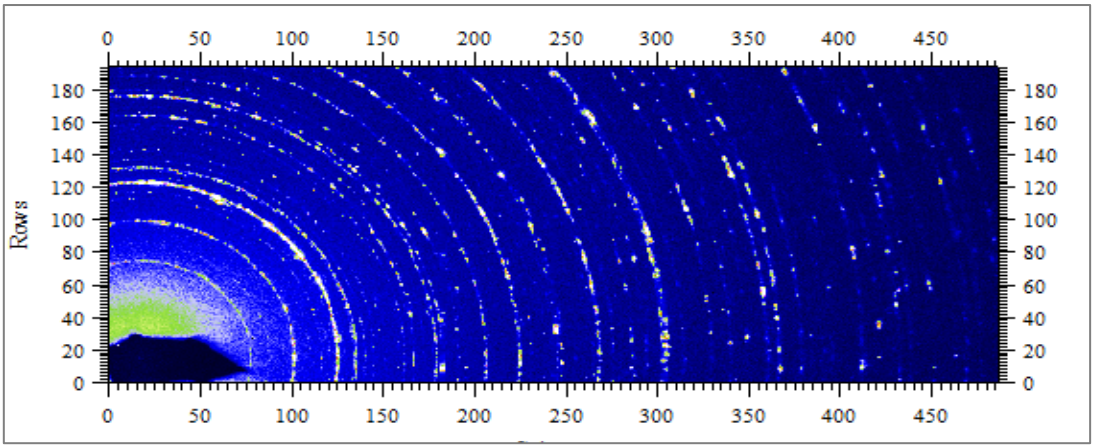

Figure 6.14: 2-D diffraction patterns for spot 1 (from Fan, 2013)

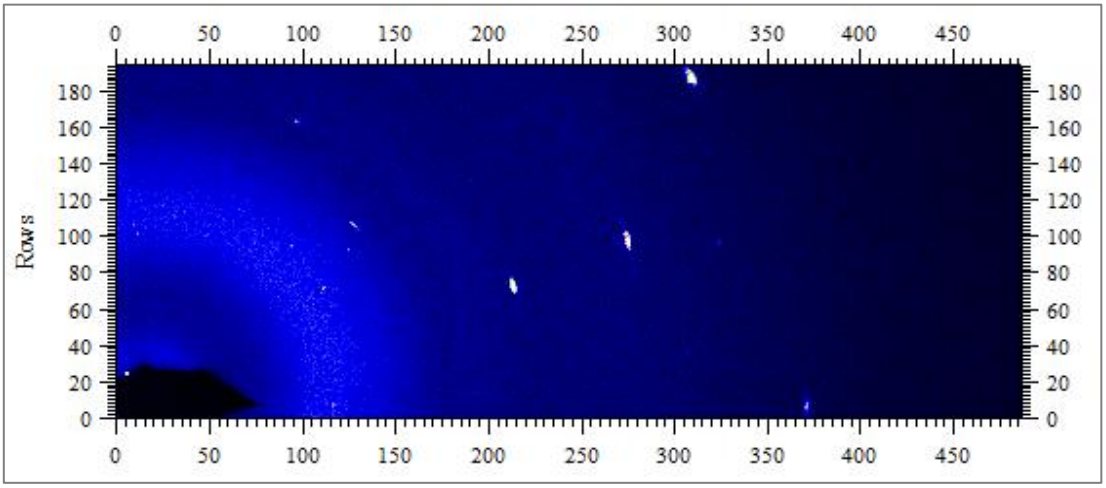

Figure 6.15: 2-D diffraction patterns for spot 3 (from Fan, 2013)

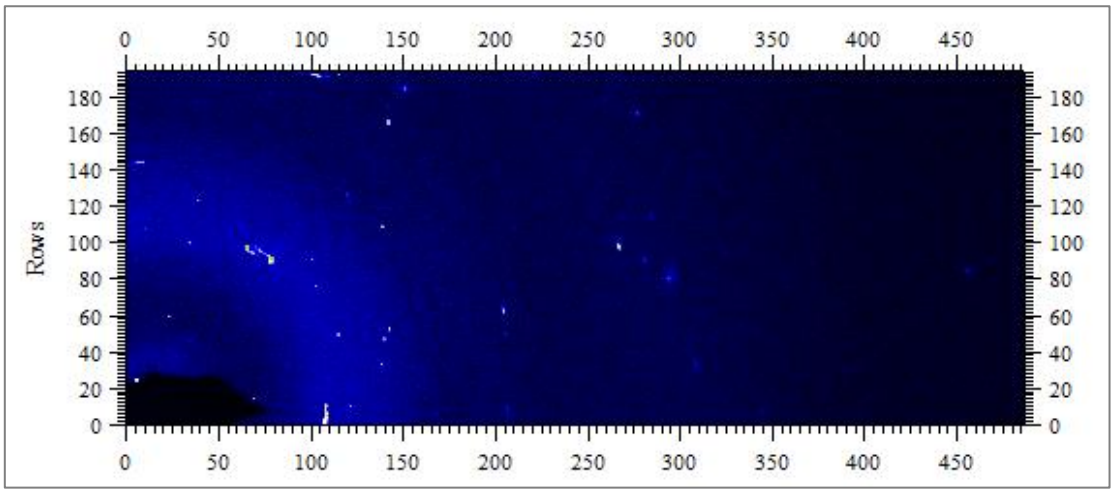

Figure 6.16: 2-D diffraction patterns for spot 4 (from Fan, 2013)

The results of XANES analyses of the Ag hotspots and standards are presented in Figure 6.17. From the XANES, spots 1 and 2 matched with the acanthite standard, indicating that it was probably an intergrowth grain that contained quartz and acanthite (Ag_2S). For spot 3, the curve did not match with any standard but, by incorporating the information gathered by SXRF, this was nominally identified as iodargyrite (AgI). This was consistent with its XANES spectra, which showed different features compared to other Ag grains and sulphide standards. Spot 4 matched the standard for pearcite ($(Ag,Cu)_{13}As_2S_{11}$). Also, pyrargyrite and proustite were identified through XANES.

The XANES spectra showed clearly significant differences among the different Ag-containing sulphide mineral groups.

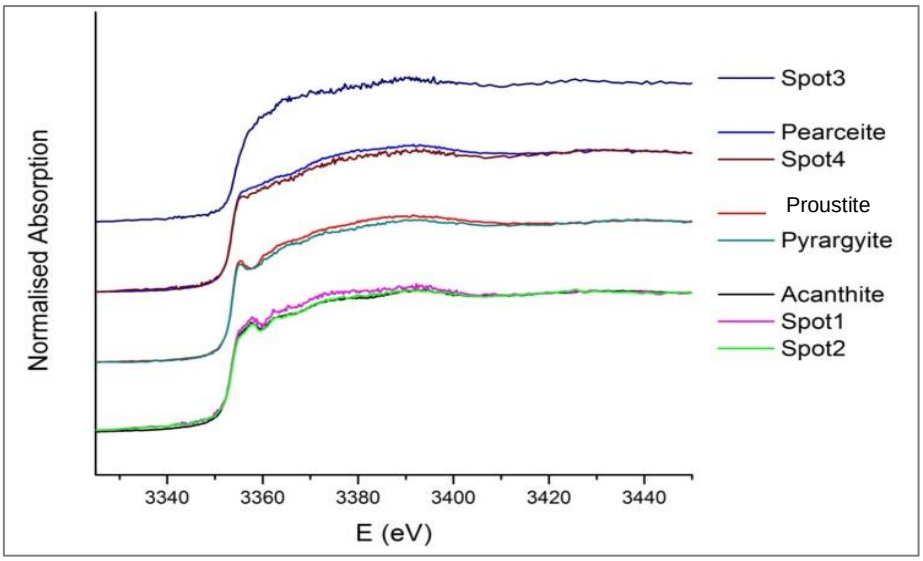

Figure 6.17: XANES analyses of Ag hotspots and standards (from Fan, 2013).

The additional silver-bearing minerals identified by the new protocol (barite_Ag, proustite and iodargyrite) were all incorporated into the MLA mineral reference library.

6.2.1.7 Mineral liberation analyser (MLA)

The results presented incorporate the spectra that were identified as a result of the new protocol established to identify previously unaccounted silver carriers. For the size fraction of -425/+300 μm, a total of 1,037,266 grains was measured in 53,220 particles. For the coarse size fraction of -1.18 mm/+850 μm, 546,620 grains in 20,968 particles were measured.

a) Modal mineralogy

The modal mineralogy (presented in Table 6.8) consisted primarily of quartz, kaolinite and feldspar and in lesser extent clays_micas and others. The modal mineralogy indicated that quartz was the main non-sulphide gangue present in the ore. However, attention was made for the quantity of kaolinite present in the ore, being this the reason why in this ore the kaolinite was separated from the group of clays_micas.

Table 6.8: Modal mineralogy for Supergene oxide ore at -425/+300 μm and -1.18mm/+850 μm with 95% confidence

Mineral	Average wt%, -425/+300 μm	Std. Dev.	Average wt%, -1.18mm/+850 μm	Std. Dev.
Ag_min	0.01±0.0	0.0	0.01±0.0	0.0
Pyrite	0.01±0.0	0.0	0.03±0.0	0.0
Quartz	50.73±0.9	1.1	56.21±2.7	3.1
Feldspar	11.66±0.7	0.8	9.51±1.5	1.7
clays_micas	7.75±1.6	1.9	6.34±1.7	1.9
Kaolinite	23.69±0.6	0.6	21.87±1.7	1.9
Fe_oxide	1.40±0.2	0.2	1.25±0.5	0.5
barite_Ag	0.01±0.00	0.0	0.04±0.02	0.0
Others	4.75±1.0	1.1	4.74±2.5	2.8

b) Elemental deportment

Figure 6.18 illustrates the evolution in the quantification of the silver deportment, using all of the techniques available for this project and considering as well the results of the metallurgical characterisation to identify the silver carriers for this complex supergene ore. The first attempt considered the MLA data for the -425/+300 μm and -1.18mm/+850 μm size fractions. For the -425/+300 μm size fraction after Level 1 and 2 characterisation, less than 20% of the silver was accounted for, with acanthite identified as the main silver mineral. After applying Level 3 characterisation, the incorporation of barite_Ag and the other identified silver minerals into the MLA mineral reference library allows the MLA to account for approximately 80% of the silver in the -1.15 mm/+850 μm size fraction, and approximately 50% of the silver in the -425/+300 μm

fraction as shown in Figure 6.18. Also it can be noticed in this figure the results from the analysis of the flotation feed samples for P80 values of 100 µm and 50 µm. For these samples, which have been homogenised by grinding and have smaller pixel resolutions during MLA measurement (allowing more effective measurement of fine mineral grains), the silver assay can be reconciled with the MLA calculated assay.

By combining the mineralogical and metallurgical characterisation, it was possible to identify the silver deportment for this supergene ore, which is clearly carried by silver minerals. Acanthite was the main carrier, followed by barite_Ag and pyrargyrite, and to a lesser extent, tetrahedrite and native silver (shown in the analysis of the recalculated flotation feed).

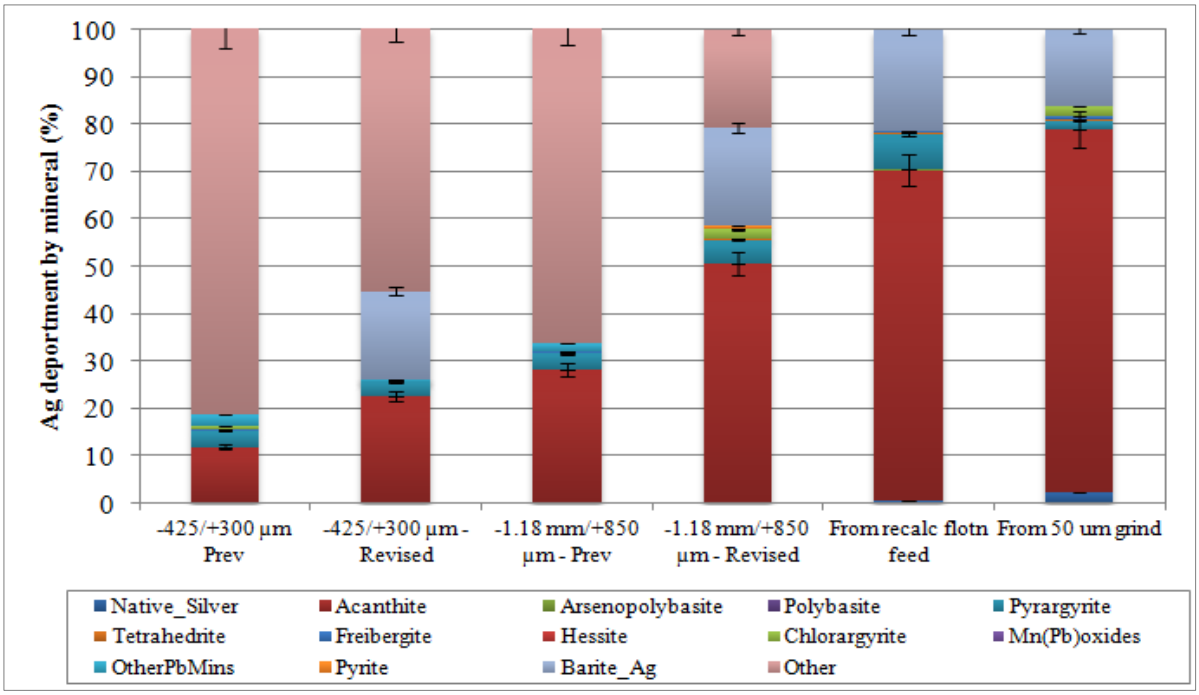

Figure 6.18: Silver deportment by mineral for Jayula ore, showing the previous results and the current results.

c) Texture:

- ***Mineral grain size:***

The grain sizes of the silver minerals in the -425/+300 µm fraction were analysed; these were native silver, acanthite, arsenopolybasite, pyrargyrite, tetrahedrite, freibergite, hessite and chlorargyrite, and barite_Ag, as shown in Figure 6.19. From this graph it can be seen that the silver minerals and barite_Ag had similar fine mineral grain sizes, with a P80 of approximately 12.5 µm. This indicated that fine grinding is required to recover these silver minerals.

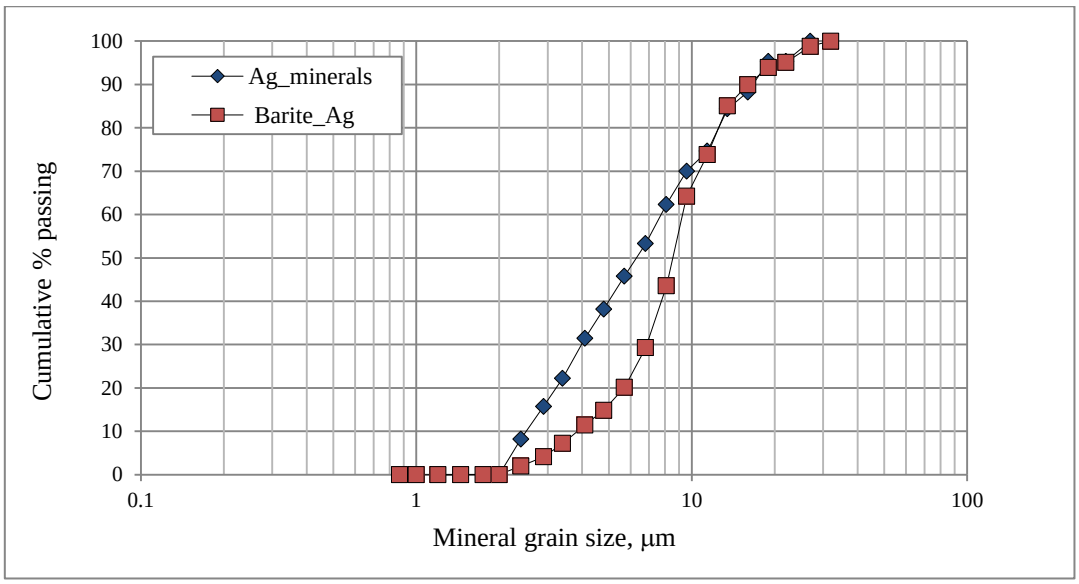

Figure 6.19: Mineral grain size distributions for Ag minerals and barite_Ag for Jayula.

❖ *Mineral association*

Based on the results from the MLA and the integration of the new protocol, the silver minerals (Figure 6.20) were strongly associated with quartz (79%), followed by carbonates (6%) and barite (3.6%) and barite_Ag (3.1%). In the case of barite_Ag (Figure 6.21), the main association was with quartz (49.9%), lead sulphates (9.8%) and the clays_ micas group (7.9%). These mineral associations do not represent troublesome cases for the flotation process. In the case of this clays_micas group the minerals identified are not problematic for flotation. The minerals identified are Muscovite, illite, biotite and kaolinite.

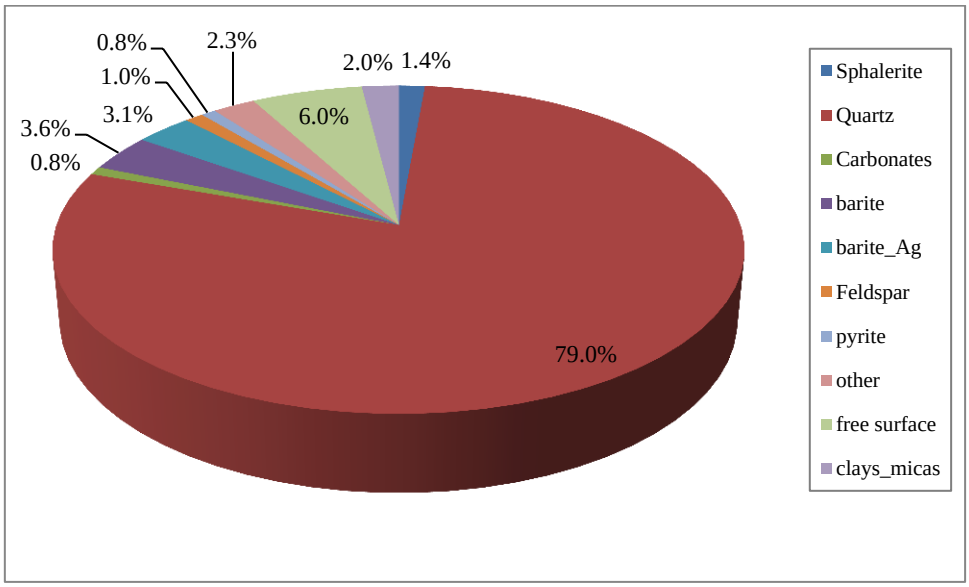

Figure 6.20: Silver mineral associations

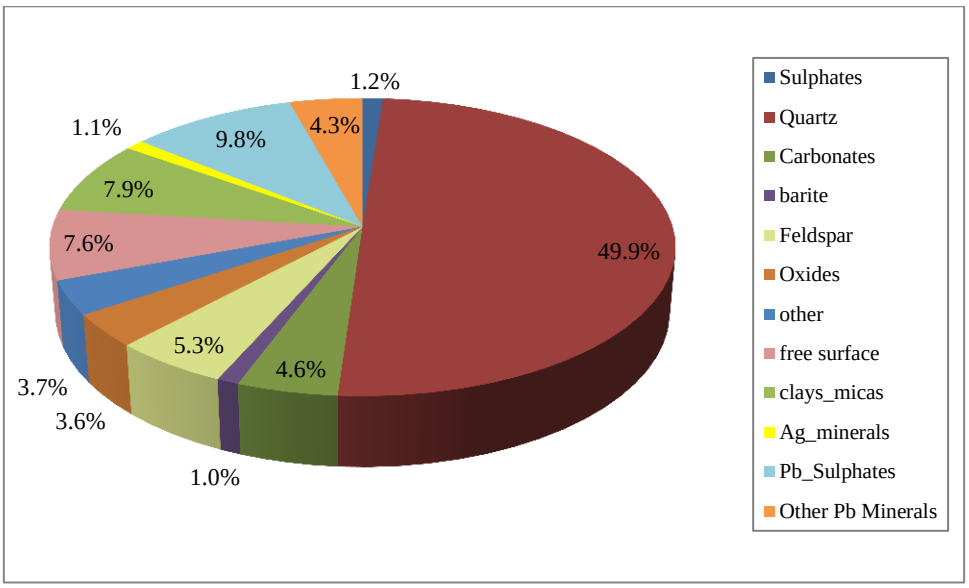

Figure 6.21: barite_Ag mineral associations

Complex textures, as described by Butcher (2010), were present in the Jayula ore. For example, in Figure 6.22 (A), which illustrates the BSE and the MLA processing images, a particle can be seen in the top-right corner that contains silver mineral rimmed by sulphate minerals, while Figures 6. 22 (B and C) show particles that contain disseminated inclusions of barite_Ag in barite. Clearly, the presence of these complex textures directly affects the liberation and thereby the potential flotation response of the silver minerals that are present in this supergene ore.

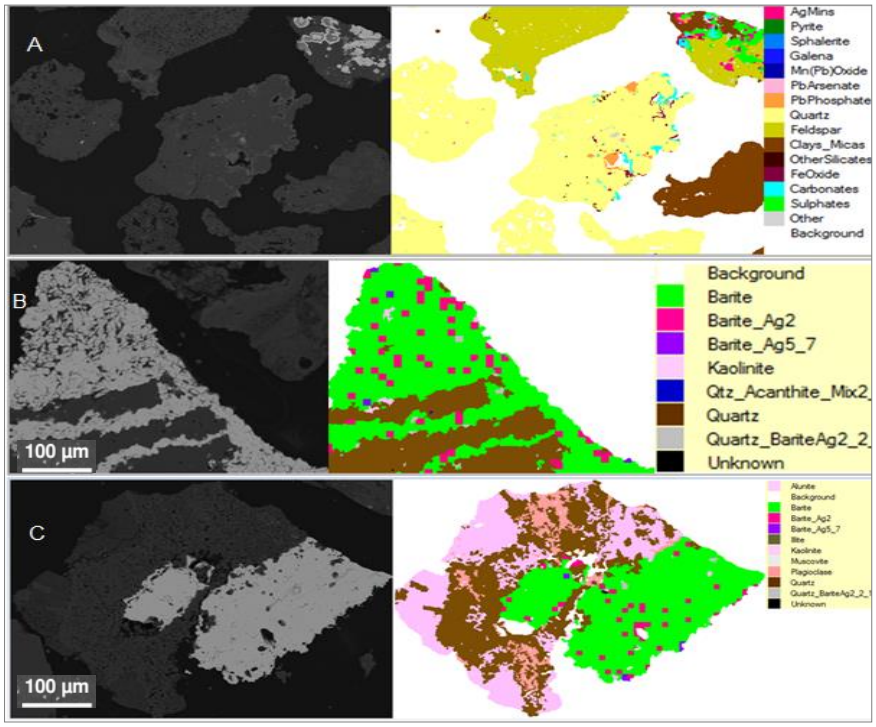

Figure 6.22: BSE and MLA images showing complex textures present in Jayula ore at -425/+300 µm.

- ***Assessment from Level 3***

The outcomes of the new protocol were the identification of barite_Ag association, proustite and iodargyrite. The barite_ Ag association was found using the manual SEM not using the synchrotron methods. In fact with the XANES spectra two new minerals: proustite and iodargyrite were found. These minerals were added to the MLA library to complement the deportment of silver. Table 6.9 illustrates a summary of the analytical techniques used on Level 3.

Table 6.9: Assessment of Level 3

Techniques	**Chemical assay**	**XRD**	**Oxide mineral characterisation**	**Optical microscopy**	**LA-ICP-MS**	**Novel Methodology**	**MLA**
Comment	Recalculated head assay for Ag is 104 ppm	Dominant gangue quartz, follows by kaolinite and feldspar	Pb ox. mineral: 10.4% Zn ox. mineral: 5.6%	Congruent with gangue mineralogy reported by XRD. Ore present complex textures. Ag deportment: acanthite and Native Ag.	Pb phosphate grains contain Ag in ss with a value of 9±5.4ppm of Ag in Pb phosphates. Pb arsenates grains contains 267±442 ppm of Ag. Jarosite present a value of 173±109 ppm of Ag as ss.	New discoveries are barite_Ag, pearceite and iodargyrite	In agreement with XRD and Op microscopy for gangue mineralogy. Ag deportment: acanthite, barite_Ag, chlorargyrite, pyrargyrite, native. Ag between other Ag mins. Silver minerals and barite_Ag present a P80 of 12 μm requiring a fine grinding to recover Ag.

6.2.2 Flotation feed characterisation for Jayula ore

The flotation feed characterisation included liberation analysis for the rougher feed material at a P80 of 100 μm using MLA analysis. Table 6.10 illustrates the results of this and indicates that 30.9% of the silver minerals were liberated i.e. there was poor liberation for the silver minerals, as expected from the mineralogical characterisation, which showed that the grain size of the silver minerals was <20 microns. However, analysing the liberation levels for the non-sulphide gangue showed that it was highly liberated (96.8%) at a feed sizing of 80 per cent passing 100 μm.

The interpretation of these results was that the flotation feed needed to be ground to a finer P80 in order to liberate the silver minerals to the extent that they would be amenable to recovery via selective flotation. However, it was known that increasing the liberation of the minerals of interest had the consequence of increasing the fineness of the NSG, which can result in an increase in the

recovery of NSG through entrainment, which is based on particle size and not the level of liberation, and a decrease in the concentrate grade.

Table 6.10: Calculation of overall liberation value for silver minerals and NSG at 80% passing 100 µm

Size fraction	Ag minerals distribution	Ag minerals liberation value (%)	Units of liberated Ag minerals	NSG distribution	NSG liberation value (%)	Units of liberated NSG
+106 µm	22.3	4.7	1.5	15.5	96.3	15.0
+53 µm	40	16.5	6.6	23.1	96	22.2
+35 µm	2.7	0.0	0.0	8.2	96	7.8
+17 µm	18.9	74.5	14.1	12.0	96.9	11.6
+14 µm	6.1	54.3	3.3	3.7	97.5	3.6
-14 µm	10	54.3	5.4	37.5	97.5	36.6
Total	100		30.9	100		96.8

Key findings of mineralogical characterisation

The mineralogical characterisation of the Jayula ore was complex because it required a high level in conjunction with the metallurgical results to finally understand the nature of the silver deportment. As a number of analytical and microscopic techniques were used for the ore, a new protocol was developed to systematically identify unknown Ag minerals and Ag minerals not in the MLA library. In terms of Ag deportment, acanthite, barite_Ag and pyrargyrite are the main silver carriers.

The gangue mineralogy indicated that quartz is the main non-sulphide gangue mineral present, followed by kaolinite and other clays. It is possible that these could produce problems via inadequate dispersion and increased pulp viscosities for a given percentage of solids in the pulp. The textures present in the ore are complex, particularly with respect to the fine grained nature of the silver minerals. As a consequence, the liberation level for the combined silver minerals in the rougher feed at a P80 of 100 µm was low (30.5%) indicating a finer flotation feed size is needed to liberate the silver minerals adequately for flotation to be effective.

Due to the nature of the silver minerals present selective flotation was selected. As with the Toldos ore, a combination of reagents is an important factor in enhancing the recovery of the Ag minerals.

6.3 Results of metallurgical characterisation for Jayula ore

6.3.1 Preliminary preflotation results

For the Jayula ore, the preflotation test revealed that there were no minerals present in significant quantities in the ore that displayed a strong level of natural flotation. However, some natural hydrophobicity was observed. The silver recovery was intermediate to the values for the Toldos ore

and the Tesorera ore; it is possible that the acanthite in this sample caused the observed response, as discussed for Toldos ore (Section 4.2.1). After 8 minutes of preflotation, 1.5% of the solids were recovered, with the following elemental recoveries: 19.0% silver, 7.0% copper, 1.7% iron, 2.0% lead, 3.5% sulphur and 8.6% zinc (Table 6.11).

Table 6.11: Preflotation results for each concentrate and for the combined concentrate for Jayula ore

Streams	Mass		Assays						Recovery (%)					
	grams	%	Ag *	Cu *	Fe (%)	Pb *	S (%)	Zn *	Ag	Cu	Fe	Pb	S	Zn
Feed	1000													
Con 1	6.5	0.7	2080	630	3.3	8310	1.1	5670	12.4	3.9	0.7	0.9	1.8	4.2
Con 2	4.7	0.5	938	410	3.2	7800	0.8	3130	4.0	1.8	0.5	0.6	0.9	1.7
Con 3	3.3	0.3	838	430	3.4	7870	1.1	7250	2.5	1.3	0.4	0.4	0.9	2.7
Total Con	14.5	1.5	1426	513	3.3	8044	1.0	5208	18.9	7.0	1.7	2.0	3.5	8.6
Tail	978.4	98.5	90	100	2.8	5810	0.4	820	81.0	93.0	98.3	98.0	96.5	91.4
Recal Feed	992.8	100	109	106	2.8	5843	0.4	884	100	100	100	100	100	100

*ppm

6.3.2 Flotation flow sheet for Jayula ore

A considerable number of flotation tests were performed, trying to obtain a desirable silver recovery (over 60%) and a mass recovery close to 10%, as this was the constraint put in place by MSC for incorporating the ore in the plant feed. All these tests gave unsatisfactory silver recoveries and adequate silver selectivity was difficult to achieve.

6.3.2.1 Flow sheet design

Figure 6.23 illustrates the path used for the preliminary flotation tests. It started with a preflotation test, followed by sulphide flotation, followed by sulphidisation and non-sulphide flotation. It then continued by exploring non-sulphide mineral flotation with de-sliming, then the use of non-sulphide mineral flotation with regrinding. At this point, the information on the silver deportment was very incomplete or misleading. When the characterisation of the key mineralogical attributes of silver were completed it became apparent that silver mineral grain size was a key limiting factor in the flotation response and as a result the flotation feed size was reduced to 25 microns.

The following approaches were applied to testing of this supergene ore:

Preflotation test was used to identify possible hydrophobic minerals present in the ore and the behaviour of the valuable minerals present in the ore, in the absence of collector.

Sulphide flotation followed by sulphidisation and non-sulphide flotation. This type of flotation was used successfully in the previous chapter to produce a bulk concentrate. The strategy was to recover all sulphide minerals first using standard reagent conditions, and to then sulphidise the pulp to recover any oxide minerals that responded to sulphidisation and that had not floated in the first step of flotation.

Non-sulphide mineral flotation used chelating collectors to recover silver minerals / non-sulphide minerals that may be carriers for silver minerals. There was a presumption that a significant portion of the silver was associated with some non-sulphide gangue minerals.

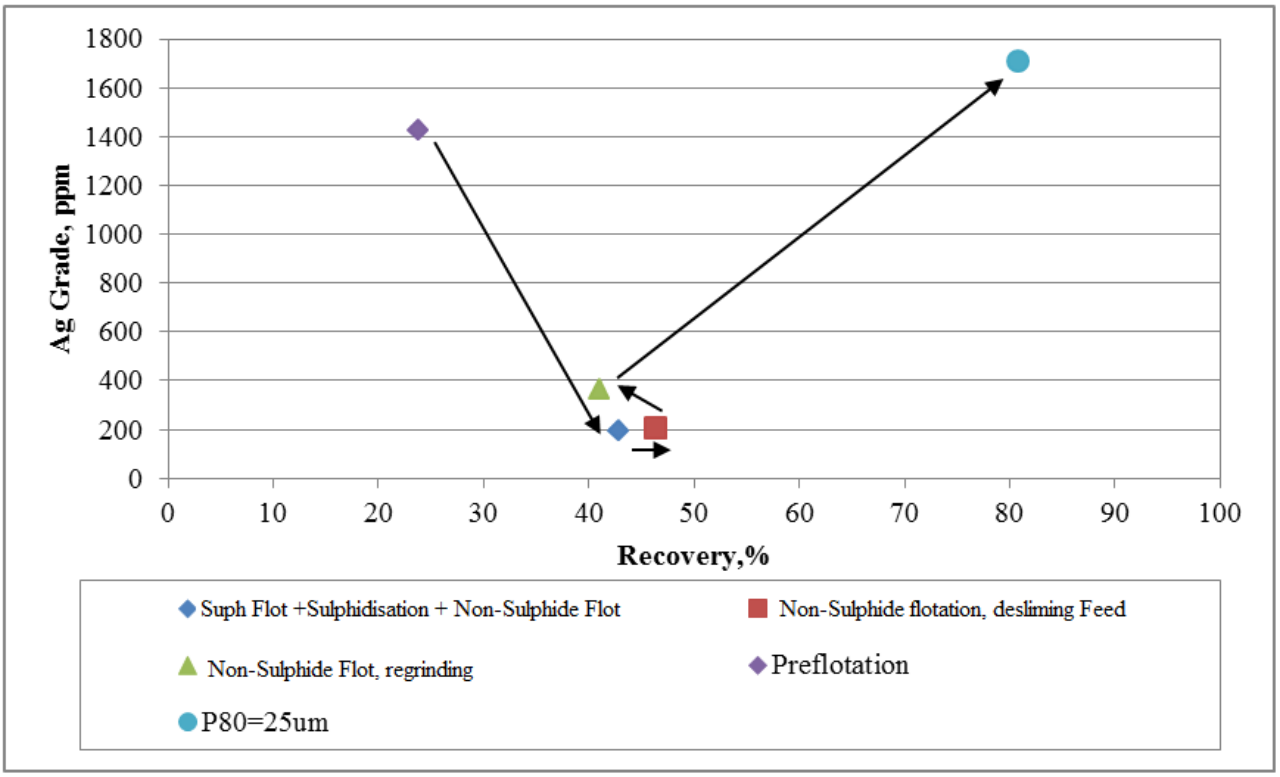

Figure 6.23: Path of flotation tests used in the supergene ore

None of these approaches was successful in achieving the required silver recovery target. Selective flotation was then applied, using the knowledge gained at the completion of all the strategies used previously for this supergene ore. To find the best flotation flow sheet, an experimental design was required to limit the number of tests required for this purpose.

- **Final flow sheet for Jayula ore**

Grinding time was selected to fit the experimental design, with a P80 of 25 microns requiring a grinding time of 23 minutes.

Selective flotation was used according to the low or nil presence of sulphide minerals in the ore. Five concentrates were obtained after different flotation times, of 30 sec, 2 minutes (con 2, 3 and 4) and after 4 minutes for con 5. The scheme of reagents is shown in Table 6.12. The best flow sheet for the Jayula ore is shown in Figure 6.24.

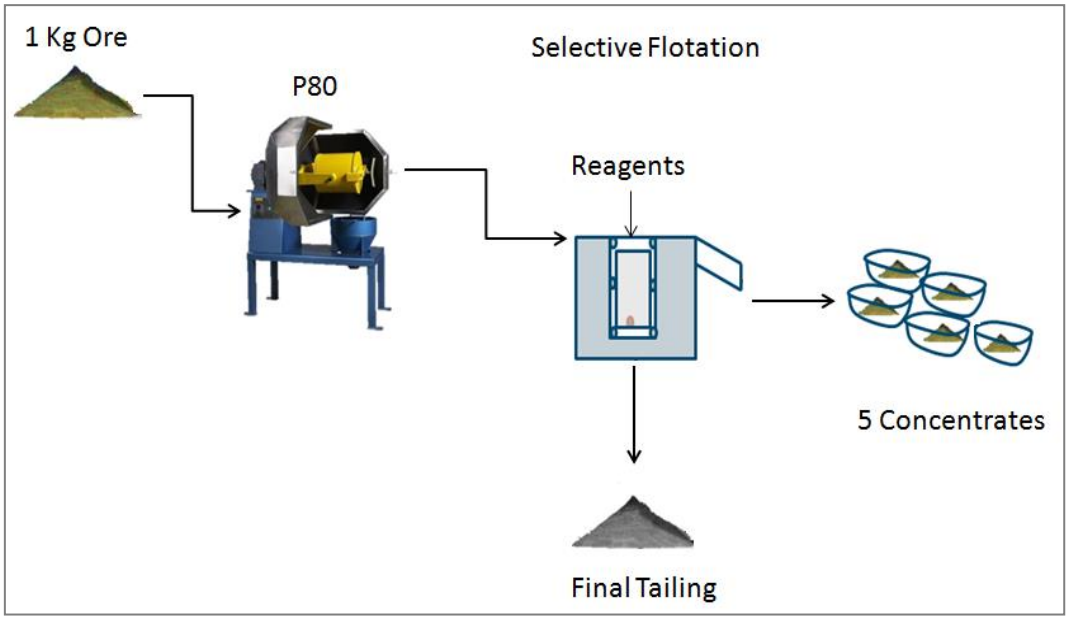

Figure 6.24: Flow sheet used for supergene Jayula ore

Table 6.12: Reagents used on the Jayula ore.

Reagent	Addition (g/t) in selective flotation
D919*	300
Copper Sulphate	600
Aero 3418A	220
Aero 404	250
PAX	300
MIBC	85
Lime	21.5

*D919 lignosulfonates (Dispersant)

Each of the five concentrates and the tailing were sized. In total, six size fractions (+38 μm, +C1/+C2, +C3, +C4, +C5 and –C5) were obtained by wet and dry sieving and cyclosizing; these were submitted for characterisation of the flotation products.

6.3.3 Experimental design

A factorial experimental design was chosen based on the preliminary flotation tests (described in the previous section) to be applied with the selective flotation strategy. The parameters that were considered to affect the behaviour of this kind of flotation were P80 values of 100 and 25 microns and collector dosage for 3418A (160 g/t and 550 g/t). The aim was to achieve the highest silver grade possible through selective flotation.

The results of this experimental design are presented in Table 6.13, and indicate that Test A achieved the highest cumulative grade for silver, with a value of 458 ppm, followed by D (153 ppm of Ag), B (145 ppm of Ag) and C, with 137 ppm of Ag.

Table 6.13: Results of the two-factorial experimental design

Test	P80, µm	Collector Dosage, g/t	Rec, %	Grade, ppm	Mass rec, %
A	25	160	80.0	458	13.2
B	25	550	78.4	145	60.1
C	100	550	58.5	137	46.6
D	100	160	47.4	153	33.2

Figure 6.25 illustrates the grade recovery curves for the tests shown in Table 6.13. The Y-axis represents the grade of each concentrate, while the X-axis represents the recovery of Ag for each concentrate. From the figure it can also be seen that A achieved the best performance for Concentrate 1 in terms of Ag grade.

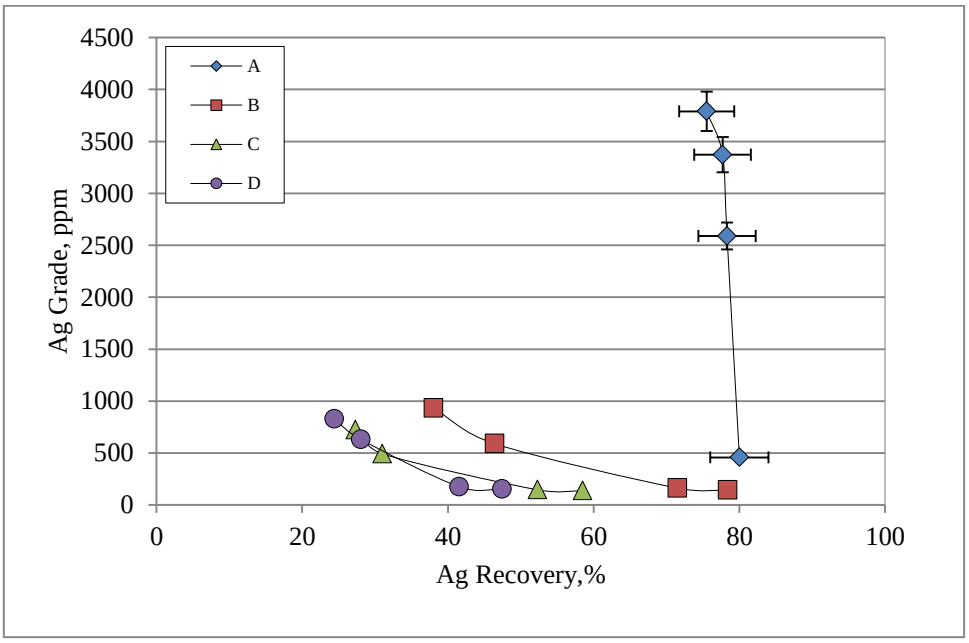

Figure 6.25: Grade-recovery curves for experimental design for Test A, B, C and D.

6.3.4 Batch flotation results of test A from the experimental design

The use of selective flotation was discussed in the literature review and in Chapter 3. This method was chosen due to the features present in the ore, i.e. the deportment of silver minerals and the low amount of sulphide minerals present. The flotation feed sizing, and hence the degree of liberation, was chosen according to the silver mineral grain size (Figure 6.19) from the flotation feed characterisation. The selected feed particle size distribution used in the experimental design was a

P80 of 25 μm, as well as 100 μm. The finer flotation feed sizing allowed additional liberation of grains that contained silver, enabling the process to recover a higher amount of silver with improved concentrate grade and reduced mass recovery.

The results of this flow sheet configuration are given in Table 6.14. The recovery of silver reached a value of 80.8% with a grade of 1709 ppm. The other elements achieved recoveries that were between 10.6% and 24.9%, showing that selective flotation to recover silver was successful.

Table 6.14: Flotation results for selective flotation of silver (P80 of 25 μm)

		Cumulative grade						Cumulative recovery,%					
Streams	Mass, (g)	Ag	Ba	Fe	Pb	S	Zn	Ag	Ba	Fe	Pb	S	Zn
Con 1	62.2	3372	3370	3.5	9168	1.00	2093	74.5	5.1	6.9	9.9	13.18	17.3
Con 2	87.2	2564	3236	3.4	8752	0.88	1766	79.4	6.9	9.5	13.3	16.26	20.4
Con 3	133.2	1709	3258	3.3	7834	0.73	1409	80.8	10.6	14.3	18.2	20.63	24.9
Tail	872.0	62	4180	3.1	5390	0.43	650	19.2	89.4	85.7	81.8	79.37	75.1
Rec. Feed	1005.1	280	4058	3.1	5714	0.47	751	100	100	100	100	100	100

Figure 6.26 presents the grade recovery curves for Ag, Ba and S. These elements were chosen because they are the most representative elements for the minerals that carried silver. In the cases of Ag and S, the curves are consistent with the behaviour of this type of curve – as the grade decreased, the recovery increased. Only 10.6% of the barium was recovered. Barium was known to exist in the feed as barite and barite_Ag.

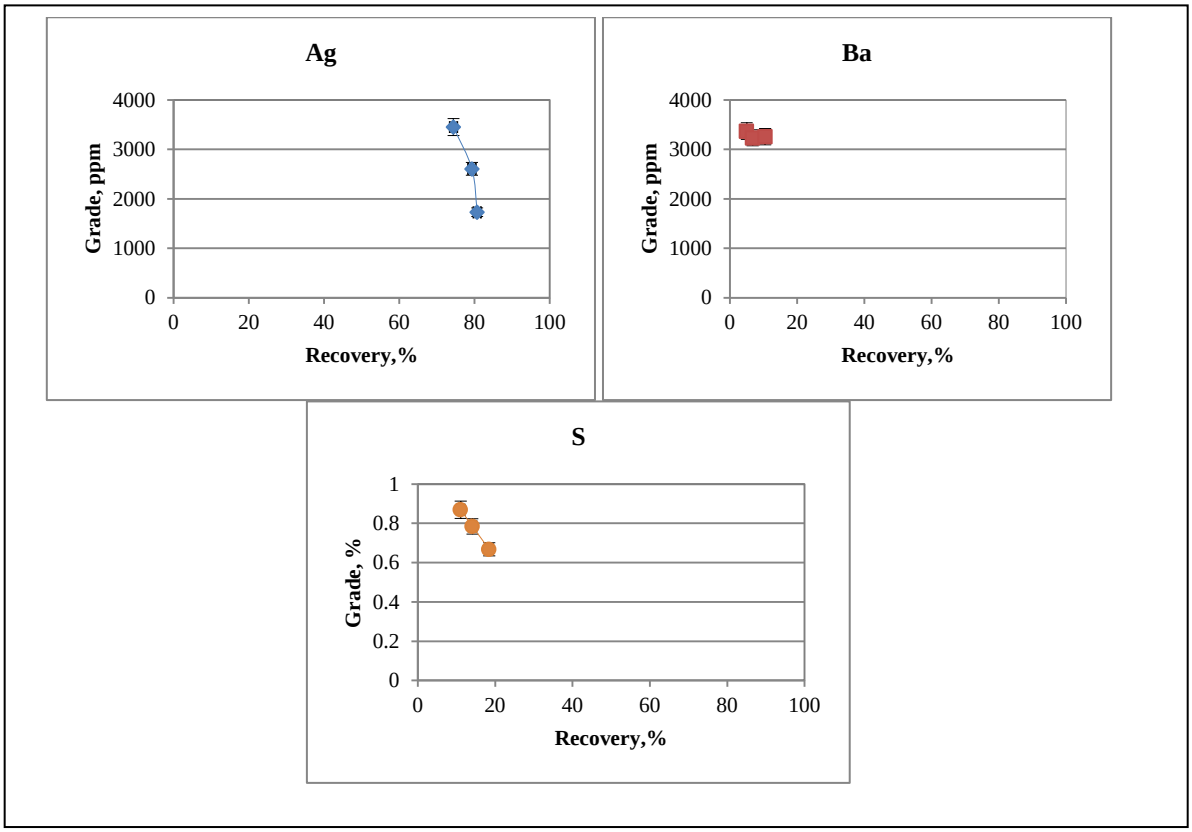

Figure 6.26: Grade-recovery curves for Ag, Ba, and S.

The kinetics of the flotation test on an unsized elemental basis were studied and are shown in Figure 6.27. Silver exhibited a fast rate of flotation, especially at the first concentrate. These data also demonstrate that the flotation was selective for silver when compared to the other elements that are part of this study.

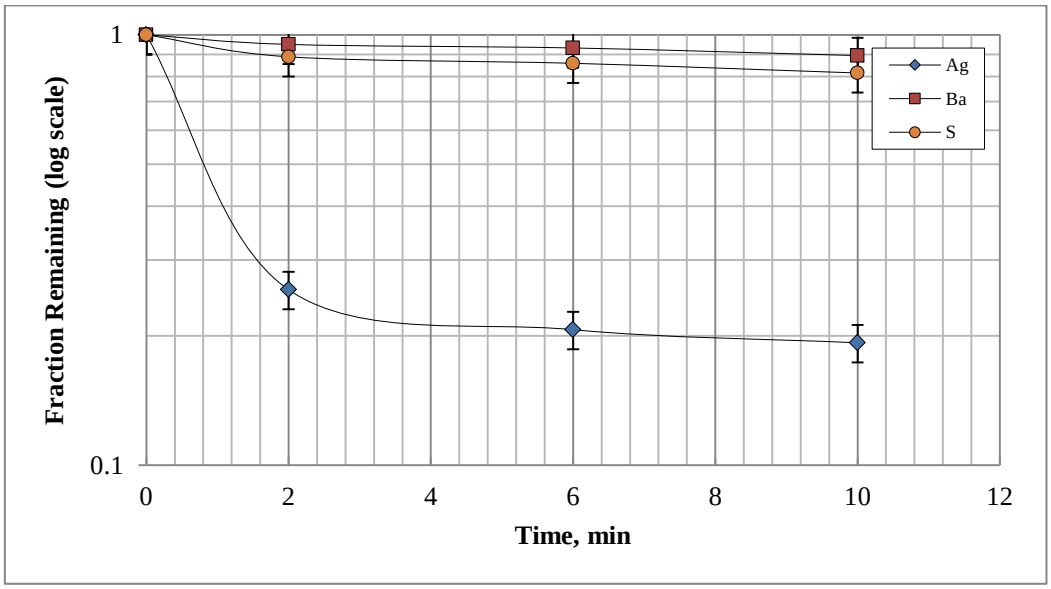

Figure 6.27: Fraction remaining (log scale) versus time for selected elements, with 95% confidence limits.

6.4 Results of flotation product characterisation

6.4.1 Mineral recovery by size

Silver was found predominantly in known silver minerals and also in barite_Ag. The main silver minerals present in the concentrates were acanthite, pyrargyrite and barite_Ag. Figure 6.28 illustrates the recovery-by-size data for the silver minerals, barite_Ag and non-sulphide gangue (NSG). For the Ag minerals, the overall recovery was 81.9% while the recovery by size was >90% for sizes less than 11 microns with recovery decreasing for the coarser size fractions. The recovery behaviour for barite_Ag was similar to that of NSG indicating that this mineral is not recovered by true flotation i.e. particle–bubble collisions under the conditions used. The recovery of barite_Ag and NSG was consistent with recovery by entrainment with the overall water recovery being 32.6%.

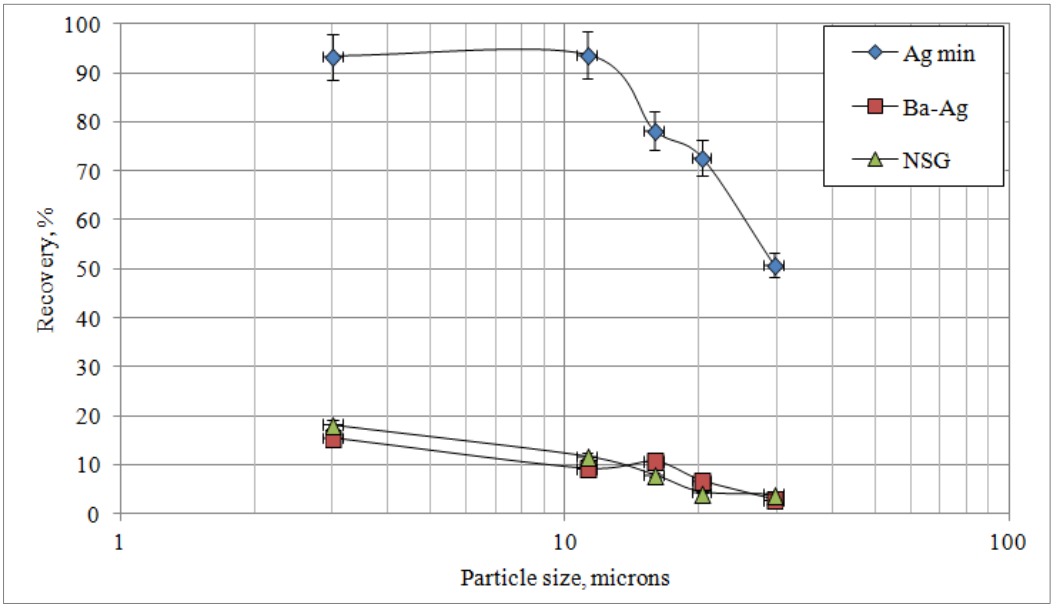

Figure 6.28: Recovery-by-size for silver minerals, barite-Ag and NSG

6.4.2 Recovery-by-size and liberation

To analyse the recovery-by-size and liberation, all the results previously shown were used to calculate the mass flow of liberated particles. The minerals analyses were silver minerals and NSG. The results of these analyses are shown in the following figures (6.29 and 6.30). For silver minerals, the recoveries-by-size for liberated particles show the typical inverted-U shape for this type of analysis, where this curve shows higher recoveries than for the curve with overall recovery of Ag minerals. The fine particles tended to be recovered as liberated particles, as well as composite particles with NSG and barite_Ag. The coarse particles are mainly recovery as liberated particles.

Figure 6.30 illustrates silver loss in tailings. Silver was lost in the tailings mainly in the coarse size fraction (30 µm) and in the finest size fraction (3 µm) as liberated particles, while in binary composites with barite_Ag the main loss is in the finest size fraction. The silver losses as composites with NSG are in the ends of the curves i.e. in the finest and in the coarsest size fractions.

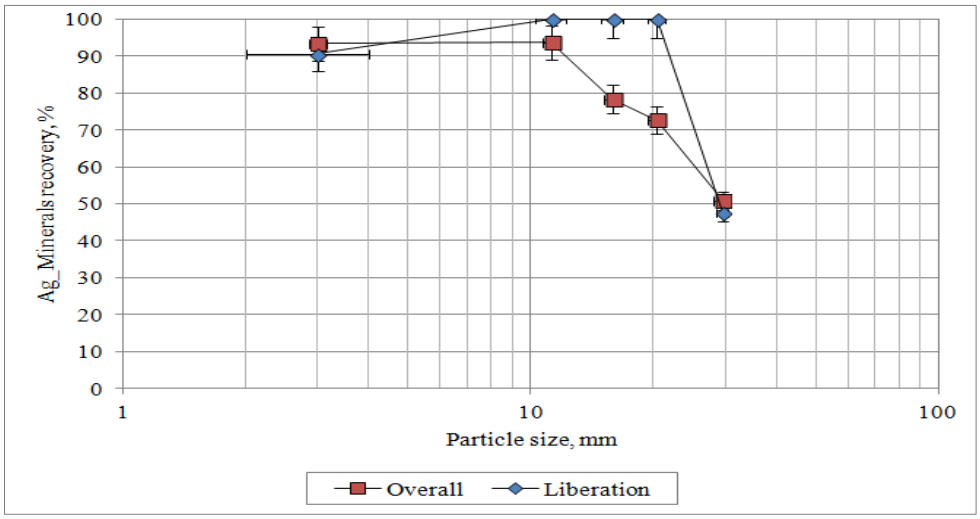

Figure 6.29: Recovery of Ag minerals (liberated and overall)

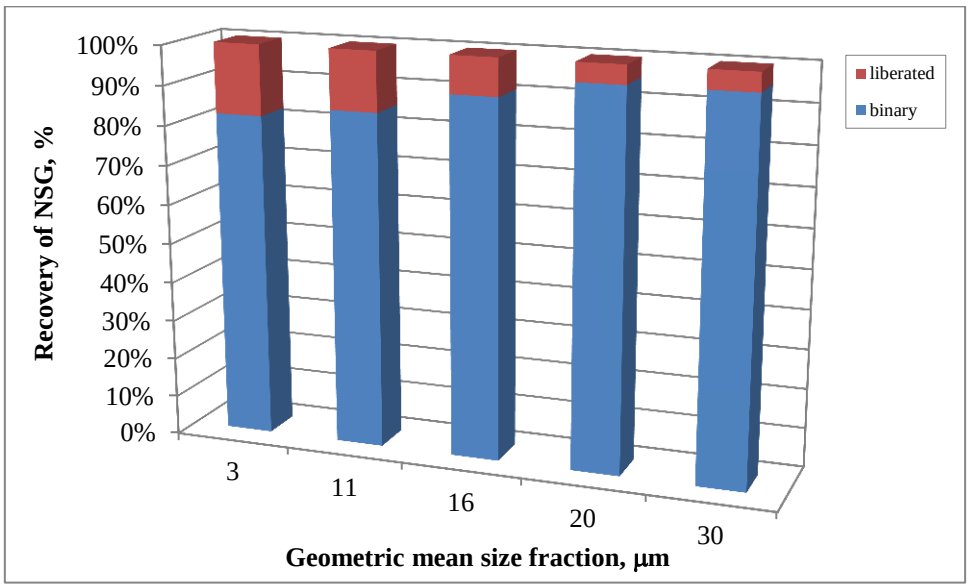

Figure 6.30: Ag loss in tailing

6.5 Key findings

Jayula ore was characterised primarily by using Level 3 mineral characterisation. This is an extension of the Level 2 mineral characterisation, and also includes a new protocol to identify the deportment of those silver minerals that could not be identified in the previous levels of mineral characterisation. The protocol for identifying the silver deportment was primarily devised to

improve the understanding of silver deportment. During this process a new association was found between silver and barite (barite_Ag), and other silver minerals, proustite and iodargyrite that were not in the MLA library. These were incorporated in the MLA mineral reference library and used to reanalyse the data. By using the insights gained from Level 3 characterisation in combination with the results that were being achieved in the metallurgical testing, it was possible to quantify the silver deportment in this ore.

In terms of processing, the difficulty in quantifying the silver deportment and the complexity of Level 3 characterisation made it difficult to choose a unique strategy for floating the silver in the early phases of the metallurgical characterisation. After a long investigation of the mineralogical behaviour of the ore, in terms of grain size and texture, it was possible to achieve a recovery of 80.8% of silver with a grade of 1709 ppm, after allowing increased liberation of silver minerals from a reduction in the size distribution of the ore from a P80 of 100 μm to 25 μm.

At the conclusion of this case study, it can be demonstrated that a full understanding of the application of mineralogical analysis combined with metallurgical expertise can be used to obtain an acceptable separation using flotation for this ore.

Chapter VII:

Discussion

This chapter discusses the key mineralogical attributes for the three ores that came from the same deposit and their impact on the development of an effective flotation strategy. Based on the knowledge gained through the mineralogical characterisation and the metallurgical characterisation, a new concept of refractoriness for silver ores is introduced.

7.1 Context

The main driver for this work was to identify the key mineralogical attributes for three different ores from MSC, a magmatic-hydrothermal (MH) deposit, so that an effective beneficiation process to recover silver could be developed. Different questions were raised during the identification of these attributes, which became key to understanding the behaviour of these ores when froth flotation was used as the separation process. These questions are answered in this Chapter, which demonstrates how the characteristics of the different ores influence the development of an effective separation process.

7.2 The systematic approach developed to characterise silver

As discussed in the literature review, there is currently no established methodology for carrying out systematic mineralogical characterisation of silver ores. This thesis proposes the systematic application of a series of characterisation tools to identify the silver deportment and other key mineralogical attributes in complex low-grade silver ores.

The most common microscopic techniques used for characterisation of silver ores are optical microscopy, SEM-based analysis and EMPA. Based on these techniques, the proposed framework to characterise systematically silver minerals is presented in Figure 7.1. It consists of three levels of characterisation. The first Level 1 uses all the techniques that are routinely used to find the mineralogical attributes required to develop a process design. The deportment of the valuable element, in this case silver, must be identified because it is the key factor that helps the mineralogist and metallurgist to identify the issues that can cause the losses of the silver in the tailings. If silver is carried by sulphide minerals in solid solution, then a second phase, Level 2, in the study is

applied. If the silver deportment is not identified sufficiently by Level 2, then more sophisticated analyses to identify unknown silver carriers are used and this is referred to as Level 3.

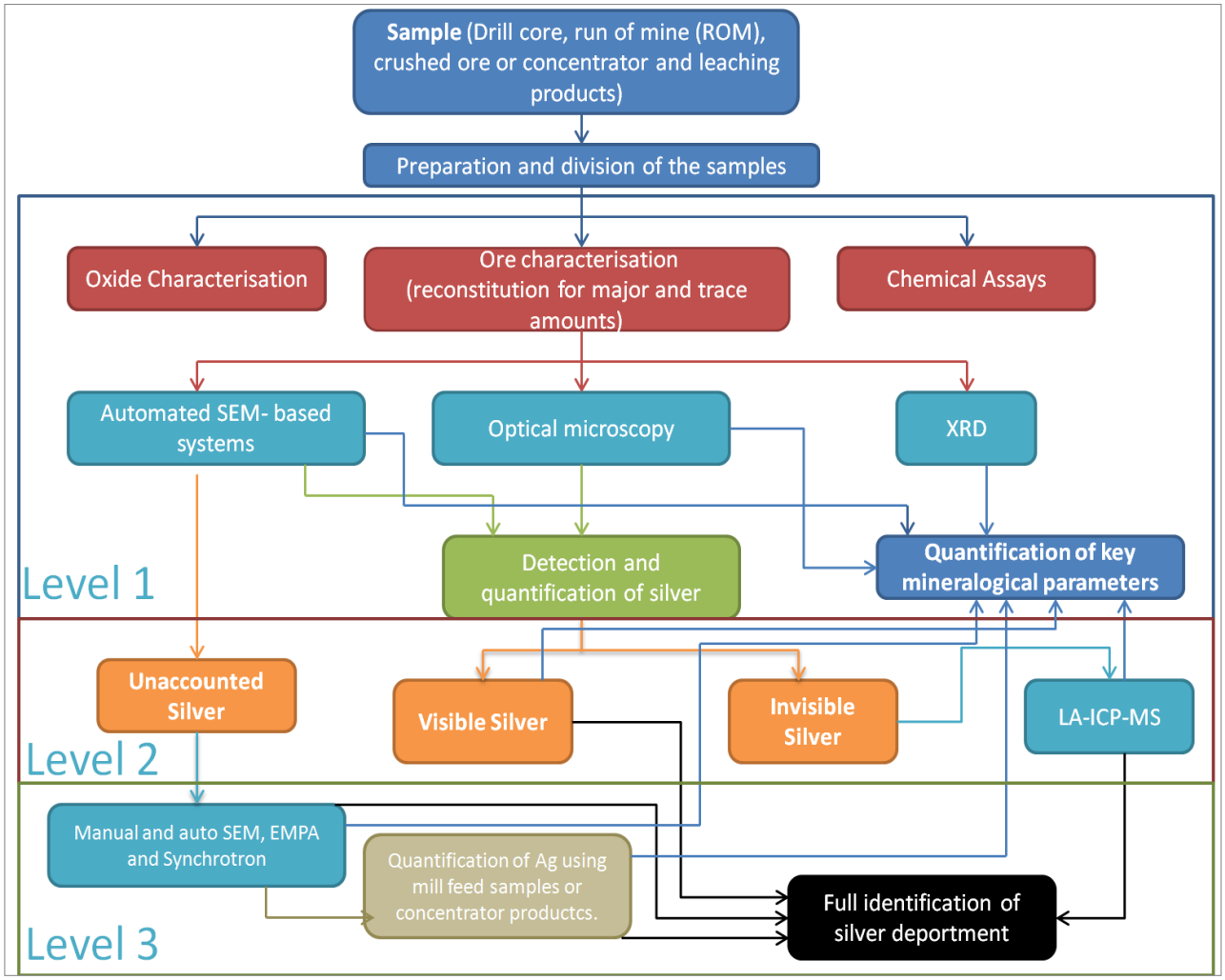

Figure 7.1: Systematic approach for identifying mineralogical attributes

The advantage of this approach is that unknown Ag minerals, which are identified through an automated SEM-based system, can be investigated in a quicker manner.

7.3 Key mineralogical attributes

As the key mineralogical attributes were established i.e. modal mineralogy, elemental deportment, texture (mineral association and grain size) and liberation of the ores, it became possible to develop a flow sheet design for processing the ores. The way in which each of the attributes impacted on the development of an effective flotation strategy is discussed in the following sections.

❖ **Modal mineralogy:** the ores used in this work come from different pits of the same mine site and contain similar gangue minerals in different proportions. The gangue was important to characterise so that any minerals that could potentially interfere with flotation could be identified.

An abundance of non-sulphide gangue existed in the three ores. The feldspar group is the most prevalent for oxide (Toldos) ore and for the sulphide (Tesorera) ore with 54.9±1.6% and 67.6±1.3%, respectively, while the supergene oxide (Jayula) ore contains only 11.7±0.7% feldspar. Another mineral which is present in all ores is quartz, being dominant in Jayula ore with 50.7±0.9%. The clays_micas group is also present in the ores, having a major presence in Jayula ore rather than in the oxide and sulphide ores. Carbonate minerals have a large presence in the oxide ore when compared with the other two ores. The sulphide minerals are most prevalent in the sulphide ore. In the context of flotation the gangue matrix does not present any obvious minerals that could potentially be detrimental to flotation. A comparison of the modal mineralogy of the ores is shown in Figure 7.2.

❖ **Silver deportment:** In order to characterise the silver deportment, different characterisation levels were required for each ore. For the oxide ore Level 1 analysis was sufficient, from which it was determined that the predominant silver carriers for the ore were chlorargyrite and acanthite which account for more than 60% of the silver in the ore. For the sulphide ore Level 2 analysis was required as the majority of the silver was present at ppm levels in pyrite. For the supergene oxide ore Level 3 analysis was required due to the fine grained nature of the ore and the more complex associations of silver, such as that with barite, a previously unreported association for silver. The total silver content and its distribution by mineral is shown in Figure 7.3. In the development of a flotation flow sheet for each ore, the silver deportment was critical in determining the most appropriate reagent suite to use for each ore. The Ag carriers were very different for all ores indicating that different flotation strategies i.e. flow sheet design and reagent schemes, were needed to recover silver from the ores.

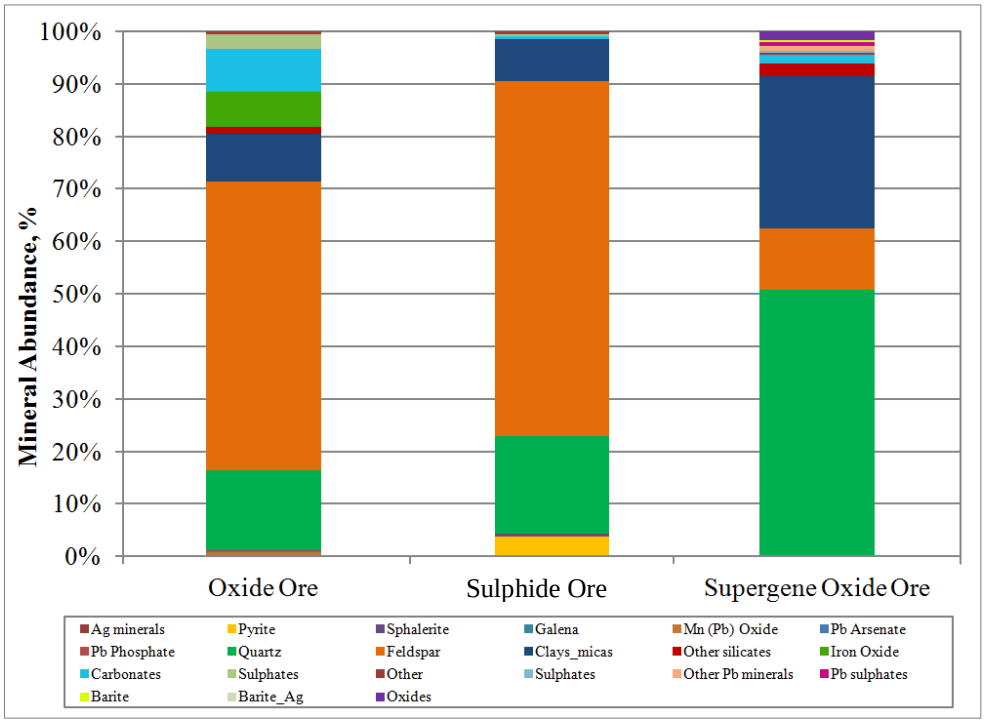

Figure 7.2: Modal mineralogy for Tesorera ore (sulphide ore), Toldos ore (oxide ore) and Jayula ore (supergene oxide ore).

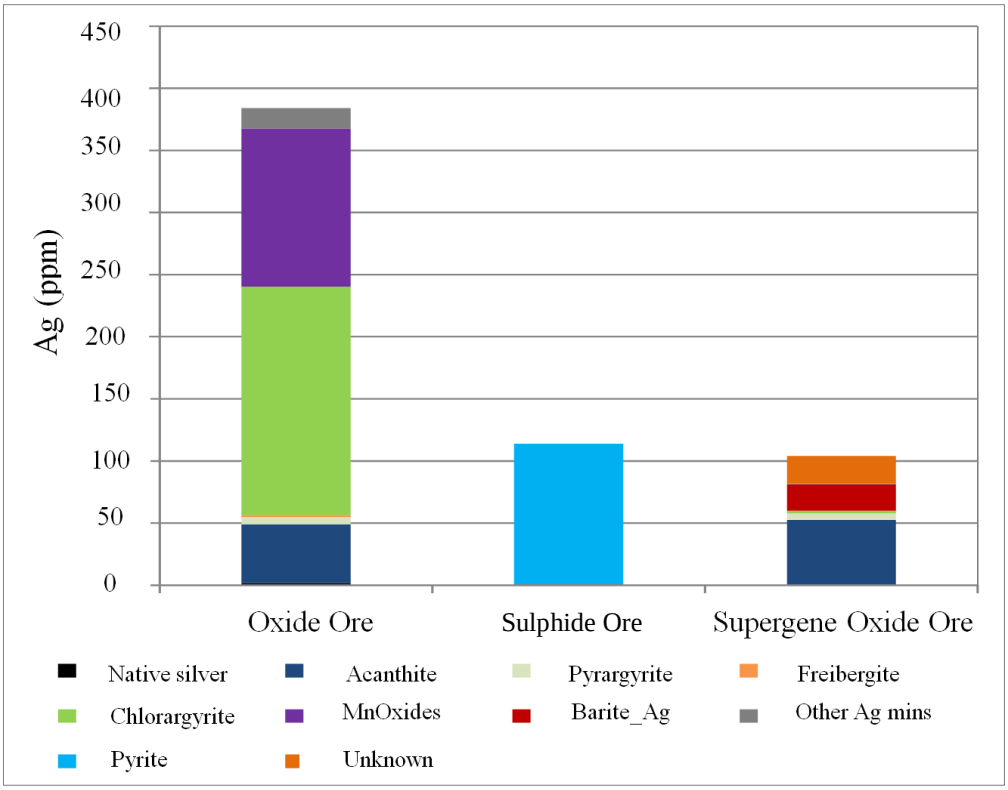

Figure 7.3: Silver deportment for Toldos ore (oxide ore), Tesorera ore (sulphide ore) and Jayula ore (supergene oxide ore).

❖ **Texture of ores:**

➢ **Mineral association:** The mineral associations for Toldos and Jayula ores were focussed on silver-bearing minerals while, for Tesorera ore, the focus was on pyrite because its associations have an impact on the flotation of the pyrite.

➢ **Mineral Grain size:** For Toldos ore the grain size of Ag-minerals was quite large showing a P80 of approximately of 240 μm in the +300 μm size fraction. For Tesorera the pyrite grain size was a P80 of 115 μm in the +300 μm size fraction while, for Jayula ore, the Ag-mineral grain size was 12.5 μm in the +300 μm size fraction.

❖ **Degree of liberation:** In order to identify the most appropriate grind P80 for each ore, the liberation characteristics and grain size of the predominant silver minerals were investigated. For the oxide ore at a P80 of 100 μm the overall liberation of the combined silver minerals was greater than 50%; in addition the predominant silver mineral, chlorargyrite, had a P80 grain size of 240 μm indicating that a target grind of 100 μm should provide sufficient liberation for rougher flotation. For the sulphide ore only 40% of the pyrite was liberated at a grind size of 100 μm, and in order to improve the liberation of pyrite, additional grinding was carried out on the +75 μm fraction in the flotation feed to generate a flotation feed P80 of 56 μm. The supergene oxide ore, due to the fine grained nature of the identified silver minerals, was only 30% liberated at a 100 μm flotation feed size and required grinding to 25 μm (P80 value).

7.3.1 Mineralogical drivers for flotation

Figure 7.4 illustrates how the mineralogical drivers, deportment and grain size, influenced the flotation each of the ores. Deportment in this context relates to the deportment of silver minerals based on their response to flotation i.e. they are classified as floatable silver minerals (which include all of the silver sulphides) and silver occurring in solid solution. Non floatable silver minerals include minerals such as barite_Ag (whose flotation response is similar to that of NSG). In this case Jayula ore contains floatable Ag bearing minerals as carriers, however the grain size of these minerals is relatively small and, from a metallurgical perspective, ultrafine grinding was required and was the motivation for decreasing the size of the flotation feed to 25 μm (P80 value). Toldos ore also contains floatable Ag-bearing minerals as carriers and, based on the coarse grain size of these minerals the standard grind size for flotation was adequate to recover Ag. Tesorera ore contained pyrite as the main Ag carrier as Ag in solid solution; liberation studies indicate that the degree of pyrite liberation at a P80 of 100 μm was not enough to recover pyrite and in addition the distribution of silver by size indicated that a large proportion of the silver was present in coarser

size fractions. Therefore, a modification of the grinding procedure was introduced (MIG), to reduce flotation feed size to 56 microns.

The mineralogical drivers provide insights into the likely behaviour of the silver-bearing minerals found in each of the ores during flotation and how this can be used to develop a framework for assessing the refractoriness of each ore.

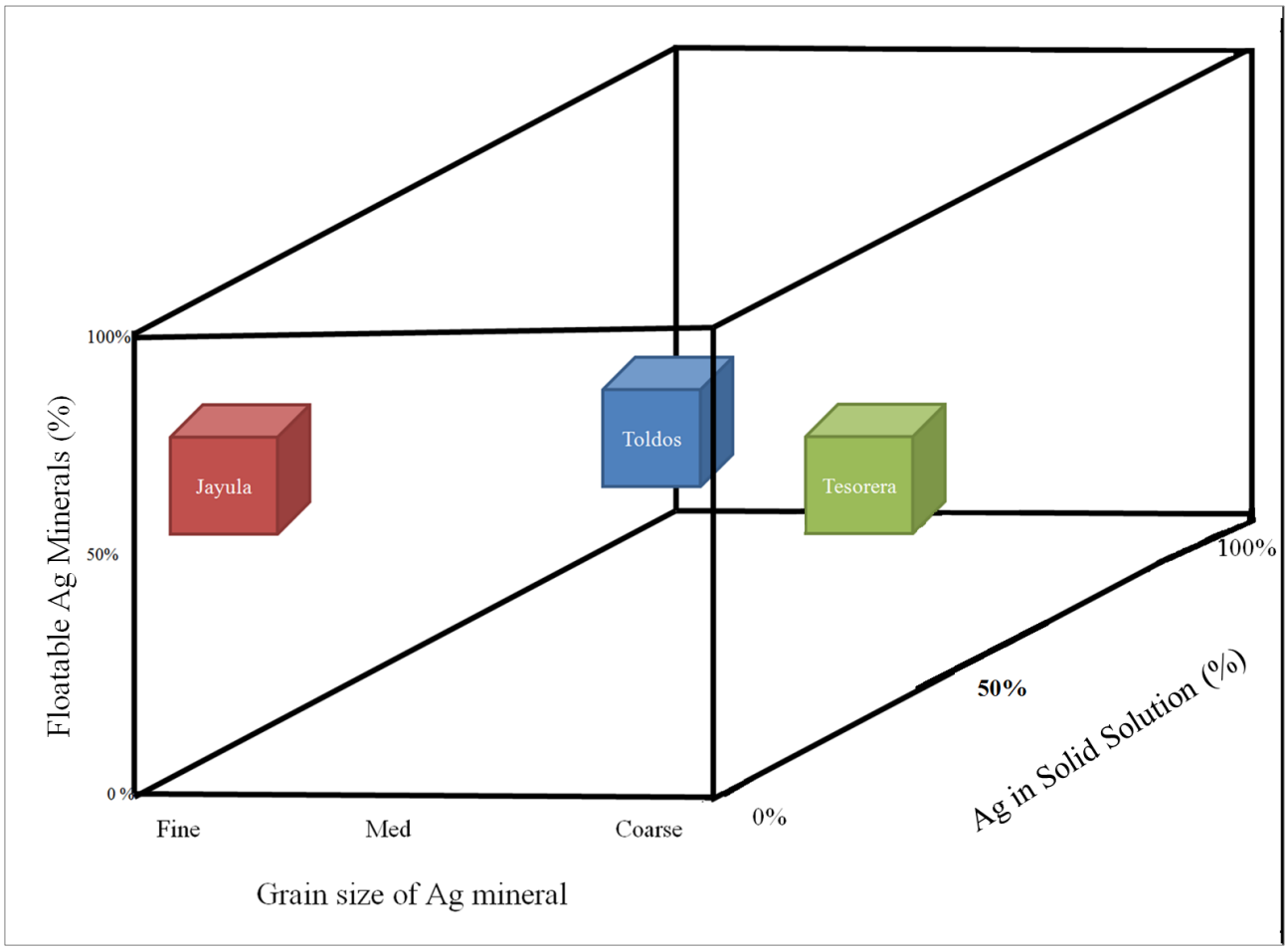

Figure 7.4: Mineralogical drivers – deportment (% Floatable Ag Minerals (y axis) and % Ag in Solid Solution (z axis)) and grain size (x axis) for ores under study.

The information from mineralogical characterisation resulted in the creation of different flotation flow sheets for each of the ores which were able to achieve the target recovery (over 80%). Figures 7.5 and 7.6 show the flow sheets used for the ores.

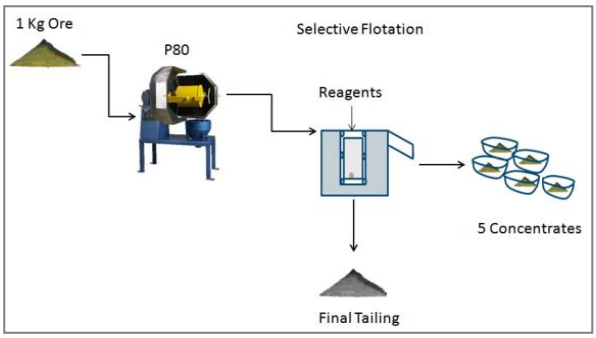

Figure 7.5: Flotation flow sheet for oxide ore (P80=100 µm) and supergene oxide ores (P80=25 µm).

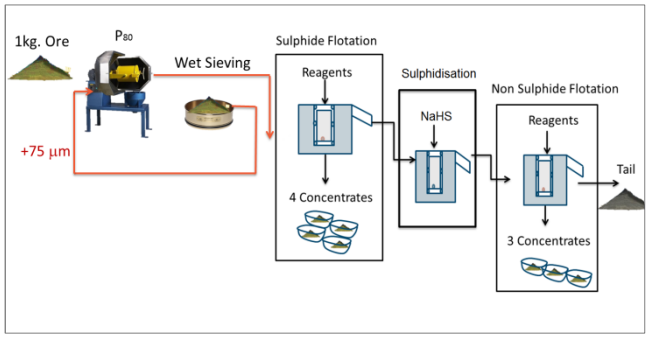

Figure 7.6: Flotation flow sheet for sulphide ore (P80=55 µm).

7.4 Consequences for flotation

Figure 7.7 shows a graph of the cumulative silver recovery (x-axis) versus cumulative silver grade (y-axis) for each ore. For the oxide ore it can be seen that concentrate 1 has a slightly lower grade than concentrate 2, then for concentrates 3, 4 and 5 the cumulative grade decreases as expected in this type of graph. The final recovery of silver for this ore is 83.8% at a grade of 4404 ppm.

The grade recovery curve for the sulphide ore is also shown in Figure 7.7. The trend that is presented for silver illustrates that between concentrates 4 and 5 there is a discontinuity gap which represents the effect of the sulphidisation stage used in this flotation process that aims to maximize the Ag recovery through a pyritic concentrate, which has an average grade of Ag in pyrite of approximately 2900 ppm, representing the maximum silver grade that could be achieved theoretically. Also, this additional stage of sulphidisation allows a significantly improved position of the Ag grade/recovery curve, by increasing the silver recovery. The final recovery of silver for this ore is 87.2% at a grade of 485 ppm.

The flow sheet presented in Figure 7.5 which includes grinding the flotation feed to a P80 of 25 µm to improve the degree of liberation of the silver minerals in the supergene ore results in a final recovery of over 80% as seen in Figure 7.7. The fine particle size in the flotation feed contributes to the lower grade seen in this ore, in comparison to the oxide ore, due to the increased entrainment of gangue resulting in a final silver grade of 1709 ppm.

The relative positions of the grade recovery curves shown in Figure 7.7 reflect the silver mineralogy for each of the ores. The rougher concentrate produced from flotation of the Toldos ore has the highest grade due to the presence of silver in silver sulphides/halides with a high silver composition (see *Appendix A*). Despite Jayula also containing silver sulphide minerals the grade is lower as a consequence of the fine grinding required to achieve liberation, which as a consequence increased entrainment of NSG and reduced rougher concentrate grade. The lowest final rougher concentrate was achieved with the Tesorera ore which was limited by Ag occurrence at ppm levels in pyrite.

The occurrence of the silver in pyrite also required the use of a sulphidisation stage to ensure adequate recovery of tarnished pyrite.

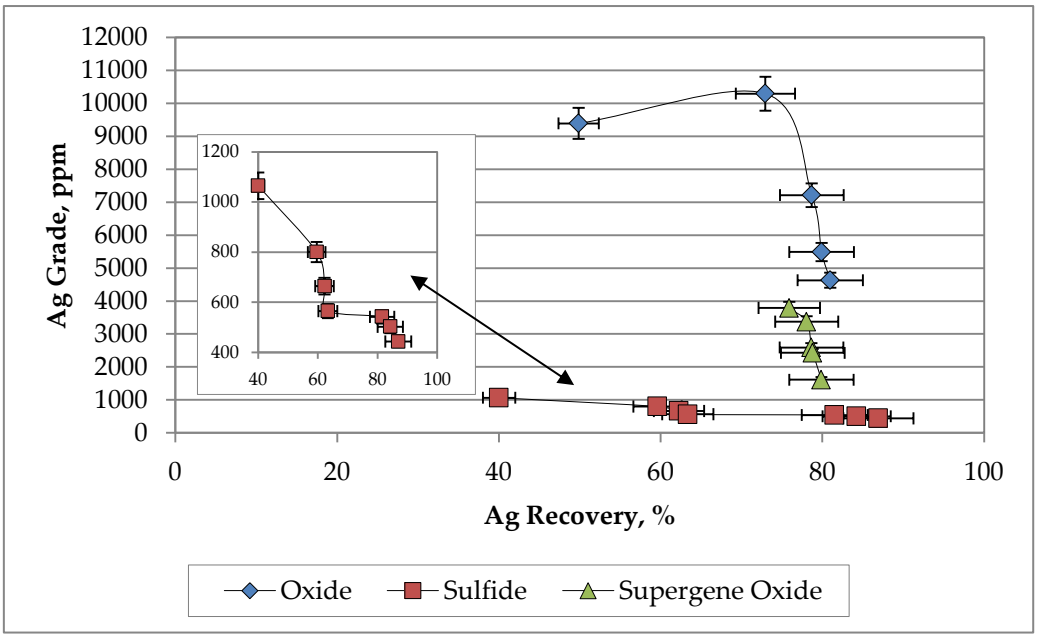

Figure 7.7: Grade – recovery curves of Ag for each ore.

❖ Kinetics

The kinetic response of each ore is presented in Figure 7.8, which shows the fraction remaining (log scale) for silver in the tail with respect to the flotation time for silver. The data illustrate that silver has faster kinetics in the supergene oxide ore followed by the oxide ore with the sulphide ore having the slowest. For the sulphide ore the slope of the curve between 8 and 10 minutes showed that pyrite, which hosts the silver, responded well to the sulphidisation stage.

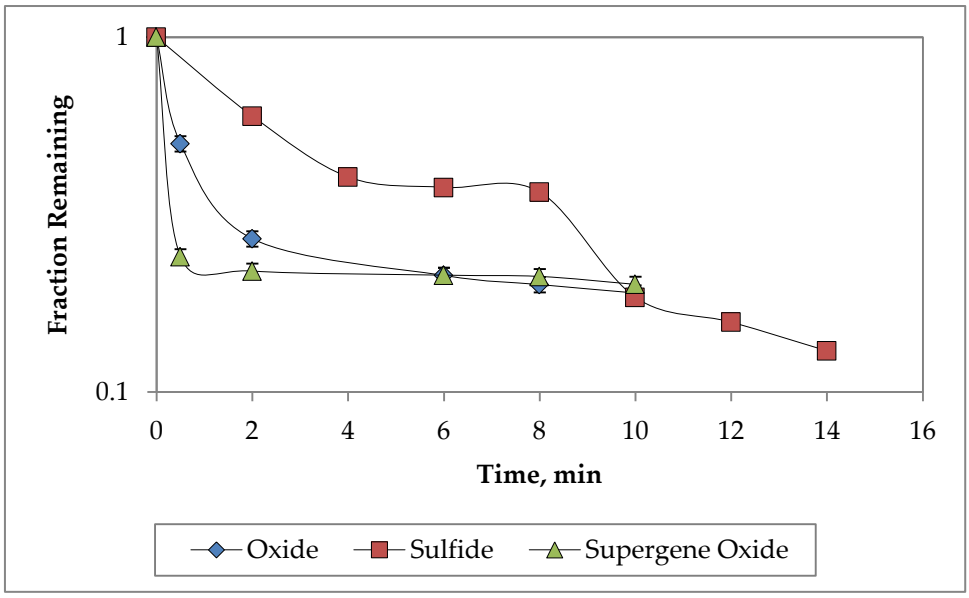

Figure 7.8: Silver kinetics for each ore

❖ **Size-by-liberation**

In the oxide ore Ag minerals were recovered as liberated particles in each of the size fractions studied. The main losses of Ag were in the coarse size fraction as binary composites. In Tesorera ore (sulphide ore) pyrite was recovered in the liberated form (50% of the total) followed by binary composites with NSG. The main losses of pyrite were in the liberated form in the finest size fraction, while the composites particles containing pyrite caused losses in the 45 μm fraction. For Jayula ore (supergene ore), Ag minerals were mainly recovered as liberated particles. The main losses of silver were in the finest size fraction for liberated and in binary composite with barite_Ag which is considered non-floatable. Also, in the coarse size fraction, the main loss was as liberated Ag minerals.

7.5 Refractoriness of silver

The term refractory is used to encapsulate the degree of difficulty in extracting a particular element from an ore and depends on the mineralogical characteristic of the ore. The use of this term is not well defined for silver minerals as discussed in the literature review, and as such, the concept of refractory in the context of silver that unifies all definitions from the previous authors and considers the results from this thesis is presented. ***Refractory silver ore*** contains visible silver minerals that are difficult to recover using a standard test, either by hydrometallurgical methods or flotation. ***Double refractory silver ore*** contains at least one mineral where silver is present as submicroscopic silver e.g. as solid solution in sulphides. Ores that contain both silver in solid solution and non-floatable silver minerals would potentially be more difficult to process than either refractory or double refractory ores.

Table 7.1 illustrates a classification of silver occurrences based on Zhou (2010).

Table 7.1: Classification of silver by nature and carriers (after Zhou, 2010)

Form	Microscopic Silver	Sub-microscopic Silver
Nature	Visible under microscope, i.e. Scanning electron microscope (SEM)	Invisible under microscope, i.e. Scanning electron microscope (SEM)
Carriers	Native silver, silver-gold alloys, silver sulphides, silver tellurides, silver selenides, silver antimonides, silver sulphosalts and silver halides	Present in galena, sphalerite, pyrite, bornite, chalcopyrite, covellite, tetrahedrite, tennantite, boulangerite, bournonite, arsenopyrite, manganese oxide and kaolinite.

The standard flotation test for MSC ore includes grinding of ores to a P80 of 100 μm. Preliminary results of these tests, shown in *Appendix L*, indicate that with grinding the ores to this fixed P80, the silver recovery was varied across the ores as a result of their key mineralogical attributes (as described in previous sections). These data suggest that it would be useful for a metallurgist to have a simple test to diagnose the ease of processing silver ores. This concept is analogous to that used for gold where a simple cyanidation test is used to define the difficulty with which gold ores can be

processed. In this work the "degree of refractoriness of silver ore" (how refractory the ore is for processing by flotation) is given by when the flotation recovery (based on a standard flotation test) is less than 30%; or as a general concept, a refractory silver ore is one that is resistant to recovery in a normal flotation processes with a feed sizing of 100 μm (P80 value). Table 7.2 shows the classification proposed for the degree of refractoriness of silver.

Table 7.2: Classification of refractoriness based on standard flotation test

Rougher Recovery, %	**Classification**	**Ore Study under standard flotation test**
< 30 % recovery	Highly refractory	Jayula ore
30 – 60 % recovery	Mildly refractory	Tesorera ore
60 – 100 % recovery	Weakly refractory	Toldos ore

7.6 Summary

A range of various mineralogical characterisation tools was applied for each ore in order to provide the information required to develop a flow sheet that would successfully recover more than 80% of the silver in each ore in roughing. The marked differences in the mineralogical attributes of the ores are reflected in the different approaches used to recover the silver in each case and demonstrate the value of process mineralogy as a tool for metallurgists in optimising the recovery in increasingly complex low-grade ores.

Chapter VIII:

Conclusions

This thesis sought to address the following hypothesis:

Key mineralogical factors (elemental deportment, liberation and association) can be determined using a systematic application of mineralogical characterisation tools, from which an effective flotation strategy for low-grade silver ores can be developed.

To assess the above hypothesis, a framework of analysis was developed and the conclusions drawn from these investigations are presented below. The objectives as described in Chapter 1 and how they were achieved are discussed in the following sections.

8.1 To develop a systematic approach to characterise the silver deportment, association and texture in ores that begins with using traditional microscopic techniques and uses more advanced and sophisticated techniques when needed.

The three ores studied in this work were all characterised using Level 1 methodology with new, more sophisticated and advanced methodologies then used for the mineralogical characterisation if Level 1 was insufficient to fully define the key mineralogical parameters.

Level 1 characterisation involved two standard procedures, chemical characterisation and mineralogical characterisation. Chemical characterisation was carried out on an unsized and size-by-size basis for the ore feed, while the mineralogical characterisation was based on standard mineralogical characterisation techniques using different particle sizes for each technique. These included X-ray diffraction (XRD), oxide characterisation of lead and zinc, optical microscopy and mineral liberation analysis (via the use of the MLA system) to characterise the ore mineralogy in each sample. For the Toldos ore, Level 1 characterisation was sufficient to fully identify the key mineralogical parameters and indicated that silver occurred mainly in the silver minerals.

Tesorera ore also required Level 2 characterisation which included laser ablation inductively coupled plasma mass spectrometry (LA-ICP-MS), to quantify the composition of pyrite which

contained silver in solid solution. At the conclusion of this analysis, more than 95% of the silver was found to occur in solid solution with pyrite.

Level 3 characterisation was required to fully understand the key mineralogical parameters for Jayula ore. The challenges encountered for this ore were the grain size of the silver minerals and their composition. The detection limits of the techniques used also constituted another challenge given the nature of the silver in the ore. Results from the metallurgical test work were used in combination from the insights gained from Level 3 characterisation to understand fully the behaviour of the ore. While most of the silver was present as silver minerals, a new association with barite was identified (barite_Ag) which behaved in a similar way to the non-sulphide gangue minerals during flotation, rendering this component of the silver non-recoverable. The presence of barite_Ag together with the extremely fine-grained nature of the remaining silver minerals made it challenging to develop the final flow sheet.

8.2 To develop a method to identify unknown spectra from MLA analysis, with specific focus on the identification of silver-bearing minerals.

The Level 3 characterisation approach was developed specifically to identify minerals that contained silver that had not been identified in the existing MLA mineral reference library. This required detailed examination of the samples using a range of techniques including EMPA, manual and auto-SEM and synchrotron from which the following minerals were identified and incorporated into the mineral reference library: barite_Ag, iodargyrite and proustite.

The results of combining and applying the different levels of mineralogical characterisation allowed for the development of a novel and systematic methodology to identify unknown silver minerals that may have been missing from conventional ore microscopic routines used for ore mineralogy. Figure 8.1 describes the new methodology used in this work.

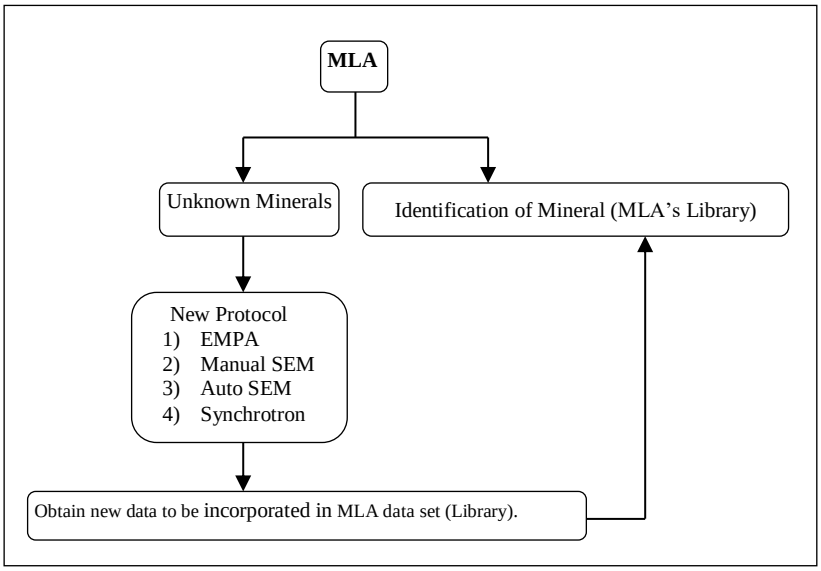

Figure 8.1: Novel methodology to identify unknown silver spectrum

8.3 Using the information from mineralogical characterisation to develop an appropriate flotation strategy in order to obtain greater than 80% recovery of silver in laboratory rougher flotation test.

Once the ore characterisation was performed and the information regarding modal mineralogy, silver deportment, mineral association, grain size and texture of the ores was established, it was possible to propose adequate strategies for ore treatment, through a flotation process at laboratory scale to obtain a rougher concentrate with the required characteristics. Two typical flotation strategies are in use to recover silver. These are selective and bulk flotation: the first aims to selectively float silver minerals and to then float low-grade base metals; and bulk flotation aims to recover all sulphide minerals into a single concentrate which includes silver. Both flotation techniques were successfully used, where suitable in this research to produce rougher flotation concentrates. The challenges in the development of the flotation flow sheets were adequate preparation of the flotation feed and selection of the appropriate reagent scheme to produce a rougher concentrate that met the required characteristics. For the Toldos and Jayula ores, the focus was on selective flotation because of the occurrence of silver in the ores as discrete minerals and the absence of other sulphide minerals. Bulk flotation was used for the Tesorera ore to recover a pyritic concentrate that contained silver in a two – stage process. Suitable reagents, conditions and dosages were selected based on preliminary test work that was carried out.

This work has shown that it is possible to use flotation as a separation technique for low-grade complex silver ores, by selecting appropriate feed preparation and reagent addition strategies which are based on understanding the key mineralogical attributes of the ore.

8.4 Development of a consistent framework that can be used to quantify refractoriness of silver bearing ores.

This thesis has developed a framework that unifies the definition of refractory silver and introduces the concept of double refractory ore. This definition is based on the amount of silver present in floatable silver minerals, the amount of silver present in solid solution and the grain size of silver-bearing minerals. The framework developed will allow the development of a more standardised approach to describing refractoriness in silver ores and will assist metallurgists in understanding the impact of these types of ores in terms of process response.

8.5 Future work

Following from this novel methodology for ore characterisation of unknown silver minerals, it is recommended that further work is carried out to characterise barite_Ag to the extent that it meets the criteria to be identified as a new mineral i.e., isolation of the grain, high resolution XRD and other type of microscopic analyses.

More EMPA analysis should be done on barite_Ag to quantify the content of Ag on the grains to explain the nature or composition of barite_Ag association. This will help to understand the lack of recovery of the barite_Ag.

It is suggested that the methodologies developed in this work can be applied to other complex silver deposits to validate the usefulness of the approach. One of the areas of further work recommended for the methodology is the refinement of the MLA measurement settings to target finely grained silver minerals. This would involve modifying the resolution and X-ray collection to the smallest grain size possible, and modifying the BSE search threshold.

To broaden the area of this research and to incorporate geometallurgy aspects, the geological units, i.e. Toldos ore (oxide ore), Tesorera ore (sulphide ore) and Jayula ore (supergene ore), could be analysed, using the principal component analysis (PCA) or the affinity test for geometallurgy developed by Aminpro (Ameluxen, 2014), in order to create geometallurgical units (UGM) to ensure good recovery from blending these ores.

An investigation into the effects of clay minerals in low-grade silver ores, in terms of viscosity of the pulp and the effects in the froth phase is also recommended. It is also suggested that other

processing routes, such as leaching, could be investigated for these ores in order to determine what the most suitable method for processing these ores is.

In terms of water, it is suggested that the ores should be treated by flotation using the water from the processing plant (mine site) as some conditions can be changed when the experiments are performed using fresh water from Brisbane.

It is suggested that more analysis need to be done for the metallurgical accountability in terms of grade and possible penalty elements, for example As in the concentrate that has a high penalty for selling it to the smelters.

References

Adams, M. D., 2005. Advances in Gold Ore Processing, Elsevier Vol. 15, pp.73-332.

Ahlfeld, F., 1967. Metallogenetic epochs and provinces of Bolivia: Mineralium Deposita, Vol. 2, pp. 291-311.

Allan, G., and Woodcock, J., 2001. Review of the flotation of native gold and electrum, Minerals Engineering, Vol. 14, No.9, pp. 931-962.

Amelunxen, P., 2014. Personal communications.

Amoros, J., Lunar, R., and Tavira, P., 1981. Jarosite: a silver bearing mineral of the gossan of Rio Tinto (Huelva) and La Union (Cartagena, Spain), Mineral Deposita, Vol. 16, pp. 205-213.

Basto, M., Figuerido, M.O., Legrand, F., Chevallier, P., Melo, Z., and Ramos, M.T., 1995. Gold assessment in micas by XRF using synchrotron radiation. Chemical Geology 124 , pp. 1–2 and pp. 83–90.

Baum, W., 1988. Mineralogy-related processing problems of epithermal gold-silver ores, Process Mineralogy VIII, Ed. D. Carson and A. Vassiliou, TMS, pp. 3-20.

Baum, W., Lotter, N.O., and Whittaker, P.J., 2004. Process Mineralogy – A New Generation for Ore Characterization and Plant Optimization. In: SME Annual Meeting, Denver, Pre-print 04–12, pp. 1–5.

Becker, M., Brough, C., Smith, D., and Bradshaw, D., 2008. Geometallurgical characterisation of the Merensky Reef and Northam platinum mine; comparison of normal, pothole and transitional reef types. International Congress for Applied Mineralogy, Brisbane, Queensland, Conference Proceedings, pp. 391-399.

Benzaazoua, M., Marion, P., Robaut, F., and Pinto, A., 2007. Gold-bearing arsenopyrite and pyrite in refractory ores: analytical refinements and new understanding of gold mineralogy. Mineral Mag 71, pp. 123–142.

Benzaazoua, M., Marion, P., Liouville-Bourgeois, L., Joussemet, R., Houot, R., Franco, A., and Pinto, A., 2002. Mineralogical distribution of some minor and trace elements during a laboratory flotation processing of Nerves-Corvo ore (Portugal). Int. J. Miner. Process. Vol. 66, pp. 163-181.

Bojcevski, D., 2004. Metallurgical characterisation of George Fisher meso-textures and micro-textures. Masters Thesis, School of Engineering, The University of Queensland. 376pp.

Bonnici, N.K., 2012. The mineralogical and textural characteristics of copper-gold deposits linked to mineral processing attributes. PhD thesis, University of Tasmania. 249pp.

Boyard, G., 1954. Etude de différents problémes posés par la flottation des carbonates de plomb a la laverie de Toussit. Rev. Ind. Min., Vol. 35, pp.167-172.

Boyle, R.W., 1968. The geochemistry of silver and its deposits: Geological survey of Canada Bulletin No. 160.

Butcher, A., 2010. Chapter 4 A practical Guide to Some Aspects of Mineralogy that Affect Flotation. Spectrum Series 16, Flotation plant Optimisation, pp. 83-93.

Cabri, L. J., Harris, D. C., and Nobiling, R., 1984. Trace Silver Analyses by Proton Microprobe in Ore Evaluation, Precious Metals: Mining, Extraction and Processing; Los Angeles, Calif.; U.S.A.; 27-29 Feb; pp. 93 – 100.

Carter, J., 1957. The milling of silver-cobalt, in The Milling of Canadian Ores, 6Th Commonwealth Mining and Metallurgical Congress, Northern Miner Press Ltd., pp. 165-170.

Chemical register, 2014. http://www.chemicalregister.com/register/whylist.asp access on 18/12/2014 02:30 PM.

Chen, T., and Dutrizac J., 1988. Mineralogical characterisation of silver flotation concentrates made from zinc neutral leach residues, Metallurgical Transactions B, Vol. 19B, October, pp. 803-817.

Chryssoulis, S.L., Surges, L.J. and Salter, R.S., 1985. Silver mineralogy at Brunswick Mining and Smelting and its implications for enhanced recovery. In Complex Sulphides: Processing of Ores, Concentrates and by-products. Eds.Zunkel, A.D., Boorman, R.S., Morris, A.E., and Wesely, R.J., Warrendale, pp. 815-830.

Chryssoulis, S.L., and Surges, L.J., 1988. Behaviour of tetrahedrite in the mill circuits of Brunswick Mining and Smelting Corporation Limited: Inst. Mining Metallurgy Internat. Conf. Silver, Mexico City, Nov. 1988, Proc., pp. 205-216.

Chryssoulis, S., Venter, D., and Dimov, S., 2003. On the floatability of gold grains, 35th Annual Meeting Canadian Mineral Processors, Ottawa, pp. 455-472.

Chryssoulis, S., Dunne, R., and Coetzee, A., 2004. Diagnostic microbeam technology in gold ore processing, Journal of Metals, July, pp. 53-57.

CMM, 2014. http://www.uq.edu.au/nanoworld/index.html?page=35655&pid=35502 access on 18/12/2014 at 11:55 AM.

Collins, M.J., Yuan, D., Masters, I.M., and Kalanchey, R., 2013. Pilot plant pressure Oxidation of a refractory gold-silver concentrate. CIM Journal, Vol. 4, No.3, pp.160-166.

Craig, J.R., 2001. Ore-mineral textures and the tales they tell. The Canadian Mineralogist. Vol.39, pp. 937-956.

Crawford, W.E., 1934. Cyanide milling practice of The Fresnillo Company, Trans. Amer. Inst. Min. Metall. Engineers, 112, pp. 734-750.

Cserna, Z., 1976. Mexico – geotechnics and mineral deposits: New Mex. Geol. Society, Spec. Publ. 6, pp. 18-25.

CSIRO, 2011. http://www.csiro.au/Organisation-Structure/Divisions/Process-Science-and-Engineering/XRD-analysis.aspx accessed on 13/10/2013 at 17:55 hrs.

Cytec , 2010. Cytec Mining Chemicals Handbook.

Dana, 1963. Dana's System of Mineralogy, 7th Ed., Vol. 2, Wiley, New York.

Di Prisco, G., Leroux, D., and Scott, D., 2002. Determination of silver bearing minerals in the Lady Loretta ore, 34th Annual Meeting Canadian Mineral Processors, Ottawa, pp. 57-75.

Dorr, J., and Bosqui, F., 1950. Cyanidation and Concentration of Gold and Silver Ores, 2nd edition, McGraw Hill.

Dunne, R., Levier, M., Acar, S., and Kappes, R., 2009. Keynote address: Newmont's contribution to gold technology, in Proceedings World Gold Conference 2009, The Southern African Institute of Mining and Metallurgy: Johannesburg, pp. 221-230.

Duran, P., and Block, V., 2012. Silver recovery from polymetallic flotation tailings. Expomin 2012. Presentation.

Elger, K., 2003. Analysis of deformation and tectonic history of the Southern Altiplano Plateau (Bolivia) and their importance for plateau formation. GeoForschungsZentrum Postdam, Scientific technical report STR 03/05, pp. 1-152.

Engel, A.L., and Jackson, T.A., 1949. Flotation of silver chloride from an oxide ore. Bureau of Mines, Report of Investigation 4574.

Essa, 2002. http://essa.vividcluster.crox.net.au/backend/EssaPurchasing/upload/Model/-130717335/docs/Ball_and_Rod_Mills.pdf . Accessed on 11/11/2013 at 10:24 AM

Evans, C.L., 2010. 'Development of a methodology to estimate flotation separability from ore microtexture', PhD Thesis, JKMRC, The University of Queensland.

Evans, C.L., Napier-Munn, T.J., 2013. Estimating error in measurements of mineral grain size distribution. Minerals Engineering, Vol. 52, pp. 198-203.

Fa, K., Miller J.D., Jiang, T., and Li, G., 2005. Sulphidisation flotation for recovery of lead and zinc from oxide-sulphide ores. Transactions Nonferrous Metals Society of China- English edition. Vol. 15, No.5, October 2005, pp. 1138-1144.

Fan, R., 2013. Synchrotron Analysis of Jayula ore. Confidential report.

Fan, R., and Gerson, A., 2014. Development of advanced methods for examination of Ag mineralogy and flotation losses. International Mineral Processing Congress (IMPC 2014), Chapter 14, pp. 32-42.

Fandrich, R.G., Bearman, R.A., Boland, J. and Lim, W., 2007. Mineral liberation by particle bed breakage, Minerals Engineering, Vol. 10, No. 2, pp. 175-187.

Figueiredo, M.O., Basto, M.J., Abbas, K,. Chevallier P., Melo Z., Ramos, M.T., 1993. Synchrotron X-ray-fluorescence analysis of heavy trace-elements in light silicate minerals, X-ray spectrometry, 22 Vol. 4, pp. 248-251.

Finch, J.A., *et al.*, 1979. Laboratory simulation of a closed circuit grind for a heterogeneous ore. CIM Bull. 72 (803), pp. 198-200.

First, 2014. http://www.first.ethz.ch/infrastructure/equipment/xrd. Accessed on 17/12/2014 at 11:28 AM.

Fleming, M.G., 1953. Effects of soluble sulphide in the flotation of secondary lead minerals. In: Recent Developments in Mineral Dressing. The Institution of Mining and Metallurgy, London, pp. 521-548.

Fuerstenau, D.W., 2007. In Froth flotation: a century of innovation (Eds.: Fuerstenau, M.C., Jameson, G.J., Yoon, R.-H. Australasian Institute of Mining and Metallurgy), Society for Mining Metallurgy and Exploration, Littleton, Colo., 3.

Fuerstenau, M.C., Chander, S., Woods, R., 2007. Froth flotation: a century of innovation (Eds.: Fuerstenau, M.C., Jameson, G.J., Yoon, R.-H. Australasian Institute of Mining and Metallurgy), Society for Mining Metallurgy and Exploration, Littleton, Colo., 425p.

Garcia-Zuñiga, H., 1935. The efficiency obtained by flotation is an exponential function of time. Boletin Minero, Soc. Nac. Minera, Santiago, Chile, 47, pp. 83-86.

Garret, P.R., 1979. The Effect of Polytetrafluoroethylene Particles on the Foamability of Aqueous Surfactant Solutions. Journal of Colloid and Interface Science. Vol. 69, No. 1, pp. 107- 121.

Gasparrini, C., 1983. The mineralogy of gold and its significance in metal extraction, CIM Bulletin, Vol. 76, 851, pp. 144-153.

Gasparrini, C., 1984A. The mineralogy of silver and its significance in metal extraction, CIM Bulletin, June, pp. 99-110.

Gasparrini, C., 1984B. The Metallurgy of the Precious Metals as Affected by Their Mineralogy and Manner of Occurrence in Their Ores. In Precious metals. Metallurgical Society of AIME. Los Angeles, pp. 101-109.

Gasparrini, C., and Lowell, G., 1985. Silver-bearing inclusions in “argentiferous” galena from the Silvermine District in southeastern Missouri, Canadian Mineralogist, Vol. 23, pp. 99-102.

Gasparrini, C., 1993. Gold and Other Precious Metals From Ore to Market. Springer-Verlag.

Gaudin, A. M., 1957. Flotation. McGraw-Hill Book Company, New York, pp. 326-368.

Gemmell, J.B., Zantop, H., and Birnie, R.W., 1989. Silver sulfosalts of the Santo Niño vein, Fresnillo district, Zacatecas, Mexico. Canadian Mineralogy 27, pp. 401-418.

Gieser, H.S., 1931. Experimental flotation of oxidized silver ores. American Institute of Mining and Metallurgical Engineers, Technical publication No. 401.

Goodall,W.R., and Scales, P.J., 2007. An overview of the advantages and disadvantages of the determination of gold mineralogy by automated mineralogy. Minerals Engineering 20 Vol. 5, pp. 506-517.

Gottlieb, P., Wilkie, G., Sutherland, D., Ho-Tun, E., Suthers, S., Perera, K., Jenkins, B., Spencer, S., Butcher, A., and Rayner, J., 2000. Using Quantitative Electron Microscopy for Process Mineral Applications. Journal of Metals, Vol. 52, pp. 24-25.

Graybeal, F.T., and Vikre, P.G., 2010. A Review of silver-rich mineral deposits and their metallogeny. Presented at the SEG 2010 Conference.

Gu, Y., 2003. Automated Scanning Electron Microscope Based Mineral Liberation analysis. Journal of Minerals and Materials Characterisation and Engineering, Vol. 2, pp. 33-41.

Guay, W. J. 1981. The Treatment of Refractory Gold Ores Containing Carbonaceous Material and Sulfides. Gold and Silver Leaching: Recovery and Economics, W. J. Schlitt, W. C. Larson, and J. B. Hiskey, (Eds.), SME, Littleton, pp. 17-22.

Guerra, C., 1988. Interference of manganese oxide minerals in recovery of silver from oxidized silver-bearing ores from Guanacevi mining district, Durango, Mexico, In Proceedings Silver – Exploration, Mining and Treatment, IMM, Mexico City, pp. 269-277.

Hagni, R.D., 1982. The influence of original host rock character on alteration and mineralization in the tri-state district of Missouri, Kansas and Oklahoma, U.S.A., Editors Amstutz, G.C., Goresy, A.E., Frenzel, G., Kluth, C., Moh, G., Wauchkuhn, A., and Zimmermann, R.A. , Ore genesis: The state of the art, Berlin, Springer-Verlag, pp. 99-107.

Hagni, R.D., 1986. Process Mineralogy VI (Editor), TMS-AIME.

Hahn, A.W., 1927. Flotation of Oxidized Lead-Silver Ores, Technical Publication No.10, American Institute of Mining and Metallurgical Engineers, August, pp. 1-5.

Hahn, A.W., 1929. Silver-bearing Minerals of Some Ores from the Tintic Mining District. New York Meeting, February, pp. 325-329.

Hausen, D., 1982. Process mineralogy of auriferous pyritic ores at Carlin, Nevada, Process Mineralogy II, Ed. Hagni, R., TMS, pp. 271-289.

Hausen, D., and Hill, D., 1994. Mineralogical and metallurgical characterization of silver bearing ore from Sonora, Mexico, Process Mineralogy XII, Ed. Petruk, W., and Rule, A., TMS, pp. 161-170.

Henley, K.J., 1983. Ore-dressing mineralogy – a review of techniques, applications and recent developments. Special Publication for Geological Society of South Africa, Vol. 7, pp.175–200.

Holloway, B., Clarke, G., and Lumsden, B., 2008. Improving fine lead and silver flotation recovery at BHP-Billiton's Cannington Mine, 40th Annual Meeting of Canada Mineral Processors, CIM, pp. 347-361.

Hoover, T. J., 1914. Concentrating ores by flotation. The Mining Magazine: London. 2nd ed., 37.

Horwood, E. J., 1909. British Patent 1789. Reported in Hoover, 1914, 37.

Hu, Y., Sun, W., and Wang, D., 2009. Electrochemistry of Flotation of Sulphide Minerals. Springer 304pp.

Jameson, G.J., Nam, S., and Moo Young, M., 1977. Physical Factors Affecting Recovery Rates in Flotation. Miner. Sci. Engrg., Vol. 9, pp. 103-118.

JKTech., 2011. JKSimfloat software (Version 6) [Computer Program]. Available at http://www.jktech.com.au/jksimfloat . Accessed 28 November 2014.

Johnson, N. W., and Munro, P. D., 2002. Overview of Flotation Technology and Plant Practice for Complex Sulphide Ores. In: Mineral Processing Plant Design Practice and Control, Vol. 1, SME, USA, pp. 1097-1123.

Jones, M.P., 1987, Applied Mineralogy : A Quantitative Approach, Graham and Trotman, London.

Jones, M.P., and Gavrilovic, J., 1970. Automatic quantitative mineralogy in minerals technology. Rudy, Vol. 5, pp. 189-197.

Jones, M.H., and Woodcock, J.T, 1979. Control of laboratory sulphidization with a sulphide ion selective electrode before flotation of oxidized lead-zinc-silver dump material. International Journal of Mineral Processing, Vol. 6, pp. 17-30.

Kelly, E.G., and Spottiswood, D.J., 1982. Introduction to Mineral Processing, Chapter 3, John Wiley and Son.

Kim, J., and Stanley, R., 1988. Flotation of silver minerals and precipitates in acidic media, In Proceedings Silver – Exploration, Mining and Treatment, IMM, Mexico City, pp. 247-260.

Kleeman, J.R., 1968. Treatment of old tailing dumps at Broken Hill South Ltd. In Broken Hill Mines . Edited by Radmanovich, M., and Woodcock, J.T., Melbourne: The Australiasian Institute of Mining and Metallurgy, pp. 437-457.

Klein, C., 2002. Mineral Science, Wiley and Sons, pp. 351-352.

Knights, J., and Patterson, D., 1988. Process mineralogy of silver in lead-zinc-silver ores at Mount Isa, Australia, In Proceedings Silver – Exploration, Mining and Treatment, IMM, Mexico City, pp. 101-110.

Knights, J., 2011. hrltesting Technical Memorandum No.562 Jayula, Tesorera, Toldos ores. Confidential.

Kohli, R., and Mittal, K.L., 2011. Developments in surface contamination and cleaning-detection, characterization, and analysis of contaminants. Elsevier. 331p.

Krismer, M., Vavtar, F., Tropper, P., Sartroy, B., and Kaindl, R., 2011. Mineralogy, mineral chemistry and petrology of the Ag-bearing Cu-Fe-Pb-Zn sulfide mineralizations of the Pfunderer Berg South Tyrol, Italy. Austrian Journal of earth sciences, Vol. 104, pp.36-48.

La Brooy, S.R., Linge, H.G., and Walker, G.S., 1994. Review of gold extraction fromores, Minerals Engineering, Vol.7, pp. 1213-1241.

Lamberg, P., 2011. Particles – The bridge between geology and metallurgy: Proceedings Conference in Mineral Engineering, Luleå, Sweden, pp. 1-16.

Lara, C., 1988. Flotation at the David Contreras Unit, La Encantada, Coahuila, Mexico, In Proceedings Silver – Exploration, Mining and Treatment, IMM, Mexico City, pp. 239-245.

Lastra R., 2007. Seven practical application cases of liberation analysis. International Journal of Mineral Processing, Vol., 84, pp. 337-347.

Leaver, E., and Woolf, J., 1939. Flotation of silver minerals, research Investigation 3436, US Bureau of Mines.

Lord, J.A., and Markovic, S., 1970. Control of the liquid phase composition in the differential flotation of some complex Peruvian ores. Proc. Int. Miner. Process. Congr., 9th, Prague, 1, pp. 259-269.

Lynch, A.J., Johnson, N.W., Manlapig, E.V., and Thorn, C.G., 1981. Mineral and Coal Flotation Circuits—Their Simulation and Control. Elsevier, Amsterdam. 285.

Lynch, A.J., Harbort, G.J., and Nelson, M.G., 2010. History of Flotation. AusIMM Spectrum Series No. 18, AusIMM, pp. 57-59.

Malhotra, D., Ramadorai, G., and Purdy, K., 1987. Plant Practice in Sulphide Flotation, Chapter in Chemical Reagents in the Mineral Processing Industry, Ed. Malhotra, D., and Riggs, W., SME-AIME, Colorado, pp. 21-37.

Malhotra, D., and Harris, L., 1999. Review of plant practice of flotation of gold and silver ores, in Advances in Flotation Technology, Ed. Parekh, B., and Miller, J., SME, pp. 167-181.

Mann A.W., 1984. Mobility of gold and silver in lateritic weathering profiles; some observations from Western Australia. Economic Geology, February 1984, Vol. 79, pp. 38-49.

Marley, F., and Hagni, R., 1982. Mexican silver ores: their mineralogical occurrence and treatment, Process Mineralogy II, Ed. Hausen D., and Park W., TMS, pp. 151-169.

Marsden, J., and House, L., 1992. The chemistry of gold extraction. Ellis Horwood, 597.

Marsden, J.O., and House, C.I., 2006. Chemistry of Gold Extraction, second edition. Society for Mining, Metallurgy and Exploration: Littleton.

McArthur, G.J., 1996. Textural evolution of the Hellyer massive sulfide deposit. Unpublished PhD thesis, University of Tasmania, Hobart, Australia. 272pp.

McQueen, K.G., 2005. Ore deposit types and their primary expressions. In Butt, C.R.M. *et al* (eds.) "Regolith expression of Australia ore systems: a compilation of exploration case histories with conceptual dispersion, process and exploration models" CRC LEME (Cooperative Research Centre for Landscape Environments and Mineral Exploration) Vol.1, pp. 1-14.

MLA., 2009. MLA System User Training Course. JKTech.

Mudd, G. M., 2010, The Environmental Sustainability of Mining in Australia: Key Mega-Trends and Looming Constraints. Resources Policy, 35 Vol. 2, pp. 98-115.

Nanotech-now, 2014. http://www.nanotech-now.com/news.cgi?story_id=42519. Accessed on 18/12/2014 at 11:52 AM.

Newbury, D. E., Joy, D. C., Echlin, P., Fiori, C. E., and Goldstein, J. I., 1986. Advanced Scanning Electron Microscopy and X-ray Microanalvsis. Plenum Press, New York. 454 pp.

Nguyen, A.V., and Schulze, H.J., 2004. Colloidal Sciences of flotation. New York: Marcel Dekerr.

Nicnas, 2014. http://www.nicnas.gov.au/chemical-information/imap-assessments/imap-assessment-details?assessment_id=167. Accessed on 18/12/2014 at 13:36 PM.

NIST, 2014. http://www.nist.gov/cnst/nanofab/toolset-metrology.cfm .Accessed on 18th December 2014 at 12:24 PM.

NMMU, 2014. http://chrtem.nmmu.ac.za/jeol-jsm-7001f . Accessed on 18/12/2014 at 12:05 PM.

Oancea, D., 2007. Silver deposits – Geochemistry, TechnoMine website. http://technology.infomine.com/articles/1/323/silver-exploration.silver-geochemistry.multi-element/silver.deposits.geochemistry.aspx . Accessed on 14th November 2013 at 11:58 AM.

Onal, G., Bulut G., Gul, A., Kangal, O., Perek, K., and Arslan, F., 2005. Flotation of Aladag oxide lead-zinc ores. Minerals Engineering. Vol. 18, pp. 279-282.

Parashyniak, P. and Phillips, R., 1978. Echo Bay Mines Limited, in Milling Practice in Canada, CIM Special, Vol. 16, pp. 62-63.

Pearson, F., Clark, K., and Gonzales, O., 1988. Ore mineralogy and silver distribution at Real de Angeles, Zacatecas, Mexico, In Proceedings Silver – Exploration, Mining and Treatment, IMM, Mexico City, pp. 73-99.

Petruk, W., 2000. Applied mineralogy in the mining industry, Elsevier Science, Amsterdam. 268.

Petruk, W., and Schnarr, J., 1982. The behaviour of galena, chalcopyrite and tetrahedrite during flotation of a fine-grained base metal ore in the concentrator of Brunswick Mining and Smelting Limited, Process Mineralogy II, Ed. Hausen, D., and Park, W., TMS, pp. 201-212.

Pitard, F.F., 2010. Theoretical, practical, and economic difficulties in sampling for trace constituents. The Journal of The Southern African Institute of Mining and Metallurgy, Vol. 110, pp. 313-321.

Pryor, E.J., 1953. Some aspect of the flotation of oxidized minerals. Recent developments in mineral dressing. The Institute of Mining and Metallurgy, London.

Pryor, E.J., 1965. Mineral Processing, Elsevier Publishing Co. Ltd. Great Britain. 784pp.

Qing,, W., He, M., and Chen, Y., 2008. Improvement of flotation behaviour of Mengzi lead-silver-zinc ore by pulp potential control flotation. Transactions of Nonferrous Metals Society of China. Vol. 18, pp. 949-954.

Ramadorai, G., 1991. Roasting options for improved gold-silver recoveries, Process Mineralogy XII, Ed. Hausen, D., Petruk, W., Hagni, R., and Vassiliou, A,. TMS, pp. 95-105.

Reed, S.J.B., 2005. Electron Microprobe Analysis and Scanning Electron Microscopy in Geology. Second Edition, Cambridge University Press.

Reflex, 2012. ioGAS software 2012 (Version 4.1)[Computer program]. Available at http://reflexnow.com/iogas/ . Accessed 28 November 2014.

Rey, M., 1954. Flotation of oxidized ores of lead, copper and zinc. Bull. Inst. Min. Metall., 574: pp. 541-548.

Rule, C.M., 2011. Stirred milling – new comminution technology in the PGM industry. The Journal of The Southern African Institute of Mining and Metallurgy, Vol. 111, February 2011, pp. 101-107.

Sack, R., and Brackebusch, F., 2004. Fahlore as an indicator of mineralization temperature and gold fineness, CIM Bulletin, Vol. 97, No. 1081. pp. 78-83.

Sandoval-Zambrano, G.E., 2013. Development of a novel strategy to estimate flotation recovery as a function of particle size and mineral liberation. PhD, JKMRC, The University of Queensland. 237pp.

Savassi, O.N., Alexander, D.J., Franzidis, J.P., and Manlapig, E.V., 1998. An empirical model for entrainment in industrial flotation plants, Minerals Engineering, Vol. 11, No. 3, pp. 243-256.

Shaede, E., Manning, L. and Rescoe, R., 1978. Terra Mining and Exploration, Limited – Silver Bear Mine, in Milling Practice in Canada, CIM Special, Vol. 16, pp. 76-78.

Silver Institute, 2013. https://www.silverinstitute.org/site/supply-demand/silver-production/ Accessed on 14th November 2013 at 11:59 am.

Silver Institute, 2015. The World Silver Survey 2015 A Summary. https://www.silverinstitute.org/site/wp-content/uploads/2011/06/WSS2015Summary.pdf Accessed on 22nd January 2016 at 11:35 am.

Silver Wheaton, 2013. RBC Capital Markets 9th Annual Silver Conference. Presentation, December 2013.

Smith, D., 1988. Geology of silver deposits along western American cordillera, in Proceedings Silver – Exploration, Mining and Treatment, IMM, Mexico City, pp. 11-24.

Stone, J.B., and McCarthy, J.C., 1942. Mineral and metal variations in the veins of Fresnillo, Zacatecas, Mexico: Am. Inst. Mining and Metall. Engineers, Tech. Publ. 1500, 16.

Taggart, A.F., 1945. Handbook of Mineral Dressing, Wiley New York.

Tãmas, C.G., Bailly, L., Ghergari, L., O'Connor, G., and Minut, A., 2006. New occurrences of tellurides and argyrodite in Rosia Montanã, Apuseni Mountains, Romania, and their metallogenic significance: Canadian Mineralogist, Vol. 44, pp. 367-383.

Thompson, P., 2002. The selection of flotation reagents via batch flotation tests, in Proceedings Mineral Processing Plant Design, Practice, and Control, Ed. by Mular, A., Halbe, D., and Barratt, D., Vol. 1, TMS, pp. 136-144.

Trahar, W.J., 1981. A rational interpretation of role of particle size in flotation. International Journal of Mineral Processing Vol. 2, pp. 289–327.

Tretbar, and Romano, 2009. Minera San Cristobal Zn-Pb-Ag Mine Bolivia (power point presentation).

UTAS, 2014. http://www.utas.edu.au/earth-sciences/facilities/laicpms-laboratory. Accesssed on 18/12/2014 12:13 PM.

Viljoen, E.A., and Johnson, L.A., 1983. Microbeam techniques in applied mineralogy. Special Publications of the GSSA 7, pp. 499-506.

Wandke, A., and Martinez, J., 1928. The Guanajuato mining district, Guanajuato, Mexico: Economic Geology, Vol. 23, pp. 1-44.

Warman International, 1981. Warman Cyclosizer Manual.

Warnaars, F., Atkinson, W., and Ambrus, J., 1987. Chanarcillo: an epithermal vein-type and disseminated silver deposit in Chile, Process Mineralogy VII, Ed. Vassiliou, A., Hausen, D., and Carson , TMS, pp. 273-279.

Watling, R.J., Herbert, H.K., and Abell, I.D., 1995. The application of laser ablation - inductively coupled plasma - mass spectrometry (LA-ICP-MS) to the analysis of selected sulphide minerals, Chemical Geology 124, pp. 67-81.

Webster, J.G., and Mann, A.W., 1984. The influence of climate, geomorphology and primary geology on the supergene migration of gold and silver Journal of Geochemical Exploration Vol. 22, Issues 1–3, September 1984, pp. 21–42.

Wightman, E., 2011. Characterisation of Minera San Cristobal oxide ores (Jayula, Tesorera and Toldos). Confidential report.

Wilkie, G., and Bojcevski, D., 1997. Applied Mineralogy as a Diagnostic Metallurgical tool for silver bearing base metal Sulphide Ores, in proceeding of 'Sixth Mill Operators Conference', Madang, New Guinea, 6-8 October 1997, pp. 199-203.

Wills, B.A., 1998. Mineral Processing Technology, Chapter 12, 6th Edition, Pergamon Press.

Wills, B.A., and Napier-Munn, T., 2006. Wills' Mineral Processing Technology (Seventh Edition), Butterworth-Heinemann, Oxford.

Withers, P.J., 2013. Chapter 7: Synchrotron X-ray Diffraction. Practical Residual Stress Measurement Methods. First Edition. Edited by Gary S. Schajer. John Wiley & Sons. Ltd. pp. 163-194.

Woodcock, J.T., Henley, K.J., Cathro, K.J., 1976. Metallurgy of gold and silver with reference to other precious metals. Course Notes for an Australian Mineral Foundation Workshop Course. Australian Mineral Foundation. 5-9 April. 343pp.

Woodcock, J.T., Sparrow, G.J., and Bruckard, W.J., 2007. Flotation of precious metals and their minerals. In Fuerstenau, M. C., Jameson, G., and Yoon, R.-H., (Eds.), Froth flotation, a century of innovation, SME, pp. 575–609.

Zhang, J., Zhang, Y., Richmond, W., and Wang., H, 2006. Processing technologies for gold-telluride ores, International Journal of Minerals, Metallurgy, and Materials, 17, pp. 1-10.

Zhou, J., Jago, B., and Martin, C., 2004. Establishing the process mineralogy of gold ores, 36th Annual Meeting Canadian Mineral Processors, Ottawa. pp. 199-226.

Zhou, J., Martin, C., Blatter, P., Bosse, P.A., and Robitaille, J., 2005. The process mineralogy of precious metals in LaRonde flotation products and its effect on process optimization, 44th Annual Conference Of Metallurgists CIM held in conjunciton with the 35th Annual Hydrometallurgy Meeting. Calgary, Alberta, Canada, Met Soc, pp. 93-109.

Zhou, J., 2010. Process mineralogy of silver ores and applications in flowsheet design and plant optimization, 42nd Annual Meeting Canadian Mineral Processors, Ottawa. pp.143-161.

Zhou, J., 2013. Mineralogy and predictive metallurgy of major types of gold ores. CIM Journal, Vol. 4, No. 3. pp. 201-209.

Appendix A - List of silver - bearing minerals

Table A.1: List of silver – bearing minerals (after Gasparrini,1984 & 1993 and webmineral)

No.	Name	Formula	Comment	Others Comments
1	Acanthite	Ag_2S	Silver is an essential constituent	Also called silver glance. Orthohombic, stable below 1750 °C
2	Aguilarite	Ag_4SeS	Silver is an essential constituent	
3	Alaskaite	$Pb(Ag, Cu)_2Bi_4S_8$	Silver is an essential constituent	
4	Allargentum	Ag_6Sb	Silver is an essential constituent	
5	Altaite	PbTe	Silver may occur in minor ammounts (<5%)	
6	Amalgam	Ag_2Hg_3		
7	Andorite	$PbAgSb_3S_6$	Silver is an essential constituent	
8	Angelaite	$Cu_2AgPbBiS_4$		
9	Antimonial silver	(Ag, Sb)	Silver is an essential constituent	
10	Antimonpearceite	$[Ag_9CuS_4][(Ag,Cu)_6(Sb,As)_2S_7]$		
11	Aramayoite	$Ag(Bi,Sb)S_2$	Silver is an essential constituent	
12	Arcubisite	Ag_6CuBiS_4	Silver is an essential constituent	
13	Argentian pentlandite	$(Fe,Ni)_8AgS_8$	Silver is an essential constituent	
14	Argentian plumbojarosite	$(Pb,Ag)Fe_3^{-6}(SO_4)_2^{-4}(OH)_6^{-12}$	Silver is an essential constituent	
15	Argentite	$Ag_2S.$	Silver is an essential constituent	Isometric Stable above 1750 °C
16	Argentojarosite	$AgFe_3(SO_4)_2(OH)_6$	Silver is an essential constituent	
17	Argentopentlandite	$Ag(Fe,Ni)_8S_8$		
18	Argentopyrite	$AgFe_2S_3$	Silver is an essential constituent	
19	Argentotennantite	$(Ag,Cu)_{10}(Zn,Fe)_2(As,Sb)_4S_{13}$		
20	Argyrodite	Ag_8GeS_6	Silver is an essential constituent	
21	Argyropyrite	$Ag_3Fe_7S_{11}$	Silver is an essential constituent	
22	Arsenpolybasite	$[Ag_9CuS_4][(Ag,Cu)_6(As,Sb)_2S_7]$		

23	Aurorite	$(Ag,Ba,Ca,Mn...)Mn_3O_7*3H_2O$	Silver is an essential constituent	
24	Balkanite	$Cu_9Ag_5HgS_9$	Silver is an essential constituent	
25	Baumhauerite	$Pb_{12}As_{16}S_{36}$	Silver may occur in minor ammounts (<5%)	
26	Baumstarkite	$Ag_3(Sb,As)_2SbS_6$		
27	Benjaminite	$Pb_2(Ag,Cu)_2Bi_4S_9$	Silver is an essential constituent	
28	Benleonardite	$Ag_8(Sb,As)Te_2S_3$		
29	Berryite	$Pb_2(Cu,Ag)_3Bi_5S_{11}$	Silver is an essential constituent	
30	Berzelianite	Cu_2Se	Silver may occur in minor ammounts (<5%)	
31	Betechtinite	$(Cu,Fe)_{11}(Pb,Ag)S_7$	Silver is an essential constituent	
32	Bideauxite	$Pb_2AgC_{l3}(F,OH)_2$	Silver is an essential constituent	
33	Billingsleyite	$Ag_7(As,Sb)S_6$	Silver is an essential constituent	
34	Bismuthinite	Bi_2S_3	Silver may occur in minor ammounts (<5%)	
35	Bohdanowiczite	$AgBiSe_2$		
36	Boleite	$KPb_{26}Cu_{24}Ag_9Cl_{62}(OH)_{48}$	Silver is an essential constituent	
37	Bornite	Cu_5FeS_4	Silver may occur in minor ammounts (<5%)	
38	Borodaevite	$Ag_5(Bi,Sb)_9S_{16}$		
39	Boulangerite	$Pb_2{}^{-5}Sb_2{}^{-4}Sb_2{}^{-4}S_5{}^{-11}$	Silver may occur in minor ammounts (<5%)	
40	Bournonite	$PbCuSbS_3$	Silver may occur in minor ammounts (<5%)	
41	Bromyrite	$AgBr$	Silver is an essential constituent	Also called Bromargyrite
42	Bursaite	$Pb_5Bi_4S_{11}$		
43	Calaverite	$AuTe_2$	Silver may occur in minor ammounts (<5%)	
44	Cameronite	$AgCu_7Te_{10}$		
45	Canfieldite	$A_{g8}(Sn,Ge)S_6$	Silver is an essential constituent	
46	Capgaronnite	$HgAg(Cl,Br,I)S$		
47	Catamarcaite	Cu_6GeWS_8		
48	Cervelleite	Ag_4TeS		
49	Chalcostibnite	$CuSbS_2$		
50	Chalcosite	Cu_2S	Silver may occur in minor ammounts (<5%)	
51	Chalcopyrite	$CuFeS_2$	Silver may occur in minor ammounts (<5%)	

52	Chalcostibnite	$CuSb_2$	Silver may occur in minor ammounts (<5%)	
53	Chenguodaite	$Ag_9FeTe_2S_4$		
54	Chilenite	Mixture of cuprite and silver	Silver is an essential constituent	Bi-bearing silver
55	Chlorargyrite	AgCl	Silver is an essential constituent	Also called Cerargyrite
56	Chrisstanleyite	$Ag_2Pd_3Se_4$		
57	Cinnabar	HgS	Silver may occur in minor ammounts (<5%)	
58	Clausthalite	PbSe	Silver may occur in minor ammounts (<5%)	
59	Cocinerite	Cu_4AgS	Silver is an essential constituent	
60	Coiraite	$(Pb,Sn)_{12.5}As_3Sn_5FeS_{28}$		
61	Cooperite	PtS	Silver may occur in minor ammounts (<5%)	
62	Coronadite	$Pb(Mn_6^{4+}Mn_2^{3+})O_{16}$		
63	Cosalite	$Pb_2Bi_2S_5$	Silver may occur in minor ammounts (<5%)	
64	Covellite	CuS	Silver may occur in minor ammounts (<5%)	
65	Criddleite	$TlAg_2Au_3Sb_{10}S_{10}$		
66	Crookesite	$(Cu,Ti,Ag)_2Se$	Silver is an essential constituent	
67	Cuboargyrite	AgSbS		
68	Cuprobismuthinite	$Cu_{10}Bi_{12}S_{23}$	Silver may occur in minor ammounts (<5%)	
69	Cupromakovickyite	$Cu_4AgPb_2Bi_9S_{18}$		
70	Cupropavonite	$AgPbCu_2Bi_5S_{10}$		
71	Cupropearceite	$[Cu_6As_2S_7][Ag_9CuS_4]$		
72	Cupropolybasite	$[Cu_6Sb_2S_7][Ag_9CuS_4]$		
73	Cylindrite	$Pb_3Sn_4Sb_2S_{14}$	Silver may occur in minor ammounts (<5%)	
74	Danielsite	$(Cu,Ag)_{14}HgS_8$		
75	Dervillite	Ag_2AsS_2		
76	Diaphorite	$Ag_3Pb_2Sb_3S_8$	Silver is an essential constituent	
77	Digenite	Cu_9S_5	Silver may occur in minor ammounts (<5%)	
78	Dyscrasite	Ag_3Sb	Silver is an essential constituent	
79	Electrum	(Au,Ag)	Silver is an essential constituent	
80	Embolite	Ag(Br,Cl)	Silver is an essential constituent	

81	Empressite	$AgTe$	Silver is an essential constituent	
82	Enargite	Cu_3AsS_4	Silver may occur in minor ammounts (<5%)	
83	Eskimoite	$Ag_{1.75}Pb_{1.75}Bi_{3.75}S_9$		
84	Eucairite	$AgCuSe$	Silver is an essential constituent	
85	Eugenite	Ag_9Hg_2		
86	Famatinite	$Cu_3(Sb,As)S_4$	Silver may occur in minor ammounts (<5%)	
87	Felbertalite	$Cu_2Pb_6Bi_8S_{19}$		
88	Fettelite	$[Ag_6As_2S_7][Ag_{10}HgAs_2S_8]$		
89	Fischesserite	Ag_3AuSe_2	Silver is an essential constituent	
90	Fizelyite	$Ag_2Pb_5Sb_8S_{18}$	Silver is an essential constituent	
91	Franckeite	$Pb_5Sn_3Sb_2S_{14}$	Silver may occur in minor ammounts (<5%)	
92	Freibergite	$(Ag,Cu,Fe)_{12}(Sb,As)_4S_{13}$	Silver is an essential constituent	$(Ag_{4+2x}Cu_{2-2x})[(Cu,Ag)_4(Fe,Zn)_2]Sb_4S_{12}S_{1-x}$ $(0< x <1)$
93	Freieslebenite	$Ag_5Pb_3Sb_5S_{12}$	Silver is an essential constituent	
94	Friesite	$Ag_2Fe_5S_8$	Silver is an essential constituent	
95	Furutobeite	$(Cu,Ag)_6PbS_4$		
96	Gabrielite	$Tl_2AgCu_2As_3S_7$		
97	Gabrielsonite	$PbFe(AsO_4)(OH)$		
98	Galena	PbS	Silver may occur in minor ammounts (<5%)	
99	Geffroyite	$(Ag,Cu,Fe)_9(Se,S)_8$		
100	Geochronite	$Pb_5(SbAs)_2S_8$	Silver may occur in minor ammounts (<5%)	
101	Giessenite	$Pb_{13}(Cu,Ag)(Bi,Sb)_9S_{28}(?)$		
102	Giraudite	$(Cu,Zn,Ag)_{12}(As,Sb)_4(Se,S)_{13}$		
103	Goldamalgam	$(Au,Ag)Hg$		
104	Gustavite	$Bi_{11}Pb_5Ag_3S_{24}$	Silver is an essential constituent	
105	Hatchite	$(Pb,Tl)_2AgAs_2S_5$		
106	Henryite	$Cu_4Ag_3Te_4$		
107	Hessite	Ag_2Te	Silver is an essential constituent	
108	Heyrovskyite	$Pb_{10}AgBi_5S_{18}$		

109	Hocartite	Ag_2SnFeS_4	Silver is an essential constituent	
110	Huantajayite	(Na,Ag)Cl	Silver is an essential constituent	
111	Hunchunite	$(Au,Ag)_2Pb$		
112	Hutchinsonite	$(Pb,Tl)(Cu,Ag)As_5S_{10}$	Silver is an essential constituent	
113	Iltisite	HgSAg(Cl,Br)		
114	IMA2005-036	$Cu_8Pb_4Ag_3Bi_{19}S_{38}$		
115	IMA2008-058	$Ag_5Bi_{13}S_{22}$		
116	Imiterite	Ag_2HgS_2		
117	Incaite	$(Pb,Ag)_4FeSn_4Sb_2S_{13}$	Silver is an essential constituent	
118	Iodargyrite	AgI	Silver is an essential constituent	Also Called iodyrite
119	Jagueite	$Cu_2Pd_3Se_4$		
120	Jalpaite	Ag_3CuS_2	Silver is an essential constituent	
121	Jamesonite	$Pb_4FeSb_6S_{14}$	Silver may occur in minor ammounts (<5%)	
122	Jonassonite	$Au(Bi,Pb)_5S_4$		
123	Kitaibelite	$Ag_{10}PbBi_{30}S_{51}$		
124	Kittlite	HgAgSCuSe mineral.correct formula not available	Silver is an essential constituent	
125	Klockmannite	CuSe	Silver may occur in minor ammounts (<5%)	
126	Kobellite	$Pb_2(Bi,Sb)_2S_5$	Silver may occur in minor ammounts (<5%)	
127	Krennerite	$AuAgTe_4$	Silver is an essential constituent	
128	Krennerite	$AuTe_4$	Silver may occur in minor ammounts (<5%)	
129	Kupcikite	$Cu_{3.4}Fe_{0.6}Bi_5S_{10}$		
130	Kurilite	$(Ag,Au)_2(Te,Se,S)$		
131	Kutinaite	Cu_2AgAs	Silver is an essential constituent	
132	Laffittite	$AgHgAsS_3$	Silver is an essential constituent	
133	Laforetite	$AgInS_2$		
134	Larosite	$(Cu,Ag)_{21}(Pb,Bi)_2S_{13}$	Silver is an essential constituent	
135	Lautite	CuAsS	Silver may occur in minor ammounts (<5%)	
136	Lenaite	$AgFeS_2$		
137	Lengenbachite	$Pb_6(Ag,Cu)_2As_4S_{13}$	Silver is an essential constituent	

138	Luanheite	Ag_3Hg		
139	Makovickyite	$Ag_{1.5}Bi_{5.5}S_9$		
140	Marrite	$PbAgAsS_3$	Silver is an essential constituent	
141	Matildite	$AgBiS_2$	Silver is an essential constituent	
142	Mazzettiite	$Ag_3HgPbSbTe_5$		
143	Mckinstryite	$Cu_{0,8+x}Ag_{1.2-x}S$	Silver is an essential constituent	
144	Meneghinite	$CuPb_{18}Sb_7S_{24}$	Silver may occur in minor ammounts (<5%)	
145	Melonite	$NiTe_2$	Silver may occur in minor ammounts (<5%)	
146	Miargyrite	$AgSbS_2$	Silver is an essential constituent	
147	Miersite	(Ag,Cu)I	Silver is an essential constituent	
148	Milotaite	PdSbSe		
149	Montbrayite	Au_2Te_3		
150	Moschellandsbergite	Ag_2Hg_3	Silver is an essential constituent	
151	Mummeite	$Cu_{0.58}Ag_{3.11}Pb_{1.10}Bi_{6.65}S_{13}$		
152	Muthmannite	(Ag,Au)Te	Silver is an essential constituent	
153	Nagyagite	$Pb_5Au(Te,Sb)_4S_{5-8}$	Silver may occur in minor ammounts (<5%)	
154	Native bismuth	Bi	Silver may occur in minor ammounts (<5%)	
155	Native copper	Cu	Silver may occur in minor ammounts (<5%)	
156	Native gold	Au	Silver may occur in minor ammounts (<5%)	
157	Native silver	Ag	Silver is an essential constituent	
158	Native telluriun	Te	Silver may occur in minor ammounts (<5%)	
159	Naumannite	Ag_2Se	Silver is an essential constituent	
160	Neyite	$Pb_7(Cu,Ag)_2Bi_6S_{17}$	Silver is an essential constituent	
161	Novakite	$(Cu,Ag)_4As_3$		
162	Ostwaldite	AgCl	Silver is an essential constituent	colloidal like AgCl
163	Ourayite	$Pb_4Ag_3Bi_5S_{13}$		
164	Ouryite	$Ag_{12.5}Pb_{15}Bi_{20.5}S_{52}$	Silver is an essential constituent	
165	Owyheeite	$Pb_5Ag_2Sb_6S_{15}$	Silver is an essential constituent	
166	Paderaite	$Cu_7((Cu,Ag)_{0.33}Pb_{1.33}Bi_{11.33})_{13}S_{22}$		

167	Para-schachnerite	Ag_3Hg_2	Silver is an essential constituent	
168	Pavonite	$AgSb_3S_5$	Silver is an essential constituent	
169	Pearceite	$[Ag_9CuS_4][(Ag,Cu)_6(As,Sb)_2S_7]$		
170	Pellouxite	$(Cu,Ag)Pb_{10}Sb_{12}S_{27}(Cl,S)_{0.60}$		
171	Penroseite	$(Ni,Cu,Pb)Se_2$	Silver may occur in minor ammounts (<5%)	
172	Penzhinite	$(Ag,Cu)_4Au(S,Se)_4$		
173	Perceite	$(Ag,Cu)_{16}As_2S_{11}$	Silver is an essential constituent	
174	Perroudite	$Hg_{5-x}Ag_{4+x}S_{5-x}(Cl,I,Br)_{4+x}$		
175	Petrovskaite	$AuAg(S,Se)$		
176	Petrukite	$(Cu,Fe,Zn)_2(Sn,In)S_4$		
177	Petzite	Ag_3AuTe_2	Silver is an essential constituent	
178	Pirquitasite	Ag_2ZnSnS_4		
179	Plumbopalladinite	Pd_3Pb_2	Silver may occur in minor ammounts (<5%)	
180	Plagionite	$Pb_5Sb_8S_{17}$	Silver may occur in minor ammounts (<5%)	
181	Polyargyrite	$Ag_{24}Sb_2S_{15}$	Silver is an essential constituent	
182	Polybasite	$(Ag,Cu)_{16}Sb_2S_{11}$	Silver is an essential constituent	
183	Proudite	$Cu_{1.9}Ag_{0.1}Pb_{15.6}Bi_{20.4}Sb_{0.1}S_{32.4}Se_{14.5}$		
184	Proustite	Ag_3AsS_3	Silver is an essential constituent	Also called ruby silver
185	Putzite	$(Cu_{4.7}Ag_{3.3})GeS_6$		
186	Pyrargyrite	Ag_3SbS_3	Silver is an essential constituent	Also called ruby silver
187	Pyrostilpnite	Ag_3SbS_3	Silver is an essential constituent	
188	Quadratite	$Ag(Cd,Pb)AsS_3$		
189	Ramdohrite	$Ag_2Pb_3Sb_6S_{13}$	Silver is an essential constituent	
190	Rathite	$Pb_8Pb_{4-x}(Tl_2As_2)x(Ag_2As_2)As_{16}S_{40}$		
191	Rathite-I	$Pb_{12-x}Tl_{x/2}As_{18-x}Ag_2S_{40}$	Silver is an essential constituent	
192	Rayite	$(Ag,Tl)_2Pb_8Sb_8S_{21}$		
193	Roshchinite	$Ag_{19}Pb_{10}Sb_{51}S_{96}$ or $Pb(Ag,Cu)_2(Sb,As)_5S_{10}$		
194	Rozhkovite	$(Cu,Pd)_3Au_2$	Silver may occur in minor ammounts (<5%)	
195	Sakuraiite	$(Cu,Ag)_2(In,Sn)(Zn,Fe)S_4$	Silver is an essential constituent	

196	Samsonite	$Ag_4MnSb_2S_6$	Silver is an essential constituent	
197	Schachnerite	$Ag_{1.1}Hg_{0.9}$		
198	Schapbachite	$AgBiS_2$		
199	Schirmerite	$PbAg_4Bi_4S_9$	Silver is an essential constituent	
200	Schlemaite	$(Cu,[\ ])_6(Pb,Bi)Se_4$		
201	Schwazite	Hg-bearing tetrahedrite	Silver is an essential constituent	Hg-bearing tetrahedrite
202	Selenocosalite	$Pb_2Bi_2(S,Se)_5$	Silver may occur in minor ammounts (<5%)	
203	Selenojalpaite	Ag_3CuSe_2		
204	Selenokobellite	$Pb_2(Bi,Sb)_2(S,Se)_5$	Silver may occur in minor ammounts (<5%)	
205	Selenopolybasite	$[(Ag,Cu)_6(Sb,As)_2(S,Se)_7][Ag_9Cu(S,Se)_2Se_2]$		
206	Selenostephanite	$Ag_5Sb(Se,S)_4$		
207	Semseyite	$Pb_9Sb_8S_{21}$	Silver may occur in minor ammounts (<5%)	
208	Sicherite	$TlAg_2(As,Sb)_3S_6$		
209	Silver	Ag		
210	Silver amalgam	(Ag,Hg)	Silver is an essential constituent	
211	Silver jarosite	$Ag_2Fe_5(OH)_{12}(SO_4)_4$	Silver is an essential constituent	
212	Smithite	$AgAsS_2$	Silver is an essential constituent	
213	Sopcheite	$Ag_4Pd_3Te_4$		
214	Stannite	Cu_2FeSnS_4	Silver may occur in minor ammounts (<5%)	
215	Stannite(?)III	$CuAgSn_2S_4$	Silver is an essential constituent	
216	Stannite(?)IV	Sn-Ag-Zn-bearing tetrahedrite	Silver is an essential constituent	Sn-Ag-Zn-bearing tetrahedrite
217	Stephanite	Ag_5SbS_4	Silver is an essential constituent	
218	Sternbergite	$AgFe_2S_3$	Silver is an essential constituent	
219	Sterryite	$Ag_2Pb_{10}(Sb,As)_{12}S_{29}$		
220	Stetefeldtite	$Ag*CuO*FeO*Sb_2O_{5*}S$	Silver is an essential constituent	
221	Stibnite	Sb_2S_3	Silver may occur in minor ammounts (<5%)	
222	Stromeyerite	$Cu_{1+x}Ag_{1-x}S$	Silver is an essential constituent	
223	Stuetzite	$Ag_{5-x}Te_3$	Silver is an essential constituent	
224	Stutzite	$Ag_{5-x}Te_3,(_{x=0.24-0.36})$		

225	Stylotypite	$(Ag,Cu,Fe)_3SbS_3$	Silver is an essential constituent	
226	Suredaite	$PbSnS_3$		
227	Sylvanite	$(Au,Ag)Te_4$	Silver is an essential constituent	
228	Teallite	$PbSnS_2$	Silver may occur in minor ammounts (<5%)	
229	Telargpalite	$(Pd,Ag,Pb,Bi)_{4+x}(Te,Se)$	Silver is an essential constituent	
230	Tennantite	$(Cu,Ag,Fe)_{12}As_4S_{13}$	Silver is an essential constituent	
231	Tetrahedrite	$(Cu,Ag,Fe)_{12}Sb_4S_{13}$	Silver is an essential constituent	Also called gray copper
232	Tillmannsite	$(Ag_3Hg)(V,As)O_4$		
233	Tintinaite	$Pb_{22}Cu^{+4}(Sb,Bi)_{30}S_{69}$		
234	Tischendorfite	$Pd_8Hg_3Se_9$		
235	Tocornalite	$(Ag,Hg)I(?)$		
236	Toyohaite	$Ag_2FeSn_3S_8$		
237	Treasurite	$Ag_7Pb_6Bi_{15}S_{32}$		
238	Trechmanite	$AgAsS_2$	Silver is an essential constituent	
239	Tsnigriite	$Ag_9SbTe_3(S,Se)_3$		
240	Uchucchacuaite	$AgPb_3MnSb_5S_{12}$		
241	Umangite	Cu_3Se_2	Silver may occur in minor ammounts (<5%)	
242	Uytenbogaardtite	Ag_3AuS_2	Silver is an essential constituent	
243	Vikingite	$Ag_{1.25}Pb_2Bi_{3.25}S_{7.5}$	Silver is an essential constituent	
244	Volinskite	$AgBi_{1.6}Te_2$	Silver is an essential constituent	
245	Volynskite	$AgBiTe_2$		
246	Wallisite	$PbTl(Cu,Ag)As_2S_5$		
247	Wehrlite	$Bi_{2+x}Te_{3-x}(?)$	Silver may occur in minor ammounts (<5%)	
248	Weishanite	$(Au,Ag)_3Hg_2$		
249	Wittichenite	Cu_3BiS_3	Silver may occur in minor ammounts (<5%)	
250	Wittite	$Bi_6Pb_5(Se,S)_{14}$	Silver may occur in minor ammounts (<5%)	
251	Xanthoconite	Ag_3AsS_3	Silver is an essential constituent	
252	Zinkenite	$Pb_6Sb_{14}S_{27}$	Silver may occur in minor ammounts (<5%)	
253	Zoubekite	$AgPb_4Sb_4S_{10}$		

Table A.2: Silver bearing minerals encountered in the study

No.	Name	Formula	Comment	Others Comments
1	Coronadite	$Pb(Mn_6^{4+}Mn_2^{3+})O_{16}$		
2	Gabrielstonite	$PbFe(AsO_4)(OH)$		
3	Barite-Ag	Ag,Ba,S,Fe	Unique Chemical association found in the thesis	Insolation of the grain is difficult do to that the grain size is between 2-5 microns

Appendix B – Minera San Cristobal, Bolivia

B.1 Context

The ores used in this study come from Minera San Cristobal (MSC), which is a Ag-Pb-Zn deposit located in district of Potosi, Bolivia. These ores are treated as individual case studies under this research *Toldos ore*, an oxide low-grade silver ore; *Tesorera ore*, a complex sulphide low-grade silver ore and *Jayula ore*, complex oxide low-grade silver ore.

B.2 Description of Minera San Cristobal S.A (MSC)

MSC is 500 km to the South of La Paz, at 90 km southwest of Uyuni (altiplano) and at 4000 metres above sea level. MSC is a subsidiary of Sumitomo Corporation, Japan, and is the 3rd largest silver mine and 5th largest zinc mine worldwide (Duran and Block, 2012). Figure B.1 is a map showing the location of Minera San Cristobal, Figure B.2 shows the location of the pit and Figure B.3 the actual land location of the pits from MSC.

Figure B.1: Location of Minera San Cristobal (After Jacobson *et al.*, 1969)

MSC comprises a number of different sites, according to Jacobson *et al.*, (1969); the first mine operated was the Hedionda Mine at Jayula reported by a Spanish priest, Barba, in 1637, however repeated attempts to mine silver failed because of the presence of carbon dioxide (CO_2) gas which caused the death of many miners. After that, a Polish engineer Josef Jackowski operated the Hedionda Mine at Jayula from 1896-1901 and 1927-1936, resolving the problem of CO_2. Toldos mine was operated between 1870 and 1921 by the Compañia Minera de San Cristóbal, producing a product that contained 0.2-0.5% of silver (Ahlfeld, 1944). Other sites are Tesorera, Trapiche,

Bertha, Colon and Animas mines. Figure B.2 shows the district of San Cristóbal and the type of rock present in the area. Also, the area limited by blue indicates the current status of the mine features (pits that were study under this thesis). For example in the cases of Hedionda Mine (Jayula) and Tesorera mine the rock are Quehua Fm (Oligocene-Miocene) and in the case of Toldos mine the rock is from Potoco Fm. (Eocene-Oligocene).

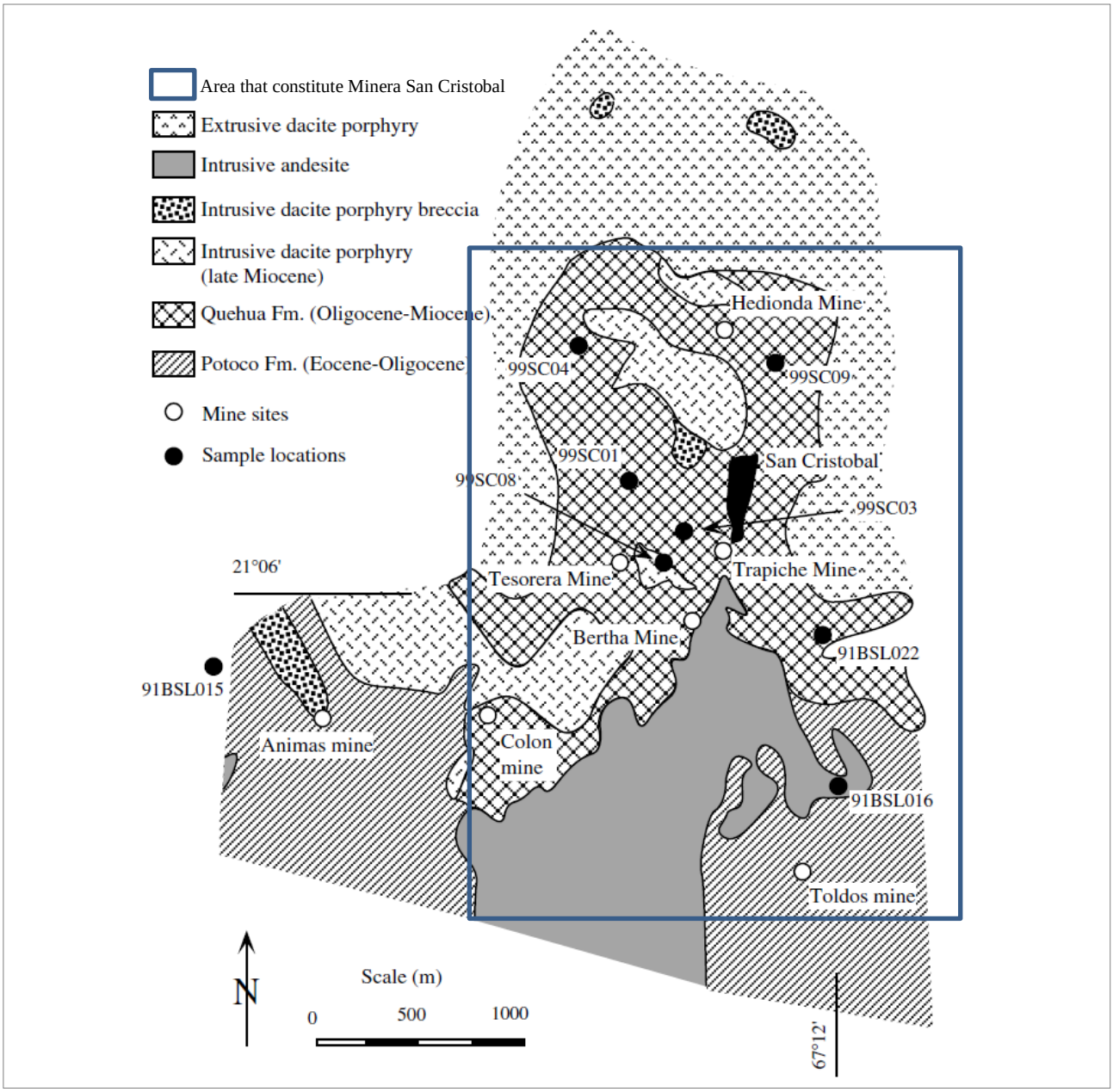

Figure B.2: Minera San Cristobal (After Jacobson *et al.*, 1969; Long *et al.*, 1991 and Kamenov *et al.*, 2002)

Figure B.3 shows the land positions of the pits of Jayula, Tesorera and Toldos. Also, in the right photo shows the legend for the areas that have been drilled for reserves others under review and other type of mineralization present in Minera San Cristobal.

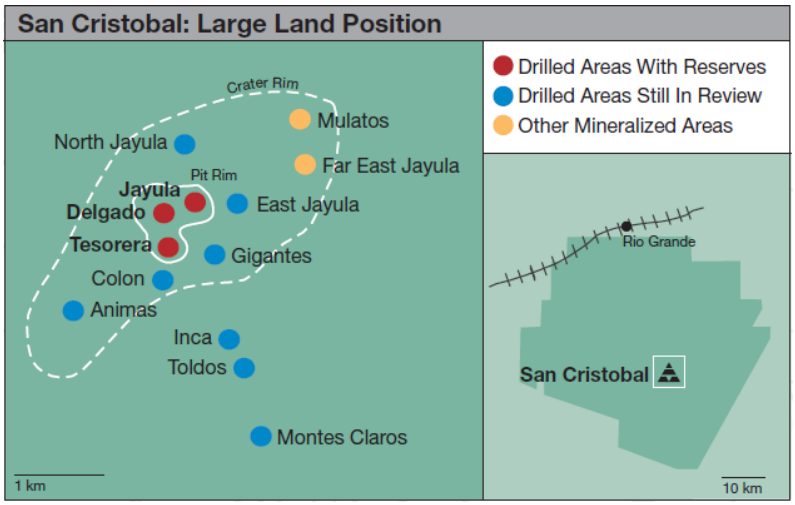

Figure B.3: Land position of MSC pits and drilled areas studied by Tretbar and Romano, 2009.

The regional geology of MSC indicates that it is situated in the Bolivia altiplano within the Central Andean Volcanic Zone of South America. It is situated between Occidental & Oriental Ranges of the Central Andean Cordillera. Tretbar and Romano, 2009 stated that "The deposit geology indicated that is located on the Khenayani-Uyuni Fault Zone (KUFZ)". Figure B.4 A, shows three photos that illustrate the relief of the topography of the Central Andes with a close-up in the right size, showing the KUFZ fault while in the botton there is a schematic cross-section of the Central Andean Plateau at ~21o S. WF = Western Flank and Precordillera, WC = Western Cordillera, AP = Altiplano, EC = Eastern Cordillera, IA = Interandean, SA = Subandean (Engle, 2003).

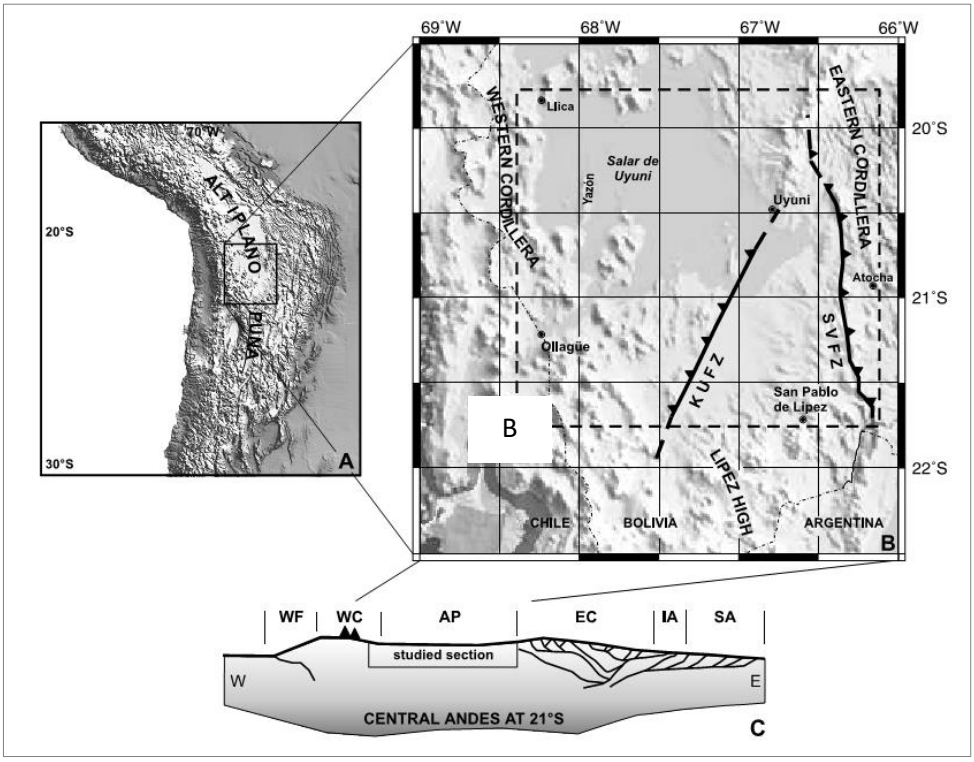

Figure B.4: Topography of the Cetral Andes where MSC is located (From Elger, 2003)

B.3 Ore mineralogy of MSC

The main mineralization of MSC is shown conceptually in Figure B.5, which illustrates Colon, Tesorera, Don Jose and Jayula pits. According to Tretbar and Romano (2009) MSC is "hosted in intrusives (vein, stockwork), contact breccias, and lower volcanoclastic sediments".

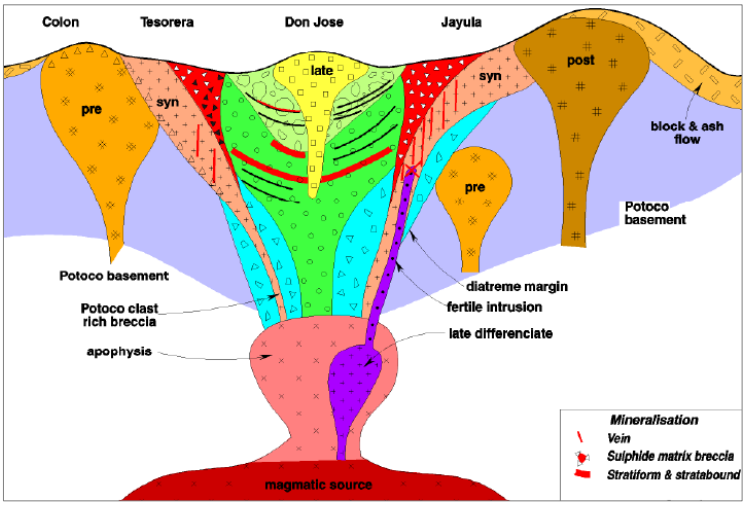

Figure B.5: MSC mineralization (From Tretbar and Romano, 2009)

MSC is classified as a magmatic hydrothermal low sulphide ore deposit containing Pb, Zn and Ag. The main minerals present are galena for Pb, sphalerite for Zn, and silver which occurs mainly as acanthite, pyrargyrite, and to a lesser extent tetrahedrite and freibergite. Silver is also present as solid solution with galena, sphalerite and pyrite, respectively. The main sulphide gangue is pyrite, clays are also present but in a relatively small quantities. Examples of the microtextures present in Tesorera and Jayula ores are shown in Figures B.6 and B.7. For both Tesorera and Jayula ores Tretbar and Romano (2009) identified fine-grained intergrowth minerals in both ores.

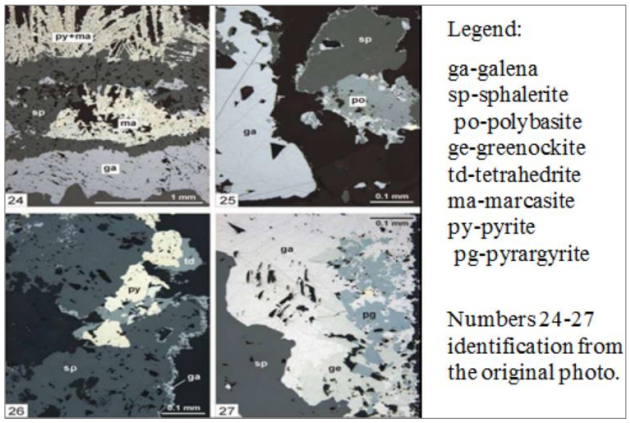

Figure B.6: Microtextures present in Tesorera Ore (From Tretbar and Romano, 2009)

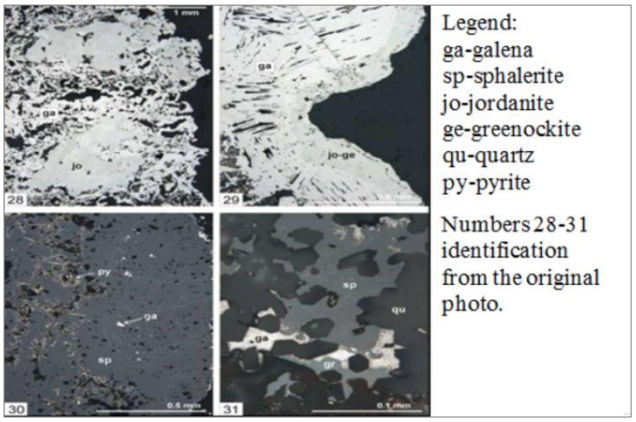

Figure B.7: Microtextures present in Jayula Ore (From Tretbar and Romano, 2009)

B.4 Description of ores used in the thesis

B.4.1 Toldos ore

Toldos ore is located at an elevation of 4100 m and is 2 km away from San Cristobal. Toldos is an old pit which has been geologically described by Ahlfeld (1967) as forming at "high temperatures with the formation of large quantities of crystalline specular hematite with glassy quartz" and Jacobson *et al.*, 1969 as "oxide veins containing iron and silver associated with andesite porphyry intrusive". The ore mineralogy is complex; some of the minerals present include arsenopyrite, barite, pyrite, quartz, native silver, stromeyerite, galena, sphalerite, tetrahedrite, chalcopyrite, pyrargyrite and polybasite.

B.4.2 Tesorera Ore

Tesorera ore is described as volcanoclastic sediments Tvs-1 from Tesorera's pit at MSC. Figure B.8 shows the location of this ore zone in the pit.

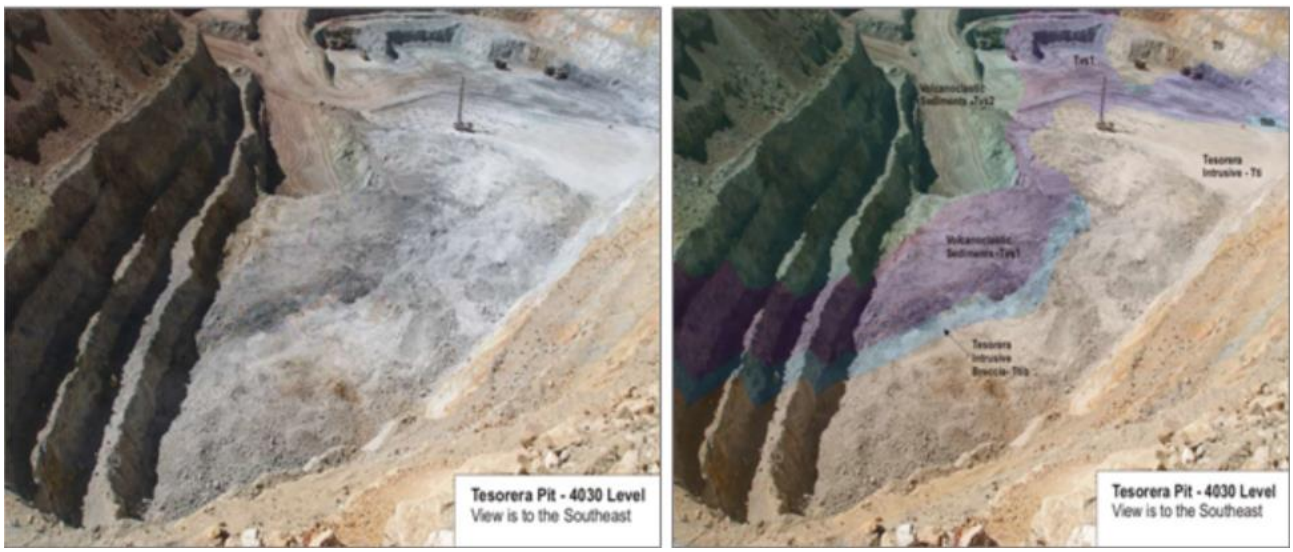

Figure B.8: Photographs from Tesorera's pit

B.4.3 Jayula ore

The geological genesis is represented by the silica cap zone of the Jayula pit at Minera San Cristobal. Figure B.9, shows a picture which indicates the zone of where the sample is from. The yellow colour is one of the main features that distinguishes this ore visually.

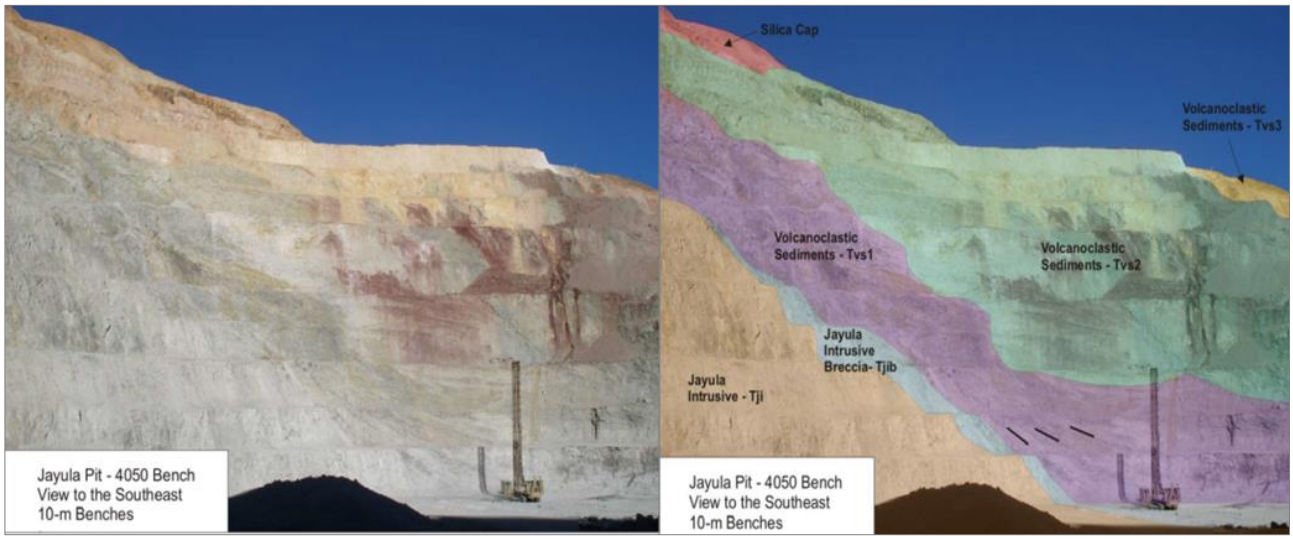

Figure B.9: Photographs from Jayula's pit

B.5 Flow sheet used at MSC

In terms of production MSC was positioned in the third place as a project in 2002 with an estimated average production of 28 Million ounces for the first five years (Apex, 2003) while the reserves in 2008 were measured at 223.9 Million tonnes at a grade of 56.5 g/t of Ag, 1.44% Zn and 0.53% Pb as commented by Tretbar and Romano (2009).

The circuit design for the flotation processes is illustrated in Figure B.8. The flotation circuit consists of lead flotation follow by zinc flotation. The lead flotation circuit consists of two parallel banks of rougher cells. The combined rougher concentrate is reground in a vertical stirred mill in closed circuit with cyclones prior to cleaning. There are four stages of cleaning, the first three stages use mechanical cells and the final stage uses a column. The cleaner tailings returns to the head of the rougher. Based on the plant configuration a P80 of 100 microns was selected as the initial flotation feed size for performing batch flotation tests on the three ores.

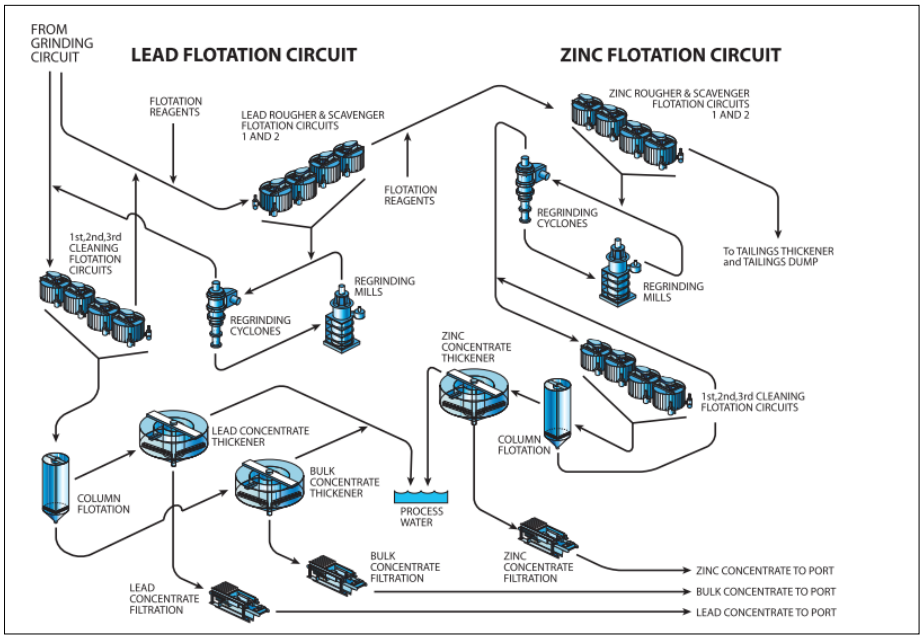

Figure B.10: Flotation circuit at MSC (From FLSmith, 2009)

B.6 References

Ahlfeld, F., 1944. La geología del mineral de San Cristóbal de Lipez (Bolivia): Minería Boliviana, Vol. 1, No. 8, 9-15.

Ahlfeld, F., 1967. Metallogenetic epochs and provinces of Bolivia: Mineralium Deposita, Vol. 2, 291-311.

Apex, 2003. Apex Silver Mines Limited Reports Third Quarter 2003 Results.

Duran, P., and Block, V., 2012. Silver recovery from polymetallic flotation tailings. Expomin 2012. Presentation.

Elger, K., 2003. Analysis of deformation and tectonic history of the Southern Altiplano Plateau (Bolivia) and their importance for plateau formation. GeoForschungsZentrum Postdam, Scientific technical report STR 03/05, 1-152.

FLSmith, 2009. Highlights Cement & Minerals Magazine, May 2009, 12-16.

Jacobson, H.S., and Murillo, C., 1969. Geology and Mineral Resources of the San Cristobal District, Villa Martin Province, Potosi, Bolivia: U.S. Geological Survey Bulletin 1273, 22p.

Kamenov, G., MacFarlane, A.W., and Riciputi, L., 2002. Sources of Lead in the San Cristobal, Pulacayo, and Potosí Mining Districts, Bolivia, and a Reevaluation of Regional Ore Lead Isotope Provinces, Economic Geology, Vol. 97, 573-592.

Long, K.R., Ludington,S., and Richter, D., 1991. Mineral Deposits and Occurrences of the Bolivian Altiplano and Cordillera Occidental, Compiled by the U.S. Geological Survey and Servicio Geologico de Bolivia, Open-File Report 91-0286, 355p.

Tretbar, D., and Romano, M., 2009. Minera San Cristobal Zn-Pb-Ag Mine Bolivia (power point presentation). December, 2009. Confidential.

Appendix C – Equipment and apparatuses used in the metallurgical and flotation characterisation

C.1. Equipment and techniques used in the mineralogical and metallurgical characterisation

This appendix has the objective to describe all the equipment and techniques used during the development of this thesis work. First all the techniques used in the mineralogical characterisation are explained in broad to then describe all the equipment used in the metallurgical characterisation.

C.1.1 Mineralogical Characterisation

The equipment and techniques used in the mineralogical characterisation i.e., for ore characterisation, mil product characterisation and flotation product characterisation are described.

a) Chemical assays

All samples were submitted for analysis using four acid digestion methods followed by inductive coupled plasma atomic emission spectroscopy (ICP-AES) to assay the elements present in each size fraction submitted. The analysis was made for 33 different elements at ALS and hrltesting, both laboratories located in Brisbane, Australia. In Table C1, the elements that were analysed by this technique and the detection limits for each are shown.

Table C1: Detection limit for chemical assays. Ranges given for detection limits for ICP-MS at ALS laboratory, located in Brisbane. The low limit is located at the left side and the upper limit is located at right side.

Element	Range (ppm or %)	Element	Range (ppm or %)
Ag	1-200	**Mo**	10-50000
Al	0.05%-30%	**Na**	0.05%-30%
As	50-100000	**Ni**	10-100000
Ba	50-50000	**P**	50-100000
Be	10-10000	**Pb**	20-100000
Bi	20-50000	**S**	0.05%-10%
Ca	0.05%-50%	**Sb**	50-50000
Cd	10-10000	**Sc**	10-50000
Co	10-50000	**Sr**	10-100000
Cr	10-100000	**Th**	50-50000
Cu	10-100000	**Ti**	0.05%-30%
Fe	0.05%-50%	**Tl**	50-50000
Ga	50-50000	**U**	50-50000
K	0.1%-30%	**V**	10-100000
La	50-50000	**W**	50-50000
Mg	0.05%-50%	**Zn**	20-100000
Mn	10-100000		

b) Oxide characterisation for lead and zinc mineral

This characterisation was performed to quantify the soluble and insoluble lead and zinc present in the samples, with the analysis performed by AMDEL, in Melbourne. For lead oxide assays, leaching with ammonium acetate solution was used to selectively dissolve oxides, and an atomic absorption spectrometer (AAS) analysis was then performed. For zinc oxide assays, a digestion in weak sulphuric acid solution (0.02N) was carried out to extract oxides, followed by an AAS analysis.

c) X-ray diffraction (XRD)

X-ray Diffraction was performed to provide qualitative information on the non-sulphide gangue (NSG) minerals present in the ores. These analyses were performed by AMDEL (this laboratory is located in Melbourne). Figure C.1 shows the XRD used by AMDEL.

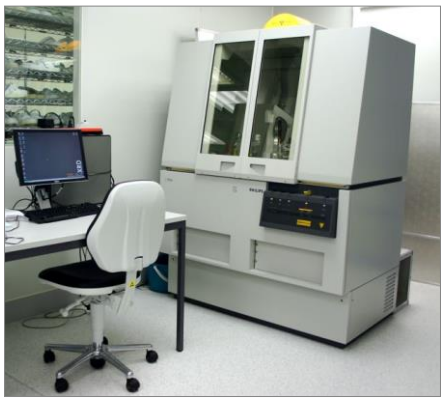

Figure C.1: Panalytical X'Pert PRO XRD used at AMDEL (from First centre, 2014).

d) Optical microscopy

The aim of this analysis was to identify the non-sulphide gangue present in the samples received, as well as to establish the level of complexity of the silver mineralogy and petrographic textures present in these ores, using the selected size fraction of -425/+300 μm from the ore head. Each ore was mounted in an epoxy polished block section and submitted to optical microscopy by reflected light at hrltesting, located in Brisbane. Figure C.2 shows an optical microscope used for these types of analyses.

Figure C.2: Optical microscope (from NIST, 2014).

e) Mineral Liberation Analyser (MLA)

The MLA was used to quantify the key mineralogical attributes for each of the ores. The main attributes studied using this technique were modal mineralogy, elemental deportment and texture (grain size, and mineral association) for the ore characterisation while for the mill and flotation products liberation studies of liberation were added to the main attributes. The system housed at the JKMRC consists of an FEI Quanta 600 SEM (scanning electron microscope) equipped with an energy dispersive X-ray analysis (EDAX) detector (Figure C.3). MLA software uses BSE (backscattered electron) images to define the mineral boundaries, while X-ray signals are used for mineral identification. Using a combination of BSE and X-ray, eight different modes of analysis can be offered by MLA: standard BSE liberation analysis (BSE), extended BSE liberation analysis (XBSE), Ford analysis or grain based x-ray mapping (GXMAP), sparse phase liberation analysis (SPL), X-ray modal analysis (XMOD), rare phase search (RPS), Latti analysis (SXBSE) and Schouwstra analysis (SPL-Dual Zoom) (Fandrich *et al.*, 2007). Each of these modes may measure more than 10,000 particles in a sample.

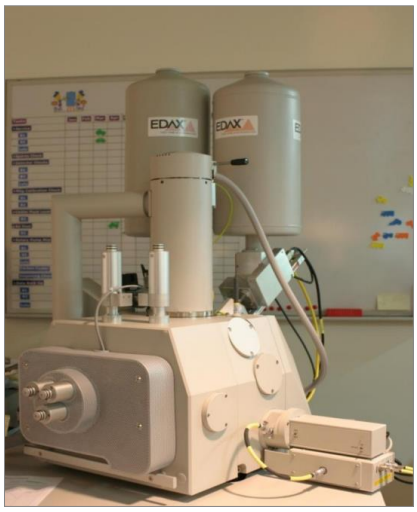

Figure C.3: MLA at JKMRC (from MLA, 2009)

The detection limits of the MLA depend on the mode of occurrence of the minerals but in general the MLA is capable of accurately quantifying mineral content down to approximately 0.01% with a minimum pixel resolution of 0.2 µm.

f) Laser ablation inductively coupled plasma mass spectroscopy (LA-ICP-MS)

Laser ablation inductively coupled plasma mass spectroscopy (LA-ICP-MS) was used to complement the MLA measurement for silver deportment, aiming to specifically analyse mineral grains which may have contained silver in solid solution.

The selected size fraction for this analysis was -212/+106 microns for Tesorera (sulphide ore) and Jayula (supergene oxide ore) ores; both blocks were submitted to MODA (McArthur Ore Deposit Assessments Pty Ltd, located in Burnie, Tasmania) Figure C.4 shows the equipment. The specific mineral grains analysed for Tesorera ore (sulphide ore) were pyrite with a spot size measurement of 35 µm. In the case of the Jayula ore (supergene oxide ore), three specific minerals were analysed to find silver as solid solution; these were jarosite, Pb-phosphates and Pb-arsenates. The spot size of the measurement was also 35 µm.

Figure C.4: LA-ICP-MS at MODA (from UTAS, 2014).

g) Electron microprobe analysis (EMPA) map

EMPA mapping was used to identify which elements were associated with silver. It was performed by J. Quinteros and D. Steel using CAMECA SX 50 equipment housed at the JKMRC (Figure C.5), and the sample analysed was -425/+300 µm. To obtain a map for key elements, the experiment was carried out at 10 kV, with the following elements measured by EMPA: aluminium (Al), arsenic (As), calcium (Ca), iron (Fe), potassium (K), lead (Pb), phosphorus (P), silicon (Si), silver (Ag) and

sulphur (S). These data were combined through a ternary diagram to determine elemental associations as described in *Appendix E*.

Figure C.5: Cameca SX 50 at JKMRC (from JKTech, 2014)

h) Manual SEM-EDS

Manual SEM-EDS was performed on Jayula's sample prepared in different sample blocks of 25 mm diameter. The preparation of these samples took into consideration the high proportion of clay in the sample (~25% kaolinite). The samples were prepared as follows: 1 kg of ore was separated in a rotary splitter to create a sample of 125 g. One aliquot was further split to create a sample for assay (60 g). The remaining splits were combined in three sets A, B and C.

Set A, B and C were wet sieved at 38 microns. The +38 microns was washed with ethanol and then was allowed to dry for 156 hrs. The remaining fine fraction (-38microns) was filtered in a filter press and then washed with ethanol and allowed to dry in an oven for 156 hrs at 40 degrees Celsius.

These block of -1.18 mm/+850 μm and -425/+300 μm size fractions, was measured using a SEM – EDS microscope, Philips XL-30 equipped with EDS (Figure C.6), held at the Centre for Microscopy & Microanalysis (CMM) at the University of Queensland (UQ) and operated by J. Quinteros. The SEM-EDS was operated at 20 kV. Table C.2 shows the sample blocks that were measured and the energy used to perform the analyses.

Table C.2: Conditions used for the manual SEM-EDS on samples of Jayula ore (supergene oxide ore).

Sample block	Size analysed	Energy used, kV
Sample 2	-425/+300 μm	20
Sample 3	-1.18mm/+850 μm	20

Figure C.6: Philips XL-30 equipped with EDS at CMM (from CMM, 2014)

i) AutoSEM

The auto SEM used was a Jeol 7001F equipped with EDS and Inca software (Figure C.7), located at Queensland University of Technology (QUT) and operated by J.Quinteros. Inca software helped to set the microscope to be an automated SEM-EDS working under fixed conditions.

Figure C.7: Jeol 7001F equipped with EDS at QUT (from NMMU, 2014).

Two samples blocks of 25 mm (-1.18mm/+850 µm and 425/+300 µm) were remeasured twice by auto SEM-EDS at 15 kV, with the objective of confirming statistically the unique spectra of barite_Ag.

j) Synchrotron Methods

Synchrotron XRF (SXRF) and synchrotron XRD (SXRD) analyses were performed by Minerals and Materials Science & Technology (MMaST) at the University of South Australia. *Appendix F* shows details of the results from for synchrotron analysis.

1. SXRF were performed in a section of a substrate of a polished section of 1 cm thick at +850 μm. The substrate has a thickness of 500 μm to map the elements at mapping size (6,100 μm horizontal × 5,400 μm vertical), mapping performed for Ag, K, S, Fe, Cu, Zn, As, Pb, Sr.
2. SXRD measured the grains that contained Ag to then identify possible Ag minerals.
3. The XANES (X-ray absorption near edge spectroscopy) is used to complement the SXRF and SXRD analysis to verify the Ag minerals present in the ore. The XANES used a bulk analysis of different silver minerals (acanthite, proustite, freibergite and pearcite) as mineral references to check the minerals found through the SXRD and SXRF.

C.2 Metallurgical and flotation product characterisation

All of the equipment and apparatuses used at some stage in the metallurgical and flotation characterisation are presented in the following paragraphs.

The main equipment used in the laboratory were:

a) Sample preparation benches

Work areas for sample preparation, which included dust extraction.

b) Analytical balances (210g x 0.01 g; 510 g x 0.1 mg & 64 kg x 0.1 g):

Used to weigh the ore sub-samples, water bottles, filter papers, concentrates, tailings, etc.

c) Bench-top sample riffler

Used to subdivide samples from ore head, Mill product, concentrate and tailings.

d) Retsch PT100 rotary sample splitter

Used to subdivide samples from feed, concentrate and tailings obtained from a flotation test.

e) Quantachrome rotary micro-splitter

Used to prepare representative sub-samples for chemical assay (unsized and size-by-size) and MLA analysis.

f) Sieve sets

Used to obtain the particle size distribution (PSD) of + 38 μm material. The common screen apertures used were 212 μm, 150 μm, 106 μm, 75 μm, 53 μm and 38 μm, sieve and bottom pan.

g) Ro-Tap sieve shaker

Used to shake the sieve screens containing the ore in order to classify the particles according to their size for a duration of 10 min.

h) Wet sieving bench

The wet sieving bench contained the following equipment used for sample preparation:

❖ **Vibratory wet screens**

Used to separate -38 µm material from a sample prior to dry screening.

❖ **Ultrasonic probe (Hielscher UP100H)**

Used to disperse slurry samples prior to wet sieving at 38 µm, and prior to classification in the Warman Cyclosizer.

i) Laboratory rod mill

The mill used to perform the grinding of the ore was the laboratory rod mill at the JKMRC. It was used to perform the grind calibration curves to achieve the required eighty percent passing size for each ore. The mill's barrel is mounted in a rotating yoke assembly which is driven through a gearbox from a three phase electric motor. The set of operational conditions was as follows: 42 rpm, 13.7 kg of stainless steel rods, pulp at 50% solids.

j) Flotation cell

The 5-litre bottom-driven JKMRC batch flotation cell (Figure C.8) was used to perform the flotation experiments for the three case studies. This cell uses a stator and impeller in the bottom of the cell to distribute the injected air through it. In this cell, the air flow and the impeller speed can be adjusted for specific conditions in the experiments or before starting any experiments. Table C.3 shows the conditions of the 5-L cell as set for the three case studies.

Figure C.8: 5-L Flotation cell used for the experiments A: Toldos ore (oxide ore); B: Tesorera ore (sulphide ore) and C: Jayula ore (supergene ore) (Photos taken by J. Quinteros, 2013)

Table C.3: Conditions for 5-L cell used for the three case studies

Parameter	Unit	Value
Cell volume	L	5
Air flow-rate	L/min	10
Impeller speed	rpm	1000
Percent of solid	wt%	20
Water used in flotation exp.		Brisbane tap water

k) Pressure filters & vacuum filters

Used to filter tailing and concentrate samples from the flotation test-work.

l) Cyclosizer

The cyclosizer is the most commonly used instrument to prepare "size fractions" of particles with diameters smaller than 38 microns. It is made up of five hydrocyclones in series. In its design, by varying the diameters of the hydrocyclone inlets and outlets, it is possible to increase the fluid velocity and the centrifugal force to separate particles of successively smaller and smaller diameters. These diameters are specified by the manufacturer (Warman Int., 1981) for each hydrocyclone with relation to the density of solids. Consequently, the separation of particles is carried out based on two compounded attributes: the diameter and density of particles. The particle shape may also contribute. Figure C.9 illustrates the cyclosizer used at JKMRC. The set of operational conditions, such as temperature, vary depending on the weather conditions prevailing when the experiment is run. As the temperature goes up, it is possible to alter the pressure to hold the cyclosizer in a "fixed condition". The elutriation time used in this study was 10 minutes and the flow meter was fixed at 165 (mm) in the rotameter.

The procedure for using the Warman Cyclosizer is set out below:

i. Ore samples were first wet screened at 38 μm to remove oversize material. Once the samples were dried, the minus 38 μm material was kept for work in the Cyclosizer (the plus 38 μm material was sized in a set of screening sieves).
ii. Once dried, the minus 38 μm material was split to obtain a representative sample with an approximate weight of 40 g. The dry sample was then mixed with water to obtain 200 mL of slurry, which was then placed in an ultrasonic bath for 10 min to aid in the dispersal of aggregates.
iii. Samples were then transferred to the feed cylinder. The water flow rate was turned to maximum and the valve on the feed cylinder was slowly opened to introduce the sample to the cyclosizer.

iv. Once the entire sample had left the feed cylinder, the valve was closed and the flow rate adjusted to 165 (mm). Elutriation then continued for 10 min, following the manufacturer's instructions (Warman Int., 1981). Pressure and water temperature values were taken at the end of the process to allow calibration factors to be calculated to determine the cut size to be established.

v. Once elutriation was complete, the water flow rate was again turned up to the maximum value and the sample was removed from each of the cyclone collection chambers. The samples were then dried in the oven at 40°C or 70°C and weighed.

m) Malvern Master Sizer

The Malvern master sizer was used to measure the particle size distributions from some ores**.** The protocol established was to measure samples in triplicate.

n) Buckets

Used to collect –C5 fraction from cyclosizer and the undersized particles from wet sieving at 38 µm.

o) Oven

Used to dry samples at 70 °C for Toldos ore (oxide ore) and Tesorera (sulphide ore) ores; for Jayula ore (supergene oxide ore), 40 °C was used due to the amount of clay present in the ore.

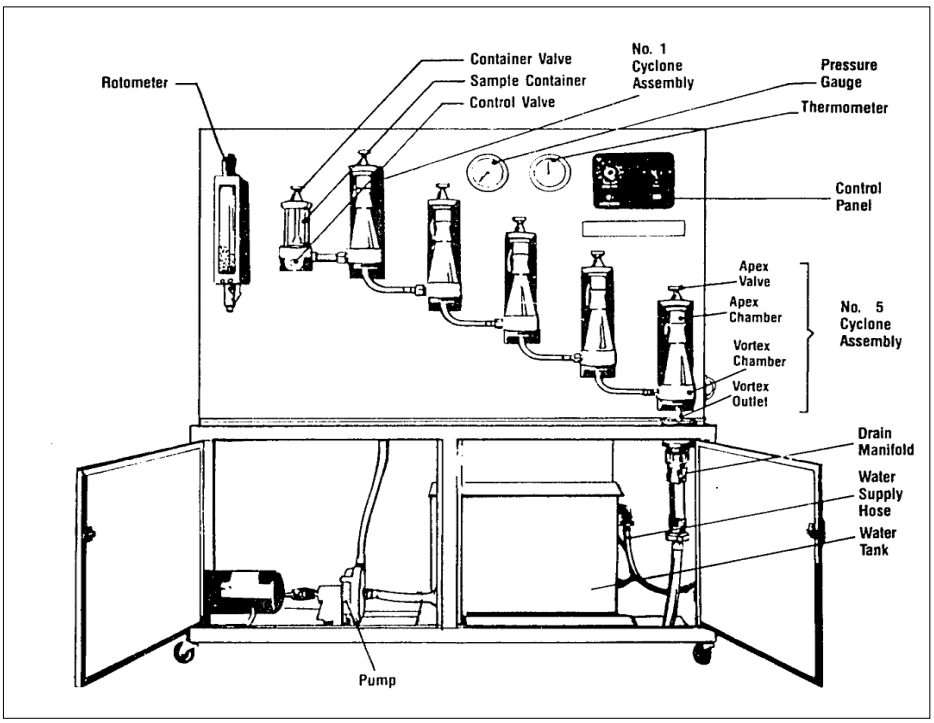

Figure C.9: Cyclosizer used for particles under 38 microns (from Warman Int., 1981).

Appendix D - Mineral grouping for each ore in MLA

Table D.1: Mineral group for Ore Characterisation and mill product Toldos Ore

Mineral Group	Mineral	Formula
Ag_minerals	Native_Silver	Ag
	Acanthite	Ag_2S
	Arsenopolybasite	$(Ag,Cu)_{16}(As,Sb)_2S_{11}$
	Polybasite	$(Ag,Cu)_{16}Sb_2S_{11}$
	Pyrargyrite	Ag_3SbS_3
	Tetrahedrite	$(Cu+,Ag)_6[Cu_4^+,(Fe,Zn,Hg)_2](Sb,As)_4S_{13}$
	Freibergite	$(Ag,Cu,Fe)_{12}(Sb,As)_4S_{13}$
	Hessite	Ag_2Te
	Chlorargyrite	AgCl
Pyrite	Pyrite	FeS_2
	Pyrrhotite	FeS
	Arsenopyrite	Fe_3^+AsS
Sphalerite	Sphalerite_Fe	(Zn,Fe)S
	Sphalerite	ZnS
Galena	Galena	PbS
Mn (Pb) Oxide	Coronadite(?)	$Pb(Mn^{++++},Mn^{++})_8O_{16}$
	Cesarolite(?)	$PbH_2Mn_4^+{}_3O_8$
Pb Arsenate	Beudantite	$PbFe^{+++}{}_3(AsO_4)(SO_4)(OH)_6$
	Gabrielsonite	$PbFe_2^+(AsO_4)(OH)$
Pb Phosphate	Hinsdalite	$(Pb,Sr)Al_3(PO_4)(SO_4)(OH)_6$
	Pyromorphite	$Pb_{10}(PO_4)_6O$
Quartz	Quartz	(SiO_2)
Feldspar	Orthoclase	$KAlSi_3O_8$
	Plagioclase	$Na_{0.5}Ca_{0.5}Si_3AlO_8$
Clays_micas	Muscovite	$KAl_3Si_3O_{10}(OH)_{1.9}F_{0.1}$
	Illite	$(K,H_3O)_{0.65}(Al,Mg,Fe)_2(Si,Al)_4O_{10}([OH]_2,H_2)$
	Chlorite	$(Mg_3,Fe_2)Al(AlSi_3)O_{10}(OH)_8$
	Biotite	$KMg_{2.5}Fe_2^+0.5AlSi_3O_{10}(OH)_{1.75}F_{0.25}$
	Kaolinite	$Al_2Si_2O_5(OH)_4$
Other Silicates	Pyroxene	$CaMg(Si_2O_6)$
	Enstatite	$(Mg,Fe)SiO_3$
	Amphibole	$(Na,K)(Ca,Na)_2[(Fe_2^+,Mg)_{1.5}(Fe_3^+,Al)_{1.5}(Fe_2^+,Fe_3^+,Al,Mg)_2][Si_{5.5}(Al)_{0.5}(Si,Al)_2]O_{22}(OH,F)_2$
	Garnet	$Fe_2^+3Al_2(SiO_4)_3$
Fe Oxide	Haematite	$Fe_3^{++}2O_3$
Carbonates	Smithsonite	$ZnCO_3$
	Siderite	$Fe_2^+(CO_3)$
	Rhodochrosite_Siderite	$(Mn,Fe_2^+)CO_3$
	Calcite	$(Ca,Mn)CO_3$
Sulphates	Barite	$Ba(SO_4)$
	Jarosite	$KFe_3^+3(SO_4)2(OH)_6$
	Alunite	$KAl_3(SO_4)_2(OH)_6$
Other	Chalcopyrite	$CuFe_2^+S_2$
	Covellite	CuS
	Enargite	Cu_3AsS_4
	Greenockite	CdS
	Rutile	TiO_2
	Apatite	$Ca_5(PO_4)(F,Cl,OH)$
	Florencite	$CeAl_3(PO_4)_2(OH)_6$
	Xenotime	YPO_4
	Goyazite	$SrAl_3[PO_4]_2[OH]_5.H_2O$
	Nolanite	$V_3^+6.9Fe_3^+1.6Fe_2^+0.5Ti_{0.6}Al_{0.3}O_{14}(OH)_2$
	Unknown	
	Low_Counts	
	No_XRay	

Table D.2: Ag Mineral group for flotation product of Toldos ore and Ag content in each mineral

Mineral	Formula	Ag (%)
Native_Silver	Ag	100.00
Acanthite	Ag_2S	87.06
Arsenopolybasite	$(Ag,Cu)_{16}(As,Sb)_2S_{11}$	70.70
Polybasite	$(Ag,Cu)_{16}Sb_2S_{11}$	66.96
Pyrargyrite	Ag_3SbS_3	59.76
Tetrahedrite	$(Cu^+,Ag)_6[Cu_4^+,(Fe,Zn,Hg)_2](Sb,As)_4S_{13}$	9.12
Freibergite	$(Ag,Cu,Fe)_{12}(Sb,As)_4S_{13}$	40.25
Hessite	Ag_2Te	59.25
Chlorargyrite	AgCl	75.26
Coronadite(?)	$Pb(Mn^{++++},Mn^{++})_8O_{16}$	4.30
Gabrielsonite	$PbFe_2^+(AsO_4)(OH)$	1.36

Table D.3: Mineral group for Flotation Product of Toldos Ore

Mineral Group	Mineral	Formula
Ag_Minerals	Native_Silver	Ag
	Acanthite	Ag_2S
	Arsenopolybasite	$(Ag,Cu)_{16}(As,Sb)_2S_{11}$
	Polybasite	$(Ag,Cu)_{16}Sb_2S_{11}$
	Pyrargyrite	Ag_3SbS_3
	Tetrahedrite	$(Cu^+,Ag)_6[Cu_4^+,(Fe,Zn,Hg)_2](Sb,As)_4S_{13}$
	Freibergite	$(Ag,Cu,Fe)_{12}(Sb,As)_4S_{13}$
	Hessite	Ag_2Te
	Chlorargyrite	AgCl
	Coronadite(?)	$Pb(Mn^{++++},Mn^{++})_8O_{16}$
	Gabrielsonite	$PbFe_2^+(AsO_4)(OH)$
Pyrite	Pyrite	FeS_2
Sphalerite	Sphalerite_Fe	(Zn,Fe)S
	Sphalerite	ZnS
Galena	Galena	PbS
	Galena_As	PbS
Quartz	Quartz	(SiO_2)
Feldspar	Orthoclase	$KAlSi_3O_8$
	Plagioclase	$Na_{0.5}Ca_{0.5}Si_3AlO_8$
Clays_micas	Muscovite	$KAl_3Si_3O_{10}(OH)_{1.9}F_{0.1}$
	Illite	$(K,H_3O)_{0.65}(Al,Mg,Fe)_2(Si,Al)_4O_{10}([OH]_2,H_2)$
	Chlorite	$(Mg_3,Fe_2)Al(AlSi_3)O_{10}(OH)_8$
	Biotite	$KMg_2Fe_2^+0.5AlSi_3O_{10}(OH)_{1.75}F_{0.25}$
	Kaolinite	$Al_2Si_2O_5(OH)_4$
Fe Oxides	Haematite	$Fe_3^+2O_3$
Carbonates	Smithsonite	$ZnCO_3$
	Siderite	$Fe_2^+(CO_3)$
	Rhodochrosite_Siderite	$(Mn,Fe_2^+)CO_3$
	Calcite	$(Ca,Mn)CO_3$
Other Silicates	Pyroxene	$CaMg(Si_2O_6)$
	Enstatite	$(Mg,Fe)SiO_3$
	Amphibole	$(Na,K)(Ca,Na)_2[(Fe_2^+,Mg)_{1.5}(Fe_3^+,Al)_{1.5}(Fe_2^+,Fe_3^+,Al,Mg)_2][Si_{5.5}(Al)_{0.5}(Si,Al)_2]O_{22}(OH,F)_2$
	Garnet	$Fe_2^+3Al_2(SiO_4)_3$
Sulphates	Barite	$Ba(SO_4)$
	Jarosite	$KFe_3^+3(SO_4)_2(OH)_6$
	Alunite	$KAl_3(SO_4)_2(OH)_6$
Other	Pyrrhotite	FeS
	Arsenopyrite	Fe_3^+AsS
	Chalcopyrite	$CuFe_2^+S_2$
	Covellite	CuS
	Enargite	Cu_3AsS_4
	Arsenic	As
	Realgar	AsS
	Greenockite	CdS
	Tenorite_Cuprite	CuO
	Rutile	TiO_2
	Ankerite	$Ca(Fe,Mg,Mn)(CO_3)_2$
	Apatite	$Ca_5(PO_4)(F,Cl,OH)$
	Florencite	$CeAl_3(PO_4)_2(OH)_6$
	Xenotime	YPO_4
	Goyazite	$SrAl_3[PO_4]_2[OH]_5.H_2O$
	Nolanite	$V_3^+6.9Fe_3^+1.6Fe_2^+0.5Ti_{0.6}Al_{0.3}O_{14}(OH)_2$
	Cesarolite(?)	$PbH_2Mn_4^+3O_8$
	Beudantite	$PbFe^{+++}3(AsO_4)(SO_4)(OH)_6$
	Hinsdalite	$(Pb,Sr)Al_3(PO_4)(SO_4)(OH)_6$
	Pyromorphite	$Pb_{10}(PO_4)_6O$
	Anglesite	$Pb(SO_4)$
	Carbon	
	Unknown	
	Low_Counts	
	No_XRay	

Table D.4: Mineral group for Ore Characterisation and mill product Tesorera Ore

Mineral Group	Mineral	Formula
Ag_minerals	Native_Silver	Ag
	Acanthite	Ag_2S
	Arsenopolybasite	$(Ag,Cu)_{16}(As,Sb)_2S_{11}$
	Polybasite	$(Ag,Cu)_{16}Sb_2S_{11}$
	Pyrargyrite	Ag_3SbS_3
	Tetrahedrite	$(Cu+,Ag)_6[Cu_4^+,(Fe,Zn,Hg)_2](Sb,As)_4S_{13}$
	Freibergite	$(Ag,Cu,Fe)_{12}(Sb,As)_4S_{13}$
	Hessite	Ag_2Te
	Chlorargyrite	AgCl
Pyrite	Pyrite	FeS_2
	Pyrrhotite	FeS
	Arsenopyrite	Fe_3^+AsS
Sphalerite	Sphalerite_Fe	(Zn,Fe)S
	Sphalerite	ZnS
Galena	Galena	PbS
Mn (Pb) Oxide	Coronadite(?)	$Pb(Mn^{++++},Mn^{++})_8O_{16}$
	Cesarolite(?)	$PbH_2Mn_4^+{}_3O_8$
Pb Arsenate	Beudantite	$PbFe^{+++}{}_3(AsO_4)(SO_4)(OH)_6$
	Gabrielsonite	$PbFe_2^+(AsO_4)(OH)$
Pb Phosphate	Hinsdalite	$(Pb,Sr)Al_3(PO_4)(SO_4)(OH)_6$
	Pyromorphite	$Pb_{10}(PO_4)_6O$
Quartz	Quartz	(SiO_2)
Feldspar	Orthoclase	$KAlSi_3O_8$
	Plagioclase	$Na_{0.5}Ca_{0.5}Si_3AlO_8$
Clays_micas	Muscovite	$KAl_3Si_3O_{10}(OH)_{1.9}F_{0.1}$
	Illite	$(K,H_3O)_{0.65}(Al,Mg,Fe)_2(Si,Al)_4O_{10}([OH]_2,H_2)$
	Chlorite	$(Mg_3,Fe_2)Al(AlSi_3)O_{10}(OH)_8$
	Biotite	$KMg_{2.5}Fe_2^+0.5AlSi_3O_{10}(OH)_{1.75}F_{0.25}$
	Kaolinite	$Al_2Si_2O_5(OH)_4$
Other Silicates	Pyroxene	$CaMg(Si_2O_6)$
	Enstatite	$(Mg,Fe)SiO_3$
	Amphibole	$(Na,K)(Ca,Na)_2[(Fe_2^+,Mg)_{1.5}(Fe_3^+,Al)_{1.5}(Fe_2^+,Fe_3^+,Al,Mg)_2][Si_{5.5}(Al)_{0.5}(Si,Al)_2]O_{22}(OH,F)_2$
	Garnet	$Fe_2^+3Al_2(SiO_4)_3$
Fe Oxide	Haematite	$Fe_3^+2O_3$
Carbonates	Smithsonite	$ZnCO_3$
	Siderite	$Fe_2^+(CO_3)$
	Rhodochrosite_Siderite	$(Mn,Fe_2^+)CO_3$
	Calcite	$(Ca,Mn)CO_3$
Sulphates	Barite	$Ba(SO_4)$
	Jarosite	$KFe_3^+3(SO_4)2(OH)_6$
	Alunite	$KAl_3(SO_4)_2(OH)_6$
Other	Chalcopyrite	$CuFe_2^+S_2$
	Covellite	CuS
	Enargite	Cu_3AsS_4
	Greenockite	CdS
	Rutile	TiO_2
	Apatite	$Ca_5(PO_4)(F,Cl,OH)$
	Florencite	$CeAl_3(PO_4)_2(OH)_6$
	Xenotime	YPO_4
	Goyazite	$SrAl_3[PO_4]_2[OH]_5.H_2O$
	Nolanite	$V_3^+6.9Fe_3^+1.6Fe_2^+0.5Ti_{0.6}Al_{0.3}O_{14}(OH)_2$
	Unknown	
	Low_Counts	
	No_XRay	

Table D.5: Ag Mineral group for flotation product of Tesorera Ore and Ag content in each mineral

Mineral	Formula	Ag %
Native_Silver	Ag	100.00
Acanthite	Ag_2S	87.06
Arsenopolybasite	$(Ag,Cu)_{16}(As,Sb)_2S_{11}$	70.70
Polybasite	$(Ag,Cu)_{16}Sb_2S_{11}$	66.96
Pyrargyrite	Ag_3SbS_3	59.76
Tetrahedrite	$(Cu^+,Ag)_6[Cu_4^+,(Fe,Zn,Hg)_2](Sb,As)_4S_{13}$	9.12
Freibergite	$(Ag,Cu,Fe)_{12}(Sb,As)_4S_{13}$	40.25
Hessite	Ag_2Te	59.25
Chlorargyrite	AgCl	75.26
Coronadite(?)	$Pb(Mn^{++++},Mn^{++})_8O_{16}$	4.30
Gabrielsonite	$PbFe_2^+(AsO_4)(OH)$	1.36
Pyrite	FeS_2	xxx

Table D.6: Mineral group for Flotation Product of Tesorera Ore

Mineral Group	Mineral	Formula
Ag_Minerals	Native_Silver	Ag
	Acanthite	Ag_2S
	Arsenopolybasite	$(Ag,Cu)_{16}(As,Sb)_2S_{11}$
	Polybasite	$(Ag,Cu)_{16}Sb_2S_{11}$
	Pyrargyrite	Ag_3SbS_3
	Tetrahedrite	$(Cu^+,Ag)_6[Cu_4^+,(Fe,Zn,Hg)_2](Sb,As)_4S_{13}$
	Freibergite	$(Ag,Cu,Fe)_{12}(Sb,As)_4S_{13}$
	Hessite	Ag_2Te
	Chlorargyrite	AgCl
	Coronadite(?)	$Pb(Mn^{++++},Mn^{++})_8O_{16}$
	Gabrielsonite	$PbFe_2^+(AsO_4)(OH)$
Pyrite	Pyrite	FeS_2
Sphalerite	Sphalerite_Fe	(Zn,Fe)S
	Sphalerite	ZnS
Galena	Galena	PbS
	Galena_As	PbS
Quartz	Quartz	(SiO_2)
Feldspar	Orthoclase	$KAlSi_3O_8$
	Plagioclase	$Na_{0.5}Ca_{0.5}Si_3AlO_8$
Clays_micas	Muscovite	$KAl_3Si_3O_{10}(OH)_{1.9}F_{0.1}$
	Illite	$(K,H_3O)_{0.65}(Al,Mg,Fe)_2(Si,Al)_4O_{10}([OH]_2,H_2)$
	Chlorite	$(Mg_3,Fe_2)Al(AlSi_3)O_{10}(OH)_8$
	Biotite	$KMg_2\ Fe_2^+0.5AlSi_3O_{10}(OH)_{1.75}F_{0.25}$
	Kaolinite	$Al_2Si_2O_5(OH)_4$
Fe Oxides	Haematite	$Fe_3^+2O_3$
Carbonates	Smithsonite	$ZnCO_3$
	Siderite	$Fe_2^+(CO_3)$
	Rhodochrosite_Siderite	$(Mn,Fe_2^+)CO_3$
	Calcite	$(Ca,Mn)CO_3$
Other Silicates	Pyroxene	$CaMg(Si_2O_6)$
	Enstatite	$(Mg,Fe)SiO_3$
	Amphibole	$(Na,K)(Ca,Na)_2[(Fe_2^+,Mg)_{1.5}(Fe_3^+,Al)_{1.5}(Fe_2^+,Fe_3^+,Al,Mg)_2][Si_{5.5}(Al)_{0.5}(Si,Al)_2]O_{22}(OH,F)_2$
	Garnet	$Fe_2^+3Al_2(SiO_4)_3$
Sulphates	Barite	$Ba(SO_4)$
	Jarosite	$KFe_3^+3(SO_4)_2(OH)_6$
	Alunite	$KAl_3(SO_4)_2(OH)_6$
Other	Pyrrhotite	FeS
	Arsenopyrite	Fe_3^+AsS
	Chalcopyrite	$CuFe_2^+S_2$
	Covellite	CuS
	Enargite	Cu_3AsS_4
	Arsenic	As
	Realgar	AsS
	Greenockite	CdS
	Tenorite_Cuprite	CuO
	Rutile	TiO_2
	Ankerite	$Ca(Fe,Mg,Mn)(CO_3)_2$
	Apatite	$Ca_5(PO_4)(F,Cl,OH)$
	Florencite	$CeAl_3(PO_4)_2(OH)_6$
	Xenotime	YPO_4
	Goyazite	$SrAl_3[PO_4]_2[OH]_5.H_2O$
	Nolanite	$V_3^+6.9Fe_3^+1.6Fe_2^+0.5Ti_{0.6}Al_{0.3}O_{14}(OH)_2$
	Cesarolite(?)	$PbH_2Mn_4^+3O_8$
	Beudantite	$PbFe^{+++}3(AsO_4)(SO_4)(OH)_6$
	Hinsdalite	$(Pb,Sr)Al_3(PO_4)(SO_4)(OH)_6$
	Pyromorphite	$Pb_{10}(PO_4)_6O$
	Anglesite	$Pb(SO_4)$
	Carbon	
	Unknown	
	Low_Counts	
	No_XRay	

Table D.7: Mineral group for Ore Characterisation and mill product Jayula Ore

Mineral Group	Mineral	Formula
Ag Minerals	Native_Silver	Ag
	Acanthite	Ag_2S
	Arsenopolybasite	$(Ag,Cu)_{16}(As,Sb)_2S_{11}$
	Polybasite	$(Ag,Cu)_{16}Sb_2S_{11}$
	Pyrargyrite	Ag_3SbS_3
	Tetrahedrite	$(Cu^{+},Ag)_6[Cu_4^{+},(Fe,Zn,Hg)_2](Sb,As)_4S_{13}$
	Freibergite	$(Ag,Cu,Fe)_{12}(Sb,As)_4S_{13}$
	Hessite	Ag_2Te
	Chlorargyrite	AgCl
Barite_Ag	Barite_Ag10	$Ba(SO_4)$
	Barite_Ag5_7	$Ba(SO_4)$
	Barite_Ag2	$Ba(SO_4)$
Pyrite	Pyrite	FeS_2
	Pyrite_Ag	$Fe_2^{+}S_2$
Galena	Galena	PbS
Sphalerite	Sphalerite_Fe	(Zn,Fe)S
	Sphalerite	ZnS
Quartz	Quartz	(SiO_2)
Feldspar	Orthoclase	$KAlSi_3O_8$
	Plagioclase	$Na_{0.5}Ca_{0.5}Si_3AlO_8$
Clays_micas	Muscovite	$KAl_3Si_3O_{10}(OH)_{1.9}F_{0.1}$
	Illite	$(K,H_3O)_{0.65}(Al,Mg,Fe)_2(Si,Al)_4O_{10}([OH]_2,H_2)$
	Chlorite	$(Mg_3,Fe_2)Al(AlSi_3)O_{10}(OH)_8$
	Biotite	$KMg_{2.5}Fe_2^{+}0.5AlSi_3O_{10}(OH)_{1.75}F_{0.25}$
Kaolinite	Kaolinite	$Al_2Si_2O_5(OH)_4$
Other Silicates	Pyroxene	$CaMg(Si_2O_6)$
	Enstatite	$(Mg,Fe)SiO_3$
	Amphibole	$(Na,K)(Ca,Na)_2[(Fe_2^{+},Mg)_{1.5}(Fe_3^{+},Al)_{1.5}(Fe_2^{+},Fe_3^{+},Al,Mg)_2][Si_{5.5}(Al)_{0.5}(Si,Al)_2]O_{22}(OH,F)_2$
	Garnet	$Fe_2^{+}3Al_2(SiO_4)_3$
Oxides	Haematite	$Fe_3^{+}2O_3$
	Rutile	TiO_2
Carbonates	Siderite	$Fe_2^{+}(CO_3)$
	Rhodochrosite_Siderite	$(Mn,Fe_2^{+})CO_3$
	Calcite	$(Ca,Mn)CO_3$
Barite	Barite	$Ba(SO_4)$
Sulphates	Alunite	$KAl_3(SO_4)_2(OH)_6$
	Jarosite	$KFe_3^{+}3(SO_4)_2(OH)_6$
Pyrrhotite	Pyrrhotite	FeS
Arsenopyrite	Arsenopyrite	$Fe3^{+}AsS$
Other Pb Minerals	Coronadite(?)	$Pb(Mn^{++++},Mn^{++})_8O_{16}$
	Cesarolite(?)	$PbH_2Mn_4^{+}3O_8$
	Hinsdalite	$(Pb,Sr)Al_3(PO_4)(SO_4)(OH)_6$
	Pyromorphite	$Pb_{10}(PO_4)_6O$
	Beudantite	$PbFe^{+++}3(AsO_4)(SO_4)(OH)_6$
	Gabrielsonite	$PbFe_2^{+}(AsO_4)(OH)$
Others	Chalcopyrite	$CuFe_2^{+}S_2$
	Covellite	CuS
	Enargite	Cu_3AsS_4
	Smithsonite	$ZnCO_3$
	Apatite	$Ca_5(PO_4)(F,Cl,OH)$
	Florencite	$CeAl_3(PO_4)2(OH)_6$
	Xenotime	YPO_4
	Goyazite	$SrAl_3[PO_4]_2[OH]_5.H_2O$
	Nolanite	$V_3^{+}6.9Fe_3^{+}1.6Fe_2^{+}0.5Ti_{0.6}Al_{0.3}O_{14}(OH)_2$
	Greenockite	CdS
	Zircon	$ZrSiO_4$
	Unknown	
	Low_Counts	
	No_XRay	

Table D.8: Ag Mineral group for flotation product for Jayula and Ag content in each mineral

Mineral	**Formula**	**Ag (%)**
Native_Silver	Ag	100.00
Acanthite	Ag_2S	87.06
Arsenopolybasite	$(Ag,Cu)_{16}(As,Sb)_2S_{11}$	70.70
Polybasite	$(Ag,Cu)_{16}Sb_2S_{11}$	66.96
Pyrargyrite	Ag_3SbS_3	59.76
Tetrahedrite	$(Cu^{+},Ag)_6[Cu_4^{+},(Fe,Zn,Hg)_2](Sb,As)_4S_{13}$	9.12
Freibergite	$(Ag,Cu,Fe)_{12}(Sb,As)_4S_{13}$	40.25
Hessite	Ag_2Te	59.25
Chlorargyrite	AgCl	75.26
Barite_Ag10	$Ba(SO_4)$	14.20
Barite_Ag5_7	$Ba(SO_4)$	5.90
Barite_Ag2	$Ba(SO_4)$	2.00
Coronadite(?)	$Pb(Mn^{++++},Mn^{++})_8O_{16}$	4.30
Gabrielsonite	$PbFe_2^{+}(AsO_4)(OH)$	1.36

Table D.9: Mineral group for Flotation Product of Jayula Ore

Mineral Group	Mineral	Formula
Ag Minerals	Native_Silver	Ag
	Acanthite	Ag_2S
	Arsenopolybasite	$(Ag,Cu)_{16}(As,Sb)_2S_{11}$
	Polybasite	$(Ag,Cu)_{16}Sb_2S_{11}$
	Pyrargyrite	Ag_3SbS_3
	Tetrahedrite	$(Cu^{+},Ag)_6[Cu_4^{+},(Fe,Zn,Hg)_2](Sb,As)_4S_{13}$
	Freibergite	$(Ag,Cu,Fe)_{12}(Sb,As)_4S_{13}$
	Hessite	Ag_2Te
	Chlorargyrite	AgCl
Barite_Ag	Barite_Ag10	$Ba(SO_4)$
	Barite_Ag5_7	$Ba(SO_4)$
	Barite_Ag2	$Ba(SO_4)$
Pyrite	Pyrite	FeS_2
	Pyrite_Ag	$Fe_2^{+}S_2$
Galena	Galena	PbS
Sphalerite	Sphalerite_Fe	(Zn,Fe)S
	Sphalerite	ZnS
Quartz	Quartz	(SiO_2)
Feldspar	Orthoclase	$KAlSi_3O_8$
	Plagioclase	$Na_{0.5}Ca_{0.5}Si_3AlO_8$
Clays_micas	Muscovite	$KAl_3Si_3O_{10}(OH)_{1.9}F_{0.1}$
	Illite	$(K,H_3O)_{0.65}(Al,Mg,Fe)_2(Si,Al)_4O_{10}([OH]_2,H_2)$
	Chlorite	$(Mg_3,Fe_2)Al(AlSi_3)O_{10}(OH)_8$
	Biotite	$KMg_{2.5}Fe_2^{+}0.5AlSi_3O_{10}(OH)_{1.75}F_{0.25}$
Kaolinite	Kaolinite	$Al_2Si_2O_5(OH)_4$
Other Silicates	Pyroxene	$CaMg(Si_2O_6)$
	Enstatite	$(Mg,Fe)SiO_3$
	Amphibole	$(Na,K)(Ca,Na)_2[(Fe_2^{+},Mg)_{1.5}(Fe_3^{+},Al)_{1.5}(Fe_2^{+},Fe_3^{+},Al,Mg)_2][Si_{5.5}(Al)_{0.5}(Si,Al)_2]O_{22}(OH,F)_2$
	Garnet	$Fe_2^{+}3Al_2(SiO_4)_3$
Oxides	Haematite	$Fe_3^{+}2O_3$
	Rutile	TiO_2
Carbonates	Siderite	$Fe_2^{+}(CO_3)$
	Rhodochrosite_Siderite	$(Mn,Fe_2^{+})CO_3$
	Calcite	$(Ca,Mn)CO_3$
Barite	Barite	$Ba(SO_4)$
Sulphates	Alunite	$KAl_3(SO_4)_2(OH)_6$
	Jarosite	$KFe_3^{+}3(SO_4)_2(OH)_6$
Pyrrhotite	Pyrrhotite	FeS
Arsenopyrite	Arsenopyrite	$Fe3^{+}AsS$
Other Pb Minerals	Coronadite(?)	$Pb(Mn^{++++},Mn^{++})_8O_{16}$
	Cesarolite(?)	$PbH_2Mn_4^{+}3O_8$
	Hinsdalite	$(Pb,Sr)Al_3(PO_4)(SO_4)(OH)_6$
	Pyromorphite	$Pb_{10}(PO_4)_6O$
	Beudantite	$PbFe^{+++}3(AsO_4)(SO_4)(OH)_6$
	Gabrielsonite	$PbFe_2^{+}(AsO_4)(OH)$
Others	Chalcopyrite	$CuFe_2^{+}S_2$
	Covellite	CuS
	Enargite	Cu_3AsS_4
	Smithsonite	$ZnCO_3$
	Apatite	$Ca_5(PO_4)(F,Cl,OH)$
	Florencite	$CeAl_3(PO_4)2(OH)_6$
	Xenotime	YPO_4
	Goyazite	$SrAl_3[PO_4]_2[OH]_5.H_2O$
	Nolanite	$V_3^{+}6.9Fe_3^{+}1.6Fe_2^{+}0.5Ti_{0.6}Al_{0.3}O_{14}(OH)_2$
	Greenockite	CdS
	Zircon	$ZrSiO_4$
	Unknown	
	Low_Counts	
	No_XRay	
	Unknown	
	Low_Counts	
	No_XRay	

Appendix E – Finding Elemental associations

E.1 Finding elemental associations

The objective for this analysis was to find any relationship between silver and other elements to assist in the identification of potential mineral hosts for unaccounted silver using ternary diagrams. Figure E.1, shows the legend used in the ternary. The idea was to obtain any silver association that can potentially give a clue about where was the silver associated with others elements from the periodic table. At the time of this analysis Barite (Ba) was not analysed as not clue was related from the new unique chemical association discovered in this thesis. However, an important relationship was found between Ag and Si that is shown in Figure E.2, this result is confirmed by the synchrotron analysis lately.

In order to perform these analyses the following steps were used:

1. From EMPA Mapping, the data were obtained through .asci, which was introduced into a small program made in MATLAB program.
2. The small program in MATLAB was created by Quinteros and Whiten to extract the data from .acsi files and correlated Ag with other elements analysed with EMPA mapping. The output of this program was obtained through excel files.
3. IoGAS program was used to perform the relationship between silver and other two elements using a ternary diagrams. This allows to identify possible correlations between Ag and other elements, and in that way it can be possible to identify some minerals that would contain Ag and focus the work under certain minerals.

E.2 Matlab Program

As is described in step 2 a small program using MATLAB was created by Jocelyn Quinteros and Bill Whiten. The objective of this program was to obtain the data from the asci file to select certain range of values of Ag to correlated with to other elements to find any association.

_____MATLAB PROGRAM_____

Loading the data %% First the data is loaded from the asci file

```
d=load('countsall.mat');
```

Matrix without final particles %% Different Matrixes were named in order to charge the data into the program and start to analysed it.

```
names={'ag','al','as','ca','fe','k','pb','p','s','si'};
%background=[20,20,20,20,20,20,10,12,30,20];
background=[30,20,20,20,20,20,10,12,30,20];

for i=1:length(names)
   dx.(names{i})=d.(names{i})(:,1:970);
end
```

Sum of counts %%Sum of all counts peak of number to then normalize the data

```
tot=zeros(size(dx.ag));

for i=1:length(names)

   tot=tot+dx.(names{i});
end
```

Distribution of the totals %% graph the normalized data into histograms

```
 figure
   hist(tot(:),1000)
```

select particles %% Select the particles that has a threshold bigger than 250

```
figure
spy(tot>250)

%%Remove background
for i=1:length(names)

   dx.(names{i})=dx.(names{i})-background(i);
    dx.(names{i})(dx.(names{i})<0)=0;
end
```

mask for separating the particles %% make mask to reselect the data bigger than 250

```
mask=tot>250;

for i=1:length(names)
   dm.(names{i})=dx.(names{i})(mask);
end
```

Ternary plot %% Graph the ternary diagrams with MATLAB program

```
figure
name3={'ag','al','s'};
sum1=sum([dm.(name3{1}), dm.(name3{2}), dm.(name3{3})], 2);
```

```
ternplot(dm.(name3{1})./sum1, dm.(name3{2})./sum1, dm.(name3{3})./sum1,'r.')
ternlabel(name3{1},(name3{2}),(name3{3}))
```

high Ag points %% Select only the highest Ag points related with other elements

```
ag=dm.ag./sum1;
al=dm.al./sum1;
s=dm.s./sum1;
mask2=ag>0.9;
agm=ag(mask2);
alm=al(mask2);
sm=s(mask2);
disp('ag  al  s')

% [agm,alm,sm]

[dm.ag(mask2), dm.al(mask2), dm.s(mask2),]
```

F.3 Data analysis by IoGas to Ag>250 pixels

Using the data obtained with MATLAB for the pixels highest than 250. These data was introduced into the IoGas software that help to graphically discriminate the relationship (associations) between Ag and other elements.

The legend indicated the range by colours in 10 by 10 the amount of silver present in the relationship between elements. The fuchsia indicated the highest amount of silver present in that pixel, and clearly it can be associated with other minerals.

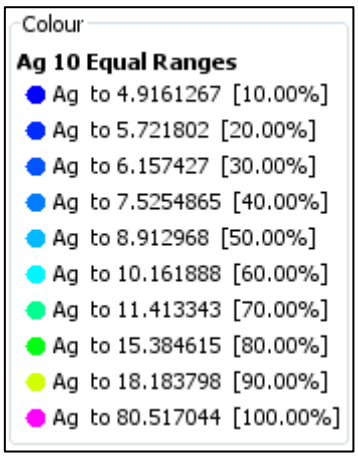

Figure E.1: Legend for the ternary diagram.

The example of the interpretation of these diagrams is presented in Chapter 6, page 125.

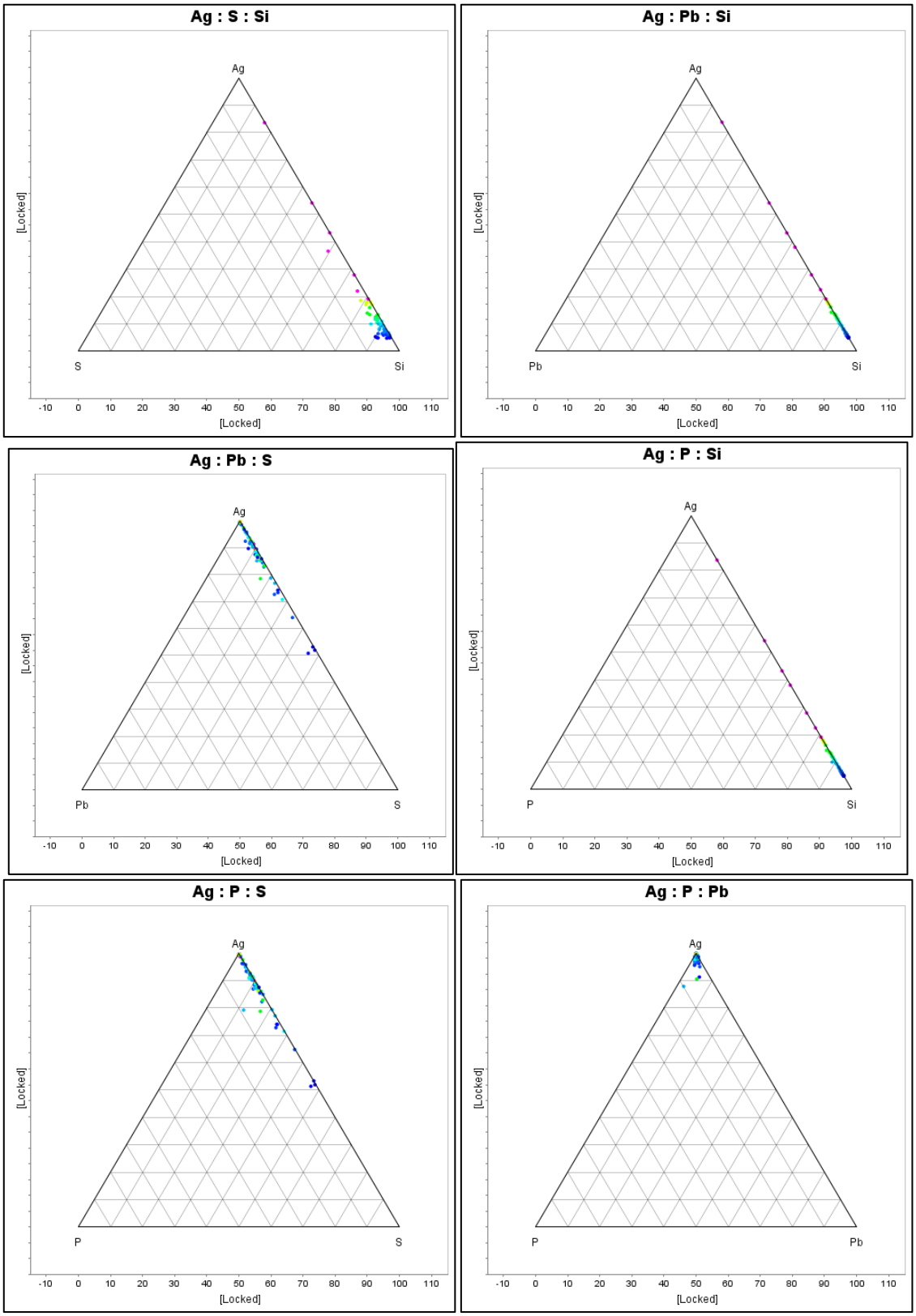

Figure E.2: Different ternary diagrams with association between Ag and other elements (Pb, P, S and Si)

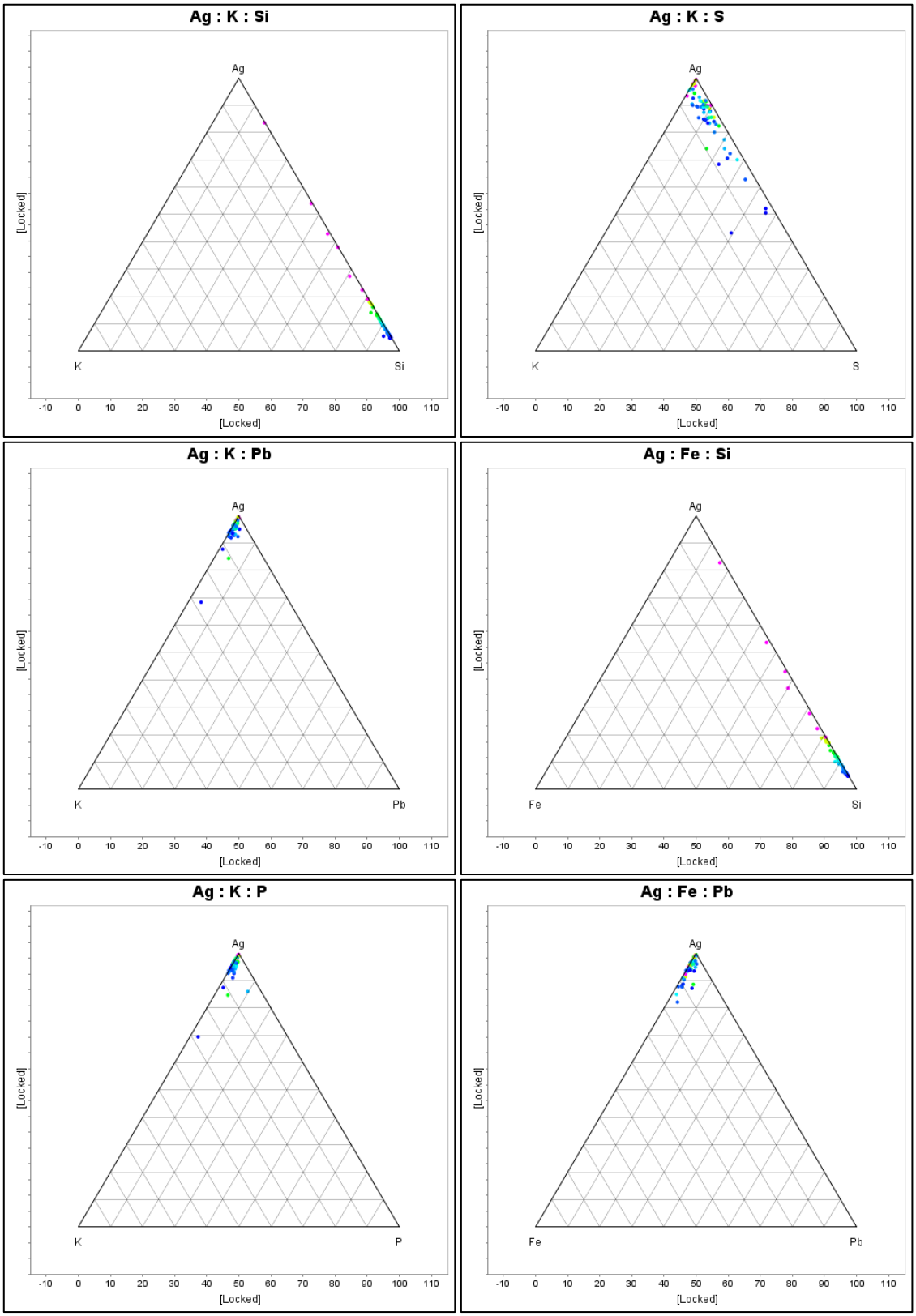

Figure E.3: Different ternary diagrams with association between Ag and other elements (Fe, K, Pb, P, S and Si)

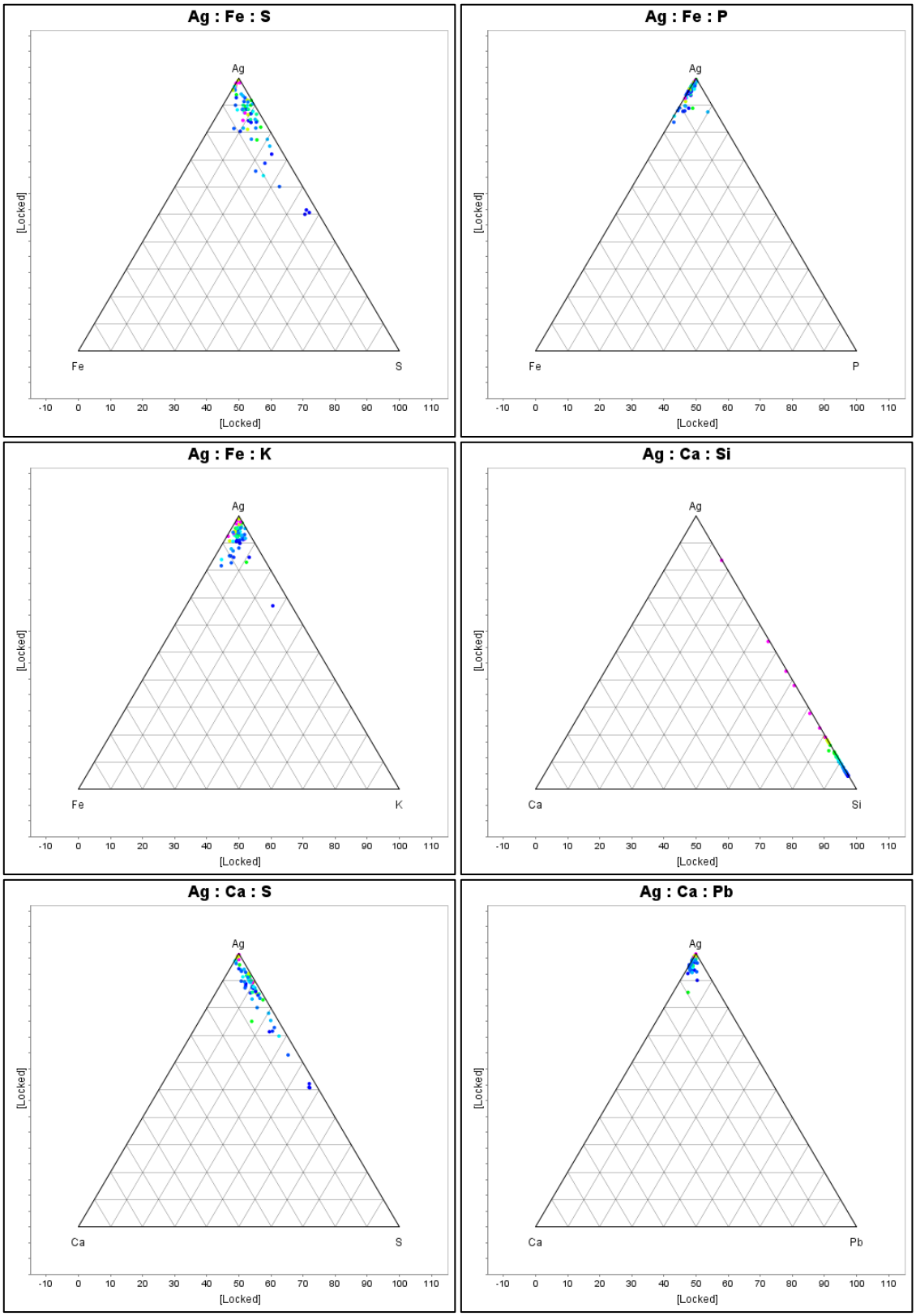

Figure E.4: Different ternary diagrams with association between Ag and other elements (Fe, K, Ca, Pb, P, S and Si)

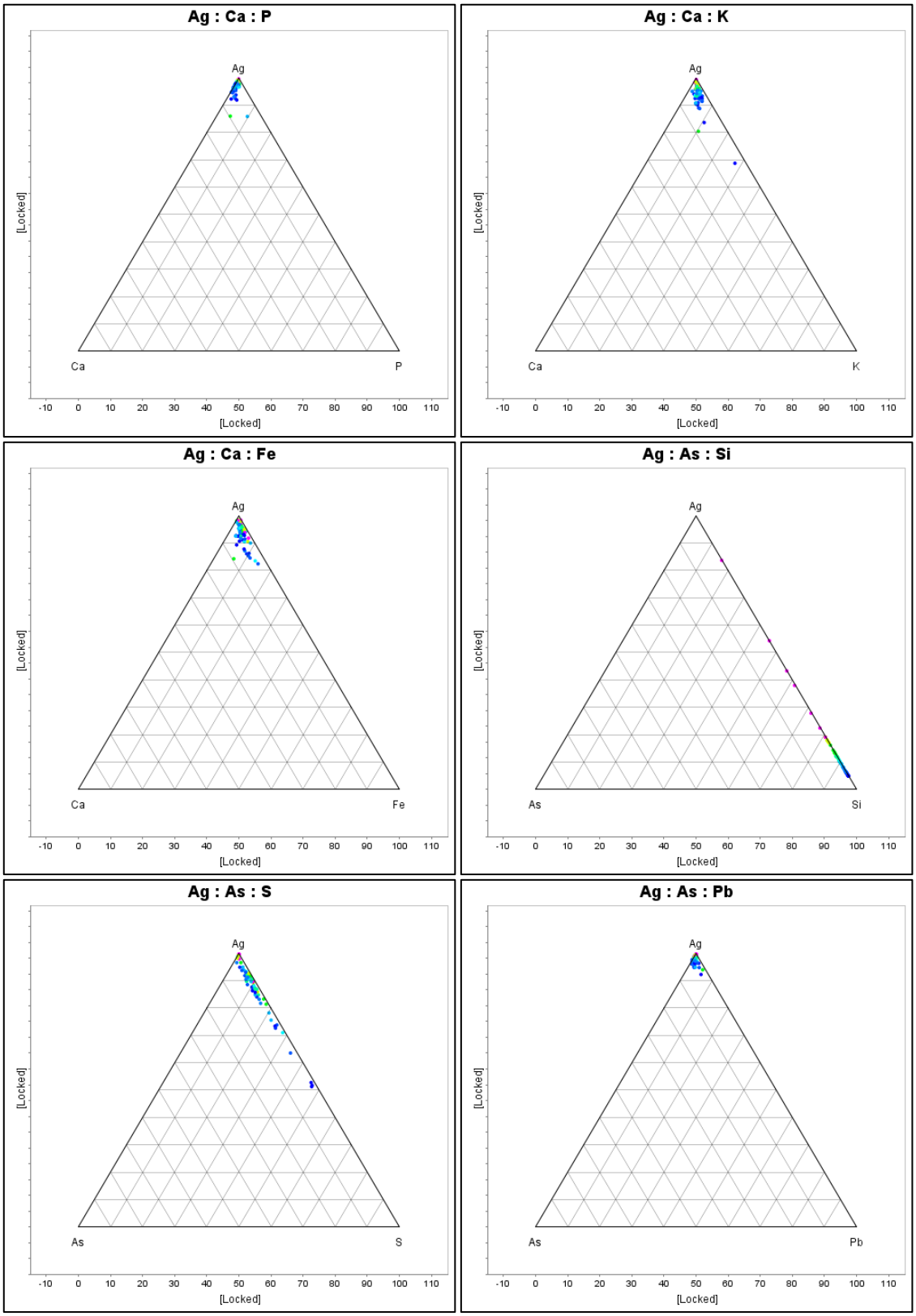

Figure E.5 Different ternary diagrams with association between Ag and other elements (As, Ca, Fe, K, Pb, P, S and Si)

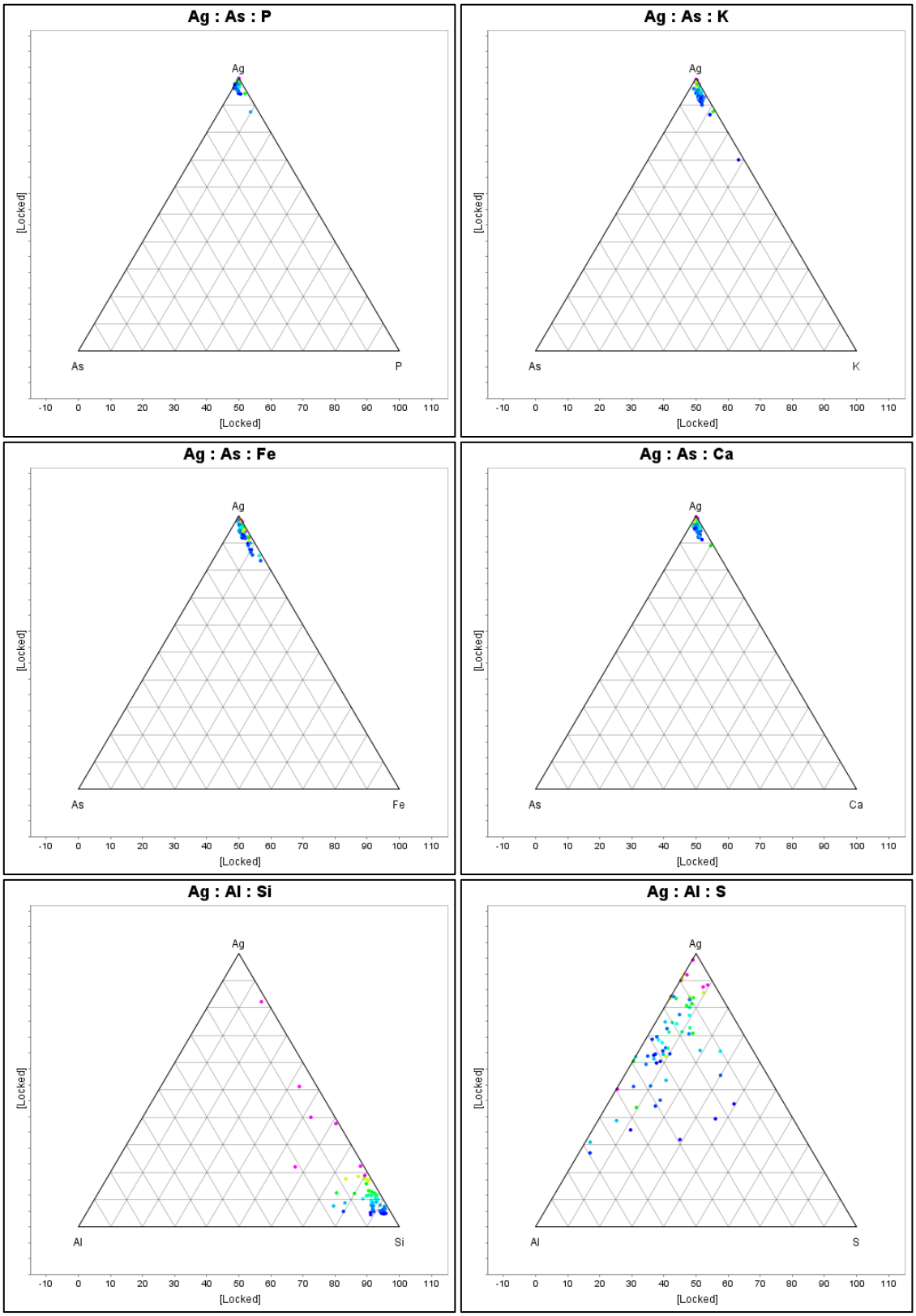

Figure E.6 Different ternary diagrams with association between Ag and other elements (As, K, P, Fe, Ca, Al and Si)

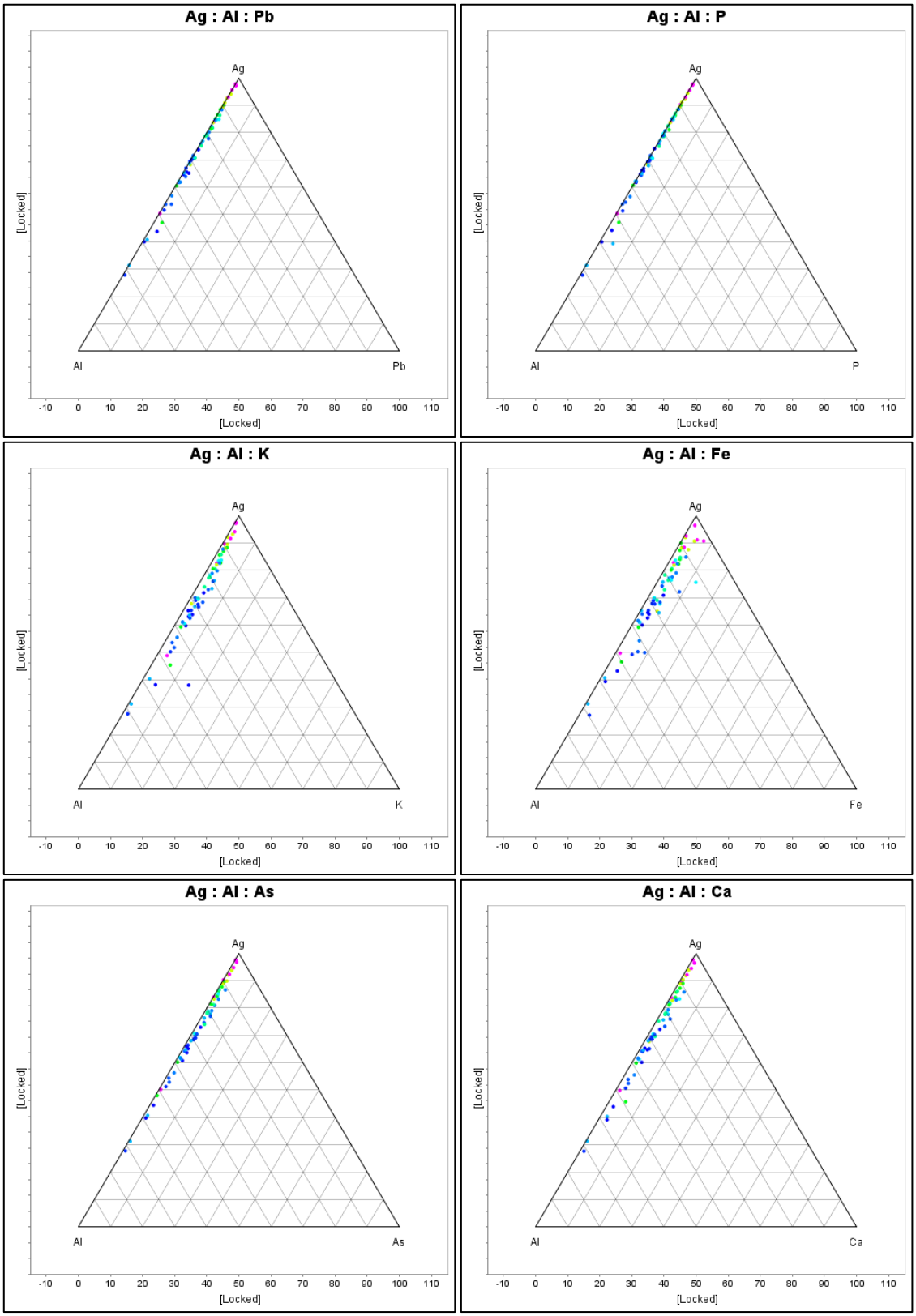

Figure E.7 Different ternary diagrams with association between Ag and other elements (Al, Ca, As, K, Fe, P and Pb)

Appendix F – Synchrotron methods from MMaST

The following Figures F.1, F.2, F.3 and F.4 are reproductions of the report provided by Rong Fan from MMaST that were incorporated into this thesis.

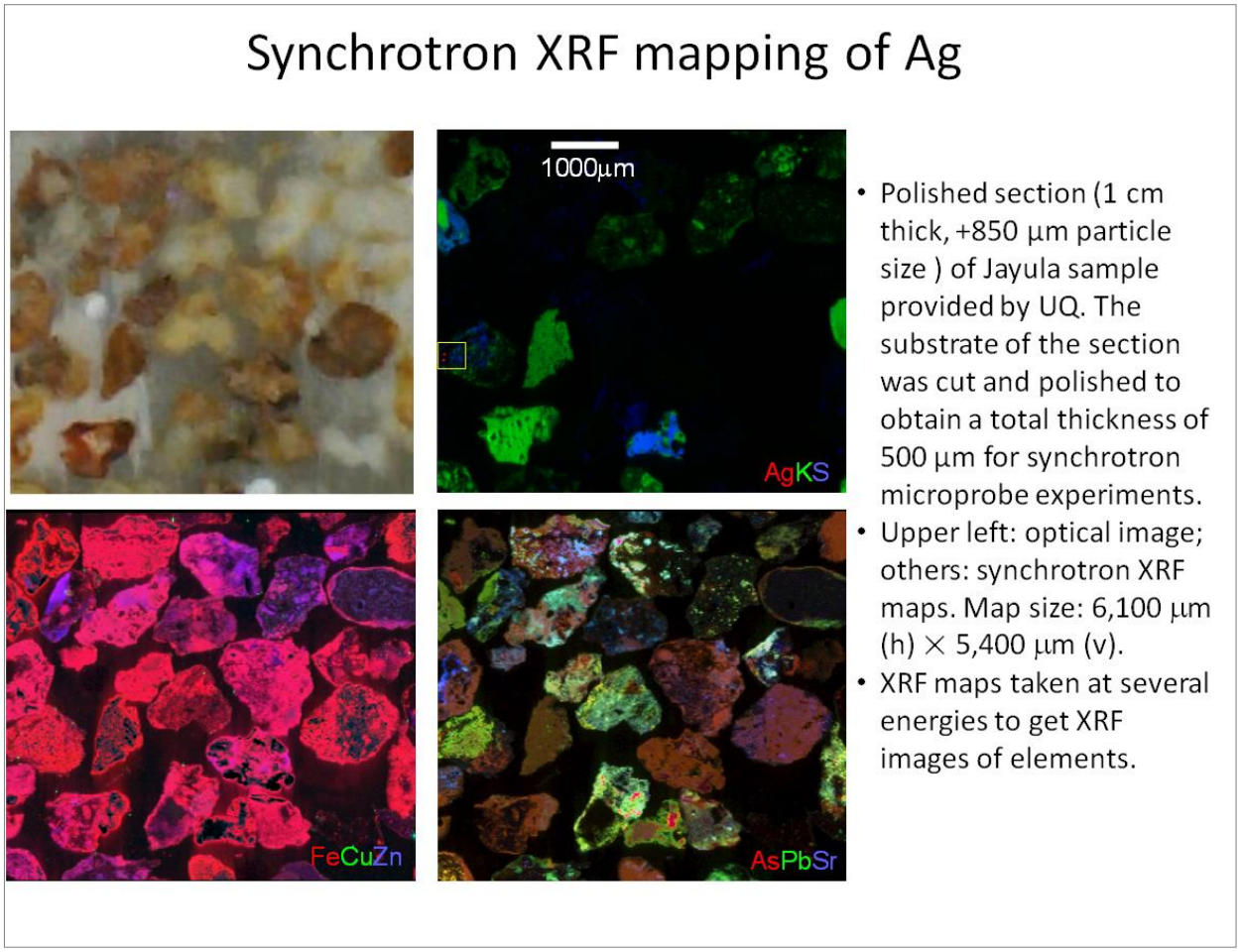

Figure F.1: From report by Fan, 2013

- Two Ag-containing hotspots (Spot 1 and Spot 2) identified and further μ-XANES and μ-XRD conducted.
- μ-XRD suggests the presence of quartz in both spots (image below shows 2D diffraction pattern of Spot 1) but no 2D diffraction rings were observed from possible Ag phases probably due to their high crystallinity (*i.e.* single crystal diffraction).

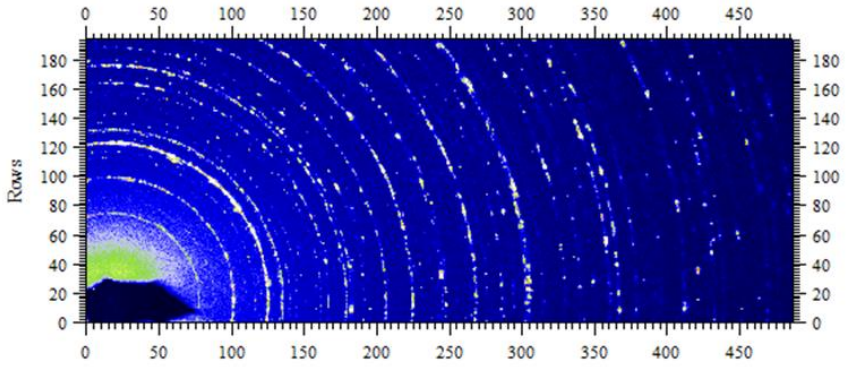

Figure F.2: From report by Fan, 2013

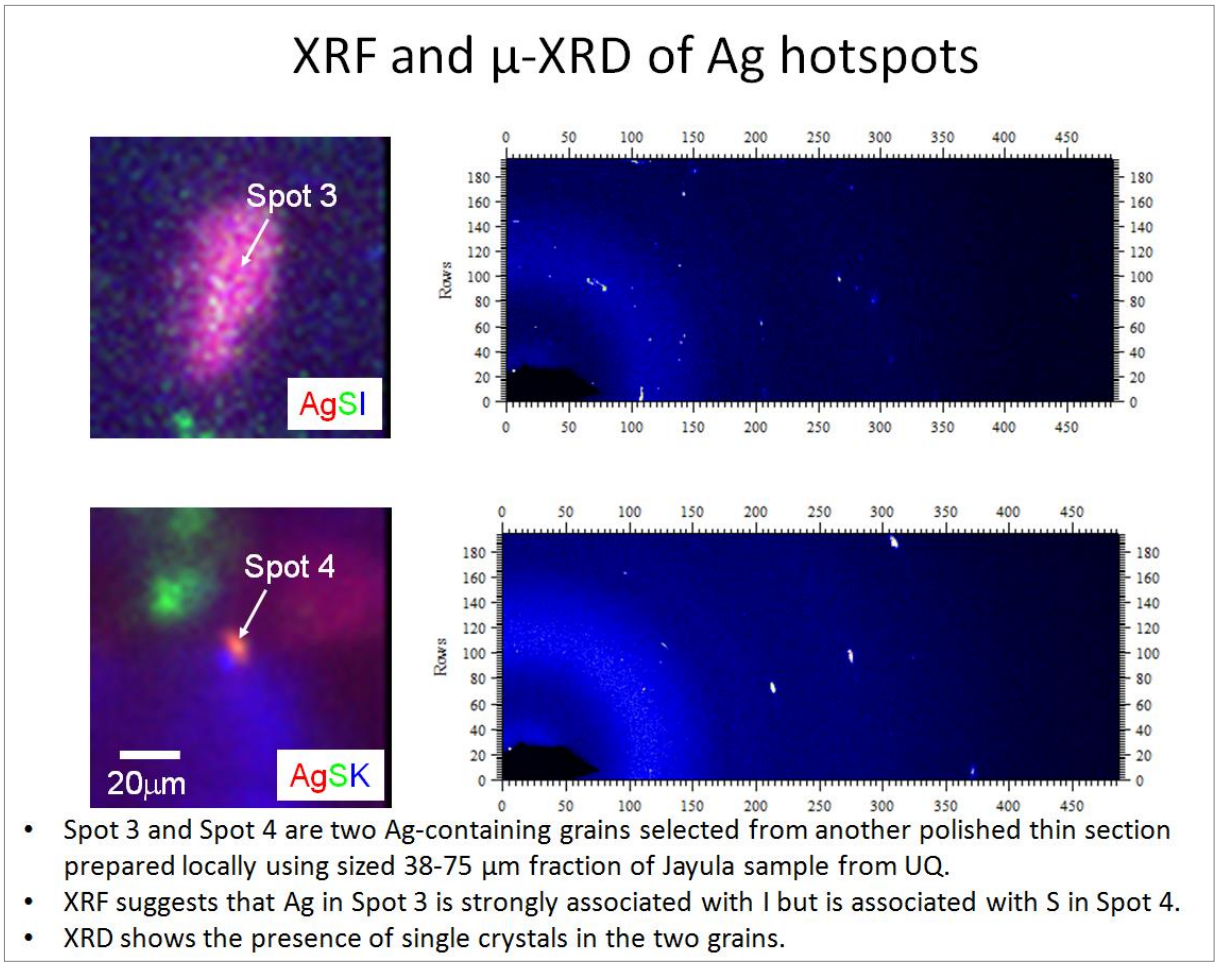

Figure F.3: From report by Fan, 2013

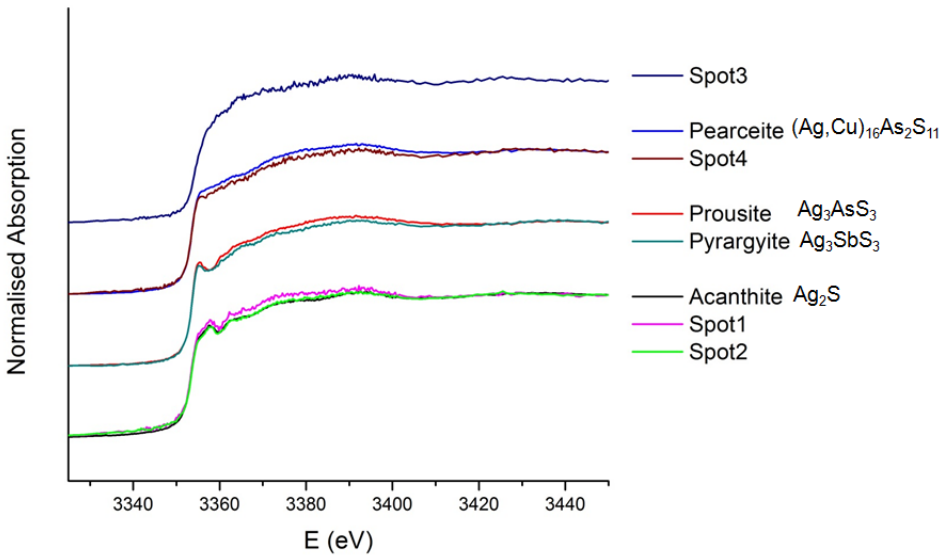

- It appears that, from µ-XANES, Ag in Spot 1 and Spot 2 is probably associated with acanthite rather other sulfides, and Ag in Spot 4 is with pearceite.
- Silver in spot 3 is likely present in iodargyrite (AgI, silver iodide). This is consistent with its XANES spectra which shows different features compared to other Ag grains and sulfide standards.
- XANES spectra shows clearly significant difference among different Ag-containing sulfide mineral groups.
- µ-XANES spectra, together with bulk XANES, can determine quantitatively the distribution of various Ag minerals in the ore by least squares fitting.

Figure F.4: From report by Fan, 2013

Appendix G – Calculation method for Liberation values

From Johnson, 2010. Existing methods for process analysis. Flotation Plant Optimisation. Spectrum Series 16, pp. 51

"(L)iberation data can also be used to identify the extent of liberation achieved at each grinding or regrinding stage at the commencement of or within a processing circuit. This information can be obtained by including samples of the combined feed and product for a grinding or regrinding circuit. For each size fraction, measurement of the liberation values for the minerals in the feed and product allows the liberation value for minerals in each stream to be calculated. For each mineral, the increase in liberation across the grinding circuit is calculated by difference".

The method consists of multiplying the mass distribution in each size fraction by the liberation value, obtained through MLA or QEMSCAN. Table G.1 shows the values of Ag minerals at P80 of 50 μm for Toldos ore.

Table G.1: Example of liberation calculation using Ag minerals at P80 of 50 μm for Toldos ore

Size	mass distribution,%	Liberation Value %	Units of liberated
+106	10.9	45.1	4.9
+53	6.7	19.3	1.3
+c2	49.0	61.6	30.2
+c3	6.6	60.0	4.0
+c4	1.6	58.2	1.0
+c5	2.0	91.1	1.8
-c5	23.0	85.2	19.6
Total	**100**		**62.8**

Therefore, the liberation value is calculated as:

$$Units\ of\ liberated = \frac{Liberation\ value\ \% * mass\ distribution,\%}{100} \quad (G.1)$$

$$Liberation\ value = \frac{\sum Units\ of\ liberated}{Total\ mass\ distribution} * 100 \quad (G.2)$$

Appendix H – Anova test

The Anova test are performed to determine if several means are significantly different to one another, as a group, using F-test to assess the significance of the variance.

H.1 Anova (Analysis of variance) for Toldos ore (oxide ore)

The variables that were tested: P80 (50 and 100 μm) and collector dosage (250 g/t and 375 g/t of 3418A). Table H.1 shows the experimental design for Toldos ore, while Table H.2 shows the results of recovery and grade for the following experimental design.

Table H.1: Experimental design for Toldos Ore

P80	***B0***	***B1***		
Test	**50**	**100**	**Collector**	**rank**
A	X		L	***A0***
B		X	L	
C		X	H	***A1***
D	X		H	

Table H.2: Result of cumulative recovery and grade

Collector	**Cum Recovery, %**		**Cum Grade, ppm**	
P80	**A_0**	**A_1**	**B_0**	**B_1**
B0	76.6	75	2577	3200
B1	74.3	73.6	4424	2771
Total	**150.9**	**148.6**	**7001**	**5972**

The Anova test was performed using Microsoft Excel. Table H.3 and H.4 shows the results of the Anova test, for recovery and grade, respectively.

The results from the ANOVA test applied to the recovery dataset of two factors, p80 and collector dosage, show that F value is smaller than the F critical and the P value is greater than 0.05. These results were found for both factors, which mean that the results are not statistically different, with a 95 % confidence. This is the case for both variables, recovery of silver and grade of silver.

Table H.3: Results of Anova test for cumulative recovery of Toldos ore.

Anova: Two-Factor Without Replication

SUMMARY	*Count*	*Sum*	*Average*	*Variance*
B0	2	151.6	75.8	1.28
B1	2	147.9	73.95	0.245
A0	2	150.9	75.45	2.645
A1	2	148.6	74.3	0.98

ANOVA

Source of Variation	*SS*	*df*	*MS*	*F*	*P-value*	*F crit*
Rows	3.4225	1	3.4225	16.90123	0.151903	161.4476
Columns	1.3225	1	1.3225	6.530864	0.237451	161.4476
Error	0.2025	1	0.2025			
Total	4.9475	3				

Table H.4: Results of Anova test for cumulative grade of Toldos ore.

Anova: Two-Factor Without Replication

SUMMARY	*Count*	*Sum*	*Average*	*Variance*
B0	2	5777.098	2888.549	194428.3
B1	2	7195.701	3597.85	1366685
A0	2	7001.253	3500.626	1707069
A1	2	5971.546	2985.773	92078.67

ANOVA

Source of Variation	*SS*	*df*	*MS*	*F*	*P-value*	*F crit*
Rows	503108.7	1	503108.7	0.388189	0.645279	161.4476
Columns	265074.1	1	265074.1	0.204526	0.729615	161.4476
Error	1296039	1	1296039			
Total	2064222	3				

H.2 Anova test for Jayula ore

The variables that were tested: P80 (50 and 100 μm) and collector dosage (220 g/t and 550 g/t of 3418A). Table H.5 shows the experimental design for Jayula ore, while Table H.6 shows the results of recovery and grade for experimental design

Table H.5: Experimental design for Jayula Ore

P_{80}	**B_0**	**B_1**		
Test	**25**	**100**	**rank**	
A	X		L	A_0
B	X		H	A_1
C		X	H	A_1
D		X	L	A_0

Table H.6: Result of cumulative recovery and grade of Jayula ore

Collector	**Cum Recovery, %**		**Cum Grade, ppm**	
P_{80}	**A_0**	**A_1**	**B_0**	**B_1**
B_0	80.0	78.4	428	296
B_1	47.4	58.5	153	137
Total	**127.4**	**136.9**	**611**	**433**

The Anova test was performed using Microsoft Excel. Table H.7 and H.8 shows the results of the Anova test, for recovery and grade, respectively.

Table H.7: Results of Anova test for cumulative recovery of Jayula ore.

Anova: Two-Factor Without Replication

SUMMARY	*Count*	*Sum*	*Average*	*Variance*
Row 1	2	158.4	79.2	1.28
Row 2	2	105.9352	52.96759	61.2152
Column 1	2	127.4352	63.71759	530.234
Column 2	2	136.9	68.45	198.005

ANOVA

Source of Variation	*SS*	*df*	*MS*	*F*	*P-value*	*F crit*
Rows	688.1395	1	688.1395	17.16082	0.150793	161.4476
Columns	22.39574	1	22.39574	0.558505	0.591423	161.4476
Error	40.09946	1	40.09946			
Total	750.6347	3				

Table H.8: Results of Anova test for cumulative grade of Jayula ore.

Anova: Two-Factor Without Replication

SUMMARY	*Count*	*Sum*	*Average*	*Variance*
Row 1	2	754	377	13122
Row 2	2	289.6251	144.8125	122.0717
Column 1	2	610.6251	305.3125	46626.92
Column 2	2	433	216.5	12640.5

ANOVA

Source of Variation	*SS*	*df*	*MS*	*F*	*P-value*	*F crit*
Rows	53911.01	1	53911.01	10.06478	0.194392	161.4476
Columns	7887.668	1	7887.668	1.472568	0.438787	161.4476
Error	5356.404	1	5356.404			
Total	67155.09	3				

H.3 Raw data of Experimental Design for Toldos ore

H.3.1 Test A for Toldos ore

Streams	Mass		Cumulative grade (%)						Cumulative Recovery (%)					
	grams	%	Ag	Cu	Fe	Pb	S	Zn	Ag	Cu	Fe	Pb	S	Zn
Feed	1000								0.0	0.0	0.0	0.0	0.0	0.0
Con 1	30.8	3.1	5220	350	7.25	2400	0.55	1900	44.8	7.1	3.1	5.0	4.1	4.7
Con 2	47.4	4.7	5388	409	7.45	2473	0.6	2015	71.0	12.8	4.9	8.0	6.3	7.7
Con 3	56.6	5.6	4670	413	7.65	2388	0.5	2073	73.6	15.5	6.0	9.2	7.2	9.5
Con 4	80.0	8.0	3375	394	7.85	2190	0.5	2087	75.2	20.9	8.7	11.9	9.3	13.5
Con 5	106.8	10.6	2577	408	8.02	2072	0.5	2130	76.6	28.8	11.8	15.1	11.6	18.3
Tail	896.0	89.4	94	120	7.14	1390	0.4	1130	23.4	71.2	88.2	84.9	88.4	81.7
Recal Feed	1002.8	100	358	151	7.23	1463	0.4	1237	100	100	100	100	100	100

H.3.2 Test B for Toldos ore

Streams	Mass		Cumulative grade (%)						Cumulative Recovery (%)					
	grams	%	Ag	Cu	Fe	Pb	S	Zn	Ag	Cu	Fe	Pb	S	Zn
Feed	1000								0.0	0.0	0.0	0.0	0.0	0.0
Con 1	17.1	1.7	9740	470	7.48	3510	0.61	2660	44.4	5.5	1.7	4.0	2.5	3.6
Con 2	23.8	2.4	10766	535	7.81	3590	0.6	2822	68.5	8.8	2.5	5.8	3.4	5.4
Con 3	30.6	3.1	8715	528	8.09	3286	0.6	2824	71.3	11.1	3.3	6.8	4.1	6.9
Con 4	49.3	4.9	5540	494	8.44	2772	0.5	2705	73.0	16.7	5.5	9.2	5.7	10.7
Con 5	62.8	6.3	4424	534	8.73	2631	0.5	2792	74.3	23.1	7.3	11.2	7.0	14.1
Tail	933.0	93.7	103	120	7.52	1410	0.4	1150	25.7	76.9	92.7	88.8	93.0	85.9
Recal Feed	995.8	100	376	146	7.60	1487	0.4	1254	100	100	100	100	100	100

H.3.3 Test C for Toldos ore

Streams	Mass		Cumulative grade (%)						Cumulative Recovery (%)					
	grams	%	Ag	Cu	Fe	Pb	S	Zn	Ag	Cu	Fe	Pb	S	Zn
Feed	1000								0.0	0.0	0.0	0.0	0.0	0.0
Con 1	29.8	3.0	6190	410	7.6	2700	0.56	2140	52.3	7.4	3.0	5.4	4.0	5.3
Con 2	41.5	4.2	5785	466	7.82	2725	0.6	2261	68.0	11.8	4.3	7.5	5.5	7.8
Con 3	50.1	5.1	4945	479	8.04	2605	0.5	2336	70.2	14.6	5.3	8.7	6.3	9.7
Con 4	61.2	6.2	4126	497	8.22	2486	0.5	2378	71.5	18.5	6.6	10.1	7.2	12.0
Con 5	93.6	9.5	2771	512	8.41	2265	0.5	2386	73.6	29.1	10.3	14.1	10.1	18.5
Tail	897.0	90.5	104	130	7.63	1440	0.4	1100	26.4	70.9	89.7	85.9	89.9	81.5
Recal Feed	990.6	100	356	166	7.70	1518	0.4	1222	100	100	100	100	100	100

H.3.4 Test D for Toldos ore

Streams	Mass		Cumulative grade (%)						Cumulative Recovery (%)					
	grams	%	Ag	Cu	Fe	Pb	S	Zn	Ag	Cu	Fe	Pb	S	Zn
Feed	1000								0.0	0.0	0.0	0.0	0.0	0.0
Con 1	29.0	2.9	6720	400	7.58	2860	0.54	2190	51.2	6.8	2.9	5.4	3.6	5.0
Con 2	39.9	4.0	6540	455	7.77	2844	0.5	2280	68.6	10.7	4.0	7.4	4.9	7.1
Con 3	51.3	5.1	5272	451	7.96	2634	0.5	2300	71.1	13.7	5.3	8.8	5.9	9.3
Con 4	63.1	6.3	4380	455	8.11	2491	0.5	2306	72.7	17.0	6.7	10.3	6.9	11.4
Con 5	89.0	8.9	3200	462	8.30	2293	0.4	2281	75.0	24.3	9.6	13.3	9.1	15.9
Tail	915.0	91.1	104	140	7.58	1450	0.4	1170	25.0	75.7	90.4	86.7	90.9	84.1
Recal Feed	1004.0	100	378	169	7.64	1525	0.4	1268	100	100	100	100	100	100

H.4 Raw data of Experimental Design for Jayula ore

H.4.1 Test A for Jayula ore

Streams	Mass	Cumulative grade (%)							Cumulative Recovery (%)					
	grams	%	Ag	Cu	Fe	Pb	S	Zn	Ag	Cu	Fe	Pb	S	Zn
Feed	1000								0.0	0.0	0.0	0.0	0.0	0.0
Con 1	53.8	5.4	3790	560	3.51	9320	1.06	2260	75.5	12.5	6.4	9.3	12.7	17.0
Con 2	62.2	6.2	3372	534	3.47	9167	1.0	2093	77.7	13.8	7.3	10.5	13.9	18.2
Con 3	81.6	8.1	2589	469	3.36	8422	0.9	1764	78.3	15.9	9.2	12.7	15.8	20.1
Con 4	133.2	13.2	458	313	2.98	6988	0.5	860	80.0	16.6	9.8	13.3	16.4	20.7
Tail	872.0	86.8	62	230	3.07	5390	0.43	650	20.0	83.4	90.2	86.7	83.6	79.3
Recal Feed	953.6	100	375	260	3.11	5772	0.5	789	100	100	100	100	100	100

H.4.2 Test B for Jayula ore

Streams	Mass		Cumulative grade (%)						Cumulative Recovery (%)					
	grams	%	Ag	Cu	Fe	Pb	S	Zn	Ag	Cu	Fe	Pb	S	Zn
Feed	1000								0.0	0.0	0.0	0.0	0.0	0.0
Con 1	44.8	4.5	934	310	3.3	6890	0.6	1120	38.0	5.2	4.8	5.5	6.0	7.2
Con 2	86.5	8.7	590	329	3.2	6982	0.5	990	46.4	10.7	9.2	10.7	10.7	12.2
Con 3	485.9	49.0	162	297	3.1	6051	0.5	776	71.5	54.1	49.1	51.9	51.1	53.9
Con 4	595.4	60.1	145	296	3.1	6022	0.5	764	78.4	65.9	60.6	63.3	61.9	65.0
Tail	395.3	39.9	60	230	3.0	5260	0.4	620	21.6	34.1	39.4	36.7	38.1	35.0
Recal Feed	881.2	100	111	269	3.1	5718	0.4	707	100	100	100	100	100	100

H.4.3. Test C for Jayula ore

Streams	Mass		Cumulative grade (%)						Cumulative Recovery (%)					
	grams	%	Ag	Cu	Fe	Pb	S	Zn	Ag	Cu	Fe	Pb	S	Zn
Feed	1000								0.0	0.0	0.0	0.0	0.0	0.0
Con 1	41.0	4.1	725	370	2.83	8060	0.6	1160	27.3	5.6	4.0	5.7	5.7	7.2
Con 2	68.6	6.9	493	418	2.80	8100	0.6	1072	31.0	10.5	6.6	9.6	9.1	11.1
Con 3	390.6	39.2	146	354	2.78	6517	0.4	773	52.3	50.7	37.2	44.1	40.4	45.7
Con 4	463.7	46.6	137	358	2.83	6510	0.4	771	58.5	60.9	44.9	52.3	48.2	54.1
Tail	532.3	53.4	85	200	3.03	5180	0.42	570	41.5	39.1	55.1	47.7	51.8	45.9
Recal Feed	923.0	100	109	273	2.94	5799	0.4	664	100	100	100	100	100	100

H.4.4 Test D for Jayula ore

Streams	Mass		Cumulative grade (%)						Cumulative Recovery (%)					
	grams	%	Ag	Cu	Fe	Pb	S	Zn	Ag	Cu	Fe	Pb	S	Zn
Feed	1000								0.0	0.0	0.0	0.0	0.0	0.0
Con 1	31.3	3.1	827	440	3.46	8790	0.67	1290	24.4	6.1	3.6	4.8	5.0	6.2
Con 2	47.3	4.8	630	450	3.36	8905	0.6	1195	28.1	9.4	5.2	7.4	7.4	8.7
Con 3	251.8	25.3	175	328	2.98	6733	0.5	809	41.5	36.5	24.7	29.9	28.0	31.2
Con 4	330.1	33.2	153	324	3.00	6651	0.5	793	47.4	47.2	32.6	38.7	36.1	40.0
Tail	664.5	66.8	84	180	3.08	5240	0.4	590	52.6	52.8	67.4	61.3	63.9	60.0
Recal Feed	916.3	100	107	228	3.05	5708	0.4	657	100	100	100	100	100	100

Appendix I– Data set of chemical assays for Toldos, Tesorera and Jayula Ore

Table I.1: complete data for chemical assay by- size for Toldos ore

SAMPLE			Ag	Al	As	Ba	Be	Bi	Ca	Cd	Co	Cr	Cu	Fe	Ga	K	La	Mg	Mn	Mo	Na	Ni	P	Pb	S	Sb	Sc	Sr	Th	Ti	Tl	U	V	W	Zn
DESCRIPTION	Size	Mass %	ppm	%	ppm	ppm	ppm	ppm	%	ppm	ppm	ppm	ppm	%	ppm	%	ppm	%	ppm	ppm	%	ppm	ppm	ppm	%	ppm	ppm	ppm	ppm	%	ppm	ppm	ppm	ppm	ppm
JK2681-3-1	Head		406	4.74	640	16850	<10	<20	0.24	10	20	30	80	7.74	<50	5.2	<50	0.14	1990	<10	0.39	<10	640	1520	0.47	80	<10	410	<50	0.18	<50	<50	30	<50	1290
JK2681-3-2	+2.36	20.22	324	4.9	520	12600	<10	<20	0.23	10	10	90	60	7.57	<50	5.7	<50	0.14	1150	<10	0.41	<10	620	1010	0.37	70	<10	330	<50	0.2	<50	<50	30	<50	990
JK2681-3-3	+1.7	17.91	326	4.54	680	13400	<10	<20	0.2	10	20	50	60	7.61	<50	5.1	<50	0.12	1080	<10	0.38	<10	590	1310	0.34	80	<10	310	<50	0.18	<50	<50	30	<50	1010
JK2681-3-4	+1.18	14.24	289	4.58	600	14950	<10	<20	0.2	10	20	60	70	8.01	<50	5.7	<50	0.12	1920	<10	0.38	<10	580	1240	0.37	70	<10	360	<50	0.18	<50	<50	30	<50	1090
JK2681-3-5	+0.850	8.64	389	4.94	610	16050	<10	<20	0.2	10	20	90	80	8.01	<50	5.3	<50	0.13	2110	<10	0.36	<10	570	1360	0.4	60	<10	380	<50	0.18	<50	<50	30	<50	1130
JK2681-3-6	+0.600	7.02	533	4.97	710	15650	<10	<20	0.21	10	20	220	100	9.1	<50	5.8	<50	0.13	2520	<10	0.37	70	610	1580	0.39	100	<10	450	<50	0.18	<50	<50	30	<50	1210
JK2681-3-7	+0.425	5.44	523	5.39	660	17500	<10	<20	0.22	10	30	200	130	8.69	<50	5.8	<50	0.16	2870	<10	0.38	40	580	1630	0.45	110	<10	520	<50	0.18	<50	<50	30	<50	1230
JK2681-3-8	+0.300	4.63	526	5.03	670	17350	<10	<20	0.22	10	30	100	120	8.66	<50	5.5	<50	0.16	2940	<10	0.38	10	580	1770	0.44	110	<10	540	<50	0.18	<50	<50	30	<50	1300
JK2681-3-9	+0.212	3.73	522	5.07	710	23600	<10	<20	0.25	10	30	100	130	8.84	<50	5.3	<50	0.18	3140	<10	0.39	10	560	1930	0.6	100	<10	610	<50	0.18	<50	<50	30	<50	1370
JK2681-3-10	+0.150	2.85	611	5.2	760	17550	<10	<20	0.29	10	20	110	160	8.95	<50	5.3	<50	0.18	3300	<10	0.41	30	580	2110	0.46	100	<10	640	<50	0.18	<50	<50	30	<50	1480
JK2681-3-11	+0.106	2.46	532	5.24	740	17200	<10	<20	0.31	10	30	120	140	8.96	<50	5	<50	0.18	3200	<10	0.4	10	620	2200	0.45	100	<10	660	<50	0.18	<50	<50	30	<50	1470
JK2681-3-12	+0.075	2.14	508	5.17	780	14500	<10	<20	0.33	10	30	140	180	9.13	<50	4.9	<50	0.17	3120	<10	0.4	20	640	2280	0.39	110	<10	680	<50	0.18	<50	<50	30	<50	1540
JK2681-3-13	+0.053	1.59	483	4.58	860	16150	<10	<20	0.35	10	30	130	280	9.29	<50	4.9	<50	0.16	3070	<10	0.38	10	760	2510	0.44	110	<10	750	<50	0.19	<50	<50	40	<50	1620
JK2681-3-14	+0.038	1.21	473	5.14	930	12800	<10	20	0.42	10	30	120	650	9.82	<50	4.5	<50	0.16	3130	<10	0.37	10	1010	2860	0.39	110	<10	760	<50	0.22	<50	<50	40	<50	1710
JK2681-3-15	-0.038	7.93	265	6.97	870	14700	<10	<20	0.49	10	30	40	290	9.81	<50	4.6	<50	0.26	2730	<10	0.31	20	1220	2660	0.41	100	10	640	<50	0.26	<50	<50	50	<50	2290
Calc Hd		**100.00**	**384**	**5.02**	**659**	**15007**	**<10**	**<20**	**0.20**	**10**	**21**	**94**	**111**	**8.3**	**<50**	**5.4**	**<50**	**0.15**	**2010**	**<10**	**0.38**	**11**	**651**	**1535**	**0.39**	**84**	**1**	**435**	**<50**	**0.19**	**<50**	**<50**	**32**	**<50**	**1236**

Table I.2: complete data for chemical assay by- size for Tesorera ore

SAMPLE			Ag	Al	As	Ba	Be	Bi	Ca	Cd	Co	Cr	Cu	Fe	Ga	K	La	Mg	Mn	Mo	Na	Ni	P	Pb	S	Sb	Sc	Sr	Th	Ti	Tl	U	V	W	Zn
DESCRIPTION	Size	Mass %	ppm	%	ppm	ppm	ppm	ppm	%	ppm	ppm	ppm	ppm	%	ppm	%	ppm	%	ppm	ppm	%	ppm	ppm	ppm	%	ppm	ppm	ppm	ppm	%	ppm	ppm	ppm	ppm	ppm
JK2681-2-1	Head		116	4.7	370	2550	<10	<20	1.06	60	60	50	30	3.73	<50	2.7	<50	0.29	1700	<10	1.33	40	1050	1930	3.15	<50	<10	550	<50	0.33	100	<50	80	<50	5640
JK2681-2-2	+2.36	12.34	185	4.53	600	880	<10	<20	0.75	160	80	60	60	4.68	<50	2.2	<50	0.22	1350	<10	0.85	60	880	3050	4.64	70	<10	460	<50	0.25	110	<50	70	<50	14900
JK2681-2-3	+1.7	13.43	127	3.93	450	1140	<10	<20	0.79	80	60	80	40	4.01	<50	2.4	<50	0.24	1630	<10	1.01	40	950	2150	3.6	50	<10	400	<50	0.3	110	<50	70	<50	8060
JK2681-2-4	+1.18	12.24	131	4.62	410	1660	<10	<20	0.87	70	60	50	50	3.87	<50	2.8	<50	0.29	1600	<10	1.18	40	1030	2050	3.4	<50	<10	450	<50	0.32	90	<50	70	<50	7230
JK2681-2-5	+0.850	9.43	113	3.93	380	1550	<10	<20	0.86	50	50	90	50	3.66	<50	2.8	<50	0.3	1420	<10	1.33	40	1010	1760	2.99	50	<10	470	<50	0.34	100	<50	80	<50	5340
JK2681-2-6	+0.600	8.78	103	4.81	360	1640	<10	<20	1.1	50	50	60	50	3.67	<50	2.9	<50	0.33	1500	<10	1.59	30	950	1700	2.82	<50	<10	580	<50	0.34	80	<50	80	<50	5300
JK2681-2-7	+0.425	7.73	92	4.59	310	1870	<10	<20	1.17	40	40	90	50	3.24	<50	2.8	<50	0.31	1420	<10	1.74	30	900	1420	2.46	<50	<10	620	<50	0.32	80	<50	70	<50	4270
JK2681-2-8	+0.300	6.93	87	4.68	290	2120	<10	<20	1.28	40	40	60	50	3.14	<50	2.7	<50	0.27	1530	<10	1.82	30	960	1390	2.36	<50	<10	660	<50	0.31	80	<50	70	<50	3870
JK2681-2-9	+0.212	5.48	87	4.94	300	2050	<10	<20	1.38	40	40	100	70	3.29	<50	2.7	<50	0.27	1690	<10	1.85	20	1210	1420	2.43	<50	<10	690	<50	0.32	80	<50	80	<50	3800
JK2681-2-10	+0.150	4.05	87	3.91	300	1880	<10	<20	1.19	30	40	70	90	3.16	<50	2.6	<50	0.24	1630	<10	1.66	30	1270	1390	2.37	<50	<10	590	<50	0.31	80	<50	80	<50	3510
JK2681-2-11	+0.106	3.25	93	4.38	330	1420	<10	<20	1.24	40	50	220	90	3.61	<50	2.7	<50	0.25	1770	<10	1.56	90	1400	1570	2.58	<50	<10	550	<50	0.34	90	<50	90	<50	3660
JK2681-2-12	+0.075	2.69	93	5.69	340	3730	<10	<20	1.26	30	50	70	90	3.89	<50	2.7	<50	0.3	1810	<10	1.37	30	1330	1600	2.67	<50	<10	580	<50	0.34	90	<50	90	<50	3580
JK2681-2-13	+0.053	1.99	103	4.95	350	2720	<10	<20	1.13	40	50	120	160	4.22	<50	2.8	<50	0.29	1900	<10	1.27	30	1400	1840	2.98	<50	<10	530	<50	0.36	100	<50	90	<50	3710
JK2681-2-14	+0.038	1.60	110	4.35	400	1960	<10	<20	1.03	40	50	90	440	4.39	<50	2.6	<50	0.25	1890	<10	1.12	30	1340	1960	3.1	<50	<10	480	<50	0.36	110	<50	100	<50	3780
JK2681-2-15	-0.038	10.07	78	4.12	360	1910	<10	<20	0.82	30	40	60	140	3.63	<50	2.7	<50	0.26	2020	<10	1.08	40	1190	1520	2.21	<50	<10	420	<50	0.42	70	<50	110	<50	3670
Calc Hd		**100.00**	**114**	**4.43**	**394**	**1659**	**<10**	**<20**	**1**	**64**	**53**	**76**	**72**	**3.77**	**<50**	**2.6**	**<50**	**0.27**	**1599**	**<10**	**1.32**	**40**	**1045**	**1886**	**3.07**	**20**	**<10**	**510**	**<50**	**0.32**	**91**	**<50**	**79**	**<50**	**6442**

Table I.3: complete data for chemical assay by- size for Jayula ore

SAMPLE			Ag	Al	As	Ba	Be	Bi	Ca	Cd	Co	Cr	Cu	Fe	Ga	K	La	Mg	Mn	Mo	Na	Ni	P	Pb	S	Sb	Sc	Sr	Th	Ti	Tl	U	V	W	Zn
DESCRIPTION	Size	Mass %	ppm	%	ppm	ppm	ppm	ppm	%	ppm	ppm	ppm	ppm	%	ppm	%	ppm	%	ppm	ppm	%	ppm	ppm	ppm	%	ppm	ppm	ppm	ppm	%	ppm	ppm	ppm	ppm	ppm
JK2681-1-1	Head		112	3.45	530	3320	<10	<20	<0.05	<10	<10	40	90	3.17	<50	1.5	<50	<0.05	30	<10	<0.05	<10	1410	5880	0.42	100	<10	750	<50	0.28	<50	<50	160	<50	710
JK2681-1-2	+2.36	9.21	189	4.84	480	3310	<10	<20	0.06	<10	<10	80	70	4.03	<50	1.1	<50	<0.05	40	<10	0.05	<10	1170	4470	0.37	100	<10	860	<50	0.25	<50	<50	130	<50	560
JK2681-1-3	+1.7	11.66	151	3.91	490	3960	<10	<20	<0.05	<10	<10	40	70	3.64	<50	1.3	<50	<0.05	20	<10	<0.05	<10	1240	4980	0.41	90	<10	780	<50	0.25	<50	<50	130	<50	610
JK2681-1-4	+1.18	9.27	160	3.98	500	4800	<10	<20	<0.05	<10	<10	60	70	3.72	<50	1.3	<50	<0.05	20	<10	<0.05	<10	1220	4980	0.44	90	<10	790	<50	0.24	<50	<50	130	<50	600
JK2681-1-5	+0.850	7.24	138	4.4	500	3650	<10	<20	<0.05	<10	<10	60	80	3.71	<50	1.4	<50	<0.05	20	<10	<0.05	<10	1240	4930	0.39	100	<10	820	<50	0.25	<50	<50	130	<50	600
JK2681-1-6	+0.600	6.57	126	4.26	510	3940	<10	<20	<0.05	<10	<10	60	80	3.56	<50	1.4	<50	<0.05	20	<10	<0.05	<10	1260	4980	0.39	90	<10	810	<50	0.24	<50	<50	130	<50	600
JK2681-1-7	+0.425	5.77	115	3.73	510	4260	<10	<20	<0.05	<10	<10	50	90	3.34	<50	1.6	<50	<0.05	20	<10	<0.05	<10	1260	5120	0.39	90	<10	740	<50	0.24	<50	<50	140	<50	630
JK2681-1-8	+0.300	5.27	99	4.33	500	4360	<10	<20	<0.05	<10	<10	60	80	3.45	<50	1.5	<50	<0.05	20	<10	<0.05	<10	1290	5220	0.38	90	<10	800	<50	0.24	<50	<50	140	<50	640
JK2681-1-9	+0.212	4.48	98	4.11	490	5080	<10	<20	<0.05	<10	<10	50	90	3.37	<50	1.5	<50	<0.05	30	<10	<0.05	<10	1330	5400	0.4	110	<10	770	<50	0.26	<50	<50	150	<50	660
JK2681-1-10	+0.150	3.64	89	2.92	520	5660	<10	<20	<0.05	<10	<10	60	100	3.12	<50	1.6	<50	<0.05	30	<10	<0.05	<10	1330	5540	0.39	110	<10	640	<50	0.25	<50	<50	150	<50	690
JK2681-1-11	+0.106	3.28	79	4.94	530	6370	<10	<20	<0.05	<10	<10	40	90	3.66	<50	1.5	<50	0.05	30	<10	<0.05	<10	1450	5760	0.43	110	<10	880	<50	0.27	<50	<50	160	<50	710
JK2681-1-12	+0.075	3.06	78	5	530	6590	<10	<20	0.05	<10	<10	60	100	3.68	<50	1.6	<50	0.06	30	<10	<0.05	<10	1500	5920	0.45	120	<10	880	<50	0.29	<50	<50	160	<50	740
JK2681-1-13	+0.053	2.66	69	4.81	540	6180	<10	<20	0.05	<10	<10	30	120	3.76	<50	1.7	<50	0.06	30	<10	<0.05	<10	1590	6300	0.44	110	<10	920	<50	0.31	<50	<50	180	<50	800
JK2681-1-14	+0.038	2.21	64	5.8	560	5900	<10	<20	0.06	<10	<10	40	200	4	<50	1.6	<50	0.07	30	<10	<0.05	<10	1670	6470	0.46	110	<10	1050	<50	0.34	<50	<50	180	<50	820
JK2681-1-15	-0.038	25.68	31	4.86	580	2110	<10	<20	0.05	<10	<10	20	120	3	<50	1.6	<50	0.06	20	<10	<0.05	<10	1830	7580	0.46	80	<10	1000	<50	0.32	<50	<50	210	<50	850
Calc Hd		**100.00**	**104**	**4.42**	**523**	**3891**	**<10**	**<20**	**0.05**	**<10**	**<10**	**46**	**94**	**3.47**	**<50**	**1.5**	**<50**	**0.02**	**24**	**<10**	**0.00**	**<10**	**1429**	**5780**	**0.42**	**93**	**<10**	**859**	**<50**	**0.27**	**<50**	**<50**	**158**	**<50**	**690**

Appendix J – MLA DATA

Appendix J is an excel file.

Appendix K – LA-ICP-MS results

Table K.1: Tesorera Results

		Average Detection Limit (ppm)												
	pyrite	2.68	0.01	0.06	0.11	0.26	0.52	0.02	0.04	0.23	0.02	0.01	0.02	0.01

Concentrations

File	Sample Name	Mineral	Spot Size	Fe57	Co59	Ni60	Cu65	Zn66	As75	Ag107	Sb121	Te125	Au197	Tl205	Pb208	Bi209
			micron	ppm	ppm	ppm	ppm	ppm	ppm	ppm	ppm	ppm	ppm	ppm	ppm	ppm
AU19A03	JK2681-2	pyrite	35	465000	102	75	1163	46	1225	3297	126	<0.23	<0.02	1465	57763	0.02
AU19A04	JK2681-2	pyrite	35	465000	50	40	99	61	2481	3160	89	<0.23	<0.02	2072	52575	<0.01
AU19A05	JK2681-2	pyrite	35	465000	370	320	167	3610	10652	3106	407	<0.23	<0.02	2259	22318	0.70
AU19A06	JK2681-2	pyrite	35	465000	272	213	394	175	3025	5425	345	<0.23	<0.02	2403	65630	1.16
AU19A07	JK2681-2	pyrite	35	465000	249	168	2167	459	3079	5021	523	<0.23	<0.02	581	20964	0.79
AU19A08	JK2681-2	pyrite	35	465000	274	284	83	88	3893	1152	336	<0.23	<0.02	1385	27891	0.16
AU19A09	JK2681-2	pyrite	35	465000	126	72	38	34	712	2724	4	<0.23	<0.02	1930	52053	<0.01
AU19A10	JK2681-2	pyrite	35	465000	644	476	271	113	5587	4624	641	<0.23	<0.02	1488	43556	0.18
AU19A11	JK2681-2	pyrite	35	465000	366	192	40	221	3951	1219	620	<0.23	<0.02	1187	33456	0.03
AU19A12	JK2681-2	pyrite	35	465000	313	383	79	95	1114	964	254	<0.23	<0.02	376	8376	0.67
AU19A13	JK2681-2	pyrite	35	465000	42	73	1127	160	2375	3922	403	0.28	<0.02	1774	66806	2.36
AU19A14	JK2681-2	pyrite	35	465000	68	57	717	105	2674	2931	94	<0.23	<0.02	884	41739	0.46
AU19A15	JK2681-2	pyrite	35	465000	118	76	17	51	1473	1479	49	<0.23	<0.02	1574	41351	<0.01
AU19A16	JK2681-2	pyrite	35	465000	402	264	605	222	5966	6857	548	<0.23	<0.02	2085	73641	0.03
AU19A18	JK2681-2	pyrite	35	465000	121	62	2	76	2063	1940	280	<0.23	<0.02	529	19326	0.08
AU19A19	JK2681-2	pyrite	35	465000	120	96	735	34	2935	2752	279	<0.23	<0.02	796	32628	0.02
AU19A20	JK2681-2	pyrite	35	465000	172	136	61	90	8569	1918	366	<0.23	<0.02	422	22989	0.19
AU19A21	JK2681-2	pyrite	35	465000	41	27	266	76	984	2225	369	<0.23	<0.02	2440	27975	<0.01
AU19A22	JK2681-2	pyrite	35	465000	71	57	11	24	246	1721	6	<0.23	<0.02	508	20312	<0.01
AU19A23	JK2681-2	pyrite	35	465000	61	73	411	122	2059	2288	460	<0.23	0.02	640	16686	0.10
MEAN	**JK2681-2**	**pyrite**		**465000**	**199**	**157**	**423**	**293**	**3253**	**2936**	**310**	**<0.23**	**<0.02**	**1340**	**37402**	**0.35**

Table K.2: Jayula Results

	Average Detection Limit																
jarosite	0.47	518.03	7.03	1.58	4.09	0.03	0.10	0.17	0.31	0.86	0.03	0.11	0.44	0.02	0.02	0.05	0.02
Pb-arsenate	0.39	421.21	6.03	1.32	3.33	0.02	0.08	0.14	0.30	0.95	0.03	0.07	0.37	0.02	0.02	0.04	0.02
Pb-phosphate	0.45	496.78	7.28	1.78	4.27	0.02	0.12	0.18	0.35	1.10	0.03	0.08	0.40	0.02	0.02	0.05	0.02

Concentrations

File	Sample Name	Mineral	Spot Size	Al27	Si29	P31	K39	Fe57	Co59	Ni60	Cu65	Zn66	As75	Ag107	Sb121	Te125	Au197	Tl205	Pb208	Bi209
			micron	ppm	ppm	ppm	ppm	ppm	ppm	ppm	ppm	ppm	ppm	ppm	ppm	ppm	ppm	ppm	ppm	ppm
AU19A29	JK2681-1	Pb-phosphate	35	111463	25699	46548	1399	238766	4.0	3.8	328	3018	5556	8.3	373	38.6	<0.02	0.1	83548	5.8
AU19A30	JK2681-1	Pb-phosphate	35	146532	76339	43603	19514	149743	0.8	1.0	226	944	4075	8.5	92	1.1	<0.02	34.4	125323	0.5
AU19A31	JK2681-1	jarosite	35	16640	77944	1088	100551	386101	2.4	0.3	316	9097	3007	65	475	2.3	0.03	4.7	88190	0.3
AU19A32	JK2681-1	jarosite	35	794	1176	366	122099	549153	0.3	<0.1	74	889	8081	219	134	5.8	<0.02	15.4	27849	0.3
AU19A33	JK2681-1	jarosite	35	8806	38911	512	111094	493779	1.1	0.4	285	3360	4126	95	404	3.2	<0.02	6.1	43631	0.5
AU19A34	JK2681-1	Pb-phosphate	35	78544	11468	44512	11967	196629	2.6	1.4	627	3992	10702	20	185	2.1	<0.02	5.4	315627	1.0
AU19A35	JK2681-1	jarosite	35	21670	52353	1573	105873	455960	0.4	0.7	82	219	6040	370	152	5.1	<0.02	19.9	22280	1.6
AU19A36	JK2681-1	jarosite	35	1792	709	358	118924	562311	0.4	0.1	43	1855	2512	118	238	1.3	<0.02	32.5	25065	0.1
AU19A37	JK2681-1	Pb-Arsenate	35	7526	23701	630	78456	423585	1.9	0.3	807	6819	5461	57	95	7.7	0.03	3.0	176380	0.8
AU19A38	JK2681-1	Pb-phosphate	35	21667	40284	10435	4356	549152	4.8	7.4	2432	14508	7328	1.9	459	8.0	<0.02	1.0	23208	0.7
AU19A39	JK2681-1	Pb-Arsenate	35	20315	4004	23359	64966	428496	0.7	0.4	248	2299	5257	79	184	2.1	<0.02	36.5	153172	0.4
AU19A40	JK2681-1	Pb-Arsenate	35	5757	7773	2754	69100	440592	0.5	0.1	1197	296	19031	19	138	7.2	<0.02	1.1	204229	0.7
AU19A41	JK2681-1	Pb-Arsenate	35	16433	15184	4774	82967	476810	1.8	0.3	515	5025	2455	10	698	1.5	<0.02	3.5	103971	1.3
AU19A42	JK2681-1	Pb-phosphate	35	44835	61283	5285	10835	497090	11.2	10.3	518	1189	5024	3.7	973	14.6	<0.02	3.5	10676	1.7
AU19A43	JK2681-1	Pb-Arsenate	35	30883	7083	17732	79367	412273	2.3	0.5	1344	8409	3342	1167	355	3.0	<0.02	12.2	125323	4.5
AU19A44	JK2681-1	Pb-phosphate	35	34699	15468	11210	482	546555	3.2	4.6	560	3341	7380	30	880	8.7	<0.02	0.1	32491	0.9
AU19A45	JK2681-1	Pb-phosphate	35	43994	74877	11469	1226	442352	7.0	9.4	779	16355	5325	1.8	190	0.8	<0.02	0.2	50129	0.3
AU19A46	JK2681-1	Pb-phosphate	35	30166	7273	40635	21	358487	2.7	4.9	993	6665	10239	3.2	2293	8.9	<0.02	0.1	208871	2.1
AU19A47	JK2681-1	Pb-phosphate	35	60062	26709	25113	777	456167	1.9	2.9	388	3851	5879	3.1	311	1.8	<0.02	0.5	64982	0.3
AU19A48	JK2681-1	Pb-phosphate	35	139680	30909	12603	42016	350663	3.7	8.6	652	2578	4295	8.0	498	18.7	<0.02	0.2	44559	2.9
MEAN	**JK2681-1**	**Pb-phosphate**		**71164**	**37031**	**25141**	**9259**	**378560**	**4.2**	**5.4**	**750**	**5644**	**6580**	**9**	**625**	**10.3**	**<0.02**	**4.5**	**95941**	**1.6**
MEAN	**Jayula**	**Pb-arsenate**		**16183**	**11549**	**9850**	**74971**	**436351**	**1.4**	**0.3**	**822**	**4569**	**7109**	**267**	**294**	**4.3**	**<0.02**	**11.3**	**152615**	**1.6**
MEAN		**jarosite**		**9940**	**34219**	**779**	**111708**	**489461**	**0.9**	**0.3**	**160**	**3084**	**4753**	**173**	**280**	**3.5**	**<0.02**	**15.7**	**41403**	**0.5**

Appendix L – Tesorera and Jayula ores conditions and preliminary results

L.1 Conditions used for preliminary flotation test

A series of batch flotation tests was carried out for both Tesorera and Jayula ore. During all rougher flotation experiments, the per cent of solids was 20% and aeration rate in the flotation cell was 10 L/min. Combinations of different families of collectors were used such as Aero 404, Aero 3418A, Potassium amyl xanthate (PAX), and other collectors; sodium hydrosulphide (NaHS) as a sulphidising reagent; sodium silicate (Na_2SiO_3) and D919 (Lignosulphonate) as depresants; Lime, sodium hydroxide (NaOH) and sulphuric acid (H_2SO_4) as pH modifiers and methyl isobutyl carbinol (MIBC) as frother. Rougher flotation test tests were carried out over a period of 8 minutes. Table L.1 summaries the equipment conditions used for Tesorera ore.

Table L.1: Conditions for Rougher's Flotation (sulphide, sulphidization and non- sulphide flotation)

Flotation Equipment	Rougher	**Grinding Equipment**	Primary Grind
Flotation Machine	JKMRC	**Mill**	Rod
Cell size in litres	5	**Charge/Material**	15 kg/ 1000 kg JK2681-2
Aspiration	air	**Water**	1000 ml
Impeller Speed in rpm	1000		

The resume of the reagents used in each ore can be seen from Tables L.2 and L.3.

Table L.2: Reagents used on Tesorera Ore

Reagent	**Class**	**Supplier**
Aerophine 3418A	Collector (Dithiophosphinate)	Cytec
PAX	Collector (Potassium amyl xanthate)	Senmin
Aero 404	Collector (Mercaptobenzothiozole)	Cytec
MIBC	Frother (methyl isobutyl carbinol)	Not Given
Copper Sulphate	activator	Ajax Chemicals
Lime	pH modifier	Not Given
Sodium Hydroxide	pH modifier	Ajax Chemicals
Sulphuric acid	pH modifier	Not Given
Sodium Silicate	Dispersant	Not Given
EDTA (ethylenediaminetetra-acetic acid)	Dispersant	Not Given
Sodium hydrosulphide	Sulphidisation agent	Ajax Chemicals

Table L.3: Reagents used on Jayula ore

Reagent	Class	Supplier
Aerophine 3418A	Collector (Dithiophosphinate)	Cytec
PAX	Collector (Potassium amyl xanthate)	Senmin
Aero 404	Collector (Mercaptobenzothiozole)	Cytec
Aero S-9849	Collector Chelating	Cytec
Aero 3000C	Collector (Cationic)	Cytec
Aero 6494	Collector (Chelating)	Cytec
Aero 869F	Collector (Anionic)	Cytec
Aero 6697	Collector (Monothiophosphate)	Cytec
Aero XD-5002 promoter	Collector (Modified Thionocarbamate)	Cytec
Aero MX-950	Collector (Dithiocarbamate and thionocarbamate)	Cytec
MIBC	Frother (methyl isobutyl carbinol)	Not Given
Copper Sulphate	activator	Ajax Chemicals
D919	Dispersant (Lignosulfonate)	Not Given
Sodium oleate	Dispersant (Anionic oxhydryl)	Not Given
Dodecylsulfonate	Dispersant (Alkyl sulphonate)	Not Given
Sodium Silicate	Dispersant	Not Given
Lime	pH modifier	Not Given
Sodium Hydroxide	pH modifier	Ajax Chemicals
Sulphuric acid	pH modifier	Not Given
Sodium hydrosulphide	Sulphidisation agent	Ajax Chemicals

L.2 Description of the experiments

Rougher flotation tests were conducted on Tesorera and Jayula ores, after the sulphidisation step, the second non sulphide flotation step was either sulfidising with sulphidisation reagents or using non sulphide collectors. Figure L.1 shows the laboratory flow sheet for Tesorera and Jayula ores.

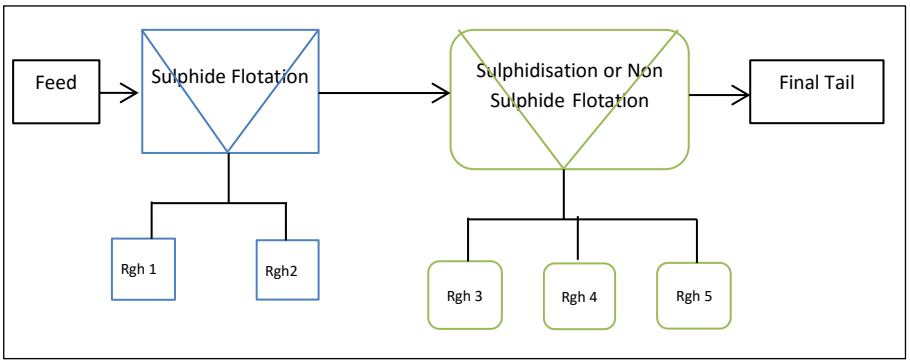

Figure L.1: Batch flotation test

L.3 Flotation experiments performed for Tesorera ore

Forty-five batch flotation tests were performed for Tesorera ore, from which thirty-nine experiments were conducted using sulphide flotation or sulphide/sulphidisation rougher flotation (Figure L.1) and six cleaner tests were done. These experiments are divided in fifteen series. Each one of the series had a different approach (conditions) for improving silver recovery on Tesorera ore. Table L.4 summarises these series.

Table L.4: Series of tests for Tesorera

Series	Tests	Aim
1	1 to 5	Characterisation of the flotation properties of the ore.
2	6 to 11	Evaluation of collector and activator addition.
3	12 to 16	Evaluation of pH and reagents.
3 to 10	17 to 39	Sulphide mineral flotation followed by Sulphidisation for non-sulphide minerals: From series 10 regrinding of feed was introduced
11 to 15	40 to 45	Sulphide mineral flotation followed by Sulphidisation for non-sulphide minerals and one stage of cleaning

Table L.5, summarises the flotation conditions for each test performed on Tesorera, which includes reagent used, pH, and global dosage for sulphide flotation and sulphidisation of non-sulphide minerals recovered by flotation.

Table L.5: Reagents, dosage and pH used in tests for Tesorera ore

Test	Step 1: Sulphide's flotation (gas: air)					Step 2: Sulphidisation's flotation				
	pH	Eh (mV)	Dispersant (g/t)	Activator (g/t)	Collectors (g/t)	gas	pH	eH (mV)	Activator (g/t)	Collectors (g/t)
1	5.7	409			MIBC (170)					
2	5.7	393			3418A (90), MIBC(120)					
3	7	306			3418A(90), MIBC(120), lime(550)					
4	7	290		$CuSO_4$(130)	3418A(90), MIBC(120), lime(650)					
5	6.7	278		$CuSO_4$(130)	3418A(60),PAX(40), MIBC(220), lime(860)					
6	7	328		$CuSO_4$(130)	3418A(90), MIBC(220), lime(900)					
7	7	325		$CuSO_4$(130)	3418A(200), MIBC(160), lime(800)					
8	7	310		$CuSO_4$(130)	3418A(45), MIBC(180), lime(750)					
9	7	298		$CuSO_4$(390)	3418A(90), MIBC(190), lime(800)					
10	7	274		$CuSO_4$(130)	3418A(90), MIBC(190), lime(800)					
11	7	280		$CuSO_4$ (130)	3418A(90), MIBC(190), lime(2000)					
12	7	230		$CuSO_4$(130)	3418A (90), MIBC(180), lime(800)					
13	7	225		$CuSO_4$(130)	3418A(90),PAX(180), MIBC (180), lime (800)					
14	7	230		$CuSO_4$(350)	3418A(90),PAX(180), MIBC (180), lime (900)					
15	8.1	158		$CuSO_4$(350)	3418A(90),PAX(180), MIBC (180), lime (2100)					
16	4.2	320		$CuSO_4$ (350)	3418A(90),PAX(180), MIBC (180), Sulphuric Acid (0.41)					
17	5.5	268		$CuSO_4$(350)	3418A(90),PAX(180), MIBC (180), lime (50)	air	11.7	-393	$CuSO_4$ (300)	NaHS(8585), PAX(300)
18	5.5	261		$CuSO_4$(350)	3418A(90),PAX(180), MIBC(180)	air	11.5	-382		NaHS(7860), Aero 3000C(450)
19	8.2	131		$CuSO_4$(450)	3418A(90),PAX(180), MIBC (140), lime (1800)	air	9.5	-417	$CuSO_4$ (300)	NaHS(5647), PAX(300)
20	8.2	157		$CuSO_4$(450)	3418A (90), Aero 404(100),PAX (180), MIBC (140), lime (1800)	air	9.6	-404	$CuSO_4$ (300)	NaHS(6089), Aero 404(150),PAX(300)
21	8.2	136		$CuSO_4$(450)	3418A (90), Aero 404(100),PAX (180), MIBC (140), lime (1750)	air	7.7	-179	$CuSO_4$ (300)	NaHS(2470), Aero 404(150),PAX(300)
22	8.2	151		$CuSO_4$(450)	3418A (90), Aero 404(110),PAX (180), MIBC (150), lime (2500)	air	10.8	-549	$CuSO_4$ (300)	NaHS(6593), Aero 404(150),PAX(300), MIBC(30)
23	8.2	91	EDTA (35)	$CuSO_4$(450)	3418A (90), Aero 404(110),PAX (180), MIBC (130), lime (4800)	air	10.4	-549	$CuSO_4$ (300)	NaHS(6372), Aero 404(150),PAX(300), MIBC(30)
24	8.2	123	Sodium Silicate (1000)	$CuSO_4$(450)	3418A (90), Aero 404(110),PAX (180), MIBC (130), lime (1400)	air	10.6	-542	$CuSO_4$ (300)	NaHS(6497), Aero 404(150),PAX(300), MIBC(30)

25	5.5	233		$CuSO_4$(450)	Aero 404(600),PAX (400), NaHS(25), MIBC(160),lime(100)	N2	8.4	-433	$CuSO_4$ (300)	NaHS(2241), Aero 404(400),PAX(400), MIBC(160)
26	5.5	178	Sodium Silicate (1000)	$CuSO_4$(450)	Aero 404(600),PAX(400), NaHS(25), MIBC(140),Sulphuric Acid (320)	N2	8.3	-433	$CuSO_4$ (300)	NaHS(2498), Aero 404(400),PAX(400), MIBC(120)
27	7	132	Sodium Silicate (1000)	$CuSO_4$(450)	Aero 404(600),PAX (400), NaHS(25), MIBC(140),Sulphuric Acid (20)	N2	8.6	-433	$CuSO_4$ (300)	NaHS(2534), Aero 404(400),PAX(400), MIBC(160)
28	7	202		$CuSO_4$(450)	Aero 404(600),PAX(400), MIBC(120),lime(800)	N2	7.1	-300	$CuSO_4$ (300)	NaHS(3290), Aero 404(400),PAX(500), MIBC(100)
29	7	177		$CuSO_4$(450)	Aero 404(600),PAX(400), MIBC(120),lime(900)	N2	7	-200	$CuSO_4$ (300)	NaHS(1200), Aero 404(400),PAX(500), MIBC(100)
30	7	198		$CuSO_4$(450)	Aero 404(600),PAX(400), MIBC(120),lime(850)	N2	8.1	-400	$CuSO_4$ (300)	NaHS(6640), Aero 404(400),PAX(500), MIBC(100)
31	5.4	226		$CuSO_4$(450)	Aero 404(600),PAX,(400) MIBC(120)	N2	6.8	-300	$CuSO_4$ (300)	NaHS(4810), Aero 404(400),PAX(400), MIBC(80)
32	5.5	207		$CuSO_4$(450)	Aero 404(600),PAX(400), MIBC(120),lime(50)	N2	6.4	-183	$CuSO_4$ (300)	NaHS(3910), Aero 404(400),PAX (500), MIBC(80)
33	5.4	217		$CuSO_4$(450)	Aero 404(600),PAX(400), MIBC(120),lime(50)	N2	7	-157	$CuSO_4$ (300)	NaHS(4580), Aero 404(400),PAX(400), MIBC(80)
34	7	165	Sodium Silicate (1000)	$CuSO_4$(450)	Aero 404(600),PAX(400), NaHS(250), MIBC(120),Sulphuric Acid (0.1)	N2	7.2	-171	$CuSO_4$ (300)	NaHS(3290), Aero 404(400),PAX(400), MIBC(80)
35	7	161	Sodium Silicate (1000)	$CuSO_4$(450)	Aero 404(600),PAX(400), MIBC(120),Sulphuric Acid (0.1)	N2/air	7.3	-85	$CuSO_4$ (300)	NaHS(1200), Aero 404(400),PAX(500), MIBC(100)
36	7	171	Sodium Silicate (1000)	$CuSO_4$(450)	Aero 404(600),PAX(400), MIBC(120),Sulphuric Acid (0.2)	N2/air	7.2	-60	$CuSO_4$ (300)	NaHS(6640),Fe^{2+} (50), Aero 404(400) ,PAX(400), MIBC(100)
37	7	162	Sodium Silicate (1000)	$CuSO_4$(450)	Aero 404(600),PAX(400), MIBC(120),lime(50)	N2/air	7.2	-74	$CuSO_4$ (300)	NaHS(3950), Aero 404(400),PAX(500), MIBC(100)
38	7	171	Sodium Silicate (1000)	$CuSO_4$(450)	Aero 404(600),PAX (400), MIBC(140),lime(100)	N2/air	7.4	-93	$CuSO_4$ (300)	NaHS(4200), Aero 404(400),PAX(500), MIBC(100)
39	7	157	Sodium Silicate (1000)	$CuSO_4$(450)	Aero 404(600),PAX(400), MIBC(120), Sulphuric Acid (1.25)	N2/air	7.7	-97	$CuSO_4$ (300)	NaHS(3990),Fe^{2+} (), Aero 404(400), PAX(500), MIBC(60)
40	7	168		$CuSO_4$(450)	Aero 404(600),PAX(400), MIBC(120), Sulphuric Acid	N2/air	6.6	-39	$CuSO_4$ (100)	NaHS(1104;), Aero 404(200),PAX(200)
41	7	199		$CuSO_4$(450)	Aero 404(600),PAX(400), MIBC(120),lime(100)	N2/air	6.5	29	$CuSO_4$ (100)	NaHS(1020), Aero 404(200),PAX(200), MIBC(100)
42	7	44		$CuSO_4$(450)	Aero 404(600),PAX(400), MIBC(),120lime(600)	N2/air	7	-42	$CuSO_4$ (100)	NaHS(1910), Aero 404(200),PAX(200), MIBC(100)
43	7	118		$CuSO_4$(450)	Aero 404(600),PAX(400), MIBC(120),lime(900)	N2/air	7	-28	$CuSO_4$ (100)	NaHS1970 (), Aero 404(200),PAX(200), MIBC(100)
44	7	126		$CuSO_4$(450)	Aero 404(600),PAX(400), MIBC(120), Sulphuric Acid (0.04)	N2/air	7	-39	$CuSO_4$ (100)	NaHS(1600), Aero 404(200),PAX(200), MIBC (100)
45	7	161		$CuSO_4$(450)	Aero 404(600),PAX(400), MIBC(120), Sulphuric Acid (0.02)	N2/air	7.5	-50	$CuSO_4$ (100)	NaHS(1600), Aero 404(200),PAX(200), MIBC(100)

The recommendation from the literature review was evaluated in this work taking the mineralogy in consideration. Recommendation 1 was applied to series 10 (more details on September 2011's report for MSc by B. Johnson) and series 14 to 15. In series 10, higher recovery of silver was acquired in test 39 with 86.9 per cent of silver and mass recovery of 24.0 %, which can be found in Table L.6. This test is a combination of sulphide and sulphidisation's flotation plus an alteration of the grinding (MIG) to ensure that there was less solid and silver in the coarse fractions, the reagents used for sulphide flotation are sodium silicate as dispersant; collectors are Aero 404, PAX and MIBC for sulphide flotation and NaHS as sulphidisation agent, ferrous ions (Fe^{2+}) to improve the pyrite recovery due to silver associated with pyrite in this ore, $CuSO_4$ as activator, Aero 404 and PAX, as collectors for sulphidisation's flotation of non-sulphide minerals. The pH of this batch flotation was 7.

Recommendation 3 was applied to series 3 to 15 and suggestion 4 was tested on series 6 to 10. It can be noted that the silver minerals were responding well to flotation under these extreme conditions (sulphidisation step and activation of pyrite).

The results of recoveries for silver, arsenic, copper, iron, lead, sulphur, antimony and zinc can be seen in Table L.6.

Table L.6: Final Recoveries for elements on Tesorera Ore

Test No.	Mass Recovery	Final Recovery, Tesorera Ore (%)							
		Ag	As	Cu	Fe	Pb	S	Sb	Zn
1	1.7	1.4	0.0	7.1	1.6	2.6	1.7	0.0	8.5
2	3.7	13.9	0.0	14.9	9.0	17.1	13.9	0.0	44.5
3	4.3	15.4	0.0	22.8	11.7	20.0	15.5	0.0	33.0
4	6.2	27.0	0.0	28.3	19.8	29.6	28.0	0.0	62.2
5	8.4	29.6	0.0	28.2	21.1	31.8	29.9	0.0	75.6
6	4.9	21.1	0.0	25.2	13.9	23.5	22.7	0.0	62.7
7	5.7	25.6	0.0	26.5	18.5	28.8	27.0	0.0	55.6
8	3.2	14.7	0.0	20.0	8.5	16.4	15.5	0.0	59.9
9	4.7	17.6	0.0	16.7	10.7	18.8	18.4	0.0	65.6
10	4.5	19.7	0.0	22.0	11.9	21.1	20.3	0.0	65.5
11	4.6	17.0	0.0	19.6	10.8	19.6	17.9	0.0	62.2
12	4.5	19.9	0.0	18.6	12.2	21.4	20.5	0.0	63.6
13	6.8	25.4	0.0	22.6	16.9	27.7	25.1	0.0	55.5
14	7.6	32.8	0.0	23.2	22.1	34.6	32.8	0.0	67.0
15	5.8	26.7	0.0	19.0	17.1	28.8	27.2	0.0	67.9
16	6.8	23.9	0.0	20.4	15.9	25.8	24.1	0.0	56.9
17	16.1	60.0	0.0	26.8	44.3	63.0	56.3	0.0	67.4
18	11.7	51.4	0.0	30.8	37.2	55.0	48.7	0.0	62.9
19	16.2	44.8	0.0	28.8	34.6	49.1	44.0	0.0	69.7
20	19.9	59.7	0.0	33.9	47.1	65.2	57.4	0.0	70.1
21	18.4	64.8	0.0	35.6	49.4	70.4	64.5	0.0	69.0
22	18.1	33.2	0.0	29.0	27.5	36.6	32.4	0.0	64.2
23	16.2	28.1	0.0	22.6	25.0	32.6	27.2	0.0	49.4
24	18.2	34.0	0.0	29.8	28.5	37.8	33.5	0.0	70.9
25	19.1	54.9	40.9	34.0	41.8	60.6	53.3	26.1	65.1
26	19.0	57.1	44.4	32.9	44.2	62.8	55.6	26.0	67.0
27	20.4	70.0	53.7	33.8	53.3	74.8	68.5	32.2	78.6
28	36.3	82.7	69.1	55.6	66.6	85.2	81.4	45.4	82.6
29	35.3	82.7	68.6	54.8	66.4	85.9	82.0	45.6	88.6
30	28.1	62.5	49.3	48.5	51.6	67.3	60.1	33.3	62.4
31	24.4	68.7	53.3	41.0	54.0	73.4	66.4	37.2	67.6
32	28.6	79.3	63.0	48.6	62.6	82.6	77.1	41.1	78.1
33	29.4	85.6	73.2	49.0	64.8	86.2	82.5	44.4	87.9
34	27.2	76.6	59.7	45.0	60.2	79.4	74.5	39.3	81.8
35	26.8	83.3	68.8	42.8	61.7	84.2	80.7	42.5	86.9
36	26.3	83.0	67.9	43.5	61.2	83.1	80.0	41.4	85.9
37	26.9	84.2	69.9	44.4	62.1	85.3	82.3	41.7	89.1
38	28.0	84.2	69.1	46.2	64.2	86.1	82.4	42.9	87.9
39	24.0	86.9	70.2	44.0	62.4	85.1	84.4	41.0	90.8
40	4.6	38.1	21.7	11.2	21.1	30.1	28.4	12.1	21.8
41	4.9	43.8	24.2	13.1	24.8	39.1	35.1	14.7	33.8

42	3.9	39.3	18.6	9.9	18.7	30.3	26.3	10.9	14.8
43	6.2	46.3	18.2	12.0	18.0	26.4	23.9	10.9	26.3
44	8.2	54.6	30.9	15.2	28.7	43.1	40.8	17.6	61.6
45	9.6	53.5	31.7	17.6	28.7	40.8	38.8	17.6	47.5

L.4 Flotation experiments performed for Jayula ore

For Jayula ore fifty seven batch flotation tests were performed, which are divided in seventeen different series, each one having a specific objective. Table L.7 summarises these series.

Table L.7: Series of test for Jayula ore

Series	Tests	Aim
1	1 to 2	Characterisation of the flotation properties of the ore.
2	9 to 13	Evaluating a protocol for sulphidisation.
3, 4, 10, 13	3 to 6; 7 to 8; 34 to 36; 45 to 47	Sulphide mineral flotation conditions followed by sulphidisation for Non Sulphide minerals.
5 to 9, 11 to 12, 14 to 17	14 to 33; 37 to 44, 58; 49 to 57	Non sulphide mineral flotation conditions. Desliming was introduced in series 10 to 13. Regrinding was introduced in series 14 and 17.

Table L.8 summarises the flotation conditions for each test performed on Jayula ore. This includes reagent used, pH, and global dosage for sulphide flotation, sulphidisation or non-sulphide flotation.

Table L.8: Reagents, dosage and pH used in tests for Jayula ore

Test	Step 1: Sulphide's flotation					Step 2: Sulphidisation or Non sulphide flotation				
	pH	eH (mV)	Dispersant (g/t)	Activator (g/t)	Collectors (g/t)	Gas	pH	Eh (mV)	Dispersant (g/t)	Activator (g/t)	Collector (g/t)
1	4.7	335			MIBC (90)						
2	7	219		$CuSO_4$ (130)	3418A(90),MIBC(105), Lime(750)						
3	7	98		$CuSO_4$ (130)	3418A(90),PAX (180),MIBC(105), Lime(700)						
4	7.2	167		$CuSO_4$ (450)	3418A(90),PAX(180),MIBC(105), Lime (900)						
5	7	177		$CuSO_4$ (450)	3418A(90),PAX(180),MIBC(120), Lime(700)	Air	11.1	-460		$CuSO_4$ (300)	NaHS(115490), PAX(300)
6	7	149		$CuSO_4$ (450)	3418A(90),PAX(180),MIBC(130), Lime(980)	Air	11.1	-460			NaHS (105150), Aero 3000C (450)
7	7.7	141		$CuSO_4$ (450)	3418A(90),PAX(180),MIBC(180), Lime(1200)	Air	9.3	-371		$CuSO_4$ (300)	NaHS(3892), PAX(300)
8	7.7	157		$CuSO_4$ (450)	3418A(90),Aero 404(130),PAX(180), MIBC(105), Lime(1600)	Air	9.7	-476		$CuSO_4$ (300)	NaHS(4003), Aero 404(150), PAX(300)
9						Air	11.5	-445			NaHS(6000),Na2S (87,780), PAX(80), 3000C(70), MIBC(70)
10						Air	7.7	-201			NaHS(4660), PAX(80),Interfroth 156(60)
11						Air	6.3	-48			NaHS (540), PAX(80) ,Interfroth 156 (60), lime(550)
12						Air	11.6	-479			NaHS(33,680), PAX(80),Interfroth 156(30)
13						Air	9	-165		$CuSO_4$ (500)	NaHS(4780), PAX(80),Interfroth 156(80)
14	5.5	161			Dodecylsulphonate(75), NaOH(230)						
15	7	138			Dodecylsulphonate (40), MIBC(40), NaOH(520)						
16	9	95			Dodecylsulphonate (45), MIBC(50), NaOH(960)						

17	4.6	214			Dodecylsulphonate(45),MIBC(50)						
18	6.5	163			AERO 6697 (1000), NaOH (200)						
19	6.7	175			AERO 6697 (900),MIBC (50), NaOH(480)						
20	8.1	128			AERO 6697 (900),MIBC (50), NaOH(1180)						
21	5.5	248			AERO 6697(900),MIBC(50)						
22	6	306			Sodium Oleate(600), MIBC(80),NaOH(410)						
23	7	253			Sodium Oleate(600), MIBC(80),NaOH (540)						
24	8.2	173			Sodium Oleate(600), MIBC(80),NaOH(1000)						
25	4.8	308			Sodium Oleate (600), MIBC (80)						
26	8.2	103		$CuSO_4$ (450)	3418A(90), Aero 404(130), PAX(180), MIBC(140), NaOH(1140)	Air	8.4	68		$CuSO_4$ (200)	Aero 404(100), PAX(200), Aero 6494(750),MIBC(100)
27	9	26		$CuSO_4$ (450)	3418A(90), Aero 404(130), PAX(180), MIBC(140), NaOH(600)	Air	9	-27	Sodium Silicate (1000)	$CuSO_4$ (200)	Aero 404(100), PAX(200), Sodium Oleate(400), MIBC(200)
28	8.2	83		$CuSO_4$ (450)	3418A(90), Aero 404(130;), PAX(180), MIBC(140), Lime(1000)	Air	4.7	215	Sodium Silicate (1000)	$CuSO_4$ (200)	Aero 404(100), PAX(200), Sodium Oleate(400), MIBC(100), H_2SO_4(140)
29	9	62	D919 (200)	$CuSO_4$ (450)	3418A(90), Aero 404(130), PAX(180), MIBC(140), NaOH(1000)	Air	9	29	D919 (200)	$CuSO_4$ (200)	Aero 404(100), PAX (200), Sodium Oleate(400), MIBC(100)
30	8.2	104	D919 (200)	$CuSO_4$ (450)	3418A(90), Aero 404(130), PAX(180), MIBC(140), Lime(1200)	Air	4	239		$CuSO_4$ (200)	Aero 404(100),PAX(200), Sodium Oleate(400), MIBC(100), H2SO4(120)
31	8.2	93	D919 (200)	$CuSO_4$ (450)	3418A (90), Aero 404(130), PAX(180), MIBC(140), NaOH(1020)	Air	8.3	40		$CuSO_4$ (200)	Aero 404(100), PAX(200), Aero 6494(750),MIBC(100)
32	8.2	112	D919 (200)	$CuSO_4$ (450)	3418A(90), Aero 404(130), PAX(180), MIBC(140), NaOH(1010)	Air	8.2	91		$CuSO_4$ (200)	Aero 404(100), PAX(200), Aero 6494(600),MIBC(100)
33	7.9	121	D919 (200)	$CuSO_4$ (450)	3418A(90), Aero 404(130), PAX(180), MIBC(140), NaOH(1850)	air	8	45		$CuSO_4$ (200)	Aero 404(100), PAX(200), Aero S-9849(1200), MIBC(100)
34	8.2	110		$CuSO_4$ (450)	3418A(90), Aero 404 (130), PAX (180), MIBC (140), Lime(1810)	air	8.2	-122		$CuSO_4$ (300)	Aero S-9849(500), Aero 404(400), PAX(400), MIBC(100)
35	8.2	106		$CuSO_4$ (450)	3418A(90), Aero 404 (130), PAX (180), MIBC (140), Lime(1900)	air	8.2	-36	Sodium Silicate (1000)	$CuSO_4$ (150)	Aero S-9849(150), Aero 404(100), PAX(40), MIBC(100)
36	8.2	131		$CuSO_4$ (450)	3418A(90), Aero 404 (130), PAX 180 (), MIBC (140), Lime(1000)	air	8.2	-42	Sodium Silicate (1000)	$CuSO_4$ (150)	Aero S-9849(150), Aero 404(100), PAX(40), MIBC(100)
37	9	64	Sodium Silicate (1000)	$CuSO_4$ (450)	3418A(90), Aero 404 (130), PAX (180), MIBC (140), Lime(400)	air	9	99			Sodium Oleate(400), MIBC(100)
38	8.2	106	D919 (200)	$CuSO_4$ (450)	3418A(90), Aero 404 (130), PAX (180), MIBC (140), Lime(750)	air	9	64			Aero 6494(750), MIBC (100)
39	9	80	Sodium Silicate (1000)	$CuSO_4$ (450)	3418A(90), Aero 404 (130), PAX (180), MIBC (140), Lime(450)	air	9	87			Sodium Oleate(800), MIBC(100)
40	8.2	65	D919 (200)	$CuSO_4$ (450)	3418A(90), Aero 404 (130), PAX (180), MIBC (140), Lime(650)	air	8.2	-35			Aero 6494(1500), MIBC(100)
41	8.2		D919 (200)	$CuSO_4$ (450)	3418A(90), Aero 404 (130), PAX (180), MIBC (140), Lime						
42	8.2	47		$CuSO_4$ (450)	3418A(90), Aero 404 (130), PAX (180), MIBC (140), Lime(750)	air	6.1	185	D919 (200)		Aero 869F(600); H_2SO_4(350)
43	8.2	64		$CuSO_4$ (450)	3418A(90), Aero 404 (130), PAX (180), MIBC (140), Lime(750)	air	6.2	111	D919 (200)		Aero 869F(1200); H_2SO_4(1000)
44	8.1	57		$CuSO_4$ (450)	3418A(90), Aero 404 (130), PAX (180), MIBC (140), Lime(100)	air	6.5	150	D919 (200)		Aero 869F(2400); H_2SO_4(1300)
45	8.1	135		$CuSO_4$ (450)	3418A(90), Aero 404 (130), PAX (180), MIBC (140), Lime(950)	N2/air	8.9	105			NaHS(1104), Lead Nitrate(100), Aero 404(400), Aero S-9849(150), PAX(400)
46	8.1	117		$CuSO_4$ (450)	3418A(90), Aero 404 (130), PAX (180), MIBC 140 (), Lime(1000)	N2/air	8.4	-139			NaHS(570), Lead Nitrate(100), Fe^{2+} (100), Aero 404(400),Aero S-9849(100), PAX(400)
47	8.2	115		$CuSO_4$ (450)	3418A(90), Aero 404 (130), PAX (180), MIBC (140), Lime(800)	N2/air	8.3	-50			NaHS (520), Lead Nitrate(150), Fe^{2+} (150), Aero 404(300),3418A(240), S-Aero 9849(120)
48	8.2	65	D919 (200)	$CuSO_4$ (450)	3418A(90), Aero 404 (130), PAX (180), MIBC (140), Lime(1200)	air	8.2	-35	D919 (200)	$CuSO_4$ (100)	Aero 404(50), PAX(100), Sodium Oleate(300)
49	8.2	107	D919 (200)	$CuSO_4$ (450)	3418A(90), Aero 404 (130), PAX (180), MIBC (140), Lime(1150)	air	8.2	115	D919 (200)	$CuSO_4$ (200)	Aero 404 (100), Pax (200), Sodium Oleate(400), MIBC(100)
50	8.2	64	D919 (400)	$CuSO_4$ (450)	3418A(90), Aero 404 (130), PAX (180), MIBC (140), Lime(1550)	air	8.2	35	D919 (400)	$CuSO_4$ (200)	Aero 404(100), PAX(200), Sodium Oleate(750)

51	8.2	64	D919 (200)	$CuSO_4$ (450)	3418A(90), Aero 404 (130), PAX (180), MIBC (140), Lime(1800)	air	8.2	70		Aero MX-950(150)
52	8.2	75	D919 (200)	$CuSO_4$ (450)	3418A(90), Aero 404 (130), PAX (180), MIBC (140), Lime(2250)	air	8.2	88		Aero 3418A(100),Aero MX-950(150)
53	8.2	96	D919 (200)	$CuSO_4$ (450)	3418A(90), Aero 404 (130), PAX (180), MIBC (140), Lime(1500)	air	8.2	102		Aero 3418A(100),Aero MX-950(150)
54	8.2	130	D919 (200)	$CuSO_4$ (450)	3418A(90), Aero 404 (130), PAX (180), MIBC (140), Lime(1900)	air	9.4	47		Aero MX-5002(400), PAX(200), Sodium Oleate(400;), MIBC(100)
55	8.2	83	D919 (200)	$CuSO_4$ (450)	3418A(90), Aero 404 (130), PAX (180), MIBC (140), Lime(900)	air	9.5	67		Aero XD-5002(80)
56	8.2	130	D919 (200)	$CuSO_4$ (450)	3418A(90), Aero 404 (130), PAX (180), MIBC (140), Lime(550)	air	8.2	132		Aero XD-5002(80)
57	8.2	69	D919 (200)	$CuSO_4$ (450)	3418A(90), Aero 404 (130), PAX (180), MIBC (140), Lime(2100)	air	8.2	127	D919 (200)	AERO 869F(1450)

As for the Tesorera ore, the mineralogy was considered in addressing the recommendation from the literature review. In this case, recommendation 1 was applied to series 14 to 17 and the results are shown in Table L.7. Regrinding of the + 74 μm of the ground feed for additional 10 minutes; desliming of the ground feed and a combination of both were evaluated.

Suggestion 2 was applied to series 5 to 7 for non-sulphide flotation, and then for series 8 to 9, following by series 11 to 12, and series 14 to 17, in which it the best recovery was obtained from silver on test 29. The reagents were tested in a range of pH from 4 to 9.5. Higher recovery of silver was obtained. The selected reagents were for Sulphide flotation: collectors Aerophine 3418A (Dithiophosphinate), Aero 404 (Mercaptobenzothiozole), PAX (Potassium amyl xanthate), frother: MIBC (methyl isobutyl carbinol), activator: Copper sulphate ($CuSO_4$), dispersant D919 (Lignosulphonate), pH modifier: Sulphuric acid and for Non-sulphide flotation, collectors: Aero 404, PAX, Sodium Oleate (Anionic oxhydryl) frother: MIBC, activator: $CuSO_4$ and dispersant D919.

Based on the laboratory batch flotation test a suitable pH of 9.0 -9.5 is recommended for floating Jayula ore. The best results for Jayula ore were test 29 with 46.1% of silver recovery and mass recovery of 23.1 per cent at pH 9. This test is a combination of sulphide and non-sulphide flotation where lignonsulphonate D919 was used as dispersant and sodium oleate as collector on non sulphide flotation. Test 53, achieved 47.5% of silver recovery and mass recovery of 18.5%. This test also is a combination between sulphide and non sulphide flotation where D919 was used as dispersant in the sulphide flotation and Aero MX-950 (CYTEC) was used as collector in the non sulphide flotation at pH 8.2.

Other collector's schemes were tried with the selected pH, grinding size and dispersants (Table L.3, shows collectors and dispersants used on Jayula ore). These were not as successful as the combination of collectors described above. For example, test 48 had 65.3% on silver recovery but high mass recovery 48.0% (Table L.9).

Recommendation 3 in presence of sulphidisation, was applied to series 3 to 4 and then series 10 and 13. The results are low on silver recoveries, where none of the tests exceeded 35% of silver recovery.

The results of recoveries for silver, arsenic, copper, iron, lead, sulphur, antimony and zinc can be seen from Table L.9.

Table L.9: Final Recoveries for elements on Jayula Ore

Test No.	Final Recovery, Jayula Ore (%)								
	Mass Recovery	Ag	As	Cu	Fe	Pb	S	Sb	Zn
1	1.5	19.0	0.0	7.0	1.7	2.0	3.5	0.0	8.6
2	5.7	28.8	0.0	12.5	6.7	8.4	11.7	0.0	22.0
3	3.8	25.9	0.0	8.4	4.2	5.5	5.7	0.0	7.8
4	7.1	24.1	0.0	13.1	8.0	10.0	8.7	0.0	11.5
5	13.3	28.0	0.0	20.0	14.2	18.1	15.7	0.0	19.5
6	13.9	27.8	0.0	23.2	14.8	17.9	14.5	0.0	19.7
7	11.9	29.2	14.2	17.7	13.7	16.1	11.7	14.8	16.8
8	14.3	31.4	16.7	20.0	16.4	18.8	13.0	13.7	20.8
9	0.9	0.4	0.0	1.4	0.8	1.0	2.6	0.0	0.7
10	0.1	5.8	0.0	1.4	0.3	0.6	0.8	0.0	0.7
11	0.3	13.3	0.0	2.5	0.4	0.6	1.2	0.0	1.5
12	0.4	1.6	0.0	1.1	0.5	0.6	1.2	0.0	0.6
13	0.8	17.2	0.0	3.6	0.9	2.2	2.3	0.0	2.5
14	7.3	21.0	9.2	12.6	9.0	10.5	10.1	8.6	11.7
15	15.5	31.4	18.1	24.0	18.0	20.3	15.1	15.5	21.3
16	7.1	20.9	8.7	12.3	8.3	9.7	9.3	8.1	11.7
17	23.4	29.0	27.4	30.4	26.7	30.4	29.7	24.8	30.9
18	55.1	63.4	59.0	60.3	58.1	60.7	56.2	51.3	62.7
19	52.7	58.9	56.5	59.4	55.7	59.3	53.7	50.5	61.9
20	49.3	57.8	53.5	56.9	53.8	56.8	51.0	50.3	60.5
21	61.8	66.6	66.3	67.3	65.6	68.1	62.0	59.3	69.8
22	22.0	24.4	30.9	33.2	29.3	37.9	41.6	29.6	30.2
23	24.2	31.9	39.0	38.7	34.1	48.0	60.7	30.2	33.1
24	39.1	42.5	49.1	49.9	45.7	55.2	61.8	42.7	46.3
25	22.0	19.9	31.6	33.3	29.3	36.5	32.5	20.6	31.3
26	13.0	38.5	19.2	23.0	17.1	20.8	19.1	14.9	20.9
27	9.6	36.6	11.4	13.9	11.3	13.7	18.4	13.6	14.9
28	15.0	31.9	21.0	26.9	18.9	22.6	20.1	15.2	23.2
29	23.1	46.1	32.4	29.5	28.3	37.4	52.5	28.3	29.5
30	14.5	32.6	18.8	25.7	17.4	21.0	18.8	15.8	19.2
31	38.7	53.7	47.4	46.7	45.4	56.6	54.2	50.4	45.8
32	21.9	36.9	28.1	37.1	26.9	31.1	28.0	24.8	30.5
33	22.1	36.1	31.5	40.4	29.0	34.7	42.1	26.0	33.1
34	36.3	47.6	46.3	52.8	44.5	51.2	46.7	45.6	46.7
35	23.8	45.1	31.8	38.7	29.8	34.9	27.8	24.2	33.4

36	14.7	36.4	26.3	36.0	25.6	31.0	41.7	26.3	31.8
37	9.6	34.4	11.8	24.6	11.0	13.6	25.8	9.0	10.1
38	18.2	40.3	17.3	44.8	21.6	26.2	32.8	2.3	24.1
39	4.3	27.0	4.9	12.7	4.9	6.2	12.2	4.4	7.7
40	36.5	52.7	44.3	63.2	42.9	49.0	59.2	43.8	42.8
41	0.0	0	0	0	0	0	0	0	0
42	5.0	18.8	6.3	14.5	6.1	7.4	7.9	4.3	7.7
43	9.5	25.6	11.5	21.6	11.0	13.5	20.6	12.0	14.0
44	9.4	26.5	12.2	24.8	11.3	13.9	18.3	9.5	14.2
45	14.4	32.9	16.9	28.1	16.3	20.1	14.6	14.4	17.2
46	21.1	38.2	26.5	38.3	24.7	29.8	33.2	21.8	26.3
47	20.0	38.5	23.2	26.9	23.4	28.2	26.2	21.1	23.8
48	48.0	65.3	52.3	50.9	51.4	55.0	55.7	52.0	54.2
49	12.2	34.2	15.0	28.0	19.7	20.4	24.5	10.8	17.7
50	37.5	45.6	44.2	54.0	37.7	46.6	48.8	35.2	46.0
51	6.7	31.6	9.0	27.2	7.5	10.2	9.6	6.8	12.0
52	10.2	32.9	12.4	19.6	11.0	13.8	12.3	9.3	15.4
53	18.5	47.5	21.9	28.5	19.3	23.1	21.4	18.2	24.8
54	11.0	34.2	13.8	20.6	12.2	14.6	14.1	10.6	16.4
55	14.3	43.8	15.9	21.2	13.8	17.0	16.4	14.3	18.5
56	0.5	6.4	0.6	1.7	0.6	0.8	1.2	0.5	1.8
57	13.0	33.3	15.4	21.3	13.2	17.2	18.5	11.9	18.8

L.5 Conclusion

❖ Tesorera Ore

The Tesorera ore responded well to the sulphide flotation step followed by a sulphidisation step as well as to decreasing the particle size to increase the liberation of pyrite.

The best results obtained for Tesorera Ore (Test 39) were 86.9% Ag recovery at a mass recovery of 24.0% and grade of 443 ppm Ag. These were obtained with a reduction of the grind size, a sulphide flotation step at pH 7 to recover the sulphide minerals, followed by sulphidisation step to recover the non sulphide minerals. In the sulphide flotation step $CuSO_4$ was the activator, sodium silicate was dispersant; collectors were Aero 404 and later PAX and the frother was MIBC. In the sulphidisation step, the Eh was reduced to -115mv Eh, with NaHS used as the sulphidisation agent, with ferrous ions (Fe^{2+}) as well as $CuSO_4$ as the activator, Aero 404 and PAX, as collectors.

Three different collectors were used for Tesorera ore: Aero 404 and PAX (Potassium amyl xanthate) was the best combination to get highest silver recovery on sulphide and sulphidisation of

non-sulphide minerals by flotation. Copper sulphide and sodium silicate were used as activator and dispersant respectively. Ferrous ions are necessary to activate pyrite to improve silver recovery.
The range of pH tested was from 4 to 8.2 and pH 7 was found to be the most adequate pH to float Tesorera ore.
Tesorera ore is recommended to be processed by Minera San Cristobal's concentrator using the adequate rate of reagents and grinding procedures developed by JKMRC personnel in this project. It is then suggested to test whether similar results can be achieved in a pilot plant testing.

- **Jayula Ore**

Mineralogical characterisation of the Jayula ore indicated that approximately 24% of the silver occurs in silver minerals such as acanthite and pyrargyrite while most of the remaining silver occurs in a lead arsenate mineral.
The liberation level for lead arsenate in the rougher feed (80% passing size of 100 μm) is modest at 49.5% while the liberation level for the combined silver minerals in the rougher feed is low at 30%. However addition of a regrind step did not improve recoveries.

The highest silver recovery obtained was 65.3 % Ag but this was with a mass recovery of 48.0%.

Overall, the best silver recovery obtained for Jayula ore in terms of both silver recovery and mass recovery, was a combination between sulphide flotation and non-sulphide flotation, where silver recovery was 46.1 % on test 29 and 47.5% of silver recovery on test 53. The selected reagents used in both tests were for Sulphide flotation; these are collectors: Aerophine 3418A (Dithiophosphinate), Aero 404 (Mercaptobenzothiozole), PAX (Potassium amyl xanthate), frother: MIBC (methyl isobutyl carbinol), activator: Copper sulphate ($CuSO_4$), dispersant: D919 (Lignosulphonate), pH modifier: Sulphuric acid and for Non-sulphide flotation test 29 collectors: Aero 404, PAX, Sodium Oleate (Anionic oxhydryl) frother: MIBC, activator: $CuSO_4$ and dispersant D919. Aero 3418A and Aero MX-950 (Dithiocarbamate and thionocarbamate) as collectors for test 53, respectively.

From the 10 collectors tested from different families, the combination of three collectors (Aerophine 3418A, Aero 404 and PAX), plus copper sulphide as activator, D919 as dispersant and sodium oleate as collector in the non-sulphide flotation were suitable to achieve the highest recovery of silver with a relatively low mass recovery on Jayula ore (46.1%).

The range of pH tested was from 4 to 9.5 and pH 9 or 8.2 is the most suitable pH to float Jayula ore based on test 29 and test 53, respectively.

A method for obtaining a strong response from the lead arsenate mineral which bears silver has not been identified in the non sulphide flotation section of this test-work. It is recommended that hydrometallurgical processes also be evaluated for Jayula ore.

REFERENCE

Johnson N.W, 2011. Literature review – flotation of silver minerals and processing of silver bearing ores. Confidential report.